Understanding the Haematopoietic Differentiation Potential of Human Pluripotent Stem Cells.

Anna L French BSc (Hons)

Brasenose College

Supervisor Prof. Suzanne Watt

Co-supervisor Dr. Lee Carpenter

Thesis submitted for the degree of Doctor of Philosophy at the University of Oxford
Trinity term 2013

Nuffield Division of Clinical Laboratory Sciences, Radcliffe Department of Medicine, University of Oxford
and NHS Blood and Transplant, Oxford

Abstract

Understanding the haematopoietic differentiation potential of human pluripotent stem cells. Anna French, Brasenose College, Degree of Doctor of Philosophy, Trinity Term 2013.

Pluripotent stem cells (PSCs), both embryonic stem (ES) and induced pluripotent stem (iPS) cells, have the capacity to generate any cell type of the body and therefore have application in disease modelling, as a drug-screening tool and as a cell source for regenerative medicine. The development of the human haematopoietic system can be investigated within a PSC differentiation system, which has been demonstrated to faithfully recapitulate aspects of haematopoietic ontogeny. Furthermore, PSC-derived haematopoietic cells may be a viable alternative, in a clinical setting, to cells isolated from bone marrow, peripheral blood or umbilical cord blood. iPS cells, which can be generated from a multitude of adult somatic tissues, have a number of advantages over ES cells, that include ethical and immunogenic implications. The aim of this thesis was to investigate the capacity of human iPS cells to give rise to B lymphocytes, an output that has challenged the field. In the context of haematopoietic differentiation from PSCs, the generation of lymphocytes provides a valuable readout that is synonymous with the definitive waves of haematopoiesis and that could be used as a disease model for numerous leukaemias. Here, B lymphocytes were robustly generated from iPS cells. These iPS-derived B cells showed a high level of similarity at the global transcriptional level with B cells generated from UCB haematopoietic stem/progenitor cells. The cellular origins of iPS-derived B cells were investigated and it was demonstrated that a putative haemogenic endothelial population could generate B lymphocytes with an 80- fold enrichment in this potential, when compared to haematopoietic progenitor fractions. Finally, the capacity of iPS-derived B cells to generate cell surface immunoglobulins has been described for the first time. Interestingly, the production of these IgM^+ cells was inhibited by the addition of recombinant IL-7.

Publications

- French A, Buckler RL, Brindley DA. Commercialization of regenerative medicine: learning from spin-outs. Rejuvenation Research 2013 Apr; 16 (2) 164-70.

- Carpenter L, Malladi R, Yang CT, French A, Pilkington KJ, Forsey RW, Sloane-Stanley J, Silk KM, Davies TJ, Fairchild PJ, Enver T, Watt SM. Human induced pluripotent stem cells are capable of B-cell lymphopoiesis. Blood 2011 Apr 14; 117 (15) 4008-11.

- English K*, French A*, Wood KJ. Mesenchymal stromal cells: facilitators of successful transplantation? Cell Stem Cell 2010 Oct 8; 7 (4) 431-42.

Manuscripts in preparation

- French A, Yang CT, Carpenter L*, Watt SM*. Human induced pluripotent stem cells generate sIgM^{+} B lymphocytes via a hemogenic endothelium intermediate.

- Brindley DA, French A, Suh J, Roberts M, Dean B et al. The Implementation of Novel Collaborative Structures for the Identification and Resolution of Barriers to Stem Cell Translation. Stem Cells and Development. *In review.*

Published meeting abstracts (lead author abstracts)

- French A, Yang CT, Carpenter L* and Watt SM* (2013). Human induced pluripotent stem cell-derived B lymphocytes are generated via a haemogenic endothelial intermediate and mature to express cell surface IgM. NHS Blood and Transplant UK R&D conference, Oxford University, Oxford, UK.
- French A, Carpenter L, Watt SM (2012). B lymphocyte development from human induced pluripotent stem cells. Keystone Symposia, The Life of a Stem Cell: From Birth to Death. Olympic Valley, CA USA.
- French A, Pilkington K, Carpenter L, Watt SM (2010). Differentiation of human iPS cells towards haematopoietic and endothelial lineages. Hydra VI: The European Summer School on Stem Cells & Regenerative Medicine. Hydra, Greece.

Awards

- Senior Hulme Scholar (2012/13), Brasenose College, University of Oxford.
- Poster presentation prize (2010). Hydra VI: The European Summer School on Stem Cells & Regenerative Medicine. Hydra, Greece.
- MRC-OSCI D.Phil Studentship Award (2009). University of Oxford.

Acknowledgements and Declaration

Foremost, I would like to thank Dr. Lee Carpenter for introducing me to such an exciting project, for his insightful scientific input and support throughout, and for allowing me the space to develop my own ideas and direction. I would also like to thank Prof. Suzanne Watt for her supervision and for the opportunity to study within her laboratory, without which, this thesis would not have been possible. I would like to recognise the Oxford Stem Cell Institute, Brasenose College and NHS Blood and Transplant for supporting and/or funding this work.

I would like to thank all the members of the SCR laboratory, past and present, for their support and company. In particular, Dominic Sweeney for discussions, both scientific and otherwise, as well as for helpful advice in the lab. Thanks to Dr. Emma Pepperell for many years of much needed social activity and conversation. I am also hugely grateful to Cheng-Tao Yang for invaluable assistance in tissue culture, that enabled me to occasionally get away from the lab, and, for his friendship. Many thanks to Dr. Enca Martin-Rendon and Dr. Sarah Hale for insightful advice and support throughout my time in SCRL. Thanks also to Dr. Cheen Khoo, Nita Fisher, Chao-Hui, Surhi Buglass, Youyi Zhang, Huajuan Zhang, Dr. Lisa McRae, Jen Greenhowe and Dr. Kate Coldwell who have all made the working environment an enjoyable one, I am very grateful for their company. Finally, thanks to Dan, Rosalba, Mark, and Francesca for bringing a new wave of fun to the lab in recent times.

I am hugely grateful for the support of my family and friends. To my mother, for her understanding, encouragement and for her inspiring determination, as well as my father, for instilling an inquisitive (and occasionally argumentative) mind. I am thankful to my brothers, Andrew, Mark and Matthew for their continual support and presence. Also, to my friends, in particular, Binky, the Ave, Sjouke and many others who continue to provide the opportunity and companionship for many enjoyable adventures and occasions.

I certify that I carried out more than 95% of the research for this thesis. The gene array was performed by Dr. Dilair Baban at the Wellcome Trust Centre for Human Genetics, University of Oxford. Assistance in the analysis of gene array data was provided by Mr. Steven Taylor, WIMM, University of Oxford. FACS was performed by trained operators at the WIMM, Nuffield Department of Medicine and Sir William Dunn School of Pathology, all University of Oxford. Injections for mouse *in vivo* studies were performed by Dr. Ou Li, Nuffield Department of Surgery, University of Oxford. I would like to thank Dr. Lee Carpenter, University of Oxford, Cheng-Tao Yang, University of Edinburgh and Dr. Polyanna Goh, UCL for providing iPS cell lines.

Contents

List of figures

List of tables

Chapter 1.

Introduction

1.1 Literature review

1.1.1 Stem Cell Subsets

1.1.1.1 Stem Cells

The two hallmarks that have been used to define a stem cell are that of self-renewal and the potential to give rise to one or more cell types. This separates stem cells from 'progenitor cells' which have more restricted self-renewal capacity and potential, and from terminally differentiated cells which feature neither of these properties. Self-renewal is a form of cell division where one (asymmetric), or both (symmetric), cells are produced with conserved potency and potential between parent and daughter cell. This enables a stem cell pool to be maintained and therefore contributes positively to a homeostatic state.

Embryonic stem (ES) cells are characterised by their ability to self-renew and are also pluripotent; pluripotency defined as the ability to form all and any cell type of the three germ layers, endoderm, ectoderm and mesoderm. Mouse ES cells and were first described in 1981 (Evans and Kaufman, 1981, Martin, 1981). Human ES cells were not isolated until 1998 (Thomson et al., 1998). ES cell lines were established from the inner cell mass of the developing blastocyst (Evans and Kaufman, 1981, Martin, 1981, Thomson

et al., 1998). In appropriate conditions, initially using mouse feeder cells and subsequently in feeder-free systems, ES cells can be grown continually in an undifferentiated state and thus represent a potentially unlimited cell source. Differences between mouse and human ES cells have been described. Human ES cells are thought to be more similar to mouse epiblast stem cells (EpiSCs) than mouse ES cells (Tesar et al., 2007, Vallier et al., 2009). Unlike their mouse counterparts, human ES cells do not require LIF to maintain pluripotency (Reubinoff et al., 2000, Thomson et al., 1998). Whilst the majority of cell surface markers used to identify ES cells are conserved between mouse and human ES cells, there are however some exceptions, such as the expression of SSEA-1 (Thomson et al., 1998). Human ES cells are also morphologically different from mouse ES cells, with flat rather than domed colonies described for the former, and have a propensity to undergo apoptosis if dissociated to generate single cells (Watanabe et al., 2007, Ohgushi et al., 2010).

Adult stem cells are described as multipotent. This means that, whilst they have the capacity to differentiate into numerous cell types, the differentiation potential of adult stem cells is limited, when compared to pluripotent cells. The haematopoietic stem cell (HSC) represents one of the earliest descriptions of an adult stem cell. HSCs are found in the bone marrow and are responsible for the production of cells of the blood lineage, from red blood cells to platelets to T and B lymphocytes throughout adult life (McCulloch and Till, 1960, Wu et al., 1967, Muller-Sieburg et al., 1986). Stem cells from a vast array of tissues have subsequently been described, including neuronal, cardiac, intestinal and mesenchymal stem cells. In comparison to embryonic stem cells, attempts to expand

adult stem cells *in vitro*, that is to promote self-renewal at the expense of differentiation, has proven to be challenging.

1.1.1.2 Induced pluripotent stem cells

Induced pluripotent stem (iPS) cells were first generated in 2006 from adult mouse fibroblasts, and subsequently from human fibroblasts in 2007, by the retroviral introduction of Oct3/4, Sox2, c-myc and Klf4 (Takahashi and Yamanaka, 2006, Takahashi et al., 2007, Yu et al., 2007). This work was pioneered by Shinya Yamanaka and colleagues. The introduction of these four transcription factors reprogrammed the somatic cells to an ES cell-like state, resulting in pluripotency and the ability to self-renew (Figure 1). Further technological advances led to the use of non-integrating viral vectors and plasmids, recombinant proteins, synthetic mRNAs and miRNAs to introduce the reprogramming factors (Kaji et al., 2009, Zhou et al., 2009, Kim et al., 2009, Warren et al., 2010, Anokye-Danso et al., 2011). More recently, mouse iPS cells have been derived using small molecules alone (Hou et al., 2013). Moreover, iPS cells have been generated without the need for feeder cells (Yu et al., 2011). Advances have also been made with regard to the starting cell type used for reprogramming. Originally generated from dermal fibroblasts, iPS cells have now been successfully derived from a diverse range of tissues, including human umbilical cord blood (UCB), adipose tissue and even cells isolated from urine (Sun et al., 2009, Zhou et al., 2012, Haase et al., 2009).

The concept of the pluripotency network, where the expression of core factors define and regulate the pluripotent state has developed, with significant contribution from Smith and colleagues (Niwa et al., 2000, Masui et al., 2007, Martello et al., 2012, Boyer et al., 2005). Whether pluripotency represents a ‘ground-state’ or a ‘metastable’ state

continues to drive discussion within this field (Marks et al., 2012, Hayashi et al., 2008, Graf and Stadtfeld, 2008). In the case of induced pluripotency, it is thought that this network is activated by the enforced expression of the core pluripotency factors. This understanding has been advanced and questioned by the demonstration that the core factors, Oct4 and Sox2, can be replaced by lineage specifiers which were postulated to act by balancing mesendoderm with ectoderm fate (Shu et al., 2013).

Whether human ES cells and iPS cells are equivalent has been intensively discussed. In addition to sharing the defining characteristics of ES cells, iPS cells have a similar morphology and express human ES cell specific genes such as SSEA-4, TRA-1-81 and TRA-1-60 (Takahashi et al., 2007, Yu et al., 2007, Andrews, 1984). A number of groups have reported epigenetic memory in iPS cells resulting from the cell of origin, as well as chromosomal aberrations and the retention of X-inactivation marks (Kim et al., 2010, Mayshar et al., 2010) (Tchieu et al., 2010). However, these findings have repeatedly been challenged, with differences between ES and iPS cells being attributed to the conditions in which the iPS cells are generated, or to the genetic background of the cell of origin (Tomoda et al., 2012)(reviewed by (Cahan and Daley, 2013). A picture is emerging which suggests that human ES and iPS are not distinct populations, but that variation between iPS cell lines is greater than observed between different ES cell lines (Bock et al., 2011). Therefore, due to their similarity, ES and iPS cells are frequently referred to as pluripotent stem cells (PSCs). The ultimate demonstration of pluripotency, which is not possible in human systems, is that described by the tetraploid complementation assay (Nagy et al., 1990). Pluripotency can also be demonstrated in non-human cells by the generation of chimaeras and subsequent germline transmission. In a direct comparison of ES and iPS

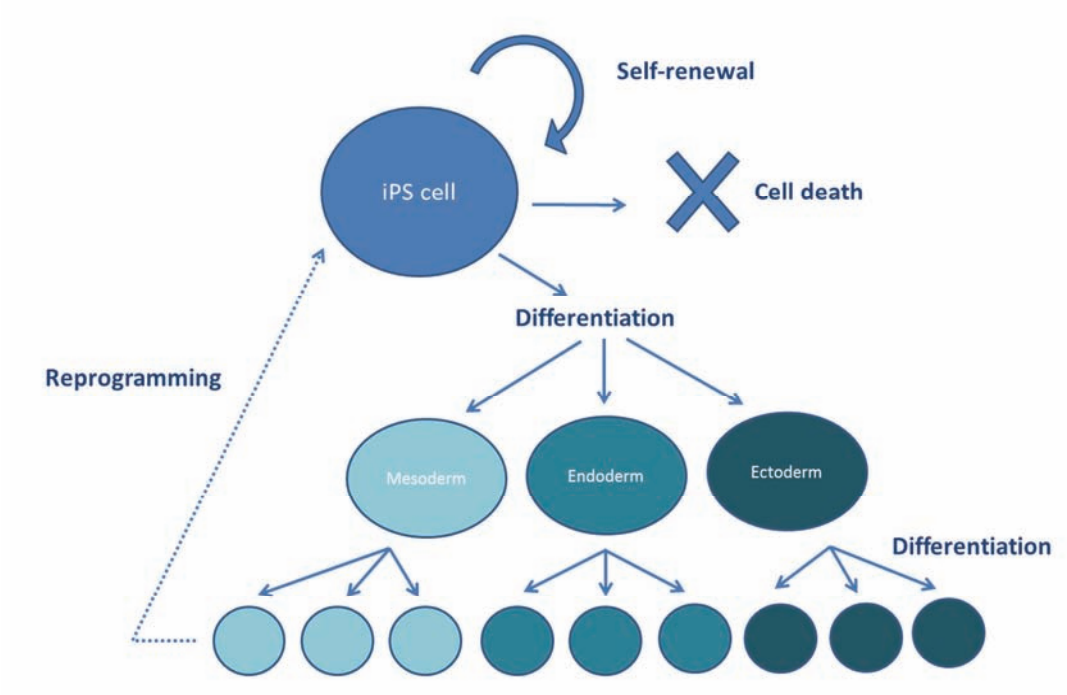

Figure 1 Alternative cell fates of induced pluripotent stem cells.
Induced pluripotent stem (iPS) cells can be generated in vitro by reprogramming adult somatic cells. iPS cells can give rise to all three germ layers: mesoderm, endoderm and ectoderm which in turn generate all of the tissues of the adult. Whilst iPS cells have the potential to self-renew, this potential is gradually lost as differentiation proceeds, cells are also thought to become increasingly specialised and lineage restricted. iPS cells also have the potential to indefinitely self-renew. An alternative cell fate is death, either by apoptosis or necrosis.

from mice with the same genetic background, Hochedlinger and colleagues demonstrated that the only difference in gene expression between the two cells types was found within the *Dlk1-Dio3* gene cluster (Stadtfeld et al., 2010). When the subfraction of iPS cell clones that were not epigenetically silenced at this locus were selected, 100% chimaerism could be observed (Stadtfeld et al., 2010). Furthermore, it was noted that the presence of ascorbic acid during reprogramming abrogated aberrant silencing at the *Dlk1-Dio3* locus (Stadtfeld et al., 2012).

The use of iPS cells as an alternative to human ES cells circumvents the ethical issues associated with embryo destruction and potentially addresses the problem of immunogenicity if these cells are to be used in an autologous transplantation setting. However, whether iPS-derived cell therapies will provoke an immune response has been hotly debated. Early studies demonstrated immunogenicity of undifferentiated iPS cells (which form teratomas when injected into mice), but importantly, this was not demonstrated for iPS-derived differentiated cells, which are of more clinical relevance (Zhao et al., 2011) (Guha et al., 2013).

In the short term, iPS cells are an invaluable tool for drug discovery and a useful model for both developmental biology and disease (Meng et al., 2010; Raya et al., 2009; Itzhaki et al., 2011; Lee et al., 2009). Here, the derivation of iPS cells from patients with genetic diseases could yield a system in which questions about pathogenesis can be probed. iPS cell lines have now been generated from patients with diseases as diverse as type 1 diabetes, Parkinson's disease, and Long QT syndrome (Soldner et al., 2009, Maehr et al., 2009, Moretti et al., 2010, Israel et al., 2012, Kondo et al., 2013). Whether iPS cell models faithfully recapitulate the disease *in vitro* remains to be determined. Promising reports of

disease-characteristic retention in a number of monogenic diseases, such as Rett Syndrome and Spinal Muscular Atrophy, have been reported (Marchetto et al., 2010, Ebert et al., 2009). Furthermore, it is possible to 'correct' genetic defects in the dish by homologous recombination, as described with Fanconi's Anaemia (Raya et al., 2009, An et al., 2012).

In a developmental context, human pluripotent stem cells, both ES and iPS, can be used as a model system. Research conducted with PSCs may complement that which has historically been conducted in non-primate species such as *Drosophila*, *Xenopus* and the mouse. Whilst a large number of genes and processes are conserved between mouse and human, a significant number are not. An estimated 1% of human genes do not have a known mouse homologue (Waterston et al., 2002). With the additional restrictions and ethical issues related to obtaining human embryos, which could otherwise be used to verify work in the mouse or provide a system to probe non-conserved genes and biochemical pathways, human PSCs stand alone in being able to fulfil such a requirement (Zhu and Huangfu, 2013).

Perturbations in the development of the blood system have far reaching implications and are associated with a vast array of diseases, from anaemia to severe combined immune-deficiency (SCID). iPS cells can thus be used to better understand these pathologies. Moreover, PSCs as a source of HSCs for transplantation could revolutionise treatment in the clinic. Currently, clinical HSC transplantation is approached using cells harvested from the bone marrow (BM), or, alternatively, from umbilical cord blood (UCB). The use of UCB has numerous advantages and disadvantages in comparison to transplantation with BM-derived HSCs. However, insufficient availability, mismatch between donor and recipient,

as well as unsuitable engraftment profiles still pose a significant clinical hurdle. PSC-derived HSCs and terminally differentiated blood cells could be used to address current shortfalls in clinical efficacy. A large segment of the pluripotent stem cell field is therefore focused on understanding blood cell development, a process termed haematopoiesis, which is also the focus of this thesis.

1.1.1.3 Haematopoietic stem cells

In the adult, HSCs reside in the bone marrow, in niches that contain mesenchymal cells/pericytes, bone, endothelium, adipocytes and/or a variety of differentiating blood cell types (Ding et al., 2012, Corselli et al., 2013, Lo Celso and Scadden, 2011). Three niches have been described, the endosteal niche (located proximally to bone), the vascular sinusoidal niche and the bone marrow proper (reviewed in (Bianco, 2011)). These are defined as being distinct entities or a continuum of niches within the bone marrow. The debate surrounding the relevance and role of the endosteal niche as opposed to the vascular niche, in relation to HSC maintenance, quiescence and proliferation continues (Kiel and Morrison, 2008). One prevailing view is that quiescent HSCs reside in the endosteal niche, with dividing and/or differentiating HSCs being located at the vascular niche (Trumpp et al., 2010, Haylock et al., 2007). Indeed, localisation of human HSCs in the endosteal niche of the trabecular bone area has recently been reported (Guezguez et al., 2013). The authors also described phenotypic and functional differences between HSCs located in the long bone and trabecular bone areas (Guezguez et al., 2013).

The HSC pool is composed of long-term HSCs, which are quiescent but that have extensive self-renewal capacity, and that are hierarchical precursors to short-term HSCs

(Weissman et al., 2001). Short-term HSCs are capable of reconstitution, but have a limited self-renewal capacity in comparison to long-term HSCs (Morrison and Weissman, 1994). Mouse HSCs are found in the $Lin^{-}Sca1^{+}c\text{-}kit^{high}$ fraction (Spangrude et al., 1988, Li and Johnson, 1995). The SLAM markers, including CD150, have been used to characterise HSCs in the mouse, as has CD34 expression, which may be absent from long-term repopulating HSCs (Osawa et al., 1996, Kiel et al., 2005, Jones et al., 1990). Human HSCs are found in both the $CD34^{-}$ and $CD34^{+}$ population (Bhatia et al., 1998, Anjos-Afonso et al., 2013, Nakamura et al., 1999). In a recent report, human $CD34^{-}CD38^{-}CD93^{hi}$ quiescent HSCs, suggested to be a precursor to $CD34^{+}$ HSCs, were able to repopulate immunodeficient mice (Anjos-Afonso et al., 2013). A $Lin^{-}CD34^{+}CD38^{-}CD45RA^{-}Thy1(CD90)^{+}Rho^{lo}CD49f^{+}$ cell surface profile was used to demonstrate transplantable HSC activity at the single cell level from human UCB (Notta et al., 2011). Whether it will be possible to define a unique cell surface phenotype to identify the adult HSC remains to be determined, but to date this has not been achieved.

Functional assays are required to identify and define HSCs. HSCs should be able to reconstitute the blood and immune system over an organism's lifespan. However, more practical functional definitions are required to enable scientific investigation. The ability to reconstitute immunodeficient mice has been frequently used as a functional surrogate test for human HSCs (Dick, 1996, Kamel-Reid and Dick, 1988). The term HSC should only be applied to cells which fulfil the most stringent criteria, that is, high level, long-term serially transplantable reconstitution (Allsopp et al., 2001, Iscove and Nawa, 1997). In reconstitution assays, greater than 1% of lymphoid and myeloid cells and more than 1% of the white blood cells in circulation for a period of greater than 16 weeks is a criteria

frequently adopted, although the stringency of this may be disputed (Miller and Eaves, 1997). Other multilineage haematopoietic cells that do not display this capability may be referred to broadly as haematopoietic progenitor cells (HPCs). Limiting dilution and competitive repopulating assays are often used to assess frequency of HSCs within a population; at a single cell level an HSC should be able to provide long term, transplantable reconstitution (Reya et al., 2003, Szilvassy et al., 1990) *In vitro*, the colony forming unit (CFU) assay has frequently been used to assess differentiation potential (Broxmeyer, 1984). This assay however only assesses myeloid potential and is therefore a limited readout that is inappropriate with which to assign HSC identity. Co-culture with stromal cells is a longer term method by which haematopoietic potential has been assayed *in vitro*, however simultaneous B and T cell readouts have been difficult to achieve (Whitlock et al., 1984).

1.1.2 Haematopoietic ontogeny

1.1.2.1 Stages of haematopoiesis

1.1.1.1.1 Overview

Embryonic haematopoiesis is a multistage process that ultimately results in the production of HSCs which persist throughout adult life. The temporal and spatial characteristics of multiple waves of haematopoiesis are still being addressed. It is generally accepted that there are three stages of haematopoiesis, first the production of embryonic red blood cells and macrophages, second the generation of a fetal multilineage progenitor with restricted capabilities and third the formation of the pre-

HSC/ HSC (Cumano and Godin, 2007, Medvinsky et al., 2011). The first stage is often referred to as 'primitive haematopoiesis' and the latter two stages, where lymphoid progeny is observed in addition to myelo-erythroid potential, as 'definitive haematopoiesis'. Additional complexity arises due to the establishment of the circulation at the onset of the heart beat at E8.25 (embryonic day 8.25) in mouse and around day 22 of gestation in humans, whereupon anatomically separate cellular compartments are mixed together into a heterogeneous milieu (Cumano et al., 1996, Tavian et al., 1999, de Vries P.A 1962).

The genetic programmes that underlie primitive and definitive haematopoiesis, whilst displaying clear commonalities, also appear to differ, as investigated in the mouse. Runx-1, a transcription factor which is known to be absolutely required for HSC generation, is dispensable for the emergence of primitive erythrocytes (Okuda et al., 1996, Cai et al., 2000, North et al., 2002). When assaying for fetal versus adult lymphocyte potential in the mouse, the introduction of Lin28b was sufficient to promote the switch to a fetal phenotype (Yuan et al., 2012). Furthermore, *Sox17* was demonstrated, by conditional deletion, to be essential for the maintenance of fetal and neonatal 'HSCs' but not for adult HSCs (Kim et al., 2007). These observations suggest key differences, and some possible independence, between the development of embryonic/fetal blood cells in relation to the adult HSC.

1.1.1.1.2 Anatomical location

The site of haematopoiesis changes throughout embryogenesis (Figure 2). The first blood cells in both mouse and human are observed in the extra-embryonic yolk sac (YS) on E7-7.5 in the mouse and as early as day 18.5 or even day 16 of human embryonic

development (although the scarcity of human embryos available from this time in gestation is limiting) (reviewed in (Palis and Yoder, 2001)). YS cells arise in sites termed 'blood islands' which feature an outer layer of endothelium and interior erythroblasts (Tavian et al., 1999, Bloom W., 1940, Kelemen, 1979). The other major primary site of haematopoiesis is an intra-embryonic region, the aorta-gonad-mesonephros (AGM), which develops from the para- aortic splanchnopleura (P-Sp) (Medvinsky and Dzierzak, 1996, Taylor et al., 2010, Ivanovs et al., 2011).

Whether definitive blood cells and/or HSCs arise in the YS or AGM has long been discussed. Early experiments employed quail-chick chimaeras and convincingly demonstrated the intra- embryonic location of definitive HSCs (Dieterlen-Lievre, 1975, Le Douarin and Jotereau, 1975). Within the developing mouse embryo, HSC activity has been observed arising in the dorsal aorta at E10-10.5 (Medvinsky and Dzierzak, 1996). Expansion of the HSC pool occurs thereafter following migration to the fetal liver, which functions as a secondary site of haematopoiesis. HSCs in the human appear between days 30-35, again in the AGM (Ivanovs et al., 2011, Oberlin et al., 2002). There is of course a possibility that emerging HSCs actually have their true origins in the YS and have subsequently migrated in the circulation and matured to a detectable stage within the AGM. To this end, in an experiment where YS cells were labelled prior to the onset of circulation, progeny could be detected in the adult bone marrow (Samokhvalov et al., 2007). Another possible interpretation of these data, however, is that YS-derived haematopoietic cells generated independently from the HSC also home to the bone marrow. Evidence against a YS origin of HSCs comes from studies in *Xenopus* where primitive and definitive haematopoietic cells originate from distinct blastomeres (Ciau-

Uitz et al., 2000). However, no such compelling evidence has been described in mammalian systems.

In addition to the YS and AGM, the placenta appears to function as both a source and niche for haematopoietic cells, with the first cells being detected in the E8-9 mouse embryo (Alvarez-Silva et al., 2003). Then, concurrently with the AGM, HSCs are observed at E10.5-11.5 (Ottersbach and Dzierzak, 2005, Gekas et al., 2005). Furthermore, in the absence of the circulation, intra-aortic clusters can still be observed, suggesting *de novo* production although HSC potential was not demonstrated (Alvarez-Silva et al., 2003, Gekas et al., 2005). Additionally, intra-aortic clusters can also be observed in the umbilical and vitelline vessels, which represent additional possible sites of HSC production (de Bruijn et al., 2000, Mizuochi et al., 2012). Recent evidence has supported a role for these extra-embryonic vessels as an autonomous site for HSC generation (Gordon-Keylock et al., 2013). Following expansion of the HSC pool in the fetal liver, the thymus (at E11), spleen (E12), and bone marrow (E16) and are then seeded (Dzierzak and Speck, 2008). The bone marrow, spleen and thymus then retain haematopoietic activity throughout adult life, with the bone marrow as the primary site of adult haematopoiesis in mouse and human.

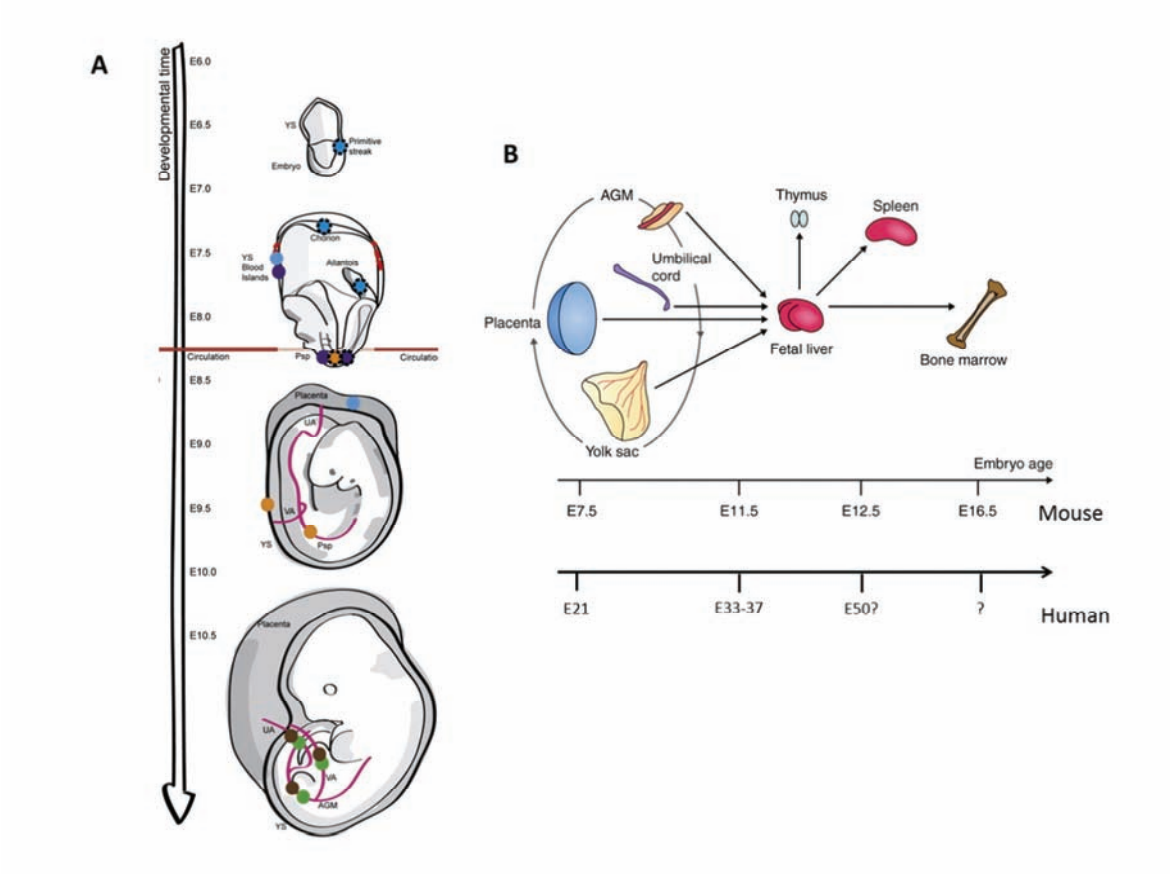

Figure 2 Timing and anatomical location of emerging haematopoietic cells during ontogeny. During haematopoietic development multiple anatomical regions of the developing mouse embryo are involved. Initially, at E7-7.5 blood cells can be detected in the extra-embryonic yolk sac, termed the primitive wave of haematopoiesis. Circulation is then established between E8-8.5 with the onset of the heartbeat. Between E10.5 and E11.5 the intra-embryonic AGM functions as a site of haematopoietic origin, generating the first HSCs. Blood cells can also be detected in the placenta and extra-embryonic vessels. The emerging HSC pool then migrates to the fetal liver where expansion occurs before cells seed the bone marrow, spleen and thymus. Timings of haematopoietic development in the human embryo are less well defined. Blood cells may be detected as early as day 16 of embryonic development, with the generation of HSCs in the AGM thought to occur around day 30. (A) Image taken from Stem cell research (Boisset and Robin, 2012). (B) Image taken and adapted from Development (Medvinsky et al., 2011).

1.1.1.1.3 The development of lymphoid potential

A pan- myeloid progenitor cell, that precedes the HSC, has been detected in the mouse YS at E8.25 and E9 AGM (Ferkowicz et al., 2003, Rampon and Huber, 2003, Palis et al., 1999). Lymphoid potential however, was initially associated with HSC activity. Indeed, when lymphopoietic potential was probed prior to the establishment of circulation in the mouse embryo, neither B cell potential nor Rag-1^{+} cells (a lymphocyte-specific protein) could be detected (Nishikawa et al., 1998b, Yokota et al., 2006). However, lymphoid cells can be detected earlier than E10.5. Multilineage potential and secondary reconstitution capacity was observed in E9.0 YS and fetal liver (Yoder et al., 1997a, Yoder et al., 1997b, Yoder and Hiatt, 1997). This capacity was only revealed when cells were introduced into a neonatal recipient (Yoder et al., 1997b, Yoder et al., 1997a, Yoder and Hiatt, 1997). One possible interpretation of this finding is that the YS-derived multilineage cells possess HSC activity but that, for this potential to be realised, the appropriate microenvironment is required. Alternatively, it is possible that, whilst this population can reconstitute the neonate, the cells are intrinsically different from the bulk of HSCs found in the adult bone marrow. In these experiments, YS cells were isolated following the establishment of circulation, although during this time window the flow of cells within the blood conduits appeared to be limited (McGrath et al., 2003). More recently, a ncx1 (-/-) mouse model, which is unable to establish a heartbeat, was used to demonstrate that B lymphoid potential can be found in the YS at E9 and, therefore, must be generated independently of the HSC (Yoshimoto et al., 2011).

1.1.2.2 Insights into the similarities and differences between differentiated haematopoietic cell types of HSC and non-HSC origins.

1.1.1.1.4 Overview

How the blood cell types generated that are HSC-derived and those that are not HSC progeny differ is an interesting question. The majority of observations, and those described in this section, have been made in the mouse. It is well known that primitive erythrocytes do not initially undergo enucleation and that they predominantly express embryonic globins (Ingram, 1972). However, enucleation does occur in this population around E12.5-16.5, (Kingsley et al., 2004, Fraser et al., 2007). Additionally, globin switching appears to be, at least partially, dependent upon the environment (Kingsley et al., 2004, Fraser et al., 2007). There is evidence to suggest that primitive macrophages differ from their HSC- derived namesake by the lack of peroxidase activity, reduction in lysozyme enzymes and absence of a monocyte precursor (Shepard and Zon, 2000). A genetic requirement for expression of the transcription factors Myb and PU.1 has also been used to separate macrophage development from YS progenitors and HSCs. YS macrophages arise independently of Myb, which is necessary for HSC generation (Schulz et al., 2012, Mucenski et al., 1991). Conversely, PU.1 was required for the generation of macrophages subsets but not HSCs (Dakic et al., 2005, DeKoter et al., 1998). In the human, there is evidence that fetal and adult stages of development yield distinct T cell populations, with a prevalence for immune tolerance amongst the fetal T cell pool (Mold et al., 2010, Havran and Allison, 1988). Key differences between B cell populations associated with fetal and adult haematopoiesis are discussed below.

1.1.1.1.5 B-1 v B-2 B cells

In the mouse, phenotypic, functional and developmental differences support the concept of distinct B lymphocyte populations termed B-1 and B-2 B cells. The predominant B cell population in the adult constitutes a key part of the adaptive immune response and are termed B-2 B cells, while the remainder of the B cell pool is made up of B-1 and Marginal Zone (MZ) B cells (Kantor, 1991a, MacLennan, 1982). In comparison to B-2 B cells, B-1 B cells arise earlier during ontogeny, are a component of the innate immune system and are found predominantly in restricted anatomical locations. Furthermore, B-1 B cells secrete antibodies without the requirement for T cell help (reviewed in (Hardy, 2006)). This B cell subset is also thought to extensively self-renew and is responsible for the majority of circulating IgM (Hayakawa et al., 1983, Hayakawa et al., 1985, Kantor, 1991b). B-1 B cells were first identified by the expression of CD5 (Hayakawa et al., 1984). However, it was soon realised that the B-1 B cell population was more diverse and could be further segmented into $CD5^+$ B-1a and $CD5^-$ B-1b cells (Kantor et al., 1992). The cellular origin of murine B-1 B cells is still very much in question. Adult mouse bone marrow was demonstrated to contain a $CD45R^{neg/low}CD19^+$ population, atypical for B cell development where the expression of CD45R usually precedes CD19 (Montecino-Rodriguez et al., 2006). $CD45R^{neg/low}CD19^+$ cells differentiated to produce B-1, but not B-2, B cells suggesting the presence of distinct progenitors (Montecino-Rodriguez et al., 2006). Studies in mice unable to establish a heartbeat demonstrated an HSC-autonomous production of B-1 B cells from haemogenic endothelium in the yolk sac (Yoshimoto et al., 2011). Further evidence has come from experiments with sort purified $Lin^-CD34^-c\text{-}kit^+Sca\text{-}1^+CD150^+$ HSCs from adult mouse bone marrow which revealed the inability of this population to produce B-1a B cells (Ghosn et al., 2012, Ghosn et al., 2011). Additionally,

B-1a B cells could be observed at E8.5, prior to HSC generation, in the splanchnopleura (Godin et al., 1993). These and other findings indicate a B-1 B cell origin that preceeds HSCs (Kantor et al., 1992). Further support for distinct B cell populations in development came from a comparison of pro-B cells isolated from mouse E16 fetal liver and adult bone marrow (Hardy and Hayakawa, 1991). Fetal cells had a greater propensity to express CD5 and were less able to generate IgG *in vivo* (Hardy and Hayakawa, 1991).

Numerous human pathologies have been postulated to have a link to B-1 B cells, including acute lymphocytic leukaemia (ALL) and a number of autoimmune diseases such as systemic lupus (Freedman et al., 1987, Caligaris-Cappio, 1996). However, human B-1 B cells have only recently been reported (Griffin et al., 2011). Rothstein and colleagues described a population of B cells with a $CD20^{+}CD43^{+}CD27^{+}$ cell surface profile in umbilical cord blood (UCB) and peripheral blood (PB), identified based upon distinct functional characteristics applied from studies in the mouse (Griffin et al., 2011). Functional criteria included, the capacity to secrete IgM in the absence of BCR stimuli, tonic intracellular signalling and the ability to stimulate T cells (Griffin et al., 2011). This description of human B-1 B cells has been met with controversy (Reynaud and Weill, 2012, Perez-Andres et al., 2011). Covens *et.al.*, characterised the $CD20^{+}CD43^{+}CD27^{+}$ population as pre-plasmablast cells (Covens et al., 2013). Much remains to be determined about the presence of analogous cells to mouse B-1 B cells in humans.

1.1.2.3 Critical signalling molecules and transcription factors in developmental haematopoiesis

Some of the key transcription factors involved in haematopoiesis include SCL, GATA family members, LMO2, c-MYB and Runx-1. SCL gene knock-out results in the complete absence of blood cells with embryonic lethality at E9.5 (Robb et al., 1995). Furthermore, mouse ES cells null for SCL are unable to form blast-colonies, but do form primitive erythrocytes and macrophages, suggesting a genetic basis for the segregation of primitive from definitive haematopoiesis (Robertson et al., 2000). Similarly, the study of c-myb in mouse and zebrafish embryos suggest that the requirement for this transcription factor can be used to distinguish primitive from definitive haematopoiesis, the latter process being abrogated in the absence of c-myb (Sumner et al., 2000, Soza-Ried et al., 2010). GATA-2 knockout is embryonically lethal at E10.5 (Tsai et al., 1994a). Both *in vivo* and *in vitro* ES cell models of GATA-2 deficiency demonstrated a large reduction, but not an absence, of primitive erythrocytes and cells of both the myeloid and lymphoid lineages (Tsai et al., 1994a, Tsai and Orkin, 1997). Recently, analysis of transcription factor expression at the single cell level in the adult mouse, revealed a role for GATA-2 in the modulation of GF1 and GF1β antagonism, as well as in the inhibition of lymphopoiesis (Moignard et al., 2013) The pivotal role of Runx-1 will be discussed in the context of the endothelial-to-haematopoietic transition below (1.1.1.1.6).

Whilst cell intrinsic mechanisms clearly have an integral, if difficult to assay, role in determining cell fate, cell extrinsic stimuli in the form of cell signalling molecules are key for the specification of the developing embryo. The blood system, and cell types such endothelium, cardiac muscle, skeletal muscle, bone and mesenchyme, are all of

mesodermal origin. Factors required for the specification of the anterior primitive streak to mesoderm in mouse embryo or ES cell cultures, include Activin A (AA) , a member of the TGF-β superfamily, in addition to Bone Morphogenetic Protein 4 (BMP-4), Wnt3a and Basic Fibroblastic Growth Factor (bFGF) (Gadue et al., 2005, Gadue et al., 2006, Tada et al., 2005, Nostro et al., 2008).

1.1.2.4 Cellular origins of the haematopoietic system

1.1.1.1.6 Haemogenic endothelium

The observation that haematopoietic and endothelial cells are closely associated in blood islands of the developing chick embryo gave rise to the proposal that these cell types share a common origin and potentially a common precursor (Murray, 1932, Peault et al., 1988, Sabin, 1920). Further support for this close association came from the commonality of genes expressed between cells of these lineages and the lack of both cell types in mice deficient in VEGFR2 (Fina et al., 1990, Kabrun et al., 1997, Murray, 1932, Sabin, 1920, Shalaby et al., 1995, Young et al., 1995). Two alternative theories emerged in relation to the cellular origins of the haematopoietic system, that of the haemangioblast and of haemogenic endothelium (Figure 3). Haemogenic endothelium (HE) describes a cell with endothelial characteristics that is capable of giving rise to haematopoietic progeny. Labelling experiments used ac-LDL (acetylated low-density lipoprotein), that specifically marks endothelium and macrophages, to probe the existence of haemogenic endothelium in the chick. Ac-LDL was introduced into the chick embryo prior to the emergence of haematopoietic cells, and was subsequently found to label both the endothelium and emerging $CD45^+$ cells in intra-aortic clusters (Jaffredo et al., 1998). More recently, the use of live cell imaging has provided convincing evidence of HE, both *in vitro*

and *in vivo* by allowing direct and continuous visualisation of single cells (Boisset et al., 2010, Eilken et al., 2009, Bertrand et al., 2010, Kissa and Herbomel, 2010). Eilken *et al.* skilfully exploited continuous live cell imaging of differentiating murine ES cells on OP9 stroma. In the ES cell/OP9 co-culture, haematopoietic cells could be observed budding off cells that were characteristically endothelial (Eilken et al., 2009). *In vivo* studies in both the mouse and zebrafish visualised the budding of haematopoietic cells from the endothelial cell wall of the dorsal aorta via a process subsequently termed 'endothelial haematopoietic transition' (EHT) (Bertrand et al., 2010, Boisset et al., 2010, Kissa and Herbomel, 2010). Unlike asymmetric cell division, EHT describes a conversion of cell states where endothelial- like cells assume the characteristics of a haematopoietic cell.

The origin of haemogenic endothelium, which is found in the ventral aspect of the dorsal aorta, has been probed. Elegant studies in the chick embryo demonstrated autonomous production of an endothelial pool possessing haematopoietic potential from splanchopleural progenitors and an endothelial population lacking this potential which was of somite origin (Pardanaud et al., 1996). Indeed, splanchopleural- derived endothelial cells which co-exist in the wall of the dorsal aorta with somite-derived endothelial cells are eventually completely replaced by the somite-derived equivalents (Pouget et al., 2006). Whether HE has a distinct origin from the remainder of the dorsal aorta endothelium in the mouse and higher organisms remains to be determined.

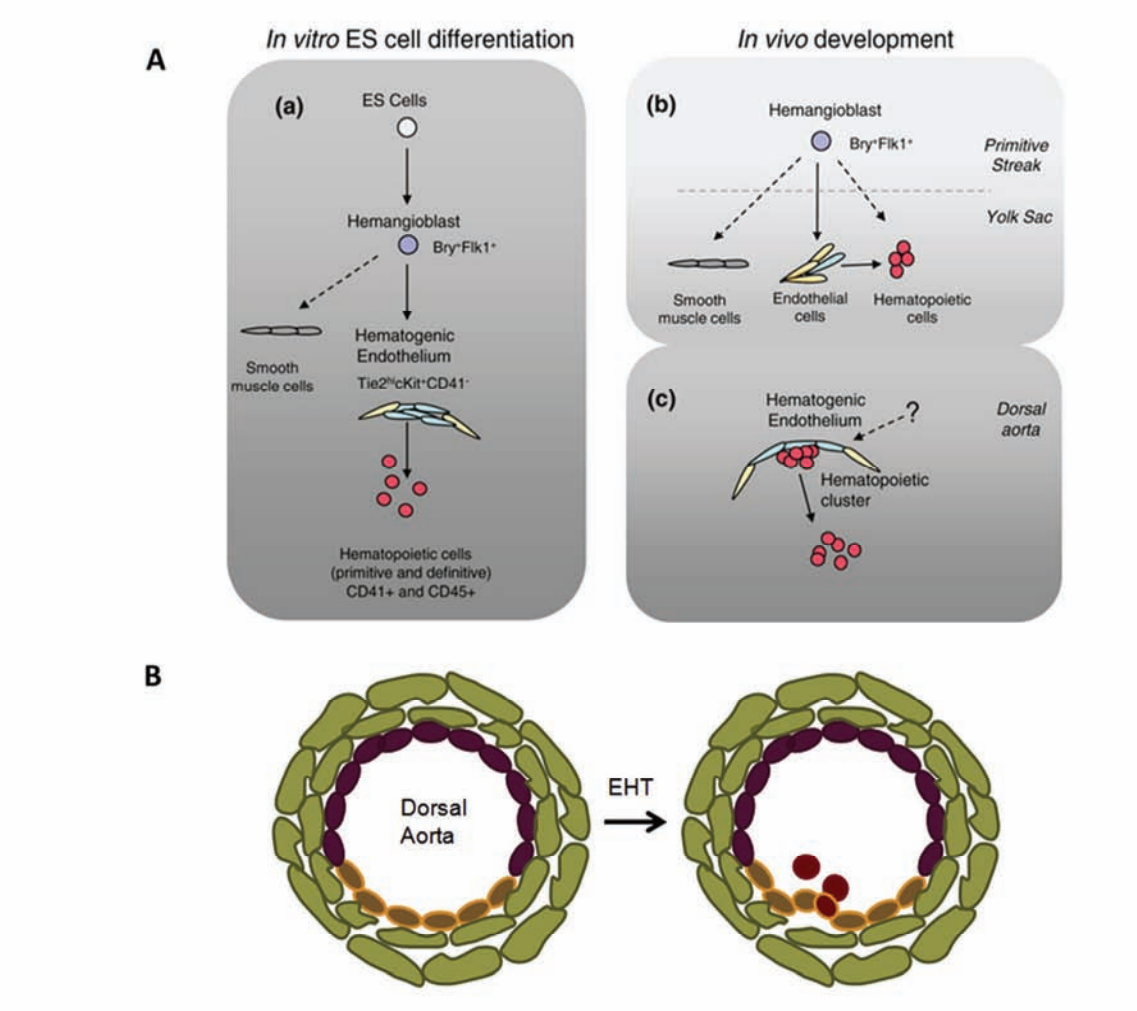

Figure 3 Models of blood development from the haemangioblast and haemogenic endothelium. (A) ES and iPS cells have frequently been used to model haematopoietic development. The generation of haemogenic endothelium (HE) from ES cells and subsequent differentiation to yield blood cells has been demonstrated with continuous time-lapse microscopy. Evidence supporting a haemangioblastic origin of ES- HE has also been described. In the developing mouse embryo, HE cells lining the dorsal aorta were demonstrated to bud off into the lumen and express haematopoietic markers. The presence of the haemangioblast in the developing yolk sac (YS) has been postulated. Additionally, haematopoietic potential of YS-derived endothelium/HE has also been described. The haemangioblast was originally described as a bipotent haematopoietic-endothelial progenitor. Whether this precursor can also form smooth muscle cells remains to be determined. (B) The endothelium of the dorsal aorta is of dual origin. The cells that line the ventral wall have haemogenic potential and can undergo EHT (endothelial to haematopoietic transition) to form budding haematopoietic cells, frequently visualised as intra-aortic clusters. (A) Image taken from BMC Biology (Gordon-Keylock and Medvinsky, 2011). (B) Image taken from The international journal of biochemistry and cell biology (Marks-Bluth and Pimanda, 2012).

Whilst direct evidence for the generation of haematopoietic cells from endothelium of the dorsal aorta has been provided from both mouse and zebrafish models, the identity and potential of these haematopoietic cells has not been assessed (Bertrand et al., 2010, Boisset et al., 2010, Kissa and Herbomel, 2010). Whether HSCs are generated via a HE intermediate is an additional question for the field to address. Interestingly, in the mouse embryo, HSCs and erythro-myeloid progenitors were demonstrated to be derived from distinct endothelial populations (Chen et al., 2011). In the model described by Chen *et al.*, the expression of CBFβ (a required Runx-1 core DNA binding factor) was placed under the control of Tek-1 and Ly6a. Tek-1 and Ly6a positive endothelial cells displayed different haematopoietic potential, thus suggesting the presence of at least two 'types' of HE (Chen et al., 2011). Distinct populations of HE were identified in a human ES cell system. Erythroid/megakaryocyte potential was observed first in an endothelial-like population before pan-myeloid potential could be detected. Lymphoid output could not be identified (Rafii et al., 2013).

At the transcript level, and therefore typically at the expense of continued cell growth, HE cells can be identified from amongst non-haemogenic endothelium by the increased expression of haematopoietic-associated genes, such as Runx-1 (North et al., 1999). However, the ability to separate HE from non-haemogenic endothelium based on cell surface marker expression would accelerate progress within the field. A unique cell surface marker to select endothelial cells and exclude other populations, such as haematopoietic and stromal cells, has not been identified. CD144 is an adhesion molecule that is expressed at cell junctions in endothelium and in a population of emerging haematopoietic cells (Figure 4) (Kim et al., 2005, Taoudi et al., 2008). *In vivo*, emerging

haematopoietic cells have been observed to express CD45 and CD41 (Taoudi et al., 2008, Ferkowicz et al., 2003, Robin et al., 2011). In pluripotent stem cell/OP9 co-culture models of haematopoietic differentiation, CD43 has been described as the first haematopoietic marker expressed (Vodyanik et al., 2006). Once a cell has begun to express CD41, CD43 or CD45 (or other haematopoietic lineage markers) it has committed to the haematopoietic lineage. It therefore can be hypothesised that the expression of CD144 in the absence of haematopoietic marker expression can be used to identify an endothelial cell. This designation however would include all endothelial cells and is therefore not a criterion for the specific identification of HE. To this end, Slukvin and colleagues characterised HE cells within PSC cultures as $CD144^{+}CD73^{-}CD43^{-}CD235a^{-}$; a cell surface phenotype that distinguishes HE from endothelium which expressed CD73 (Choi et al., 2012). This $CD144^{+}CD73^{-}CD43^{-}CD235a^{-}$ population expressed CD146, ESAM, CD31 and CD201, was capable of Ac-LDL uptake, displayed an endothelial morphology and formed tubules in the matrigel assay (Choi et al., 2012). The transient presence of $CD144^{+}CD45^{+}$ cells during development is of interest as this phenotype may identify haematopoietic cells that have recently emerged via EHT. Indeed, HSCs arising in the AGM are positive for these markers (Taoudi et al., 2008). HSCs which subsequently home to the fetal liver can also be identified within the $CD144^{+}$ pool at E13.5 in the mouse and around week 7/8 in the human before CD144 expression is downregulated (Kim et al., 2005, Oberlin et al., 2010b).

An understanding of the factors involved in the EHT transition could result in the ability to control the fate of HE. HoxA3 was identified to be such a factor, which suppressed the expression of Runx-1 and therefore inhibited EHT (Iacovino et al., 2011). The pivotal role of Runx-1 in enabling EHT is evident in zebrafish embryos. Runx-1 deficient embryos

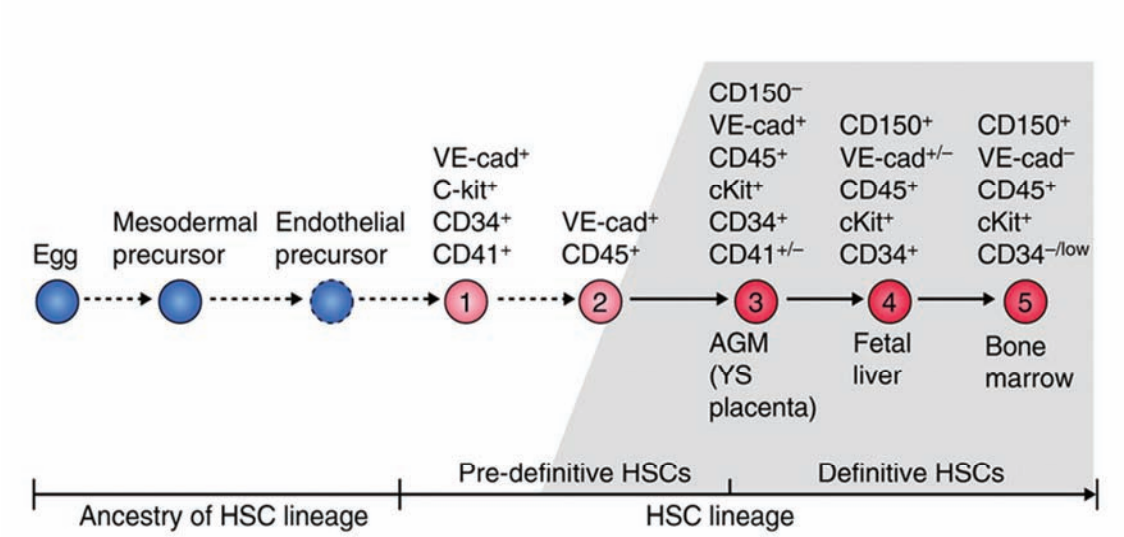

Figure 4 Model of cell marker expression in the emerging mouse HSC population.
Definitive HSCs arise from a VE-cadherin/CD144^{+}CD45^{+} population in the AGM, with cells also present in the YS and placenta. HSCs then transit to the fetal liver where CD150 is upregulated and expansion of the population occurs. HSCs in the bone marrow downregulate VE-cad/CD144. Stages leading up to the generation of VE-cadherin/CD144^{+}CD45^{+} are less well described, as represented by dotted arrows. Evidence of a VE-cadherin/CD144^{+}CD41^{+} haematopoietic precursor to the VE-cad/CD144^{+}CD45^{+} has been described in the AGM (VE-cad= VE-cadherin/CD144). Image taken from Development (Medvinsky et al., 2011).

displayed rare transition events that appeared to result in cell death (Kissa and Herbomel, 2010). A similar requirement for Runx-1 is evident in the developing mouse embryo (Chen et al., 2009). Sox-17 also appears to play a role in developing HE (Nakajima-Takagi et al., 2013, Clarke et al., 2013). In human PSC cultures, Sox17 expression was observed at a high level in $CD34^{+}CD43^{-}$ but not $CD34^{+}CD43^{+}$ cells (Nakajima-Takagi et al., 2013). In mouse ES cells, Sox17 expression distinguished endothelium with haemogenic potential from non-haemogenic endothelium. Moreover, Sox17 expression was observed in the dorsal aortic endothelium and intra-aortic clusters of E11.5 mouse embryos, where $Sox17^{+}$ haematopoietic cells were demonstrated to have multilineage reconstitution potential (Clarke et al., 2013). Furthermore, Sox17 null embryos lack $CD144^{+}CD45^{+}$ cells and are embryonically lethal at E13.5 (Clarke et al., 2013).

1.1.1.1.7 The haemangioblast

The haemangioblast is a bipotent progenitor cell with the capacity to generate both endothelium and haematopoietic progeny. It therefore, differs from HE, which is phenotypically endothelial but has haematopoietic potential. The bipotent haemangioblast-like population has been referred to as the 'blast colony- forming cell' (Choi et al., 1998, Huber et al., 2004, Zambidis et al., 2008, Kennedy et al., 2007). Seminal work has described the transient production of $CD34^{+}Flk\text{-}1^{+}CD144^{+}$ cells within day 3-3.5 mouse ES cell differentiation cultures, which gave rise to both endothelium and haematopoietic cells (Choi et al., 1998). A possible link between the haemangioblast and HE cells has been demonstrated in a mouse ES differentiation system, the haemangioblast gave rise to HE prior to the generation of haematopoietic cells (Lancrin et

al., 2009). Whether an haemangioblast cell can give rise to 'true'/non-HE endothelium remains to be determined.

1.1.2 Lymphopoiesis from HSCs

1.1.2.5 Overview

Lymphocytes can be divided into three main subsets:- T, B and innate lymphoid cells. The classical description of the haematopoietic lineage tree, shows an early split where a cell initially becomes myeloid-restricted, as a common myeloid progenitor (CMP), or lymphoid-restricted, as a common lymphoid progenitor (CLP) (Figure 5) (Kondo et al., 1997, Akashi et al., 2000). In this classical model, the CLP therefore is capable of generating T, B and NK cells in the appropriate conditions, but lacks the potential to produce red blood cells, platelets and other myeloid cell subsets. Whilst this description might provide a general overview with regard to the most common lineage choices in the adult blood system, a number of observations have challenged this hierarchical structure. Moreover, evidence for the classical model of haematopoietic differentiation has primarily and extensively been gained from studies in the mouse.

Cellular identity is typically designated based on the cell surface expression of a cohort of 'markers'. However, a number of disparities between human and mouse cells are clearly evident which adds further complexity to the concept of lineage restriction across the differentiating haematopoietic compartment. An additional consideration regarding the accuracy of haematopoietic lineage trees relates to the *in vitro* experimental settings

which may not recapitulate biologically relevant environments, and therefore may represent wholly artificial differentiation potentials (Richie Ehrlich et al., 2011).

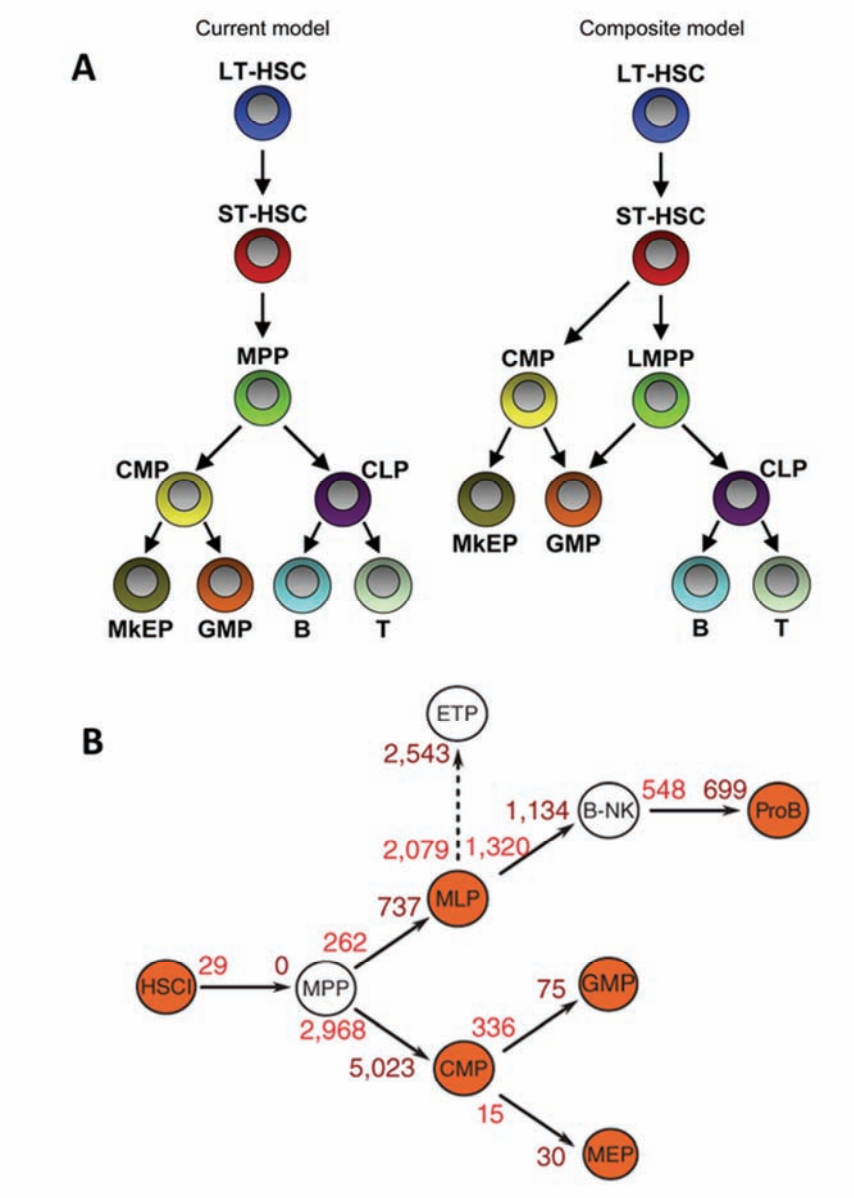

Figure 5 Alternative models of the differentiation hierarchy from the haematopoietic stem cell. (A) The original and classical/common model describes the segregation of lymphoid and myeloid potential following the first restriction. The CLP (common lymphoid progenitor) can then only generate lymphoid cells such as T and B cells, while the CMP (common myeloid potential) is limited to the production of myeloid progeny such as the megakaryocyte-erythroid progenitor (MkEP). More recent alternative models have emerged such as that describing the LMPP, the lymphoid-primed multipotent progenitor. Here, loss of myeloid potential occurs after the loss of lymphoid potential. Additionally, there are multiple different routes to generate the same cell type. B) An alternative method to characterise the haematopoietic hierarchy was adopted where differences in transcript expression, described as 'distances' between purified populations were compared. This revealed smaller, gradual changes in lymphoid commitment in comparison to myeloid commitment. (A) Image taken from Cell (Adolfsson et al., 2005) (B) Image taken from Nature Immunology (Laurenti et al., 2013a).

There is evidence from studies of human cells that the earliest restriction does not separate lymphoid from myeloid lineages but rather that lymphoid potential is lost in myeloid committed cells (Doulatov et al., 2010). Contrastingly, in this model, myeloid potential is retained in progenitors which give rise to lymphoid cells (Doulatov et al., 2010). Additionally, thymic-seeding progenitors with lymphoid and granulocyte-monocyte potential but lacking granulocyte-erythroid potential have been described in the neonatal mouse (Luc et al., 2012), The concept of 'lymphoid priming' has also been suggested, where the promiscuous expression of lymphoid-related genes can be detected in the absence of lineage commitment (Adolfsson et al., 2005, Kohn et al., 2012, Luc et al., 2008). The concept that a subset of HSCs might be lymphoid-biased has also been proposed (Benz et al., 2012, Challen et al., 2010). This may support the observation of decreasing lymphoid potential with age if a distinct population of HSCs is primarily responsible for this potential. An interesting approach was adopted by Dick and colleagues who compared the transcriptional profile of purified haematopoietic subsets. Pair-wise comparisons of differentially expressed genes overlaid onto the traditional haematopoietic hierarchy revealed that the differences between the CMP and HSC were greater than the differences between the MLP (multi-lymphoid progenitor) and HSC (Laurenti et al., 2013b). Therefore, the commitment to the lymphoid lineage is more gradual than commitment to generate myeloid progeny (Laurenti et al., 2013b). The overall emerging picture is that lineage restriction is highly plastic and that the path to mature blood cells could potentially be more variable than first thought.

Notably, this hierarchy has been constructed to represent haematopoietic differentiation from the adult HSC which resides in the bone marrow. In the developing haematopoietic

system, that precedes the large-scale production of blood cells from HSCs, it is possible that mature blood cells develop within a shorter timescale, possibly from a multipotent progenitor but with many fewer intermediate steps. Indeed, fetal macrophages are thought to be generated in the absence of a monocyte intermediate (Shepard and Zon, 2000). Moreover, a bipotent macrophage-B cell progenitor was first described in murine fetal liver (and subsequently in adult bone marrow) suggesting a much closer association between cells thought to be of distinct lineages (Cumano et al., 1992, Montecino-Rodriguez et al., 2001).

1.1.2.6 B cell development from HSCs

1.1.2.1.1 Staging of B cell differentiation

B cells are lymphocytes that are exclusively capable of secreting antibodies. They play a key role in the immune response by binding to antigens and activating multiple effector mechanisms (Roitt et al., 1969). B cells differentiate from HSCs in the post-natal bone marrow, where a number of defined stages have been characterised in the mouse based upon the expression of cell surface markers and the extent of rearrangement at the IgH locus. Following on from the CLP stage, cells committed to the B cell lineage transit through pre-pro-B, pro-B, pre-B, immature B and mature B cell stages (Figure 6) (reviewed in (Hardy and Hayakawa, 2001)) and (Hardy et al., 1991). In both mouse and human, B cells can be specifically identified with the exclusion of all other cells based on CD19 positivity which is first expressed at the pro-B cell stage. B220, a CD45 isoform, the expression of which typically precedes CD19, is also used to classify murine B cells, although it is not strictly B-cell specific (Renno et al., 1996). Differentiation from the HSC to the immature B cell stage occurs in the bone marrow, whereupon B cells transit to the

spleen and periphery to undergo further maturation (reviewed (Hardy and Hayakawa, 2001)).

1.1.2.1.2 VDJ recombination in B cell development

1.1.2.1.2.1 VDJ recombination in HSC-derived B cells

VDJ recombination is a process of DNA rearrangement, specific to lymphocytes, that generates the diversity of the B cell receptor (BCR) and T cell receptor (TCR). This process therefore is required for the specificity of interaction with a vast variety of antigens, an integral component of the immune response (reviewed in (Gellert, 2002, Jung and Alt, 2004). The BCR, a cell surface bound immunoglobulin, is composed of heavy and light chains, which contain constant and variable regions (reviewed in (Jung and Alt, 2004, Gellert, 2002)). The constant region is found at one end of the molecule and, in the secreted form of an antibody, can be recognised by effector cells of the immune system. The variable portion of the immunoglobulin contains a region of hypervariability that is produced when gene segments from the V (variable), D (diversity) and J (joining) clusters are brought together by DNA rearrangement (Figure 7) (Early et al., 1980). Additional diversity from N-additions, a limited number of randomly selected nucleotides, at the recombination sites is also observed (Tonegawa, 1983). In humans, the IgH gene locus, encoding the heavy chain, is found on chromosome 14, with the light chain encoded by regions on chromosome 22 and 2, IgL (lamba) and IgK (kappa) respectively (Croce et al., 1979, McBride et al., 1982). Recombination at the heavy chain locus begins when one of 27 D segments is brought alongside one of 9 J segments, during differentiation to form the pro-B cell (Lefranc, 2001). V-DJ segments are then aligned, using one of the 123-129 V genes, leading to the production of the pre-B cell expressing the pre-BCR (Lefranc, 2001).

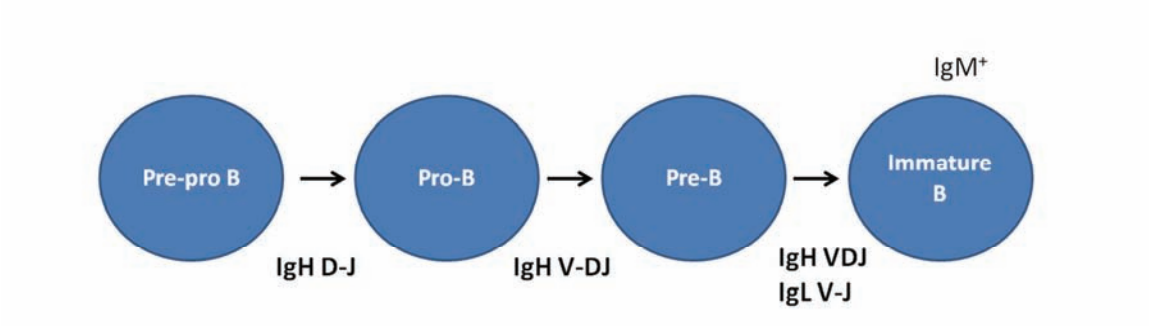

Figure 6 Stages of B cell development.
B cell development from the CLP occurs via a number of well-defined steps based on the expression of cell surface markers and genes as well as the configuration of heavy and light chain loci. Pre-pro B cells undergo D-J recombination at the heavy chain locus (IgH), forming pro-B cells. V-DJ recombination at the IgH locus then occurs in the formation of pre-B cells with express the pre-BCR. The light chains (IgL) then undergo V-J recombination which enables to expression of the BCR (B cell receptor), initially as the IgM isotype and the immature B cell is formed. Subsequent maturation and isotype switching then occurs when immature B cells leave the bone marrow and migrate to the spleen and periphery.

For a productive, protein-coding VDJ segment, DNA recombination must occur in-frame, so that codon integrity is maintained. Furthermore, N-additions must not introduce stop codons within the exon. It has been estimated that there is a 33% probability of productive recombination (Jung et al., 2006). If this productive recombination does not occur, the second locus has the opportunity for successful rearrangement (Jung et al., 2006). Developing B cells, that unproductively complete VDJ recombination at both loci, undergo apoptosis (Jung et al., 2006). Interestingly, the percentage of in-frame rearrangements appears to differ during ontogeny. When DNA from mouse fetal liver IgM^+ cells was sequenced, around 80% of heavy chain rearrangements were unproductive at E17, but by the time of birth, this had dropped to just 33% (Delassus et al., 1998). It has also been demonstrated that cells generated *in vitro* that have undergone non-productive recombination can be maintained, possibly due to the absence of positive selection (Nourrit et al., 1998). Therefore the exclusion of such populations may be dependent upon the environment and not an intrinsic property of the cell (Nourrit et al., 1998). Following VDJ recombination at the heavy chain locus, the light chain is then assembled. This results in progression to the immature B cell stage and expression of IgM on the cell surface (reviewed in (Gellert, 2002)).

1.1.2.1.2.2 VDJ recombination in B-1 B cells

In addition to anatomical locations, functional readouts and origin, fetal and adult B cells appear to differ with regard to the product of VDJ recombination at the IgH locus. It has been suggested that the preferential usage of V and D segments differs in fetal and adult B cell populations, with more frequent recombination of proximal genes in both D-J and V-(D)J rearrangements during early development (Perlmutter et al., 1985, Jeong and

Teale, 1988, Malynn et al., 1990). Other groups have argued for an increased frequency of specific D and J segment utilisation but that location in the locus is not the driving factor for this bias (Pascual et al., 1993). Additionally, studies using a model of human UCB populations differentiated on S17 stroma, revealed two alternative precursors to pro-B cells, one of which arose earlier in culture and generated far fewer N additions at V-D and D-J junctions than are found in post-natal B cell populations (Sanz et al., 2010). This was attributed to the absence of Terminal Deoxynucleotidyl Transferase (TdT) expression, a finding corroborated by work in the mouse (Sanz et al., 2010, Meek, 1990). Interestingly, artificial addition of N nucleotides in neonatal mice skewed the phosphorylcholine - binding potential of antibodies expressed by this B cell population, a property typically observed within the B-1 B cell population (Benedict and Kearney, 1999).

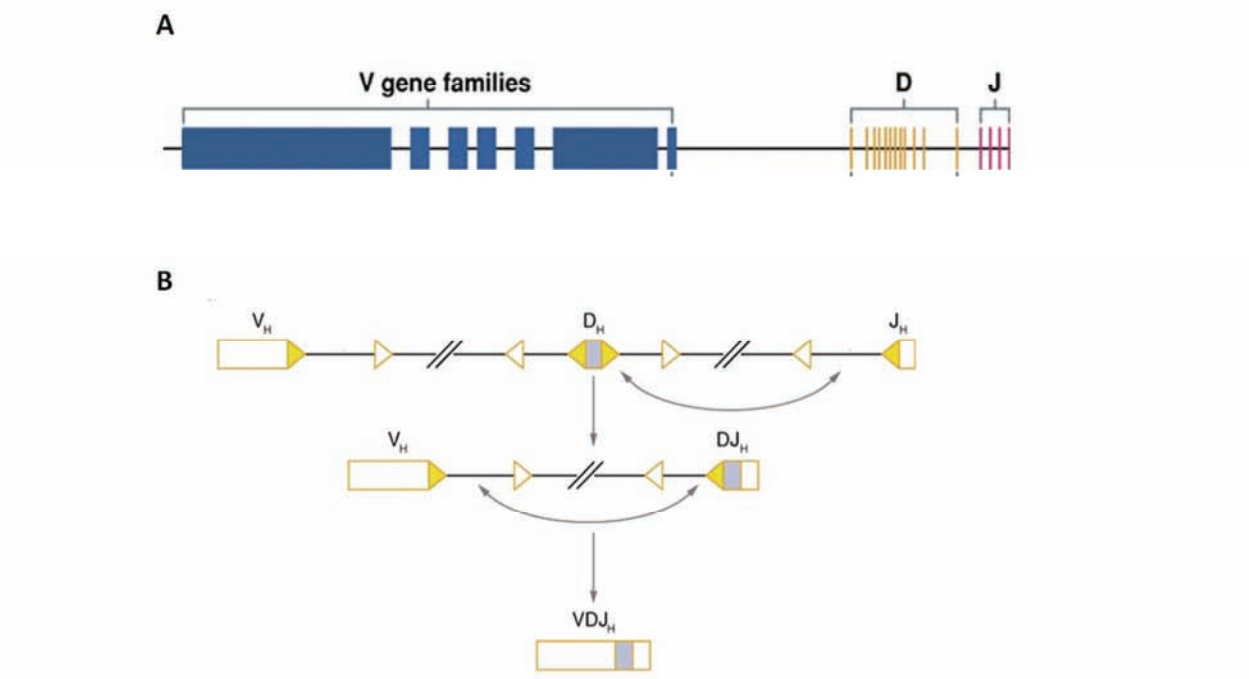

Figure 7 Schematic of VDJ recombination in B lymphocytes.
(A) Numerous V, D and J gene segments exist in the germline configuration of the genome. During B cell development VDJ recombination occurs at heavy (IgH) and light chain loci which results in the production of antigen-specific immunoglobulins. (B) During VDJ recombination, at the IgH locus, a D gene segment is spliced and rearranged next to a J segment, with the elimination of the intervening DNA. V-DJ recombination then occurs, positioning one of the V gene segments next to the DJ fragments. The recombined VDJ segment encodes the CDR3 (complementarity determining region 3), which plays a major role in antibody-antigen specificity. (A) and (B) taken and adapted from Annual Review of Immunology (Jung et al., 2006).

1.1.2.1.3 B cell differentiation in vitro

An *in vitro* system to model B cell lymphopoieisis has a range of utilities. This would enable investigation into the critical requirements for the production of antibody-expressing B cells as well as further our understanding of perturbations found in B cell-related diseases. The first description of mouse B cell maintenance, maturation and possible generation used heterogeneous adherent bone marrow stromal based Dexter-type cultures, termed Whitlock-Witte cultures (Whitlock and Witte, 1982). Mouse stromal cell lines, including S17, OP9 and MS-5 cells, were then established that permitted B cell differentiation from murine haematopoietic progenitors. These cell lines were derived from mouse bone marrow using different genetic strains and culture conditions (Collins and Dorshkind, 1987, Nakano et al., 1994, Itoh et al., 1989, Berardi et al., 1997). Observations have been made that support the need for batch testing of serum that does not promote stromal cell adipogenesis, as adiponectin, a hormone produced by fat cells, was shown to prevent B cell development in a stromal-dependent manner (Yokota et al., 2003).

Human B cell differentiation from haematopoietic progenitors has consistently proven to be more difficult to achieve. Indeed, efforts to establish cultures using human fetal bone marrow as described by Whitlock and Witte proved to be unsuccessful (LeBien, 1989). However, mouse stromal lines, most frequently S17 cells, have been shown to support B cell lymphopoiesis from human UCB $CD34^+$ cells (Sanz et al., 2010, Rawlings et al., 1995a). This human progenitor/S17 differentiation system was inefficient at promoting further development to the IgM^+ immature B cell stage. Therefore, in a two-stage protocol, $CD19^+$ cells were isolated and transferred to mouse fibroblasts transfected with human

CD40L which, in the presence of IL-4 and IL-10, generated a B cell pool with 40% IgM positivity (Fluckiger et al., 1998). The AFT024 mouse stromal cell line, derived from the fetal liver, was also able to support the differentiation of human pro-B cells to IgM^+ and latterly IgD^+ cells over a period of 4 weeks (Barker and Verfaillie, 2000). Human stromal lines have also been used for the expansion of human B cells *in vitro*, albeit typically for a limited period of time without development to the immature B cell stage (Prieyl and LeBien, 1996, Wolf et al., 1991, Moreau et al., 1993).

1.1.2.1.4 Critical transcription factors in B cell development

Transcription factors that have been described to play a role in B cell development include, but are not limited to, Pax5, PU.1, EBF (Early B cell Factor), E2A and Ikaros (Mikkola et al., 2002, Lin and Grosschedl, 1995, Kirstetter et al., 2002, Bain et al., 1994). Pax5 is required to both initiate B cell lineage commitment and prevent lineage promiscuity (Nutt et al., 1999, Mikkola et al., 2002). Macrophage and T cell development has been reported upon conditional inactivation of the Pax5 gene in murine B cells (Nutt et al., 1999, Mikkola et al., 2002). Furthermore, Pax5 controls the expression of CD19, a B cell-specific cell surface molecule involved in regulating signal transduction through the BCR (Kozmik et al., 1992). E2A and EBF, in contrast, are only required in the initial stages of B cell differentiation, during the generation of pro-B cells (Bain et al., 1994, Lin and Grosschedl, 1995). PU.1, a factor that is involved in haematopoietic ontogeny at multiple stages, and as a result is embryonically lethal, may not be required for B cell development (Ye et al., 2005, Scott et al., 1994). However, B cell numbers are reduced following PU.1 knock-out in fetal liver cells (Ye et al., 2005). In the absence of PU.1, a possible skewing of

the B cell repertoire with an increase in B-1 and decrease in B-2 B cells has been described (Ye et al., 2005).

1.1.2.1.5 IL-7 in B cell development

The IL-7 receptor is made up of two subunits, IL-7Rα (CD127) and the common γ chain/IL-2Rγ which form a heterodimer and, to which IL-7 binds (Kondo et al., 1994, Noguchi et al., 1993). Thymic stromal-derived lymphopoietin (TSLP) also signals via IL-7Rα but in conjunction with the TSLP receptor (Park et al., 2000). The common γ chain forms a heterodimer with a multitude of other subunits, thus acting as a receptor for a large family of different cytokines. Perturbations in IL-7 signalling impose severe phenotypes on lymphocyte development. A vast reduction in the thymic and splenic T cell population, to between 0.01-10% of controls, that occurs in the progenitor pool (prior to expression of CD4 or CD8), is observed in IL-7Rα$^{-/-}$ mice. These mice lack any abnormalities in red blood cell or monocyte/granulocyte cell numbers (Peschon et al., 1994). Within the B cell pool, IL-7Rα knockout resulted in a general block of B cell development at the pro-B cell stage, however a limited number of mature B and T cells were observed in the peripheral blood (Peschon et al., 1994). A similar phenotype has been observed with IL-7$^{-/-}$ mice, which characterise with a vast reduction in T and mature B cells (von Freeden-Jeffry et al., 1995). The difference in the severity of lymphopaenia between IL-7$^{-/-}$ and IL-7Rα$^{-/-}$ mice, with the later exhibiting a larger reduction in T and B cell numbers, suggests a potential role for TSLP in lymphocyte generation (von Freeden-Jeffry et al., 1995, Peschon et al., 1994, Vosshenrich et al., 2003).

The role of IL-7 in human B cell lymphopoiesis is less clear. Patients with mutations in the IL-7Rα gene have been diagnosed with T(-)B(+) severe combined immunodeficiency

(SCID), suggesting that IL-7 signalling is not required for the production of functional B cells in humans (Puel et al., 1998). This has been supported by *in vitro* data which described the lack of a significant effect of IL-7 on human fetal bone marrow $CD34^{+}CD19^{-}$ or pro-B cell populations, in the presence of supportive human bone marrow stromal cells (BMSCs) (Prieyl and LeBien, 1996). However, in co-cultures of UCB or bone marrow haematopoietic progenitor cells (HPCs) with MS-5 cells, a greater than 15- fold reduction in $CD19^{+}$ cells was observed upon addition of IL-7 neutralising antibody (Parrish et al., 2009). These data also provide evidence for the reactivity of murine IL-7 with human B cells. When human stromal cells (which produce low to undetectable levels of IL-7) were substituted with MS-5 cells, a 60-fold increase in B cell numbers occurred. In the absence of IL-7, UCB but not BM HPCs generated a small number of Flt3- dependent B cells (Parrish et al., 2009). Developmentally, there may be a changing requirement for IL-7 in B cell development. Fetal-liver derived pro-B cells were able to respond to TSLP unlike adult bone marrow equivalents (Vosshenrich et al., 2003). TSLP could possibly act as a biological substitute to IL-7 during early ontogeny. Interestingly, both fetal and adult B cell lymphopoiesis was completely prevented in Flt-$3^{-/-}$IL-7R$\alpha^{-/-}$ mice (Sitnicka et al., 2003).

The mechanism by which IL-7 functions in the development of a normal B cell pool has proven to be complex. The cytokine appears to have different roles dependent upon the stage of B cell differentiation. At the pro-B cell stage, IL-7 induced proliferation in human populations cultured with MS-5 cells (Johnson et al., 2005). The effect of IL-7 stimulation on pre-B cells is controversial. Cell lines derived from mouse fetal liver were prevented from developing into sIg^{+} cells in the presence of IL-7 (Rolink et al., 1991). B cells derived from a progenitor in adult mouse bone marrow and cultured on S17 stroma, increased

the percentage of IgM^+ cells by over 10-fold in the absence of IL-7 supplementation (Rolink et al., 1991, Montecino-Rodriguez et al., 2001). However, primary cells from the fetal liver showed a reduction in the total number of IgM^+ cells in the presence of IL-7, although the lack of cell purity may have been a complicating factor (Milne et al., 2004). A role for IL-7 in preventing rearrangement at the Ig light-chain locus has been described in human and mouse cells (Nodland et al., 2011, Johnson et al., 2008). Furthermore, inhibition of IL-7 signalling has been linked with increased levels of apoptosis in mouse B cell populations (Lu et al., 1999) (Rolink et al., 1991).

1.1.3 Haematopoietic differentiation of pluripotent stem cells

1.1.2.7 Haematopoiesis from pluripotent stem cells

When embryoid body (EB) formation is promoted from ES or iPS colonies, multiple cell types from all three germ layers, mesoderm, endoderm and ectoderm, are formed. Alternative systems to promote PSC cell differentiation include co-culture with stromal or feeder cells and monolayer cultures. Both EB and monolayer systems are potentially advantageous as, with the additional exclusion of serum, cultures can be entirely defined and the concentrations of specific cytokines closely controlled, permitting a more precise understanding of mechanisms of action. However, these modalities of promoting differentiation also have limitations. This is seen clearly in the haematopoietic lineage where, thus far, lymphocyte differentiation has only been described using a co-culture system.

OP9 stromal cells, derived from the calvaric bone marrow of op/op mice (deficient in M-CSF), have been most widely used to support the generation of haematopoietic progenitors and their differentiated progeny from pluripotent stem cells (Cho et al., 1999, Nakano et al., 1994, Vodyanik et al., 2005). Thus far, the mechanism by which OP9 stroma supports haematopoietic differentiation is unclear. This understanding would assist in the movement towards efficient, multilineage, feeder-independent haematopoietic differentiation systems. The diversity of the haematopoietic hierarchy has been reproduced in pluripotent stem cell/OP9 co-cultures in the presence of appropriate cytokines. This includes B cells, T cells (when OP9 stroma ectopically expressed the Notch ligand Delta-1), red blood cells and a whole host of other mature myeloid cell types including neutrophils, macrophages and dendritic cells (Choi et al., 2011a, Vodyanik et al., 2005, Dias et al., 2011, Timmermans et al., 2009, Cho et al., 1999). Whilst haematopoietic progenitors generated in OP9 co-culture appear to have a greater differentiation potential than phenotypically similar cells derived from EBs, the number of colony-forming cells (CFCs) produced may be reduced (Subramanian et al., 2009).

S17 cells are capable of promoting haematopoiesis from pluripotent stem cells with similar kinetics to OP9 co-cultures, although a lower percentage of $CD34^+$ cells, around 10-fold fewer, has been observed (Kaufman et al., 2001). Primary cells derived from mouse AGM and fetal liver have also been used in co-culture with hES cells, producing progenitors with the potential to generate the whole range of CFU subtypes and to engraft immunodeficient mice (Ledran et al., 2008).

One of the main aims within this field is to generate of adult-like HSCs from pluripotent stem cells, however, to date, this has not yet been achieved. Early promising studies with mouse ES cells, demonstrated primary and secondary reconstitution capacity, albeit at

low levels (Palacios et al., 1995). This was progressed by ectopically introducing HoxB4 into mouse ES cells, with the resulting haematopoietic population reconstituting primary and secondary recipients (Kyba et al., 2002). Whilst contribution of pluripotent stem cell-derived progeny in peripheral blood at 10 and 20 weeks was greater than 1%, the contribution to the lymphoid lineage was significantly below that of myeloid progeny (Kyba, 2002). Additionally, whilst long-term multilineage reconstitution is possible at the single-cell level using enriched bone marrow or UCB cells, more than 1 million ES-derived cells were required (Kyba et al., 2002). Furthermore, the requirement for the exogenous introduction of the HoxB4 transcription factor is not desirable in a clinical setting.

There has been slower progress in the move towards HSC generation from human pluripotent stem cells. This is perhaps hindered by the choice of recipient mouse strains used to assay such capabilities. NK cells, for example, present in NOD/SCID mice, were demonstrated to attack the ES cell-derived graft (Tian et al., 2006). In one of the more promising reports, hES cells were co-cultured with mouse primary AGM-explant cells and then transplanted into NOD/LtSz-Scid IL2Rγ^{null} mice. Primary and secondary engraftment was observed, although repopulation levels were generally low and multilineage potential not convincingly demonstrated (Ledran et al., 2008).

Numerous suggestions have been put forward to explain the lack of HSC activity in haematopoietic populations derived from human pluripotent stem cells. These include a lack of ability to home and migrate within recipient mice, in addition to a mismatch between the developmental stage of the pluripotent-derived cells in relation to the recipient. Furthermore, species incompatibility might hinder such investigations. For example, human pluripotent stem cell-derived haematopoietic progeny has been

demonstrated to form aggregates upon exposure to mouse serum (Wang et al., 2005b). Overall, it is unlikely that the xenogeneic transplantation setting is the main roadblock in this endeavour. A far greater issue is likely to relate to the identity of the PSC-derived haematopoietic progenitor cells and the lack of HSC characteristics.

For pluripotent cells to serve as a therapeutic source, differentiation protocols need to be devised that are efficient, robust, free of xenogeneic cells and scalable. A number of groups have demonstrated that mesodermal fate can be specified, in the absence of serum or feeder-layers, with a cocktail of cytokines including Activin A (AA), BMP-4, bFGF and Nodal amongst other factors (Irion et al., 2010, Nostro et al., 2008, Pearson et al., 2008, Purpura et al., 2008, Fehling et al., 2003, Carpenter et al., 2012). Interestingly, after a period of mesoderm induction (in the presence of AA, BMP-4 and bFGF), VEGF was found to be necessary and sufficient for the emergence of $CD43^{+}$ haematopoietic cells (Wang et al., 2012). Cocktails of known haematopoietic factors have also been used to promote the proliferation and/or differentiation of HPCs. These include, Stem Cell Factor (SCF), FMS-related Tyrosine Kinase 3 Ligand (Flt3L), IL-3, IL-6, Thrombopoietin (TPO) and Granulocyte colony- stimulating factor (G-CSF) (Chadwick et al., 2003, Niwa et al., 2011). In addition to the presence of soluble factors, other permutations in culture conditions that impact upon the generation of HPCs include the choice of extracellular matrix, the differentiation of pluripotent stem cells as colonies or as single cells and oxygen concentration (Salvagiotto et al., 2011, Niwa et al., 2011, Pick et al., 2007, Wang et al., 2012).

1.1.2.8 Lymphopoiesis from pluripotent stem cells

There is accumulating evidence that lymphoid potential may be lost more readily than myeloid potential during lineage restriction from the multipotent HSC (Luc et al., 2012). An alternative possibility is that cell fate is skewed at the HSC stage, where lymphoid or myeloid bias is experienced (Challen et al., 2010, Sieburg et al., 2006, Benz et al., 2012). A further variable that may impact upon myeloid versus lymphoid lineage readouts is that the *in vitro* and *in vivo* environmental conditions used to probe haematopoietic cell potentials may have been less well defined for lymphocyte differentiation. A concept of lymphoid-potential fragility in the context of an undefined environment, such as that which is found in pluripotent stem cell differentiation cultures, may help to explain the basis for the overwhelming position in the field. That is that pluripotent-derived haematopoietic progenitors can readily yield myeloid and erythroid cells but that lymphopoietic potential is frequently not described (Martin et al., 2008, Wada et al., 2011).

In vitro B cell differentiation potential of pluripotent cells has been demonstrated only a handful of times and just once in human systems. mES cell differentiation on OP9 stroma yielded $B220^+$ cells and $CD19^+$ cells (Cho et al., 1999, Nakano et al., 1994). The single report of human PSC-derived B cells employed a two-step culture where hES cells were first differentiated on OP9 stroma (Vodyanik et al., 2005). $CD34^+$ haematopoieitic progenitors were then isolated and cultured on MS-5 stroma with the addition of IL-3, IL-7, SCF and Flt3L, yielding $CD19^+CD45^+$ cells, albeit at a low frequency (Vodyanik et al., 2005).

1.2 Key objectives and aims of this research

The overall aim of this research was to investigate the B cell potential of human induced pluripotent stem cells. More specifically to:

1) Compare iPS-derived B cells with adult B cell populations
    - Define conditions to promote B cell lymphopoiesis from iPS cells
    - Compare global transcriptional profiles of iPS-B cells with neonatal and adult B cell populations
    - Investigate the multilineage potential of iPS-derived haematopoietic progenitors
2) Determine the cellular origin of iPS-derived B cells
    - Describe the temporal and cell surface profile of haematopoietic and endothelial populations arising during iPS differentiation
    - Identify populations with B cell potential within iPS differentiation cultures
    - Assay the potential of iPS-derived haemogenic endothelium to generate B cells
3) Investigate the potential of iPS- derived B cells to undergo maturation and express cell surface antibodies.
    - Identify *in vitro* conditions to promote iPS-B cell maturation and IgM expression
    - Determine gene segment utilisation of iPS-B cells following VDJ recombination and compare to adult B cell populations
    - Investigate the capacity of iPS-B cells to expand and mature *in vivo.*

Chapter 2.

Materials and Methods

2.1 Reagents

Table 1 Reagents and corresponding company details.

Reagent	Company
0019 clonal control	Invivoscribe Technologies Inc, San Diego, CA, USA
10 cm dish	BD Biosciences, Franklin Lakes, CA,USA
10cm bacteriology dish	Thermo Fisher Scientific, Waltham, MA, USA
2-mercaptoethanol	Sigma Aldrich Ltd., Gillingham, UK
Accutase in PBS with 0.5mM EDTA	PAA Laboratories GmbH, Pasching, Austria
Agarose	Sigma Aldrich Ltd., Gillingham, UK
Ampicillin	Sigma Aldrich Ltd., Gillingham, UK
Amplitaq gold	Life Technologies Corporation, Carlsbad, CA, USA
Anti-PE Microbead kit	Miltenyi Biotech GmbH, Bergisch Gladbach, Germany
Ascorbic acid	Sigma Aldrich Ltd., Gillingham, UK
Blood sample tube sodium citrate	BD Biosciences, Franklin Lakes, CA,USA
Bovine Gelatin, solution	Sigma Aldrich Ltd., Gillingham, UK
Bovine serum albumin (BSA)	Sigma Aldrich Ltd., Gillingham, UK
CD133 Microbead kit	Miltenyi Biotech GmbH, Bergisch Gladbach, Germany
CD34 Microbead kit	Miltenyi Biotech GmbH, Bergisch Gladbach, Germany
CD43 Microbead kit	Miltenyi Biotech GmbH, Bergisch Gladbach, Germany
CD45 Microbead hit	Miltenyi Biotech GmbH, Bergisch Gladbach,

	Germany
Collagen I bovine gel	Life Technologies Corporation, Carlsbad, CA, USA
Collagenase type IV	Life Technologies Corporation, Carlsbad, CA, USA
CompBeads Plus	BD Biosciences, Franklin Lakes, CA,USA
cRPMI	PAA Laboratories GmbH, Pasching, Austria
DAB substrate kit	Vector Laboratories Inc., Burlingame, CA, USA
DAPI	Life Technologies Corporation, Carlsbad, CA, USA
ddH_2O (double distilled water)	Life Technologies Corporation, Carlsbad, CA, USA
Defined Fetal Bovine Serum	Thermo Fisher Scientific, Waltham, MA, USA
Dexamethasone	Sigma Aldrich Ltd., Gillingham, UK
Dispase	Stem Cell Technologies, Grenoble, France
DMEM	PAA Laboratories GmbH, Pasching, Austria
DMEM/F12	Life Technologies Corporation, Carlsbad, CA, USA
DMSO	Sigma Aldrich Ltd., Gillingham, UK
EDTA	Sigma Aldrich Ltd., Gillingham, UK
EGM-2	Lonza Biologics, Tewkesbury, UK
Eprex EPO	Janssen Cilag, High Wycombe, UK
ES-qualified matrigel	BD Biosciences, Franklin Lakes, CA,USA
FcR blocking reagent	Miltenyi Biotech GmbH, Bergisch Gladbach, Germany
Gel Red Nucleic Acid Stain	Biotium Inc, Hayward, CA, USA
Hank's Balanced Salt Solution (HBSS)	PAA Laboratories GmbH, Pasching, Austria
Human IL-7 neutralising antibody	R&D systems, Minneapolis, MN, USA
Hyperladder II	Bioline, London, UK
IgH Gene Rearrangement Assay	Invivoscribe Technologies Inc, San Diego, CA, USA
LB Agar	Sigma Aldrich Ltd., Gillingham, UK
LB Broth	Sigma Aldrich Ltd., Gillingham, UK
Lipopolysaccaride	Sigma Aldrich Ltd., Gillingham, UK
LSM 1077 Lymphocyte Separation Medium	PAA Laboratories GmbH, Pasching, Austria
Methocult H4034 optimum	Stem Cell Technologies, Grenoble, France
Mouse IL-7 Neutralising antibody	R&D systems, Minneapolis, MN, USA
mTesR	Stem Cell Technologies, Grenoble, France

MTG	Sigma Aldrich Ltd., Gillingham, UK
Nuclease free water	Life Technologies Corporation, Carlsbad, CA, USA
One Shot TOP10 Chemically Competent E.Coli cells	Life Technologies Corporation, Carlsbad, CA, USA
PBS	PAA Laboratories GmbH, Pasching, Austria
pCR2.1-TOPO vector	Life Technologies Corporation, Carlsbad, CA, USA
Penicillin/Streptomycin (100x)	PAA Laboratories GmbH, Pasching, Austria
Phosphorylcholine- BSA	Biosearch Technologies Inc, Novato, CA, USA
Porcine Gelatin, powder	Sigma Aldrich Ltd., Gillingham, UK
QIAamp DNA Blood Mini Kit	Qiagen, Venlo, Netherlands
QIAprep miniprep spin kit	Qiagen, Venlo, Netherlands
QIAquick Gel Extraction Kit	Qiagen, Venlo, Netherlands
Recombinant human Activin A	Life Technologies Corporation, Carlsbad, CA, USA
Recombinant human APRIL	Peprotech, Rocky Hill, NJ, USA
Recombinant human bFGF	Life Technologies Corporation, Carlsbad, CA, USA
Recombinant human BMP-4	R&D systems, Minneapolis, MN, USA
Recombinant human CD40L	Peprotech, Rocky Hill, NJ, USA
Recombinant human Flt-3 Ligand	R&D systems, Minneapolis, MN, USA
Recombinant human IGF-1	R&D systems, Minneapolis, MN, USA
Recombinant human IL-3	R&D systems, Minneapolis, MN, USA
Recombinant human IL-4	Peprotech, Rocky Hill, NJ, USA
Recombinant human IL-5	R&D systems, Minneapolis, MN, USA
Recombinant human IL-6	R&D systems, Minneapolis, MN, USA
Recombinant human IL-7	Life Technologies Corporation, Carlsbad, CA, USA
Recombinant human SCF	R&D systems, Minneapolis, MN, USA
Recombinant human TPO	R&D systems, Minneapolis, MN, USA
Recombinant human VEGF	R&D systems, Minneapolis, MN, USA
RNAeasy minikit	Qiagen, Venlo, Netherlands
SOC medium	Life Technologies Corporation, Carlsbad, CA, USA
Sodium bicarbonate	Life Technologies Corporation, Carlsbad, CA, USA
Stempro-34	Life Technologies Corporation, Carlsbad, CA, USA
Stemspan serum-free expansion medium	Stem Cell Technologies, Grenoble, France
TBE Buffer (10x)	Life Technologies Corporation, Carlsbad, CA, USA
Trisodium Citrate	VWR International Ltd., Poole, UK

Trypan blue stain	Sigma Aldrich Ltd., Gillingham, UK
Trypsin-EDTA (1x) in PBS without Ca and Mg	PAA Laboratories GmbH, Pasching, Austria
Vectastain ABC kit	Vector Laboratories Inc., Burlingame, CA, USA
X-gal	Life Technologies Corporation, Carlsbad, CA, USA
Y-27632	Sigma Aldrich Ltd., Gillingham, UK /Stemgent, San Diego, CA, USA
α-MEM, powder	Life Technologies Corporation, Carlsbad, CA, USA

2.1.1 Media

2.1.1.1 Media components

Table 2 Media components

Media/Buffer	Media components	Fetal Calf Serum
Wash Buffer	HBSS w/o phenol red w/o Ca Mg, 3g/L Sodium Citrate, 0.5% (w/v) BSA.	NA
MACS Buffer	PBS w/o Ca Mg, 1% (w/v) BSA, 2mM EDTA (Sigma-Aldrich Ltd.)	NA
Differentiation Media	5g α-MEM powder (Life Technologies Corporation), 500ml Distilled Water (Life Technologies Corporation), 14.7ml sodium bicarbonate (Life Technologies Corporation) 100µM Monothioglycerol (Sigma) and 100U Penicillin/Streptomycin (P/S)(PAA)	10% defined (Hyclone)
OP9 Growth Media	5g α-MEM powder (Life Technologies Corporation), 500ml Distilled Water (Life Technologies Corporation), 14.7ml sodium bicarbonate (Life Technologies Corporation) 100µM Monothioglycerol (Sigma-Aldrich Ltd.) and 100U Penicillin/Streptomycin (P/S)(PAA)	20% defined (Hyclone)
MS-5 Growth Media	5g α-MEM powder (Life Technologies Corporation), 500ml Distilled Water (Life Technologies Corporation), 14.7ml sodium bicarbonate (Life Technologies Corporation) and 100U Penicillin/Streptomycin (PAA)	10% defined (Hyclone)
Stempro34^{+}	Stem Pro-34 SFM with 2mM L-glutamine, 1% (v/v) PenStrep (PAA), 400µM monothioglycerol (Sigma-Aldrich Ltd.) and 50 µg/mL ascorbic acid (Sigma-Aldrich Ltd.).	None

2.1.1.2 Media preparation

Differentiation media, OP9 growth media and MS-5 growth media were prepared by the addition of media components as indicated in Table 2. Media were then filtered through a 0.22 µm filter and stored at 4°C.

BSA was dissolved in PBS (MACS Buffer) or HBSS (Wash Buffer), Sodium Citrate was dissolved in HBSS. Solutions were filter sterilised through 0.22 µm filter. A 200mM stock EDTA solution was made up by the addition of EDTA to ddH_20. The solution was then adjusted to pH 8 and was filter sterilised. Buffer solutions were stored at 4°C.

2.2 Cells

2.2.1 Freezing and thawing of cells.

All cell culture manipulations were performed with aseptic conditions in a laminar flow hood and then cells were maintained in a humidified incubator in 5% $C0_2$ at 37°C unless otherwise indicated.

Cells, with the exception of iPS cells, were routinely frozen in 90% (v/v) defined fetal calf serum (Hyclone) and 10% (v/v) DMSO (Sigma-Aldrich Ltd.) and stored in gas-phase liquid nitrogen. iPS cells were routinely frozen in 90% mTesR (v/v) (Stem Cell Technologies) and 10% (v/v) DMSO (Sigma-Aldrich Ltd.). Unless indicated, cells were resurrected by rapid incubation at 37°C followed by the dropwise addition of the appropriate cell culture

media, centrifuged at 1,200rpm for 5 mins at room temperature (RT) and then seeded as described. Cell culture media was used within 4 weeks of preparation.

2.2.2 Cell Counts

Cell numbers were determined by one of the three following methods. If cell numbers for isolated UCB mononuclear cells (MNCs) were required, MNCs were resuspended in 10ml of MACS Buffer and a 200µl sample was taken for analysis using the Sysmex haematology analyser (Sysmex Corporation, Hyogo, Japan). White blood cell counts were produced in addition to quantification of other parameters such as red blood cell and platelet cell contaminants.

For routine cell counts, 20µl of the sample was taken and mixed 1:1 with Trypan Blue (Sigma-Aldrich Ltd.). The sample was then loaded into a haemocytometer with affixed cover slip and viable (non-blue) cells were counted at x20 magnification in the central 5 quadrants.

For heterogenous cell populations, cell counts provided as events in flow cytometry analysis were used as an estimate of cell number. Here, counts were adjusted dependent upon the proportion of total cells run per sample.

2.2.3 Cell lines

2.2.3.1 Induced pluripotent stem cells

Human C15, C18 and C19 iPS cells were obtained from Dr Lee Carpenter (NHSBT, Oxford, UK). These cell lines were derived according to protocols described by Yamanka and

colleagues (Takahashi et al., 2007, Carpenter et al., 2011). Normal Human Dermal Fibroblasts (HDFs) (Lonza Biologics) were transduced with viral supernatants generated using pMX vectors hOct4, hSox2 and hKlf4 (Addgene) with the PLATGP packaging cells (Cell Biolabs). Transduced hDFs were then cultured with mitomycin C-treated mouse embryonic fibroblasts (MEFs) in modified embryonic stem cell media, comprising: Dulbecco's modified Eagle's medium (DMEM)/F12, 20% (v/v) Knock Out Serum Replacement (Life Technologies Corporation), 10 ng/ml basic fibroblast growth factor (R&D systems), 2mM sodium pyruvate, 1x nonessential amino acids (Life Technologies Corporation), and 1µM mercaptoethanol (Sigma-Aldrich Ltd.).

Following adaptation to feeder-free conditions (as described by Ludwig et. al.,(Ludwig et al., 2006)), iPS colonies were cultured on matrigel-coated plates (BD Biosciences) in mTeSR media (Stem Cell Technologies). iPS cell lines were characterised as described in Carpenter et. al., to demonstrate an ES cell-like phenotype and pluripotent potential (Carpenter et al., 2011). iPS cell lines were shown to form teratomas in $RAG^{-/-}$ mice, were negative for the expression of transgenes and expressed pluripotent stem cell-associated markers (Carpenter et al., 2011). With the exception of C18 cells, iPS cell lines were karyotypically normal.

OPM2 and OC3 iPS cell lines were generated by Cheng-Tao Yang (NHSBT, Oxford). Briefly, human peripheral blood or umbilical cord blood mononuclear cells (MNCs) were reprogrammed by transfection of episomal plasmids containing the following factors: Oct4, Sox2, Nanog, Lin28, Klf4, and LMyc, as described by Thomson and colleagues (Yu et al., 2009). Reprogramming was performed without feeder cells in DMEM/F12 media with bFGF and N2B27 supplementation as described by Jiang and colleagues (Yu et al., 2011).

Cell lines were then characterised as described for fibroblast-derived iPS cells with the exception of the teratoma assay.

PA iPS cells were kindly provided by Dr. Polyanna Goh (UCL, UK). PA iPS cells were generated from fibroblasts grown from a skin biopsy, taken from a healthy donor. Fibroblasts were reprogrammed using plasmid delivery of OCT3/4, SOX2, KLF4, L-MYC, LIN28 and TP53 shRNA, as described in Okita at. al. (Okita et al., 2011).

All iPS cell lines were used for differentiation studies between passages 10-30, with the exception of PA iPS lines which were used between passage 40-45.

Cultures were routinely maintained in 5% CO_2 and 5% O_2 with half-media changes every 2 days. iPS colonies were passaged following a 15 minute incubation with 10µM ROCK inhibitor Y27632 (Sigma-Aldrich) supplemented in mTeSR, colonies were then washed with DMEM/F12 and incubated in 1x Dispase (Stem Cell Technologies) for 5-10 minutes. Colonies were subsequently washed in DMEM/F12 and resuspended in mTeSR media with 10µM Y27632 and manually harvested by scrapping using a 1ml pipette tip. The split ratio varied between 1:6 and 1:24 dependent upon the initial density of cells.

2.2.3.2 OP9 and MS-5 cells

OP9 and MS-5 cells were kindly provided by Professor Igor Slukvin (Department of Pathology and Laboratory Medicine, Wisconsin National Primate Research Centre, University of Wisconcin, WI, USA). OP9 cells were cultured as previously described (Nakano et al., 1994). OP9 cells were cultured on a 10cm dish, (Corning) pre-coated with 0.1% (v/v) bovine gelatin (Sigma Aldrich Ltd.) for 16 hours or greater, in 10ml of OP9 growth media: 5g α-MEM powder (Life Technologies Corporation) in 500ml Distilled

Water (Life Technologies Corporation), 14.7ml sodium bicarbonate (Life Technologies Corporation) with 20% (v/v) defined FCS (Hyclone), 100µM Monothioglycerol (MTG) (Sigma-Aldrich Ltd.) and 100U Penicillin/Streptomycin (P/S) (PAA), combined and filter-sterilized. On day 4, at 100% confluency, cells were either passaged by incubation with Trypsin-EDTA (1x) and split 1:4, or alternatively 5ml of media was aspirated and replaced with 5ml of fresh OP9 media in preparation for differentiation experiments. OP9 cells were used between passage 25 and 38. Cultures were discarded if adipogenic cells made up >10% of the total population.

MS-5 cells were cultured in 6 well plates, or T75 flasks, pre-coated with 0.1% (w/v) Porcine gelatin (Sigma-Aldrich Ltd.) in MS-5 growth media: 5g α-MEM powder (Life Technologies Corporation) in 500ml Distilled Water (Life Technologies Corporation) with 10% (v/v) defined FCS (Hyclone) and 100U P/S (PAA), combined and filter-sterilized. When MS-5 cells were confluent they were passaged by trypsin incubation and split 1:4. MS-5 cells were used between passage 6 and 9.

2.2.3.3 Human dermal fibroblasts

Human dermal fibroblasts (hDF) were purchased from Lonza Biologics, cultured in Dulbecco's Modified Eagle Medium (DMEM) (Lonza Biologics) with 10% (v/v) fetal calf serum (FCS) (PAA) and split 1:4 by Trypsin-EDTA (1x) incubation. hDFs were used up to passage 8.

2.2.4 Primary Cells

2.2.4.1 Umbilical cord blood (UCB) mononuclear cells

Human UCB was collected with written informed pre-consent and ethical approval from the Oxford Radcliffe Research Ethical Committee for the Use of Umbilical Cord Blood following Delivery as a Source of Stem Cells for Study of Cell Differentiation in Normal and Disease Conditions (CO2.313). Isolated cells were used as anonymised linked donations either under an HTA licence or with ethical permission from the Berkshire Research Ethics Committee (10/H0505/34). UCB was kept at 4°C for up to 24 hours and then enriched for MNCs by diluting 1:1 (if white blood cell (WBC) count was $<7x10^6$ cells/ml) or 1:2 (if the WBC count was $>7x10^6$ cells) in Wash Buffer: Hank's balanced salt solution (HBSS) (PAA), sodium citrate (Sigma-Aldrich Ltd.) and 0.5% (w/v) BSA (Sigma-Aldrich Ltd.) and slowly pipetted into 50ml frit tubes containing 17ml LSM 1077 (density 1.077g/ml) (PAA). Blood was then centrifuged at 1000 x g for 10 min at 22°C with the brake between 1-3 in a Hettich Rotina 46R centrifuge (DJB Labcare). The MNC layer was then collected and cells from tubes were combined, the total volume was made up to 50ml with Wash Buffer and the cells were spun at 400 x g for 10 min at 22°C with brake 9. The supernatant was then discarded and the cell pellet resuspended in Wash Buffer, 2-3 pellets were combined and the total volume was made up to 50ml with Wash Buffer before the cells were centrifuged at 200 x g for 5 min at 22°C with brake 9 to separate platelets. The supernatant was again disposed of and the remaining cell pellets were combined and a sample analysed to assess total MNC count using the Sysmex haematology analyser (Sysmex Corporation).

2.2.4.2 Peripheral blood mononuclear cells

3-5ml of peripheral blood was provided from healthy adult donors under an HTA licence or with ethical permission from the Berkshire Research Ethics Committee (10/H0505/34). Blood was diluted 1:2 with Wash Buffer and 4ml of diluted blood was layered over 3ml of LSM 1077 (PAA) in a 15ml tube. Blood was then spun and the MNC fraction isolated as described for UCB MNCs (2.2.4.1).

2.2.4.3 Human Umblical Vein Endothelial Cells

Human umbilical vein endothelial cells (HUVECS) were obtained from Dr. Emma Pepperell (NDCLS, Oxford) and cultured in complete endothelial growth medium-2 (EGM-2) (made from endothelial cell basal medium-2 (EBM-2) (Lonza Biologics) supplemented with EGM-2 Single Quots (consisting of 10ml FCS, 0.2ml hydrocortisone, 2ml fibroblast growth factor-B (hFGF-B), 0.5ml vascular endothelial growth factor (VEGF), 0.5ml long R insulin-like growth factor-1 (R_3-IGF-1), 0.5ml. ascorbic acid, 0.5ml epidermal growth factor (hEGF), 0.5ml gentamycin sulphate, amphotericin-B (GA-1000), and 0.5ml heparin per 500ml EBM-2, all from Lonza Biologics). Cells were split 1:3 for routine culture and used up to passage 4.

2.3 Antibodies

Monoclonal antibodies (mAbs) used in this study are recorded below, with the staining volumes used for analysis by flow cytometry indicated.

Table 3 Human conjugated mAbs with clone and company information.

Name	Conjugate	Clone	Company	Volume/50µl
CD10	PE	HI10a	BD Biosciences	10
CD105	FITC	166707	R&D systems	5
CD11b	FITC	ICRF44	eBioscience	2.5
CD127	PE	eBioRDR5	eBioscience	2.5
CD133	APC	293C3	Miltenyi Biotec	5
CD133	PE	293C3	Miltenyi Biotec	5
CD138	PE	DL-101	eBioscience	2.5
CD14	PeCy7	M5E2	BD Biosciences	2.5
CD144	FITC	55-7H1	BD Biosciences	10
CD144	PE	16B1	eBioscience	2.5
CD146	FITC	P1H12	Millipore	0.5
CD16	APC-eFluor780	CB16	eBioscience	2.5
CD19	FITC	HIB19	eBioscience	2.5
CD19	PerCP-Cy5.5	HIB19	eBioscience	2.5
CD19	PE	LT19	Miltenyi Biotech	5
CD20	PeCy7	2H7	eBioscience	2.5
CD235a	APC	GA-R2 (HIR2)	BD Biosciences	2.5
CD27	APC	0323	eBioscience	2.5
CD31	PE	WM59	BD Biosciences	10

CD33	FITC	P67.6	BD Biosciences	10
CD34	FITC	AC136	Miltenyi Biotec	5
CD34	APC	AC136	Miltenyi Biotech	5
CD38	FITC	HIT2	BD Biosciences	10
CD41a	APC	HIP8	BD Biosciences	10
CD41a	FITC	HIP8	BD Biosciences	10
CD43	FITC	eBio-84-3C1	eBioscience	2.5
CD43	APC	eBio-84-3C1	eBioscience	2.5
CD45	Pe-Cy7	HI30	BD Biosciences	2.5
CD45	APC-Cy7	2D1	BD Biosciences	2.5
CD45	APC	HI30	BD Biosciences	10
CD45	Alexa 488	HI30	Invitrogen	5
CD45R (B220)	FITC	RA3-6B2	BD Biosciences	2.5
CD45R (B220)	PerCP	RA3-6B2	BD Biosciences	2.5
CD56	PE	CMSSB	eBioscience	2.5
CD73	PE	AD2	BD Biosciences	10
CD90	APC	5E10	BD Biosciences	2.5
CD90	FITC	5E10	BD Biosciences	2.5
c-kit	APC	104D2	Invitrogen	5
HLA-DR	PE	LN3	Biolegend	10
IgM	APC	SA-DA4	eBioscience	2.5
IgM	PE	G20-127	BD Biosciences	10
pre-BCR	PE	HSL2	Biolegend	2.5

Volume of mAb included per 50µl staining sample for flow cytometry analysis.

Table 4 Mouse conjugated mAbs with clone and company information.

Name	Conjugate	Clone	Company	Volume/50µl
CD45	FITC	30-F11	Invitrogen	2.5
CD45	APC	30-F11	Invitrogen	2.5
Ter119	PE	TER-119	eBioscience	2.5

Volume of mAb included per 50µl staining sample for flow cytometry analysis.

2.4 Flow cytometry

2.4.1 Method

The LSR II flow cytometer (BD Biosciences) was used throughout and calibrated for analysis using Cytometer Set up and Tracking (CST) beads (BD biosciences). For detection of FITC, PE, PerCPCy5.5, PE-Cy5, PE-Cy7, APC and APC-Cy7 and Pacific Blue, the 670/14 filter was used. FITC, PE, PE-Cy5, PE-Cy7 and PerCPCy5.5 were excited by the 488 nm laser, where generally the 670/14 filter was used. When PerCP detection was required, the 660/20 filter was exchanged for the 670/14 filter. APC and APC-Cy7 were excited by the 633 nm laser and DAPI/Pacific Blue the 355 nm UV laser. Unless otherwise stated, cells for flow cytometry analysis were resuspended in 40µl MACS Buffer and 10µl FcR Blocking (Miltenyi Biotec) and incubated for 2-5 min on ice. The appropriate mAb was then added and cells were stained in the dark on ice for 20 min. Cells were then washed and resuspended in MACS Buffer for analysis with the addition of 0.1µg/ml DAPI (Life Technologies Corporation) to exclude non-viable cells. 1:100 Propidium Iodide (Sigma-Aldrich Ltd.) and 10nM TO-PRO-3 (Life Technologies Corporation) were alternatively used where indicated.

Doublet exclusion was implemented based upon SSC-H v SSC-W or FSC-H v FSC-A and isotype controls or fluorescence minus one (FMOs) were used to define negative and positive gates.

2.4.2 Antibody titration

mAbs were titrated to determine the optimum concentration for flow cytometry applications. $1x10^6$ UCB MNCs/sample were resuspended in 40µl of MACS Buffer with 10 µl human FcR blocking (Miltenyi Biotec). Antibodies were centrifuged to ensure the exclusion of antibody aggregates and the antibody diluted as indicted using MACS Buffer. The appropriate volume of mAb was then added and the sample was incubated on ice for 20 min in the dark. Cells were then washed and resuspended in MACS Buffer with 0.1µg/ml DAPI (Life Technologies). The signal/noise ratio was determined by dividing the MFI of the positive peak (signal) by the MFI of the negative peak (noise). The optimal antibody concentration is found when the signal/noise ratio is maximal. Titration of CD19 PerCPCy5.5 and CD27 APC antibodies revealed optimal concentrations of 0.625 µg/ml and 5 µg/ml respectively of the concentrations tested (Figure 8). Recommended volumes of these antibodies, produced by eBiosciences was CD19 PerCPCy5.5; 1 µg/ml and CD27 APC; 2.5 µg/ml.

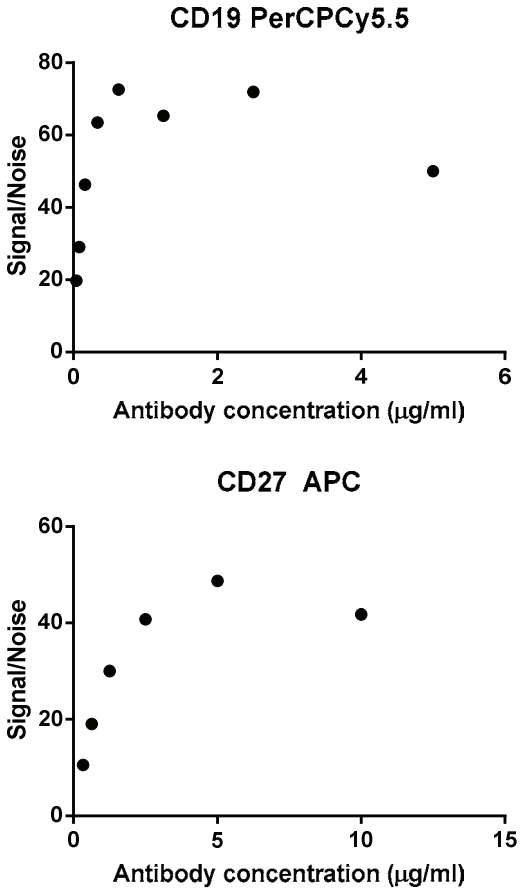

Figure 8 Antibody titration of CD19 PerCPCy5.5 and CD27 APC with UCB MNCs.
Cells were stained with the indicated concentration of antibody, washed and then analysed by flow cytometry. Signal/Noise ratio was determined by dividing the MFI of the positive peak by the MFI of the negative peak. Optimal antibody concentrations for CD19 PerCPCy5.5 was 0.625 µg/ml and 5 µg/ml for CD27 APC.

2.4.3 Compensation

PMT voltages were set using unstained cells and then compensation settings established using CompBeads Plus (BD Biosciences) as described in 'A Setup System for Compensation: BD CompBeads plus BD FACSDiva Software'. Briefly, for each flurochrome to be included in the experiment, a sample volume of antibody was added to separate tubes containing one drop of CompBeads Plus Anti-Mouse Ig Beads which were then incubated for 20 min at room temperature, in the dark. Beads were then washed with MACS Buffer and resuspended in 300µl MACS Buffer with the addition of one drop of CompBeads Plus Negative Control beads. BDFACSDiva software was used to create compensation tubes for each fluorchrome and bead samples were run and recorded. Gates were then manually set on histograms around positive and negative populations and compensation settings were calculated by the software and applied.

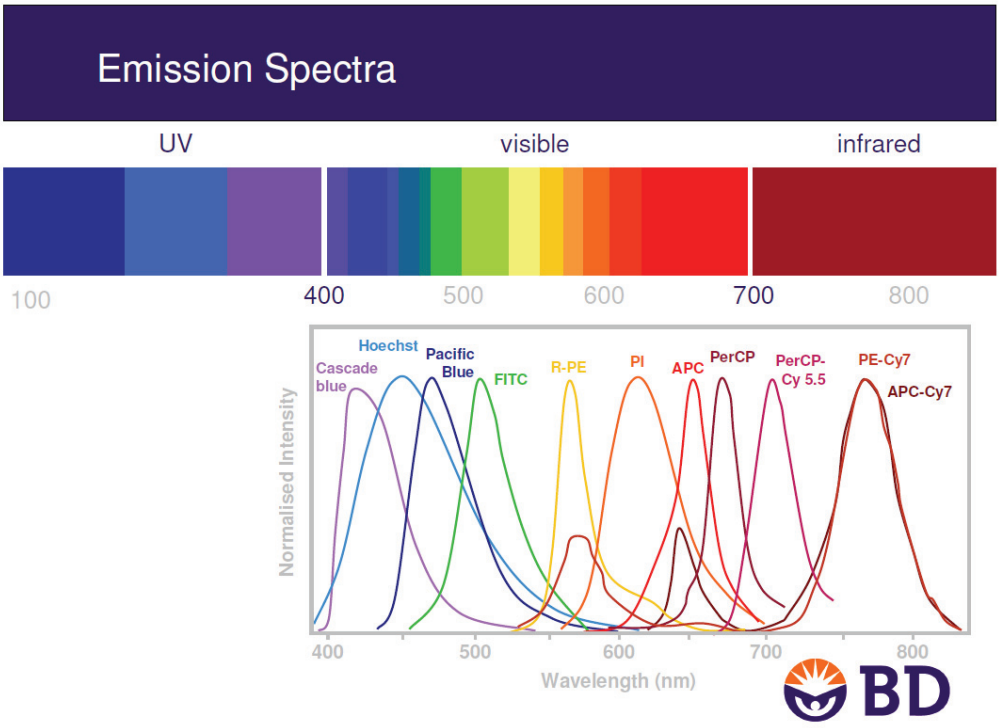

Figure 9 Emission spectra showing spectral overlaps of flurochromes detectable by the BD LSR II flow cytometer.

Flow cytometers with multiple lasers allow for the simultaneous detection of multiple flurochromes with different excitation and emission spectrums. When fluorochromes are used in combination that have overlapping emission spectra, such as FITC and PE, compensation settings are required to enable the discrimination of positive signals. Image taken from www.bdbiosciences.com.

2.5 Cell enrichment/isolation techniques

2.5.1 MACS isolation

Cells for enrichment by MACS were washed in MACS Buffer: PBS w/o Mg Ca (PAA), 1% (w/v) BSA (Sigma-Aldrich Ltd.), 2mM EDTA (Sigma-Aldrich Ltd.), centrifuged at 1,200 rpm for 5 min at 4° and resuspended in MB at the volume appropriate for the enrichment being undertaken (Table 5). The appropriate volume of microbeads was added and cells were incubated at 4° in the dark, for the time indicated. Cells were then washed with 5ml of MACS Buffer, centrifuged as above and resuspended in 500µl MACS Buffer. Cells were passed through a 30µM pre-separation filter (Miltenyi Biotec) and pre-equalibriated LS column (Miltenyi Biotec). LS columns were washed with 3ml MACS Buffer 3 times, and then cells were flushed using 5ml of MACS buffer by immediately pushing the plunger into the column. Cells were either used after enrichment with one column, or were subsequently passed through a second column, as above, where indicated.

Table 5 Enrichment regimes for MACS isolation of cell populations based on the expression of indicated cell markers.

Population to be enriched	Total maximum starting cell number	Microbeads (Miltenyi Biotech Cat. no)	Volumes used	Incubation time
CD34$^+$	<1x10^8	CD34 (130-046-702)	300µl MB, 100µl microbeads, 100µl FcR blocking	30min
CD133$^+$	<1x10^8	CD133 (130-050-801)	300µl MB, 100µl microbeads, 100µl FcR blocking	30min
CD45$^+$	<1x10^7	CD45 (130-045-801)	80µl MB, 20µl microbeads,	15min
CD43$^+$	<1x10^7	CD43 (130-091-333)	80µl MB, 20µl microbeads,	15min
CD19$^+$	<1x10^7	a) CD19-PE (130-091-247) b) anti-PE microbeads (130-048-801)	a) 100 µl MB, 10 µl CD19-PE b) 80 µl MB, 20 µl microbeads	a)10min b)15min

2.5.2 MACS enrichment profiles and purities

2.5.2.1 Day 10 iPS/OP9 co-culture, CD34$^+$ MACS enrichment.

iPS colonies were seeded onto OP9 stroma, cultured and harvested as described in section 2.6.1. CD34$^+$ cells were then selected by MACS, as described in 2.5.1. Typically, 4.6x10^5 ± 0.7 (mean ± SD) CD34$^+$ cells were harvested from one 10cm dish of C18 iPS/OP9 cells on day 10 of culture (Figure 10C). Similarly, 3.7x10^5 ± 0.6 (mean ± SD) CD34$^+$ cells were harvested from one 10cm dish of C19 iPS/OP9 cells on day 10 of culture (Figure 10C). A cell sample was then taken for analysis by flow cytometry (using a minimum of 5x10^4 cells/stain) and gates were set using FMO controls. Typically, day 10 iPS-CD34$^+$ cells were stained with mAbs to CD34 and CD43 to determine purity (CD34$^+$ cells) in addition to a broad indication of haematopoietic differentiation efficiency (CD43$^+$ cells) (Figure 10A and B). CD34-enriched fractions demonstrated purities of 87.1% ± 4.8 (C18 iPS) and 81.0% ± 3.5 (C19 iPS) (mean ± SD) (Figure 10D).

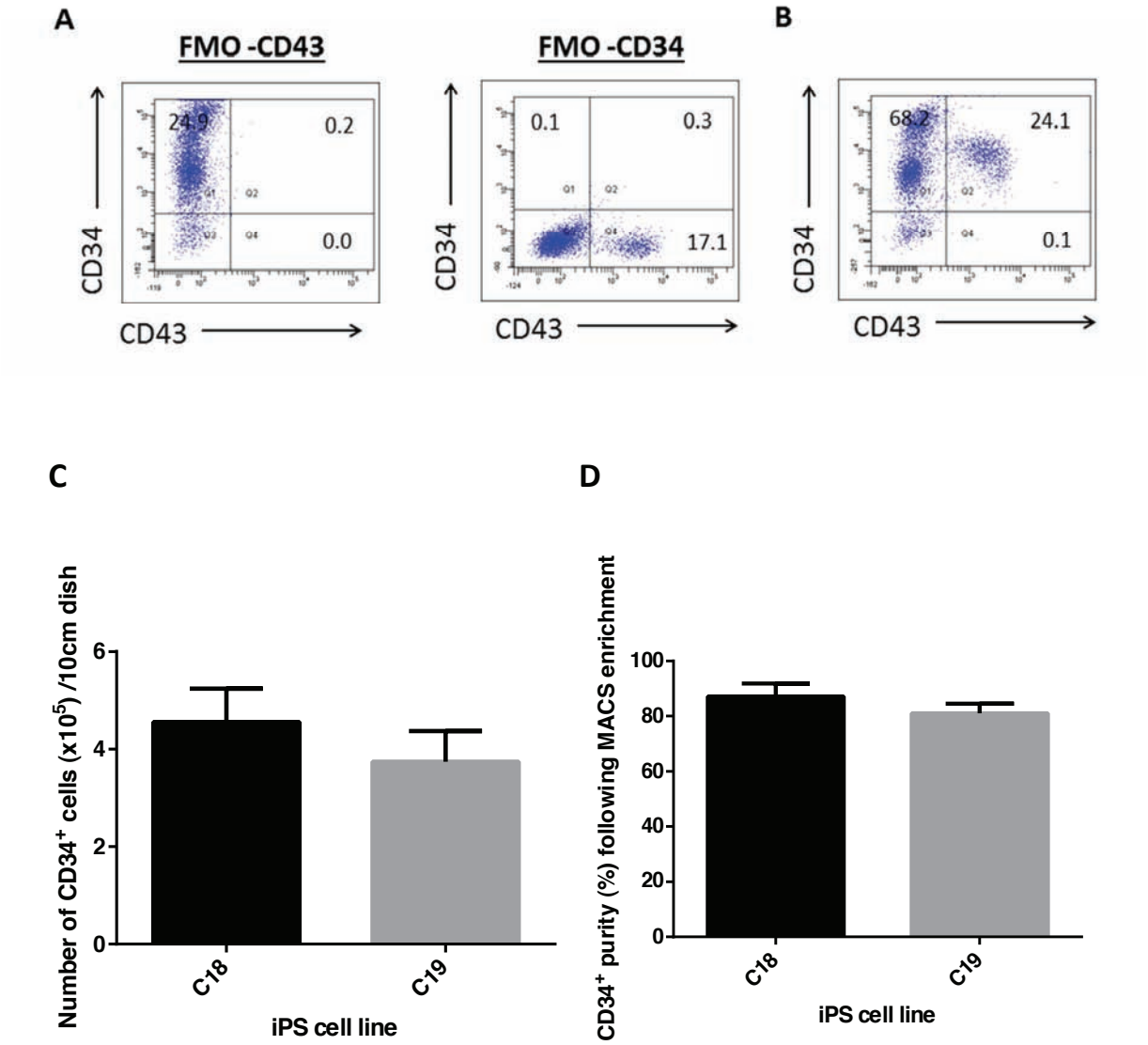

Figure 10 Profile and purity of CD34$^+$ cells isolated from day 10 iPS/OP9 co-cultures.
(A) FMO controls for flow cytometry analysis of CD34$^+$ enriched fractions. (B) Analysis of CD34 and CD43 expression was typically performed to determing the purity of MACS enrichment as well as to provide an estimate of the efficiency of haematopoietic differentiation. (C) Typical number of CD34$^+$ cells harvested from one 10cm dish of iPS/OP9 cells on day 10 of co-culture. C18, 4.6x10^5 ± 0.7; C19, 3.7x10^5 ± 0.6 (mean ± SD). (D) Typical purities, as determined by flow cytometry analysis, of CD34$^+$ cells in day 10 enriched fractions. C18, 87.1 ± 4.8; C19, 81.0 ± 3.5 (mean ± SD).

2.5.2.2 $CD43^+$ and $CD43/45^+$ MACS enrichment from iPS/OP9 co-cultures.

C18 or C19 iPS colonies were seeded onto OP9 stroma, cultures were maintained for 9 or 10 days and harvested as described in section 2.6.1. $CD43^+$ cells were then selected by MACS, as described in 2.5.1 and a sample was taken for analysis by flow cytometry. $CD43^+$ enriched fractions were 82.3% ± 8.5 (mean ± SD) positive for the expression of CD43 (Table 6). Typically, $CD43^+$ cells contained subpopulations of $CD34^+$ and $CD43^-$ cells (Figure 11A).

C18 or C19 iPS colonies were seeded onto OP9 stroma, cultures were maintained for 10 days and harvested as described in section 2.6.1. $CD34^+$ cells were enriched by MACS as detailed in 2.5.2.1 before being reseeded onto fresh OP9 stroma. Co-cultures were then maintained with a half media exchange of Differentiation media every 2 days. On day 22 co-cultures were harvested as described in 2.6.1. $CD43/45^+$ cells were then selected by MACS, as described in 2.5.1 and a sample was taken for analysis by flow cytometry. $CD43/45^+$ enriched fractions were 94.5% ± 2.1 (mean ± SD) positive for the expression of CD43 or CD45 (Table 6). Typically, $CD43/45^+$ cells were predominantly $CD43^+CD45^+$ and contained subpopulations of $CD43^+CD45^-$ and $CD43^-CD45^+$ cells (Figure 11B).

Table 6 Summary of population purities after MACS enrichment.

Selection	Culture	Fraction	Mean	SD
CD34 microbeads	Day 10 iPS/OP9	$CD34^+$	84.1	5.1
CD43 microbeads	Day 10 iPS/OP9	$CD43^+$	82.3	8.5
CD43 microbeads/ CD45 microbeads	Day 22 iPS/OP9	$CD43/45^+$	94.5	2.1
CD45 microbeads	D21 iPS-$CD34^+$/MS-5	$CD45^+$	96.1	1.5
CD19-PE, anti-PE microbeads	D21 iPS-$CD34^+$/MS-5	$CD19^+$	97.0	0.6
CD133 microbeads	Fresh UCB	$CD133^+$	87.4	2.8

Cells were generated as indicated and described in sections 2.2.4.1, 2.6.1 and 2.6.2. The indicated fraction was then isolated using MACS (2.5.1) and a sample was taken for analysis by flow cytometry. N=≥3 independent experiments.

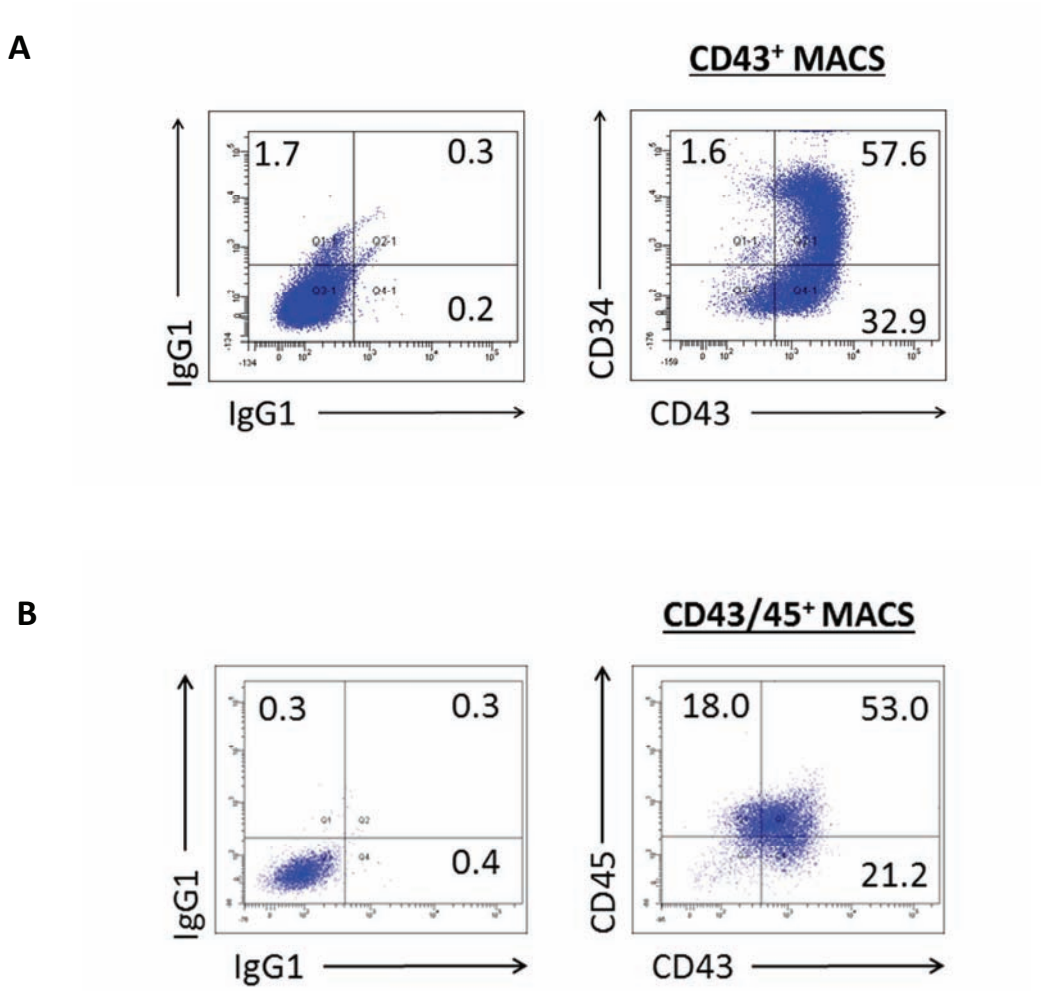

Figure 11 Flow cytometry analysis of $CD43^+$ and $CD43^+CD45^+$ MACS enriched fractions from iPS/OP9 co-cultures.

(A) C18 or C19 iPS/OP9 co-cultures were harvested on day 9 or 10 of co-culture and enriched for $CD43^+$ cells by MACS. $CD43^+$ cells contained both $CD34^+$ and $CD34^-$ cells. (B) C18 or C19 iPS/OP9 co-cultures were harvested after 10 days of co-culture and $CD34^+$ cells were enriched by MACS and reseeded onto fresh OP9 stromal cells. Cultures were then maintained for a further 12 days, harvested and enriched for the $CD43/45^+$ haematopoietic fraction by MACS. The major population was $CD43^+CD45^+$, with both $CD43^+CD45^-$ and $CD43^-CD45^+$ subpopulations. Representative images, n=3 independent experiments.

2.5.2.3 CD133$^+$ cells enrichment by MACS from UCB MNCs.

MNCs were enriched from fresh UCB, as described in 2.2.4.1. CD133$^+$ cells were then enriched by MACS (2.5.1) and a sample was taken for analysis by flow cytometry. CD133$^+$ enriched fractions had average purities of 87.4% ± 2.8 (mean ± SD) (Table 6).

2.5.2.4 CD45$^+$ and CD19$^+$ cell enrichment from day 21 iPS-CD34$^+$/MS-5 co-cultures and UCB-CD133$^+$/MS-5 co-cultures.

C19 iPS colonies were cultured with OP9 stromal cells for 10 days (2.5.2.1), cells were harvested and enriched for CD34$^+$ cells by MACS (2.5.2.1). CD34$^+$ cells were seeded onto confluent MS-5 cells and cultures, supplemented with IL-7, IL-3, SCF and Flt3L, were maintained for 21 days before being harvested (2.6.2). Cells were then enriched by MACS, either for the CD45$^+$ or CD19$^+$ population and analysed by flow cytometry. CD45$^+$ cell fractions were 96.1% ± 1.5 (mean ± SD) pure and contained a subpopulation of CD19$^+$ cells, which showed a typical low SSC profile (Table 6) (Figure 12A). When cells were isolated based on CD19 expression, CD19$^+$ cells represented 97.0% ± 0.6 (mean ± SD) of the enriched fraction (Table 6) (Figure 12B).

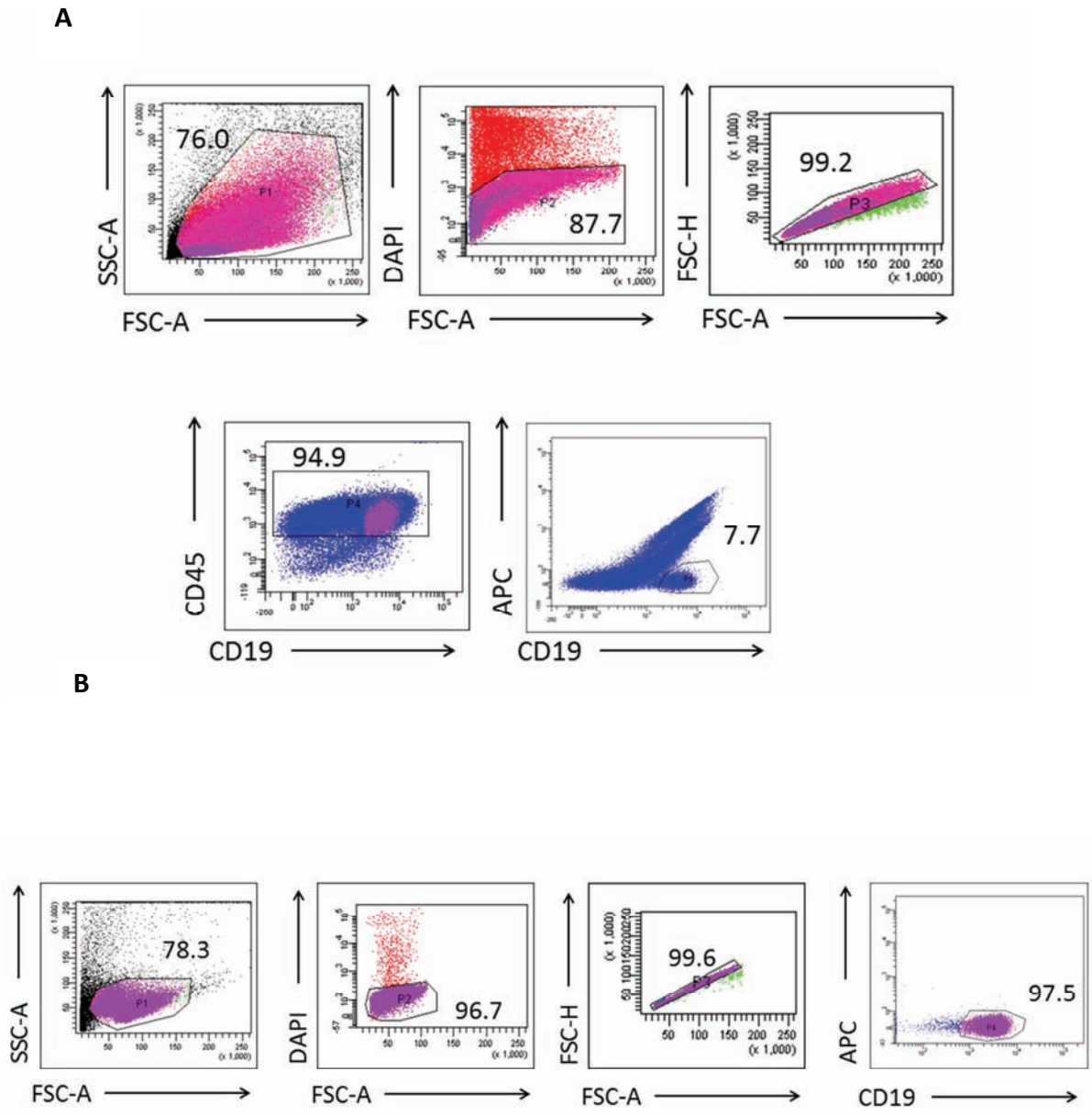

Figure 12 CD45 and CD19 MACS enrichment of cells from day 21 iPS-CD34$^+$/MS-5 co-cultures. CD34$^+$ cells, enriched from day 10 iPS/OP9 co-cultures were seeded onto confluent MS-5 stromal cells, in the presence of IL-7, IL-3, SCF and Flt3L, as described in 2.6.2. After 21 days of culture, cells were harvested and enriched by MACS for either the CD45$^+$ or CD19$^+$ fraction. (A) CD45 enrichment with purities of 96.1% ± 1.5 (mean ± SD). A subpopulation of CD45$^+$ cells expressed CD19. (B) CD19 enrichment was performed with CD19-PE and anti-PE beads. Postive fractions contained 97.0% ± 0.6 (mean ± SD) CD19$^+$ cells. Numbers in figure expressed as a percentage of the parent gate. Representative images, n=3 independent experiments.

2.5.3 Fluorescent activated cell sorting (FACS)

UCB MNCs, PB MNCs or iPS-derived cells were isolated as described and enriched by MACS for the desired cell type. Cells were then stained with the appropriate mAbs as described for flow cytometry (2.4.1), before being passed through a 35µm cap cell strainer to ensure a single cell suspension had been obtained. Cell populations were sorted by FACS at the Nuffield Department of Medicine, WIMM or Sir William Dunn School of Pathology, all University of Oxford using Aria or Becton Coulter FACS machines by the trained FACS operator. Cells were sorted into FACS tubes (BD Biosciences) containing 1-2ml media with 10-20% (v/v) serum. Cell purities were checked where sufficient cell numbers were obtained.

2.6 In vitro assays

2.6.1 Generation of HPCs from iPS/OP9 co-culture

iPS colonies cultured for 5-7 days in maintenance conditions were harvested by incubation with collagenase type IV at 1mg/ml (Life Technologies Corporation) in DMEM/F12 (Life Technologies Corporation) for 45-75 min until >70% of colonies had completely detached. Colonies were then washed three times with Differentiation media containing: 5g α-MEM powder (Life Technologies Corporation) in 500ml Distilled Water (Life Technologies Corporation), 14.7ml sodium bicarbonate (Life Technologies Corporation) with 10% (v/v) defined FCS (Hyclone), 100µM Monothioglycerol (MTG) (Sigma-Aldrich Ltd.) and 100U Penicillin/Streptomycin (P/S) (PAA) by gravity and plated

onto overgrown OP9 stroma (day 8-12 of culture) in 10ml Differentiation media. Cells were distributed homogeneously at 4-6x10^6 cells per 10cm dish. After 24 hours media was completely aspirated, removing unattached iPS colonies, and replaced with 20ml of Differentiation media. Half media changes were then performed on day 4, 6 and 8 with cells typically being harvested on day 10 of culture. When cultures were extended the feeding regime was continued.

Co-cultures were harvested, typically on day 10 cells, by removal and retention of culture media, incubation with 1mg/ml Collagenase type IV for 25 mins and subsequently with trypsin-EDTA (1x) for 7-12 minutes, until the monolayer dissociated upon gentle tapping. Trypsin was neutralised with an equal volume of Differentiation media and the homogenate was gently aspirated with a 1ml pipette tip >20 times. Cells were then passed through a 40µm cell strainer (BD Biosciences) and pelleted by centrifugation at 1,200 rpm for 5 min at RT.

2.6.2 Differentiation of iPS-CD34$^+$ or UCB-CD133$^+$ to the B cell lineage

To promote differentiation towards the B cell lineage, iPS-derived or UCB-derived haematopoietic progenitor cells (HPCs) were seeded onto confluent (day 2-4) MS-5 cells in Differentiation media supplemented with 20ng/ml IL-7 (Life Techologies Ltd.), 10ng/ml IL-3, 50ng/ml SCF and 50ng/ml Flt3L (all R&D systems). Cultures were typically seeded at 2.5x10^4 iPS-CD34$^+$ cells/ml or 0.5x10^4 UCB-CD133$^+$ cells/ml in a 6 well plate format in 2ml/ well. After 7 days, 2ml of Differentiation media supplemented with 20ng/ml IL-7, 50ng/ml SCF and 50ng/ml Flt3L was added per well. On day 14 of culture, 2ml of media, containing

non-adherent cells were aspirated, discarded and replaced with 2ml of fresh Differentiation media containing IL-7, SCF and Flt3L. Cultures were typically harvested on day 21 of culture by washing with HBSS w/o Mg Ca(PAA) and incubation with 1mg/ml collagenase IV for 25 min, and then trypsin-EDTA (1x) until cells detach. Trypsin was neutralised using Differentiation media and a single cell suspension was generated by gentle aspiration using a 1ml Gilson pipette.

2.6.3 Serum and feeder-free protocols

iPS colonies were grown as per routine culture for 5-7 days (2.2.3.1). Media was then switched to Stem Pro34^{+} media comprising: Stem Pro-34 SFM (Life Technologies Corporation), 2mM L-glutamine, 100U Penicillin/Streptomycin (PAA), 400µM monothioglycerol (Sigma-Aldrich Ltd.) and 50µg/ml ascorbic acid (Sigma-Aldrich Ltd.). Cytokines were used, were indicated, at the following concentrations; 50ng/ml (high) or 5ng/ml (low) Activin A (AA) (Life Technologies Corporation), 10ng/ml BMP-4 (R&D systems), 5ng/ml bFGF (Invitrogen), 10ng/ml VEGF (R+D systems), 20ng/ml TPO (R&D systems), 100ng/ml SCF (R&D systems) and 100ng/ml Flt3L (R&D systems). Cultures were fed every 2 days. Monolayers were harvested either by incubation with Accutase (1x) (PAA) for 7-10 min or by incubation with 1mg/ml collagenase-IV (Life Technologies Corporation) for 25 min, followed by 5-7 min with trypsin-EDTA (1x) (PAA).

2.6.4 CFU assay

Methocult H4434 (Stem Cell Technologies) was thawed and 2ml/well was added using a blunt needle into a 6 well plate. iPS- derived $CD34^+$ or $CD43/45^+$ cells were added at $5x10^3$ or $1x10^3$ cells/well as indicated, or UCB-$CD133^+$ cells at $1x10^3$ cells/well by resuspending in 50µl PBS and deposited into the methocult. Plates were then gently tipped to disperse cells in a uniformed distribution. Assays were then maintained for 14 days before colonies were scored and counted, according to the criteria depicted in Figure 3 (Figure 13) and outlined in the accompanying user manual, available at www.stemcell.com (Stem Cell Technologies).

Image removed.

Figure 13 Brightfield images of typical CFU morphologies in methocult.
The CFU assay is an in vitro readout of haematopoietic progenitor potential. Methocult, a methylcellulose-based media with supplemented cytokines, is a routinely used, commercially available product for CFU assays. Colony morphology on day 14 is used to determine progenitor potential. (A) CFU-E, indicative of relatively mature erythroid progenitors that form colonies of 50-200 cells. (B) BFU-E, indicative of erythroid progenitors with a greater proliferative potential than those that form CFU-E. (C) CFU-GM, product of granulocyte and macrophage progenitors. (D) CFU-GEMM, colonies produced by progenitors with multilineage potential that included erythroid with two or more different cell types. Magnification (A) x125, (B) x50, (C) x25, (D) x50.

2.6.5 Endothelial outgrowth colony assay

To promote endothelial differentiation iPS-derived $CD34^+$ cells were seeded onto pre-coated rat tail collagen type I coated plates (BD Biosciences) in EGM-2 media. Cultures were maintained for 14 days, fed with a half-media change every 3 days, then stained as appropriate and passaged by incubation with trypsin-EDTA (1x) (PAA). iPS-$CD34^+$ cells were designated passage 0 (P0) when introduced into the EGM-2/collagen-I conditions and were P1 upon first harvest.

2.6.6 *In vitro* tubule assay

To assess function, endothelial-like cells were seeded into an *in vitro* tubule assay previously established by the laboratory (Zhang et al., 2009). Here, endothelial-like cells were seeded onto collagen-I coated plates in co-culture with hDFs (ratios 1:3-1:6) in EGM-2 media, a half media change was performed every 3 days. After 14 days of culture, cells were fixed and stained with CD31 to visualise endothelial network formation as follows. Cultures were washed with PBS and fixed with ice-cold 70% (v/v) ethanol for 30 min at RT. Wells were then washed 3 times with PBS and incubated at 37° for 20 min with MACS Buffer to block non-specific binding. Anti-human CD31 (AbD Serotech) was diluted 1:4000 and added to cultures which were incubated overnight at 4°. Cells were washed 3 times with PBS and then incubated with MACS Buffer for 20 min at 37° before being stained with 1:200 biotinylated anti-mouse IgG (H+L) (Vector Laboratories Ltd) for 60 min at RT. After washing 3 times with PBS, equal volumes of Reagent A (Avidin) and Reagent B (Biotin), both Vectastain Elite Kit (Vector Laboratories Ltd) in 5 ml of PBS was added and incubated at RT for 30 min. The peroxidase substrate was then prepared from the

Vectastain Elite Kit by adding 4 drops of buffer, 8 drops of 3, 3'-diaminobenzidine, 4 drops of H_20_2 and 4 drops of Nickel solution to 10 ml of dH_20 (Vector Laboratories Ltd.). The tertiary antibody was removed and washed with PBS 3 times and the substrate added for 5-10 min until the tubules could be observed under a microscope. The reaction was then stopped by washing with dH_20 3 times. Cultures were allowed to dry and then images were taken using a Nikon Eclipse T300 microscope (Nikon Ltd.) and IPLab imaging software (Scanlytics, BD Biosciences). Tubule formation was then quantitated using AngioSys software (TCS Cellworks).

2.6.7 Live cell staining

For live cell imaging, CD90-FITC (1:400) and/or CD31-PE (1:100) was added to EGM-2 media, filter-sterilised and added to cell cultures for 1 hour. Cultures were then washed 3 times and visualised using a Nikon Eclipse T300 (Nikon Ltd) and IPLab imaging software (Scanlytics, BD Biosciences).

2.7 Nucleic acid isolation

DNA was isolated using the QIAamp DNA Blood Mini Kit (Qiagen, Cat no. 51104), eluted in Buffer AE and was stored at -20°C. RNA was isolated using the RNAeasy minikit (Qiagen, Cat no. 217004), eluted in RNase-free water and was stored at -80°C. DNA and RNA isolation was performed using the Spin Protocol method as described in the manufacturer's instructions. Nucleic acid concentration and purity were determined using a NanoDrop Micro-Volume UV-Vis Spectrophotometer (Thermo Fisher Scientific).

The spectrophotometer was set to zero using Nuclease-free Water (Ambion) and then 1µl of the DNA or RNA sample was analysed. The 260:280nm ratio was used as a measure of purity, readings <1.8 for DNA, or <2.0 for RNA, were deemed to be low quality and samples were not used for downstream purposes.

2.8 VDJ recombination assay

2.8.1 IgH Gene Rearrangment assay

The IgH Gene Rearragement Assay was purchased from InVivoScribe and used to assess VDJ recombination status as described in the manufacturer's protocol. Briefly, 0.25µl of AmpliTaq Gold (Life Technologies Corporation) was added to 50µl of IgH Framework Master Mixes (InVivoScribe), which contained proprietary framework and JH consensus primers, and were mixed by inversion. 5µl of sample DNA (20-100ng/µl), 5µl of IVS Control DNA (Invivoscribe) or 5µl of ddH_20 (Ambion) was added to Master Mix aliquots and reactions were run with the following programme: 95°C 7 min with 37 cycles of 94°C for 30s, 55°C for 30s, 72°C for 60s, followed by 95°C for 10 min.

2.8.2 Gel electrophoresis

To separate and visualise PCR products, DNA, mixed 5:1 with 50% (v/v) glycerol, was loaded into a 2% (w/v) agarose (Sigma-Aldrich Ltd.) TBE (Life Technologies Corporation) gel containing Gel Red Nucleic Acid Stain (Biotium) at 1:10,000 (v/v) dilution. Hyperladder

II (Bioline) was included as a molecular ladder. DNA fragments were separated in a TBE buffer by electrophoresis at 150V for 30-60 min. Images were acquired using UVi Tec Gel Version 12.6 documentation (UVITEC Cambridge) and image acquisition software.

Where appropriate bands were excised from the gel using a clean sharp scapel, visualised with a White/UV transilluminator (UVP).

2.9 Gene expression array

2.9.1.1 RNA sample preparation for gene expression profiling

For gene expression arrays, RNA was harvested from iPS cells, iPS-B cells, UCB B cells, HSC-B cells and PB-B cells. RNA was isolated from iPS cell lines cultured in mTesR media for 5-7 days by the addition of lysis buffer to adherent colonies, using the RNAeasy minikit (Qiagen, Cat no. 217004). iPS-B cells were generated following the co-culture of iPS-$CD34^+$ cells with MS-5 stroma plus IL-3, IL-7, SCF and Flt3L for 21-23 days. Cells were harvested by collagenase IV/trypsin incubation. (as described in 2.6.2). To generate HSC-B cells, UCB MNCs enriched for the $CD133^+$ fraction by MACS, were frozen and then thawed before being cultured overnight in Stemspan with Flt3L (100ng/ml), SCF (20ng/ml), TPO (100ng/ml) and IL-6 (100ng/ml). Cells were then harvested by aspiration and stained with antibodies to CD19 and CD133 (2.4.1). $CD133^+CD19^-$ cells were FACS isolated and then seeded into co-culture with MS-5 cells plus IL-3, IL-7, SCF and Flt3L for 21-23 days (as described in 2.6.2). Cells were harvested by collagenase IV/trypsin incubation.

B cells derived from iPS-$CD34^+$ and UCB-$CD133^+$ cells and those isolated from UCB and PB MNCs were enriched by MACS using CD19-PE and anti-PE beads (as described in section

2.5.1). Cells were then stained with mAbs to CD10 and isolated by FACS. Viable $CD19^{+}CD10^{+}$ cells were sorted into Differentiation media. RNA was isolated using the RNAeasy minikit (Qiagen, Cat no. 217004), eluted into nuclease-free H_20 and was stored at -80°C (as described in 2.7).

Four different iPS cell lines were used to generate biological replicates of iPS cell and iPS-B cell samples. iPS cell lines used (described in 2.2.3.1) were: C19, fibroblast-derived iPS cells generated using the retroviral delivery of Yamanaka factors (Sox2, Oct-3/4, Klf-4, c-Myc) , OPM2 and OCM3 iPS cells generated from peripheral blood MNCs (OPM2) and UCB MNCs (OC3) using non-integrating episomal vectors of Thomson factors (CT4, SOX2, L-Myc, KLF4, NANOG, and LIN28) (Kaji et al., 2009, Takahashi et al., 2007). PA iPS cells were derived from fibroblasts using plasmid delivery of OCT3/4, SOX2, KLF4, L-MYC, LIN28 and TP53 shRNA. $CD133^{+}$ cells isolated from UCB MNCs from 4 different donors were used to generate HSC-B cells. B cells were isolated from 4 different UCB MNC samples and 4 different PB MNC samples to generate biological replicates.

RNA concentration and purity were determined using a NanoDrop Micro-Volume UV-Vis Spectrophotometer (Thermo Fisher Scientific). RNA was then concentrated using vacuum centrifugation to 15 µl. 3 µl of RNA was provided for quality assessment and 12 µl for gene array at a range of concentrations: iPS 39.7-105.6 ng/ µl, iPS-B 6.8-25.7 ng/ µl, HSC-B 66.1-84.3 ng/ µl, UCB 5.2-17.4 ng/ µl, PB 1.35-3.3 ng/ µl.

2.9.1.2 Gene expression profiling

Gene arrays were performed by the High-Throughput Genomics Group, The Wellcome Trust Centre for Human Genetics, University of Oxford, using the Illumina Human-HT-12v4 expression BeadChip (Illumina). Quality controls were analysed using the

Bioanalyser and RNA was converted to biotin labelled cRNA for hybridisation. Chips were scanned using GenomeStudio (Illumina).

2.9.1.3 Gene array analysis

Data were normalised using the lumi bioconductor package and analysed using MeV software (Du et al., 2008). Data normalisation and advice on bioinformatic methods were provided by the Computational Biology Research Group, WIMM, UK.

2.10 *In vivo* experiments

BALB/c Rag2$^{-/-}$cγ$^{-/-}$ mice were housed under specific pathogen-free conditions in the Biomedical Services Unit of the John Radcliffe Hospital (Oxford, UK). Animal experiments were performed under a Home Office Licence using protocols approved by the Committee on Animal Care and Ethical Review at the University of Oxford and in accordance with the UK Animals (Scientific Procedures) Act 1986.

Mice were irradiated within 24 hours of birth with 2 doses of 2 Gy separated by 4 hours. Neonates were then injected 6-12 hours later with 5x10^5 iPS- CD45$^+$ cells or 1x10^5 UCB-CD133$^+$ cells in 50 µl of PBS-1% (w/v) BSA. Cells were administered by an intraperitoneal or intrahepatic injection. Mice were marked by foot tattoo to track animals. After 8 weeks, mice were weaned. Injections and weaning were performed by Dr. Ou Li, Nuffield Department of Surgery, University of Oxford.

Cells were prepared for injection in sterile conditions using aspectic technique. Briefly, cells were harvested from iPS-$CD34^+$/MS-5 co-cultures and enriched by MACS for the $CD45^+$ population (as described in 2.5.1). $5x10^5$ cells were resuspended in 50µl PBS-1% (w/v) BSA and kept on ice until cells were administered. UCB MNCs were isolated from fresh UCB and enriched for $CD133^+$ cells by MACS (as described in 2.5.1). Cells were frozen in 90% (v/v) FCS and 10% (v/v) DMSO. When neonates became available UCB-$CD133^+$ cells were resurrected and seeded into Stemspan media supplemented with Flt3L, SCF, TPO and IL-6 and cultured overnight. The following day, cells were harvested by aspiration and reselected for CD133 positivity by MACS. $1x10^5$ cells were resuspended in PBS-1% (w/v) BSA and kept upon ice until cells were administered.

After 4 and 8 weeks following adoptive transfer into neonates, peripheral blood was harvested via the tail vein, collecting 20-25 µl of blood per animal. 75% of blood was lysed using Red Blood Cell (RBC) Lysis buffer which contained: 15mM ammonium chloride, 10mM potassium bicarbonate, 1mM EDTA in distilled H_20 at pH 7.4. Cells were resuspended in 0.5ml RBC lysis buffer for 10 min at RT. Cells were then washed with PBS-5% (w/v) BSA. Lysed and non-lysed cell fractions were blocked using Blocking solution, comprising: PBS-5% (w/v) BSA, 10% (v/v) human FcR blocking, 5% (v/v) mouse FcR blocking, for 15 min on ice. Sample volumes were then made up to the appropriate staining volume in PBS-5% (w/v) BSA prior to the addition of mAbs. A fraction of each cell population was combined for FMO controls. Cells were stained for 20 min on ice, washed and resuspended in MACS Buffer for flow cytometry.

Animals were sacrificed after 12 weeks and cells were harvested from the spleen, bone marrow and peritoneal cavity. Peritoneal cells were extracted as described by Ray et. al.,

(Ray and Dittel, 2010). Briefly, mice were cleaned with 70% (v/v) ethanol and the outer skin of the peritoneal cavity was cut and pulled back. 5ml of ice cold PBS-1% (w/v) BSA was injected into the peritoneal cavity using a 27g needle. The peritoneal cavity was massaged to dislodge cells before a 25g needle was inserted to withdraw fluid. The peritoneum was then cut open to harvest the remaining fluid using a 1ml Gilson pipette. Solutions harvested from the peritoneal cavity were monitored for traces of blood. Splenocytes were harvested by extracting the spleen and then mashing gently with the back of a 1ml syringe in a 40µm cell strainer. Cells were washed though with ice cold PBS-5% (w/v) BSA. Bone marrow cells were harvested from femurs of the hind legs. Briefly, the ends of the femur were cut using surgical scissors and the bone marrow was flushed with PBS-5% (w/v) BSA. Single cell suspensions were generated by gentle aspiration with a 1ml Gilson pipette.

Harvested cells were then incubated with RBC lysis buffer for 10 min at RT, filtered through a 35 µl cell strainer and washed. Viable cell counts were then determined using a haemocytometer and Trypan Blue (as described in section 2.2.2). Cells were resuspended in Blocking solution and incubated on ice for 15 min before the addition of mAbs for 20 min. Samples were then analysed by flow cytometry using DAPI as a viability stain with appropriate compensation settings and FMOs (as described in section 2.4.1).

2.11 Statistical tests

Statistical tests were performed using GraphPad Prism 6 software (GraphPad Software). The statistical significance of differences was determined using the Student's t-test for unpaired data. Data are expressed throughout as mean ± standard deviation (SD). Symbols/abbreviations used are, NS= $P>0.55$, *= $P\leq0.05$, **= $P\leq0.01$, ***= $P\leq0.001$, ****= $P\leq0.0001$.

Chapter 3.

The generation of haematopoietic progenitors with multilineage potential from human induced pluripotent stem cells in vitro.

3.1 Aims and objectives

The overall aim was to establish and characterise a robust *in vitro* culture system for the differentiation of human iPS cells to produce haematopoietic progenitors. More specifically to;

1) Understand the temporal dynamics and identity of haematopoietic progenitors arising in an iPS/OP9 co-culture system.

2) Investigate the mulitilineage potential of iPS-derived $CD34^+$ haematopoietic progenitors.

3) Compare the global gene expression profile of iPS-derived and HSC-derived lymphocytes.

4) Describe a serum and feeder-free culture system for the efficient derivation of haematopoietic progenitors from iPS cells.

3.2 Background

Pluripotent stem cells have the potential to differentiate into every cell type of the three germ layers. For applications such as disease modelling, drug screening and potentially as a therapeutic cell source, pluripotent stem cell differentiation to the cell type of interest must be directed and tightly controlled. The traditional description of differentiation is illustrated by Waddington's epigenetic landscape model (Figure 14), where step-wise lineage fate choices are made upon encountering valleys and ridges that ultimately restrict and separate the terminally differentiated cells (Waddington, 1957). Elements of this model have been challenged not only by the advent of iPS cell technology *per se*, but also by the numerous accounts of direct conversion that switches one terminally differentiated cell type into another (Takahashi and Yamanaka, 2006, Vierbuchen et al., 2010, Sekiya and Suzuki, 2011).

The development of the haematopoietic system results in the production of cell types with vastly different functionality, from oxygen carrying erythrocytes to antibody producing lymphocytes. Furthermore, haematopoiesis may produce different subsets of blood cell lineages during the first and second embryonic waves of development (Yoshimoto et al., 2011, Mold et al., 2010, Schulz et al., 2012). To date, it has not been possible to produce haematopoietic stem cells *in vitro* from a pluripotent source, although a wide variety of mature blood cell types have been described (Choi et al., 2011a, Kennedy et al., 2012). How these differentiated haematopoietic cell types relate to those found in the adult and/or to cells of HSC orgin is an interesting and important question.

Assays frequently used to assess haematopoietic potential include the *in vitro* CFU assay, which provides a quantitative, accessible and cost-effective system for investigating myeloid differentiation capacity. The serial transplantation reconstitution assay remains the gold standard for assaying HSC potential but carries a high cost and does not allow for the continuous observation or accessibility of injected cells. Furthermore, in the pluripotent stem cell field where reconstituting HSCs have not been generated, techniques to permit progress towards this end goal are required.

The haematopoietic niche is primarily composed of stromal, endothelial and other blood cells which interact with haematopoietic cells and secrete factors that instruct differentiation. One approach that has been applied for the expansion of HSCs *ex vivo* and to promote haematopoiesis from pluripotent stem cells is co-culture with stromal cell lines (Nakano et al., 1994, Vodyanik et al., 2005, Taoudi et al., 2008, Harvey and Dzierzak, 2004). Interestingly, most progress has been made with mouse stromal cell lines used in hybrid culture with human cells. One such stromal cell line, OP9, supports the generation of haematopoietic cells,including rare reports of B lymphopoiesis from murine ES cells (Cho et al., 1999). Similarity between ES and iPS cells, suggests that a co-culture system with iPS colonies could also support the development of B lymphocytes. Slukvin and colleagues also described the use of MS-5 stroma in a two-step culture where human ES cells differentiated to B cells (Vodyanik et al., 2005). S17 cells have also been used to promote B lymphopoiesis from mouse tissues and from human UCB but not as a support for the generation of pluripotent stem cell-derived B lymphocytes (Rawlings et al., 1995a, Fluckiger et al., 1998). Differentiation to produce iPS- B lymphocytes may; 1) be an informative readout of HPC potential 2) provide insights into B cell diseases such as

chronic (CLL) and acute (ALL) lymphocytic leukaemias and 3) could potentially be used to produce fully human antibodies *in vitro*.

In haematopoietic ontogeny, the production of B cells can be used to discriminate definitive from primitive haematopoiesis. However, B cell potential is present that is likely to be independent of HSCs, due to timing and anatomical location (Godin et al., 1993, Sugiyama et al., 2007). B cells therefore are likely to be a product of both waves of definitive haematopoiesis. In the mouse, the early B cell population was termed B-1 as these cells arise before B-2 B cells in development. It has been reported that, in mice, HSCs generate B-2 B cells but not B-1a or MZ B cells (Kantor et al., 1992, Hayakawa et al., 1985). Fetal liver HSCs however were demonstrated to have B-1 B cell potential, although it is possible that the cell surface phenotype (Lin^-,c-kit^{high},$Sca\text{-}1^+$) may not completely exclude other non-HSC hematopoietic progenitors (Kikuchi and Kondo, 2006). Moreover, a recent publication by Yoder and colleagues demonstrated that B-1, but not B-2 B cells, are generated in the yolk sac (Yoshimoto et al., 2011). B-1 and B-2 B cells differ not only in origin but also in function. B-1 B cells are innate-like lymphocytes which produce the majority of serum IgM in the absence of infection (Hayakawa et al., 1984). Whether pluripotent stem cell-derived B cells are B-1 or B-2 B cell-like, if indeed B-1 B cells do exist in humans, is an important question for the field. As these populations have not clearly been defined in human systems, this can potentially be achieved by assessing functional characteristics that are known to be associated with mouse B-1/B-2 B cells in pluripotent-derived B cells. Alternatively, a comparison of phenotypic or functional differences between pluripotent-derived B cells and their equivalents generated from HSCs may provide such an insight.

One of the advantages of the OP9 co-culture system is that the addition of cytokines is not required. However, a complex background of cell surface and secreted factors from stromal cells, plus the variability of factors found in serum required for the culture, describe a system in which cellular mechanisms are difficult to dissect. It is therefore desirable to implement a defined culture system where the presence and concentration of all factors are known. In this regard, serum and feeder-free culture systems used to promote haematopoiesis from pluripotent stem cells have progressed with improving efficiencies (Chiang and Wong, 2011, Purpura et al., 2008, Salvagiotto et al., 2011). However, there has as yet been no reports of lymphopoiesis in a fully defined system

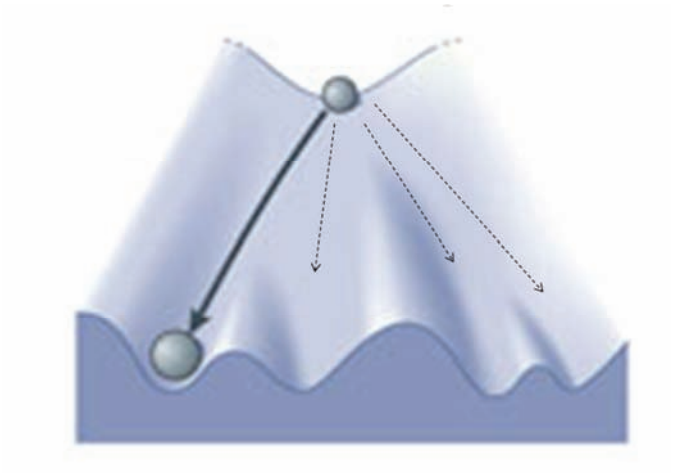

Figure 14 Waddington's landscape model.
Waddington's model described the epigenetic landscape of cell differentiation where, at the top of the hill the ball has the potential to roll in any downward direction. As the ball moves down the hill it encounters valleys and ridges, the direction the ball then places restrictions on direction. At the bottom of the hill the ball, or the terminally differentiated cell is stably positioned. Image adapted from Nature Reviews Molecular Cell Biology (Ladewig et al., 2013).

3.3 Results

3.3.1 Demonstrating the capacity of OP9 stroma to support the differentiation of iPS cells and yield populations expressing haematopoietic and endothelial markers.

3.3.1.1 Human iPS cells in co-culture with OP9 stroma differentiate to produce cells expressing endothelial- associated molecules and early haematopoieitic markers, that arise prior to the expression of CD45- the pan leukocyte marker.

OP9 stromal cells were isolated from *op/op*$^{-/-}$ mice by Nakano and colleagues in 1994 and were demonstrated to provide a supporting environment for haematopoieitic differentiation of pluripotent stem cells, without the requirement for supplementation with additional fators (Nakano et al., 1994). This co-culture system therefore appeared to be a suitable assay for promoting the generation of human iPS-haematopoieitic progenitors, as has also been described by others (Choi et al., 2009).

OP9 stromal cells undergo a gradual change of phenotype and show a reduction in supportive capacity if suboptimal conditions are introduced. Important variables in this culture system are the serum batch used, the density of cells, the feeding regime and the sourcing of media components (as described in section 2.2.3.2). OP9 cells should be flat, large cells (Figure 15) at the expense of a fibroblastic morphology and lack significant levels of adipocyte differentiation. For use as a supportive feeder layer to promote haemato-endothelial differentiation from iPS cells, OP9 stromal cells were seeded onto

bovine gelatin-coated (0.1% (v/v)) 10 cm dishes following a split ratio of 1:4 in 10 ml of OP9 Growth media. Cells were then cultured for 4 days before confluency was reached, whereupon half of the media was exchanged with fresh OP9 growth media and the cultures further maintained, without additional feeding, for use between days 8 to 12 from seeding. By day 4, OP9 cells were confluent (Figure 15 Aii), forming an overconfluent mesh by day 8 (Figure 15 Aiii).

C18 or C19 iPS colonies were harvested from routine culture by incubation with 1mg/ml collagenase IV, when colony size was maximal without allowing for spontanous differentiation, aiming to maintain colony size. Colonies, equivalent to 4-6x10^6 cells, were then plated onto day 8 to 12 OP9 stroma in Differentiation media (described in 2.1.1). Non-adherent colonies were removed by complete replacement of media after 24 hours of seeding. Thereafter, colonies were maintained in 20 ml of culture media as this has been suggested to decrease the propensity for mesenchymal differentiation when compared to lower media volumes (Vodyanik and Slukvin, 2007). The morphology and integrity of iPS colonies was generally retained for the first 3 to 4 days of co-culture (Figure 15 Bi) before cells were observed to egress from colonies and develop into more complex phase-dark sac-like and cord-like structures that have previously been associated with haematopoiesis (Vodyanik et al., 2005). Cells with an endothelial-like pebblestone morphology could also be observed (Figure 15 Biii) (Choi et al., 2011a).

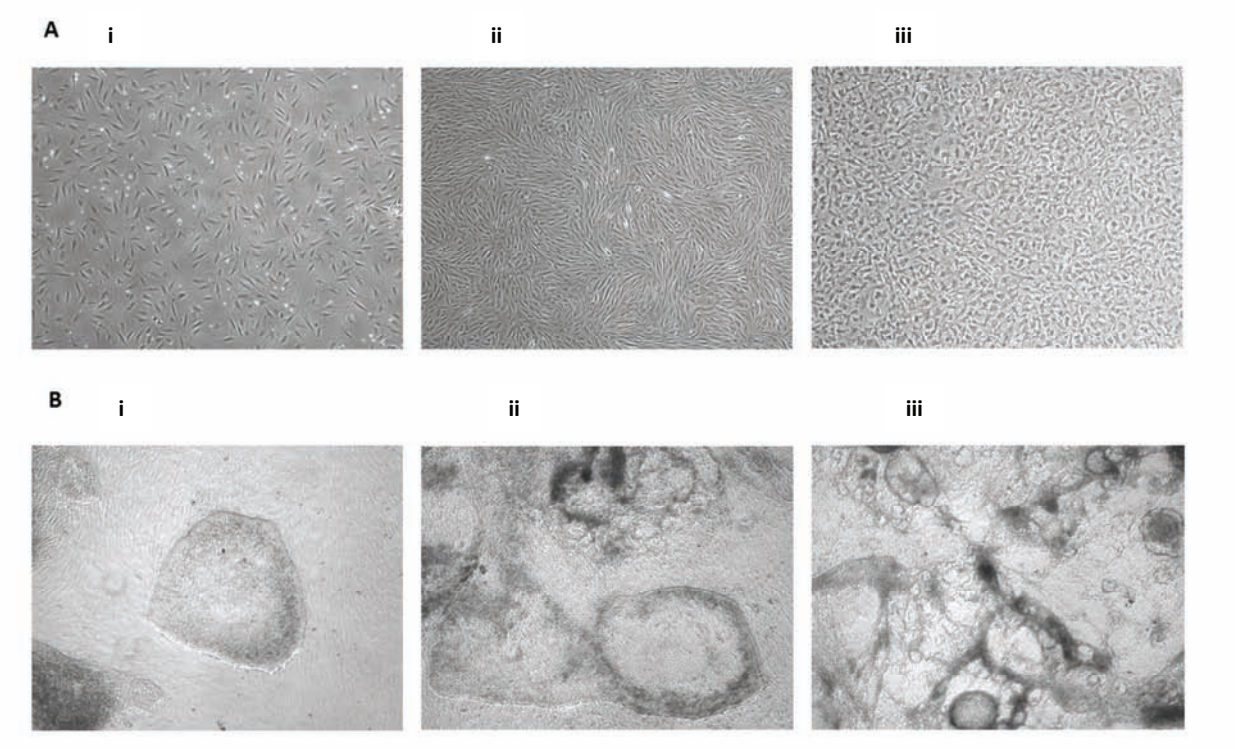

Figure 15 Morphology of OP9 stromal cells alone and in co-culture with iPS colonies.
Representative bright field images (x4 magnification) of gelatin-adapted OP9 stromal cells grown as a monoculture (A) prior to the introduction of iPS cell colonies. OP9 stromal cells were maintained at a high density as can be seen in images taken 24 hours after seeding (i), large, flat cells displaying the required morphology. Within 4 days of culture OP9 cells had become confluent, forming swirl- patterns (ii) and following a further 4 days of maintenance (iii) cells had become overgrown and were suitable for use in the co-culture assay. C18 or C19 iPS colonies were then seeded onto day 8-12 OP9 cells. Colony integrity was maintained for the first 4 days of co-culture (Bi) Coverage of OP9 cells by iPS-derived cells had increased dramatically by day 6 (ii). Cells with an endothelial-like morphology could be detected in addition to phase-dark sac-like structures and cord-like structures which have been associated with haematopoiesis, as seen on days 8 to 10 (iii).

To better understand the populations arising during differentiation, co-cultures of C18 or C19 iPS cells with OP9 stroma were established as described (2.6.1). Whole cell populations, including both adherent and non-adherent cells, were harvested at regular time points for assessment by flow cytometry. The objective was to track the expression of previously described haematopoietic and endothelial-associated cell markers. Expression of CD34, CD31 and CD144 was observed on day 5 of co-culture (day 5 $CD34^+$ cells 1.4% ± 0.7, mean ± SD) in the absence of the haematopoietic markers- CD43, CD41a and CD45 (day 5 $CD43^+$ cells 0.0% ± 0.1, mean ± SD)(Figure 16)(Appendix Table 17). This, therefore, suggested the generation of an endothelial-like population or perhaps of a progenitor with a broader potency. By day 6, a small fraction of cells were observed to express CD41a and CD43, with an increase in the proportion of cells expressing these early haematopoietic markers between days 7 to 9 (day 8 $CD43^+$ cells 3.0% ± 0.6, mean ±SD)(Figure 16)(Appendix Table 17). By day 12 of co-culture, the OP9 stromal cells had been in culture for 20 days or more and appeared, by inspection of morphology, to be largely reduced in number. Day 12 or 13 co-culture cells were harvested and the whole cell fraction was replated onto a fresh OP9 feeder layer without selection. This replating step resulted in an increase in the proportion of cells expressing haematopoietic and endothelial markers but did not significantly impact upon the relative expression of cell surface markers, when compared to assays where a replating step had not been implemented. $CD45^+$ cells were first observed on day 10 of culture and increased in number (day 8 $CD45^+$ cells 0.1% ± 0.2 and day 14 $CD45^+$ cells 1.9 ± 0.2, mean ± SD). By day 22, $CD45^+$ cells represented the predominant population, of the markers assessed, in co-

culture (day 22 $CD45^+$ cells 17.5% ± 0.9, mean ± SD)(Figure 16). In summary, the expression of endothelial-associated markers was observed prior to the presence of the early haematopoietic molecules, CD43 and CD41a which, in turn, arise before cell surface CD45 could be detected.

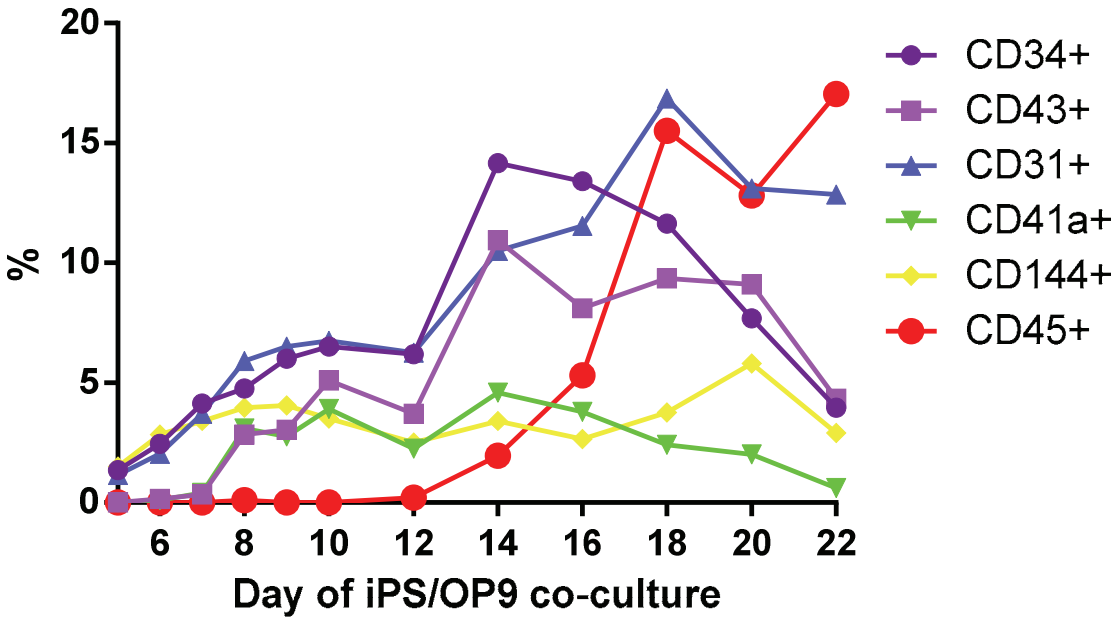

Figure 16 In co-culture with OP9 stromal cells, iPS cells differentiate and express haematopoietic and endothelial-associated cell markers.
Differentiated C18 and C19 iPS colonies on OP9 stromal cells were harvested by incubation with collagenase IV and trypsin digestion, and stained with the appropriate mAbs before being analysed by flow cytometry. A replating step was performed on day 12/13 where the whole cell fraction was reseeded onto fresh OP9 stromal cells. On day 5 of co-culture, small numbers of $CD144^+$, $CD34^+$ and $CD31^+$ cells were detected (day 5 $CD34^+$ cells 1.4% ± 0.7 SD) in the absence of the expression of haematopoietic markers (day 5 $CD43^+$ cells 0.0% ± 0.1 SD). On day 6/7, the first $CD43^+$ and $CD41a^+$ cells were observed which subsequently increased in number. CD45 expression was then detected on day 10/11 and by day 22 the $CD45^+$ cells were the predominant population in co-culture (day 8 $CD45^+$ cells 0.1% ± 0.2 and day 22 $CD45^+$ cells 17.5% ± 0.9). Values are expressed as mean percentage of cells expressing marker of total viable population ± SD where n=3 (detailed in Appendix Table 17). Data are representative of the mean from n=3 independent experiments.

3.3.1.2 CD34$^+$ cells harvested from day 10 iPS/OP9 co-cultures are heterogeneous.

To enable downstream applications it was important to identify a time point and population from which haematopoietic progenitor cells could be isolated. Two main considerations were: i) the ability to select the optimum number of cells committing to the haematopoietic lineage, and, ii) that haematopoietic cells in continued culture may become restricted in their differentiation potential. Day 10 was initially selected as a temporal window when expansion of cells expressing early haematopoietic markers could consistently be observed before a significant proportion of the population expressed CD45.

CD34$^+$ cells were enriched by MACS from day 10 C18 or C19 iPS/OP9 co-cultures and were then stained for haematopoietic and endothelial cells markers to provide a better insight into the identity of this population. CD34$^+$ cells selected from day 10 co-cultures by MACS typically had a purity of greater than 80% (C18 iPS CD34$^+$ 87.1% ± 4.7 and C19 iPS CD34$^+$ 81.6% ± 3.4, mean ± SD) (2.5.2.1). The number of CD34$^+$ cells typically harvested from one 10cm dish of day 10 iPS/OP9 cultures was in the region of $4x10^5$ CD34$^+$ cells (C18 iPS $4.5x10^5$ ± 0.7 and C19 iPS $3.7x10^5$ ± 0.6, mean ± SD) (2.5.2.1).

A subpopulation of CD34$^+$ cells co-expressed CD43, a marker that first defines cells of the haematopoietic lineage (Figure 17) (Vodyanik et al., 2006, Wang et al., 2012). Furthermore, the CD34$^+$CD43$^+$ population has been demonstrated by others to have lympho-myeloid potential (Vodyanik et al., 2006). The majority of CD34$^+$ cells were CD31$^+$, with a small fraction of CD34$^-$CD31$^+$, as well as CD34$^+$CD31$^-$ cells (Figure 17). KDR expression was detected in a subpopulation of CD34$^+$ cells, as was Tie-2 and CD144. This

$KDR^{+}Tie\text{-}2^{+}CD144^{+}$ phenotype was observed within the $CD34^{high}$ fraction, whilst $CD34^{mid}$ cells appeared mainly $KDR^{-}Tie\text{-}2^{-}CD144^{mid}$ (Figure 17). $CD34^{+}$ cells were mainly $CD45^{-}$, with less than 5% of cells expressing this marker. $CD43^{+}$ cells, within the CD34 enriched fraction, could be further sub segmented into $CD41^{+}$ and $CD41a^{-}$. All $CD41a^{+}$ cells expressed CD43 (Figure 17). Interestingly, the $CD43^{+}$ population expressed a high level of CD31, an intermediate level of CD144 and was negative for KDR (Figure 17).

To assess whether this day 10 population distribution was maintained across different iPS cell lines, both C18 and C19 iPS cells were differentiated on OP9 stromal cells and harvested for analysis by flow cytometry on day 10, where similar populations were observed. In a comparison of C18 and C19 iPS lines for the propensity of $CD34^{+}$ cells to express CD43, as a possible indicator of haematopoietic potential, there was no difference between iPS cell clones (C18 33.2% ± 10.8 and C19 30.5% ± 15.6 mean ± SD)(Figure 18). Variation in haematopoietic differentiation efficiency, as assessed by the percentage of $CD34^{+}$ cells that co-expressed CD43, was high. This variability could have been due to a number of factors, such as: colony size of iPS cells when seeded into co-culture, number of iPS colonies plates, serum batch used in culture media and passage number of iPS cells. The contribution of these potential causes of variability was not further assessed, with the exception of serum batches, which were tested prior to use in the co-culture system.

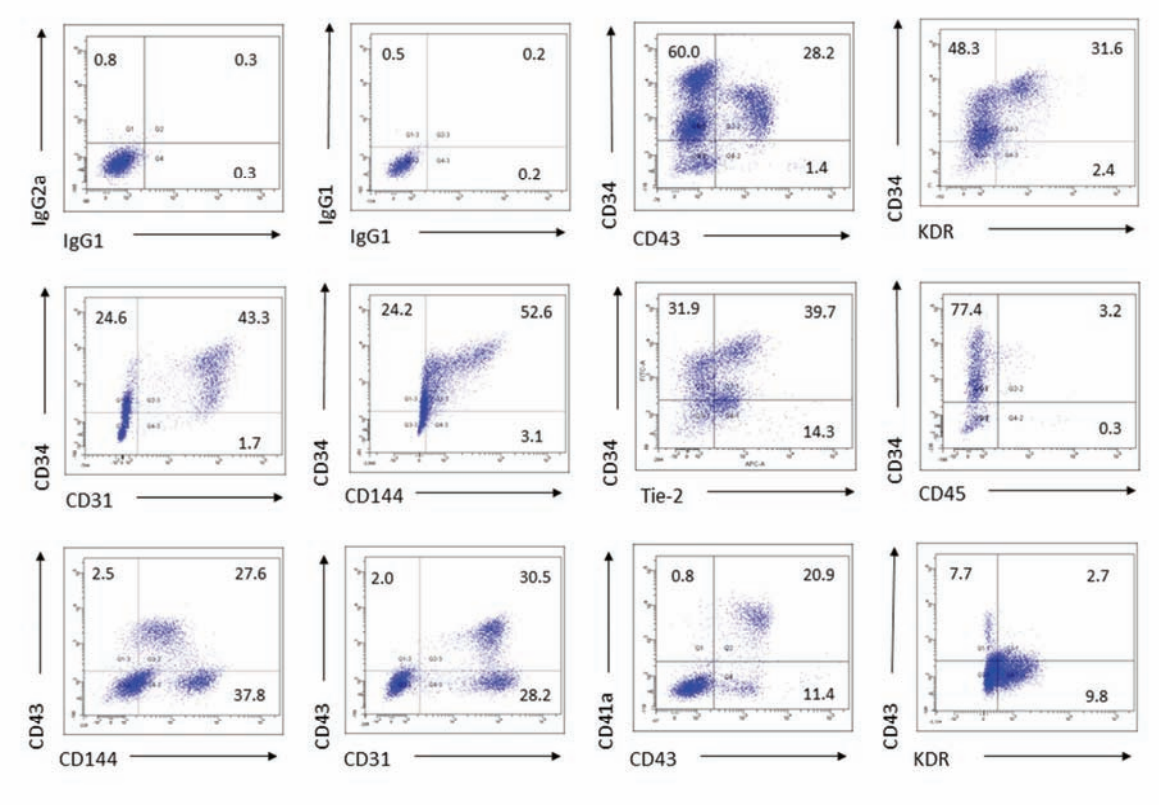

Figure 17. Expression of haematopoietic and endothelial- associated cell surface markers on iPS-CD34$^+$ cells harvested from day 10 iPS/OP9 co-cultures.

C18 iPS cells were seeded onto overconfluent OP9 stroma and maintained for 10 days as described in (2.2.3.2). Cultures were then harvested and the CD34$^+$ fraction isolated by MACS to enrich for human cells that had differentiated towards the mesodermal lineage. Purity of CD34 enrichment was typically >80% (2.5.2.1). Cells were stained with mAbs reactive to molecules known to be expressed by a range of haematopoietic and endothelial cells before being analysed by flow cytometry. Varying numbers of CD34$^+$ cells co-expressed CD43, KDR, Tie-2, CD31 and CD144. CD43$^+$ cells were CD144^{mid}, CD31$^+$, KDR$^-$ and could be subdivided into CD41a$^+$ and CD41a$^-$ fractions. Representative image, n=3 independent experiments.

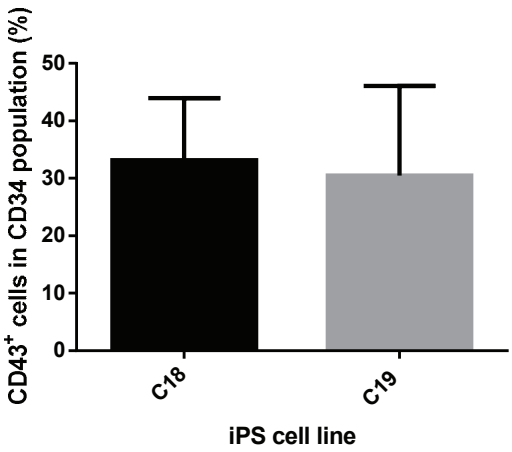

Figure 18 Comparison of C18 and C19 iPS cell lines in their capacity to produce CD43$^+$ haematopoietic cells.
The percentage of CD43$^+$ cells in the CD34 fraction isolated from day 10 co-cultures when either C19 or C18 iPS cell lines were differentiated, metric used as an indicator to assess the haematopoietic differentiation efficiency across iPS cell lines. CD43$^+$ cell number as a percentage of the total CD34 population showed no significant differences between C18 and C19 iPS cell lines (C18 33.2% ± 10.8 and C19 30.5% ± 15.6). Values are mean ± SD of n=6 independent experiments.

3.3.2 Multilineage differentiation of haematopoietic progenitor cells derived from iPS cells.

3.3.2.1 The myeloid lineage potential of haematopoietic progenitors increases with extended culture.

The colony forming unit (CFU) assay provides a quantitative and clonogenic readout of haematopoietic potential that has been well established and frequently described by many independent research laboratories. Analysis of colony morphology in the CFU assay enables the analysis of progenitor capacity at a single cell level, such as can be described with the CFU-E, BFU-E and CFU-GEMM colonies (described in 2.6.4). Red blood cells can easily be detected in a CFU assay due to their unique ability to haemoglobinise. Colonies are labelled CFU-E (erythroid), if they are made up of less than 3 clusters and less than 100 cells. If homogenous red blood cell colonies are composed of 3 or more cluster then they are designated BFU-E (burst forming unit-erythroid). In the assessment of adult haematopoietic progenitor and stem cells, CFU-E have been described as a readout for more mature erythroid progenitors with a reduced proliferation capacity, in comparison to BFU-E cells. Non-red blood cell colonies can be identified as CFU-G, CFU-M or CFU-GM dependent upon whether they are composed of morphologically distinct granulocytes, macrophages or both. For the purposes described herein, these three colonies types were not distinguished and were scored as CFU-G/GM. The final class of colonies generated in the CFU assay are CFU-GEMM (granulocyte, erythroid, macrophage, megakaryocyte) which identifies the presence of a multi-lineage myeloid progenitor.

It was initially observed that $CD43^+$ cells, isolated from day 9/10 C18 or C19 iPS/OP9 co-cultures, yielded CFU-G/GM and a small number of CFU-E, but no BFU-E or CFU-GEMM (Figure 19). Therefore, it was hypothesised that haematopoietic differentiation potential, as assessed by the CFU assay, might change with increasing time in co-culture and coincident expansion of the $CD45^+$ population. C18 or C19 iPS colonies were seeded onto OP9 stromal cells and cultured for 10 days, whereupon $CD34^+$ cells were enriched by MACS. $CD34^+$ cells were then cultured with fresh OP9 cells for a further 12 days, with half media changes every 2 days. On day 22, cells were harvested by incubation with collagenase IV/trypsin and enriched by MACS for $CD43/45^+$ cells. This was achieved by mixing one volume of CD43 microbeads with one volume of CD45 microbeads, prior to incubation. $CD43/45^+$ cells, when enriched by MACS, had typically purities of >90% (2.5.2.2). Day 22 $CD43/45^+$ cells were seeded into the CFU assay and colonies were scored after 14 days of culture.

Early (harvested from day 9/10 co-cultures) and late (from day 22 co-cultures) haematopoietic progenitors had a similar potential to produce CFU-G/GM colonies (Figure 19). Both early and late HPCs generated a limited number of CFU-E colonies (Figure 19). The clearest difference, however, was observed with the capacity to form BFU-E and CFU-GEMM. This potential was absent from the early HPC population but present in the late HPC population (Figure 19). The number of BFU-E colonies observed was greater when late HPCs were seeded, in comparison to early HPCs, this difference was statistically significant (Figure 19). CFU-GEMM colonies were never detected in early HPC seeded assays, but were present in late HPC cultures. However, the number of CFU-GEMM colonies derived from late HPCs was low and variable. Therefore, the difference

between CFU-GEMM potential in early HPC versus late HPC cultures did not reach statistical significance in 3 independent experiments (P=0.07). In summary, continued culture of iPS colonies with OP9 stromal cells coincides with an increase in multipotent myeloid progenitors, as elucidated by the CFU assay.

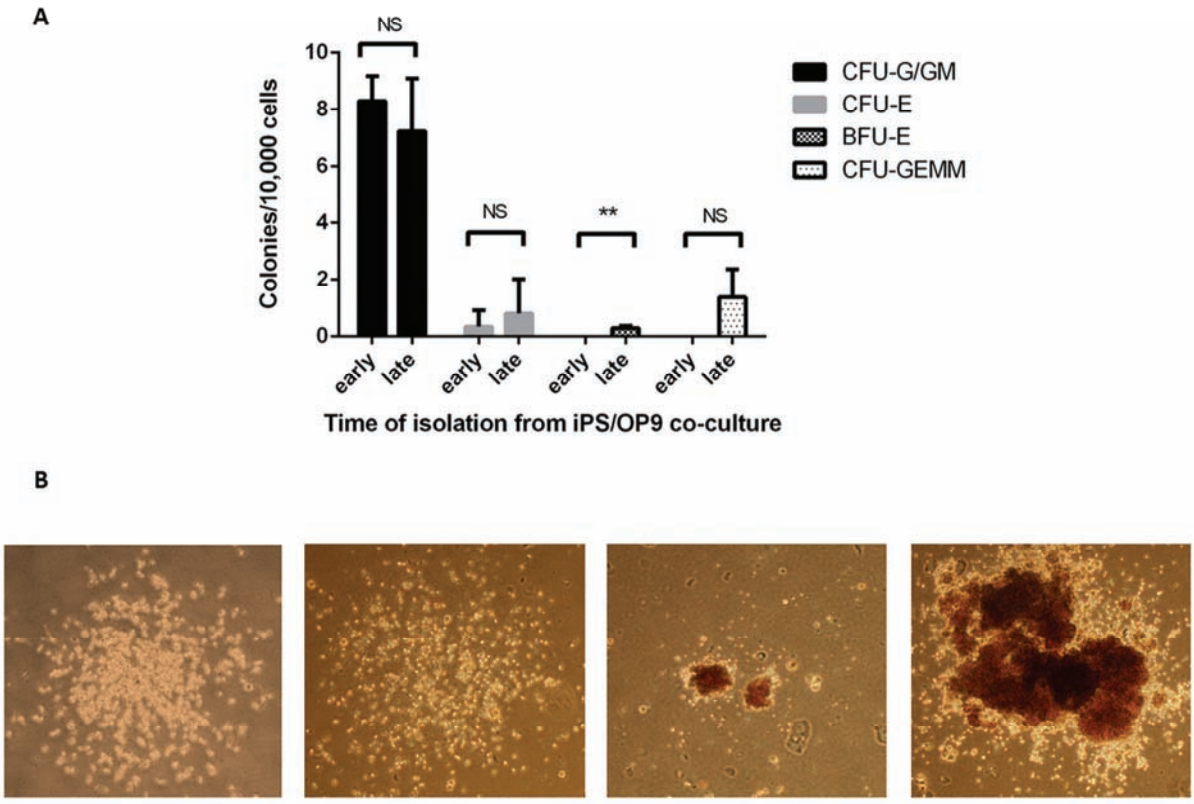

Figure 19 Comparison of day 8-10 (early) and day 22 (late) iPS- progenitor CFU potential following OP9 co-culture.

iPS colonies were co-cultured with OP9 stroma for 8-10 or 22 days respectively when populations were enriched for $CD43^+$ cells (day 8-10/early) or $CD43/45^+$ cells (day 22/late). Scoring of CFU assays (A) revealed CFU-GEMM and BFU-E potential was exclusively found in the day 22 population. Mean ± SD. Unpaired t-test, NS $P>0.05$, $**P\leq0.01$. (B) x4 brightfield images of representative CFU colonies (left to right); early CFU-G/GM, late CFU-G/GM, early CFU-E, late CFU-GEMM. n=3 independent experiments.

3.3.2.2 iPS-derived haemato-endothelial progenitors are capable of differentiation to multiple lineages.

The *in vitro* assessment of the capacity of a haematopoietic stem or progenitor cell population to differentiate into myeloid and lymphoid progeny can be seen as a functional assay to align cell surface phenotype with identity. The CFU is well described but only enables myeloid differentiation. The capacity of human pluripotent stem cells to differentiate into T lymphocytes has robustly been described with the use of OP9 stromal cells that ectopically express the Notch ligand Delta-1 (Kennedy et al., 2012, Timmermans et al., 2009). Human pluripotent stem cell differentiation to the B lymphocyte lineage however, has only been described once from human ES cells and the resulting $CD19^{+}$ fraction was not further characterised (Vodyanik et al., 2005).

The objective was to promote B cell differentiation from iPS-HPCs, alongside the production of myeloid cells, representative of both megakaryocyte-erythroid and granulocyte-macrophage lineages. As cells with an endothelial phenotype ($CD34^{high}KDR^{+}Tie\text{-}2^{+}CD144^{+}CD45^{-}$) were detected on day 10 and, as endothelial cells are a component of the adult haematopoietic niche, the outgrowth of endothelial-like cells was also an objective. Simultaneous T and B lineage differentiation has been reported to be mutually exclusive, (Calvo et al., 2012, Wilson et al., 2001). Therefore, T cell differentiation was not pursued. To promote multilineage differentiation from iPS-HPCs a variety of cytokine regimes were adopted (summarised in Table 7). IL-3, IL-7, SCF and Flt3L were used to promote B cell differentiation, as has previously been described in the human ES cell/MS-5 stromal assay (Vodyanik et al., 2005). To promote endothelial differentiation, VEGF alone was included, as it is a known growth factor for this cell type

both *in vivo* and in human ES cell cultures (James et al., 2010, Gerber et al., 1999). Red blood cell conditions were adapted from Chou *et al.* and involved the addition of IL-3, SCF, IGF-1, Dexamethasone and EPO (Chou et al., 2011). Finally, the fourth set of conditions included all of the factors listed (IL-3, IL-7, SCF, Flt3L, VEGF, IGF-1, Dexamethasone and EPO) to potentially encourage multilineage differentiation. OP9 stromal cells were used to promote haematopoietic differentiation from iPS and were therefore also used in this context, to promote multilineage differentiation, in the presence of cytokines. MS-5 stromal cells were compared to OP9 stromal cells, using the same cytokines, as this cell type had been demonstrated to support B cell differentiation from human ES cells (Vodyanik et al., 2005).

C19 iPS cells were differentiated for 10 days on OP9 stromal cells and $CD34^+$ cells were enriched by MACS as previously described (2.6.1). $2.5x10^4$ iPS-derived $CD34^+$ cells/ml were seeded onto OP9 or MS-5 stromal cells in the presence of the cytokine regimes detailed in Table 7. As this assay was not performed at the single cell level it was acknowledged that this was not an assessment of multilineage/stem cell potential but was instead a read-out at the population level. Cultures were maintained for 19 days, harvested by collagenase IV/trypsin incubation, before being stained with mAbs for flow cytometry analysis. CD19 expression was used to identify B cells, CD235a as a marker for red blood cells, CD14 to detect cells of the monocyte-macrophage lineage, CD45 as a pan-haematopoietic marker and a $CD144^+CD45^-$ phenotype as a potential indicator of an endothelial-like population (illustrated in Appendix Figure 75).

Table 7 Cytokine regimes designed to promote myeloid and lymphoid differentiation from haematopoietic progenitors in the presence of OP9 or MS-5 stroma.

	Cytokines	Reference
B cell conditions (B)	IL-3, IL-7, SCF, Flt3L	(Vodyanik et al., 2005)
RBC conditions (RBC)	IL-3, SCF, IGF-1, Dexamethasone, EPO	Adapted from (Chou et al., 2011)
Endothelial conditions (endo)	VEGF	(James et al., 2010)
All factors (All)	IL-3, SCF, IGF-1, Dexamethasone, EPO, IL-7, Flt3L, VEGF	As above

Cytokines were used at the following concentrations; SCF 50ng/ml, Flt3L 50ng/ml, IL-3 10ng/ml, IL-7 20ng/ml, VEGF 10ng/ml, EPO 3U/ml, IGF-1 40ng/ml, Dexamethasone 1µM.

$CD45^+$ haematopoietic cells could be obtained in all culture conditions, albeit at a much reduced frequency in endothelial conditions (Figure 20A). $CD45^-CD144^+$ cells, which may represent an endothelial-like population, were also present in all conditions assayed (Figure 20B). As endothelial conditions generated very few haematopoietic cells, these cultures were not analysed further. A significant number of $CD19^+$ cells were detected, but only in B cell conditions, either with MS-5 or OP9 cells (Figure 21). Variability in the number of $CD19^+$ cells produced between the 2 independent experiments was high. In general however, when the same population of $CD34^+$ cells was seeded into MS-5 or OP9 co-culture, a greater number of $CD19^+$ cells were detected from MS-5 co-cultures (Figure 21). This MS-5 co-culture system therefore was carried forward as a method to promote B cell differentiation, in addition to the generation of non-B cell haematopoietic cells and endothelial-like cells. To determine whether myeloid cells, representative of both megakaryocyte-erythroid and granulocyte-macrophage lineages, could be detected in MS-5 B cell conditions, the presence of $CD235a^+$ and $CD14^+$ cells was assessed. A small and variable number of $CD235a^+$ cells were present in MS-5 B cell conditions, in comparison to MS-5 All factor or OP9 All factor conditions (that included EPO) (Figure 22A). As the majority of $CD235a^+$ cells in MS-5 B cell conditions expressed low levels of this marker, when compared to CD235a expression levels in MS-5 All factor conditions, it can be concluded that a negligible number of red blood cells are generated in MS-5 B cell conditions. $CD14^+$ cells can be consistently detected in MS-5 B cell conditions, albeit with variable efficiencies with similar comparability between MS-5 and OP9 B cell conditions (Figure 22B).

This experiment was performed with only two independent experiments as the aim was to initially identify conditions in which a B cell, and possibly multilineage readout, could be obtained. Between these two experiments, it is evident that the efficiency of differentiation to generate different cells types was variable. This was most likely due to the use of different serum batches and/or because of different numbers of $CD43^+$ haematopoietic progenitors in the initial $CD34^+$ population seeded. To assess the variability and reproducibility of B lymphocyte generation from C18 or C19 iPS-$CD34^+$ cells in MS-5 co-culture (with B cell condition factors), this experiment was repeated with a consistent and pre-screened defined serum batch. When analysed after 21 days of co-culture, the proportion of $CD19^+$ cells as a percentage of the total cell population was 3.7% ± 0.6 (mean ± SD) and as a percentage of total $CD45^+$ cells, 4.7% ± 1.0 (mean ± SD) (Table 8). The total number of $CD45^+$ cells harvested, when $5x10^4$ $CD34^+$ cells were seeded, was $1.01x10^6$ ± $1.98x10^5$ (mean ± SD) (Table 8). Importantly, $CD19^+$ cells were generated consistently in a large number of experiments (here, 7 out of 7) and, when a number of different serum batches were used.

In summary, B lymphocytes, monocyte-macrophage and endothelial-like cells were shown to be derived from iPS-$CD34^+$ cells in MS-5 co-culture in the presence of IL-7, IL-3, SCF and Flt3L. These conditions were therefore used in the next section and throughout the thesis to promote B lymphocyte differentiation from iPS cells.

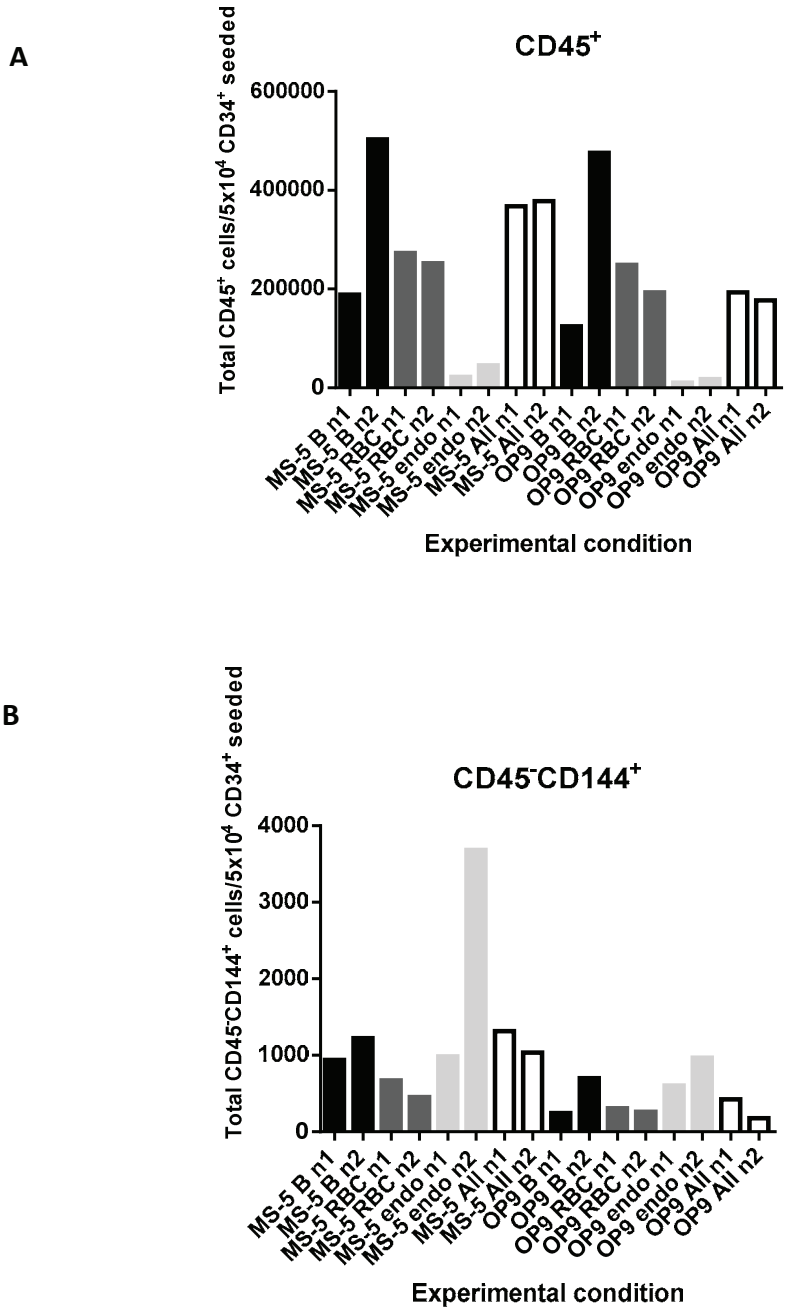

Figure 20 The effect of stromal cell environment and cytokine regime on the differentiation of iPS-CD34$^+$ cells.

CD34$^+$ cells were isolated from day 10 C19 iPS/OP9 co-cultures and seeded into an assay with either MS-5 or OP9 stroma. Cultures were supplemented with the cytokines as detailed in

Table 7. Cells were then harvested by collagenase IV/trypsin incubation on day 19 of co-culture, before being analysed by flow cytometry. (A) >150,000 haematopoietic cells staining positive for the pan-leukocyte marker CD45 could be observed in every condition assessed with the exception on both MS-5 and OP9 Endothelial (endo) cultures. (B) CD144$^+$CD45$^-$ cells, which may have an endothelial identity, were identified in the presence of all cytokine regimes. Values representative for individual experiments (n1, n2). n=2 independent experiments.

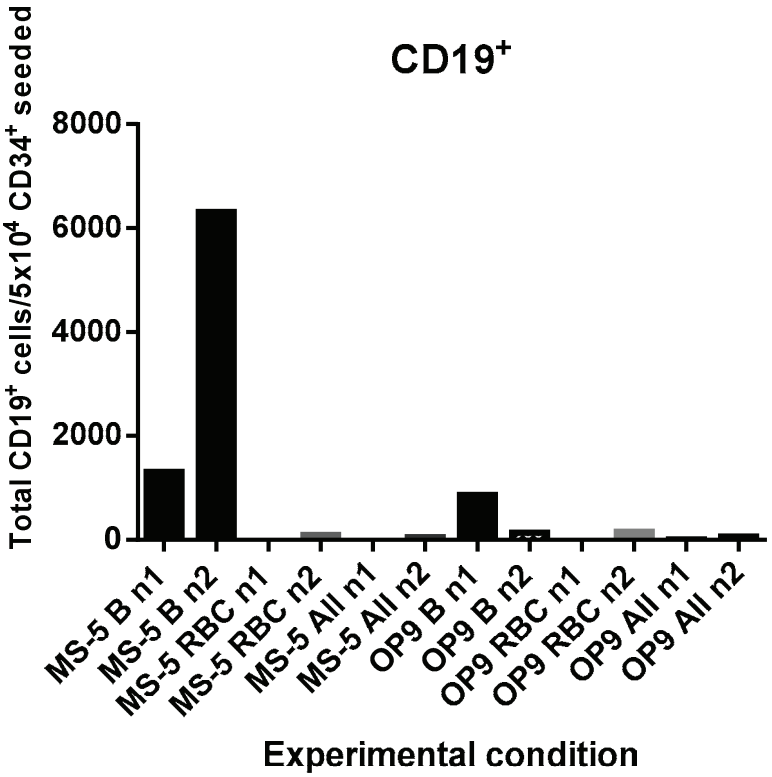

Figure 21 The effect of stromal cell environment and cytokine regime on the B cell differentiation of iPS-CD34$^+$ cells.

CD34$^+$ cells were isolated from day 10 C19 iPS/OP9 co-cultures and seeded into an assay with either MS-5 or OP9 stroma. Cultures were supplemented with the following cytokines as detailed in

Table 7. Cells were then harvested by collagenase IV/trypsin incubation on day 19, before being analysed by flow cytometry. CD19$^+$ B cells were observed in B cell (B) conditions, with greater cell numbers being obtained with MS-5 stroma than OP9 stroma co-cultures. Values representative for individual experiments (n1, n2). n=2 independent experiments.

A

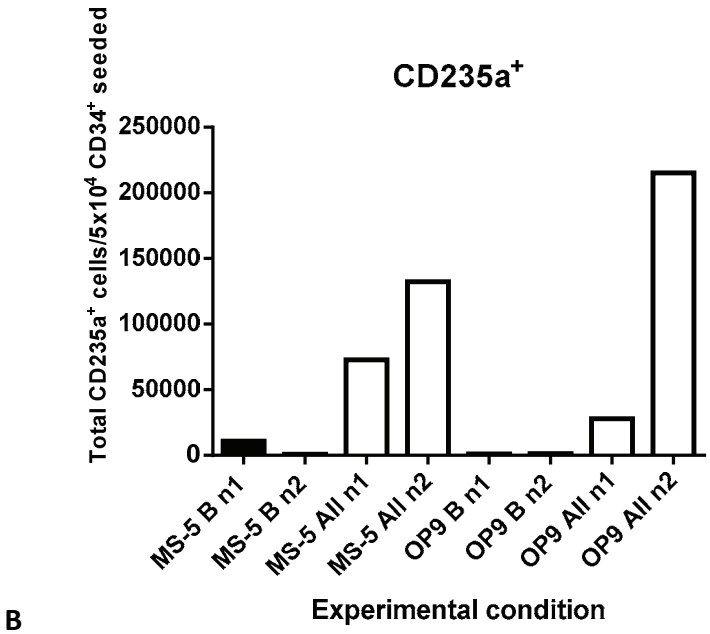

B

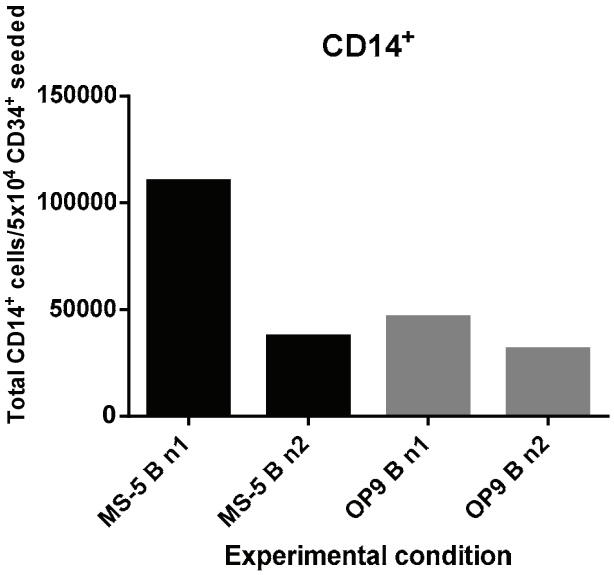

Figure 22 Assessing the presence or absence of CD235a$^+$ and CD14$^+$ cells in B cell conditions. CD34$^+$ cells were isolated from day 10 C19 iPS/OP9 co-cultures and seeded into an assay with either MS-5 or OP9 stroma. Cultures were supplemented with the following cytokines as detailed in
Table 7. Cells were then harvested by collagenase IV/trypsin incubation on day 19, before being analysed by flow cytometry. B cell (B) conditions were the only cultures permissive for B cell generation. (A) CD235a$^+$ cells were generated in MS-5 All conditions but low and variable numbers of erythrocytes were observed in MS-5 B cell conditions. (B) CD14$^+$ cells were generated in B cell conditions with MS-5 or OP9 stromal cells. Values representative for individual experiments (n1, n2). n=2 independent experiments.

Table 8 Variability of B cell differentiation from iPS-CD34$^+$ cells in MS-5 co-culture with IL-7, IL-3, SCF and Flt3L, using the same serum batch.

	Mean	Standard Deviation	Number of independent experiments
CD19$^+$ cells (% of total population)	3.68	0.59	5
CD19$^+$ cells (% of CD45$^+$ cells)	4.70	0.98	3
Total CD45$^+$ cells/5x10^4 CD34$^+$ cells seeded	1,011,428	197,942	7

iPS-CD34$^+$ cells were generated by the co-culture of C18 or C19 iPS cell colonies with OP9 stromal cells for a period of 10 days. Cells were then harvested and MACS enriched for the CD34$^+$ fraction before being reseeded onto MS-5 stroma in Differentiation media supplemented with IL-3, IL-7, SCF and Flt3L. After 21 days of culture, cells were harvested, stained with mAbs and analysed by flow cytometry.

3.3.3 Gene expression profiling of iPS-derived B cells reveals high similarity with UCB-HSC/HPC-derived B cells

3.3.3.1 Isolating $CD19^+CD10^+$ B cells from iPS, fetal and adult sources

Cell identity is frequently attributed by assessing the presence and/or absence of cell surface markers either in isolation or corroborated with expression data for a limited number of genes. Whilst the expression of key transcription factors clearly has a significant impact upon the phenotype of a cell, identity can more accurately be described by a global analysis of gene expression, when used in combination with protein markers. Genome-wide arrays produce data on the expression of known and candidate genes as well as splice variants and are therefore a powerful tool. It was hypothesised that iPS-derived B cells might be fetal-like and demonstrate major differences when compared to HSC-derived B cells.

Four different iPS cell lines were used to generate iPS-B cells. These were kindly provided by Dr. Lee Carpenter and Cheng-Tao Yang in our laboratory or Dr. Pollyanna Goh from UCL and were: i) C19, a cell line produced from dermal fibroblasts using the retroviral delivery of the Yamanaka factors, ii) OPM2, generated from peripheral blood MNCs, iii) OC3, generated from umbilical cord blood MNCs. Both OC3 and OPM2 lines were reprogrammed using episomal plasmids with the Thomson factors, and iv) PA, a cell line generated from donor dermal fibroblast cells was generated using episomal plasmids containing OCT3/4, SOX2, KLF4, TP53, LIN28 and MYCL1 as described by Okita et al. (Chou et al., 2011) (described in 2.2.3.1). iPS lines were therefore generated from a diverse range of cell types using a broad range of integrating and non-integrating reprogramming techniques and range of factors.

$CD19^+CD10^+$ pre-B cells were generated from iPS cell lines by a two-step co-culture system (Figure 23). Initially, iPS cells were co-cultured with OP9 stroma for 10 days, whereupon the $CD34^+$ population was enriched. In the second stage, $CD34^+$ cells were reseeded onto MS-5 cells and cultured with IL-7, IL-3, SCF and Flt3L as previously described for a further 21/22 days (as described in 2.6.2). Cells were then enriched for CD19 expression by MACS, before being FACS sorted to isolate the $CD19^+CD10^+$ fraction (Figure 24). B cells derived from iPS cell lines, OC3, C19 and PA ,were all generated and isolated on the same day, using the same FACS and sorting gates (Figure 24). Within the $CD19^+$ MACS isolated sample, these three cell lines contained a similar proportion of $CD19^+CD10^+$ cells (Figure 24). In comparison, B cells derived from the OPM2 iPS cell line were generated and isolated on a different day using a different FACS machine and voltage settings. OPM2-derived B cells contained a smaller proportion of $CD19^+CD10^+$ cells in the $CD19^+$ MACS enriched population (Figure 24). However, in comparison to controls, and, as $CD19^+$ cells were mainly $CD10^+$, the sorted populations were broadly comparable. RNA was then extracted from iPS-derived B cells and stored at -20°C.

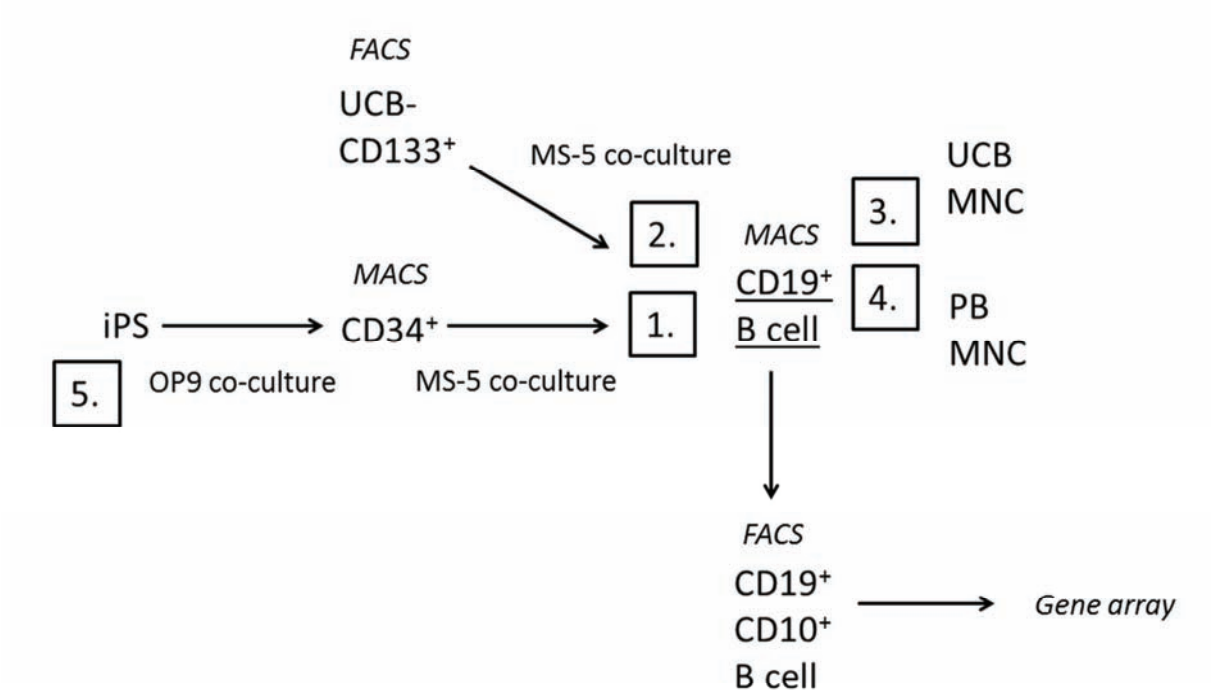

Figure 23 Schematic of B cell generation for gene array comparison.
B cells were generated from iPS cell lines (1.) by differentiation on OP9 stromal cells, isolation of the $CD34^+$ fraction and subsequent co-culture with MS-5 stroma to yield $CD19^+$ B cells. UCB-$CD133^+$ HSC/HPCs (2.) were FACS sorted and differentiated on MS-5 stroma, using the same protocol as applied to iPS cell differentiation, to generate $CD19^+$ cells. B cells were also isolated from UCB MNCs (3.) and PB MNCs (4.). $CD19^+$ cells were enriched by MACS from the 4 different cell types described (with 4 biological replicates) before being FACS isolated for the $CD19^+CD10^+$ fraction. RNA was then isolated for gene array analysis. RNA was also isolated from undifferentiated iPS cell colonies (5.).

As a comparison to iPS-B cells, HSC/HPCs were differentiated to the B cell lineage using the same culture system, MS-5 stroma supplemented with IL-7, IL-3, SCF and Flt3L (Figure 23). This would therefore allow a dissection of the impact of either environmental or cell intrinsic properties on the transcriptional landscape. UCB is a rich source of HSCs that provide long-term and serially transplantable reconstitution (Broxmeyer et al., 1991, Broxmeyer, 2008, Ito et al., 2010). Moreover, UCB is frequently used as an alternative to bone marrow HSCs in the clinic (Gluckman et al., 1989, Wagner et al., 1995, Li and Sykes, 2012, Liao et al., 2011). CD133 is a cell surface glycoprotein that is expressed on a range of cell types including haematopoietic stem and progenitor cells (Yin et al., 1997, Ito et al., 2010). $CD133^{+}CD34^{+}$ cells have been shown to be enriched for long-term repopulating potential, in comparison to $CD133^{-}CD34^{+}$ cells, and therefore potentially described the LT-HSC pool more accurately than CD34 alone (de Wynter et al., 1998, Gallacher et al., 2000, Gorgens et al., 2013). $CD133^{+}$ cells were enriched by MACS from the MNC fraction of UCB (as described in 2.5.2.3). After storage by cryopreservation, $CD133^{+}$ cells were thawed, cultured overnight in Stemspan media with Flt3L, SCF, TPO and IL-6 before being FACS isolated for $CD133^{+}CD19^{-}$ cells to ensure the exclusion of residual B cells (Figure 25). $CD133^{+}CD19^{-}$ cells were isolated from 4 different UCB donors and cells were always subsequently cultured separately to generate biological replicates. A purity check was run on FACS-sorted cells after isolation, which were 100% $CD133^{+}CD19^{-}$ (Figure 25). $CD133^{+}CD19^{-}$ UCB-HSC/HPCs (hereafter referred to as UCB-$CD133^{+}$ or HSC) were then seeded into co-culture with MS-5 stroma, supplemented with cytokines as previously described (as described in 2.6.2). After 21/22 days, cells were harvested and isolated by FACS for the $CD19^{+}CD10^{+}$ fraction (Figure 26). The sorting gate set clearly distinguished $CD19^{+}CD10^{+}$ cells from the negative population and in relation to FMO controls. The gate

was set to include the entire $CD19^{+}CD10^{+}$ population which, in the case of Sample 4, appeared to contain two subpopulations (Figure 26). The $CD19^{+/high}CD10^{+/high}$ population, comparable in fluorescence intensity to iPS-derived B cells, and a second $CD19^{+/mid}CD10^{+/mid}$ population (Figure 26). This $CD19^{+/mid}CD10^{+/mid}$ population was observed in Sample 4 and, to a lesser extent, the other three UCB-$CD133^{+}$ derived B cells. Purity check of sorted B cell populations revealed 100% purity of $CD19^{+}CD10^{+}$ cells (Figure 26). RNA was then extracted from UCB-$CD133^{+}$ derived B cells and stored at -20°C. UCB-$CD133^{+}$ cells produced a greater number of $CD19^{+}$ B cells than iPS-$CD34^{+}$ cells in the same *in vitro* culture system. This can be partially explained by the heterogeneity of the iPS-$CD34^{+}$ population which contains endothelial and mesenchymal progenitors in addition to progenitors of the haematopoietic lineage (Vodyanik et al., 2006). In comparison, the UCB-$CD133^{+}$ population is generally considered to be a haematopoietic stem/progenitor cell pool.

UCB and peripheral blood (PB) were also collected as a source of neonatal and adult B cells that had been generated without *in vitro* manipulation. Here UCB, and PB, from 4 different donors were collected and the MNC fraction was isolated by density centrifugation. B cells were then enriched by MACS selection for $CD19^{+}$ cells before FACS isolation of the $CD19^{+}CD10^{+}$ population (Figure 26). Both UCB and PB $CD19^{+}$ cells had a range of CD10 expression. Cells were therefore sorted that were $CD19^{+}CD10^{high}$. In the UCB B cell samples this gate was equivalent to around 30% of the MACS enriched $CD19^{+}$ fraction (Figure 26). In comparison, this gate only included around 5% of PB MACS enriched $CD19^{+}$ cells (Figure 26). RNA was then extracted from UCB and PB B cells and stored at -20°C.

Ideally, B cell populations from the different sources would have been FACS isolated on the same day, using the same machine and applied gates. This however was not achievable due to the availability of primary cells and limitations with equipment availability. However, overall, clearly distinct $CD19^{+}CD10^{+/high}$ cells were FACS isolated from all samples described.

As a non-B cell comparison, RNA was also isolated from iPS lines in their pluripotent, undifferentiated state. Here, iPS cell lines were cultured in mTesR until colonies were large but distinct and undifferentiated, lysis buffer was then added directly to the adherent cells and RNA was extracted.

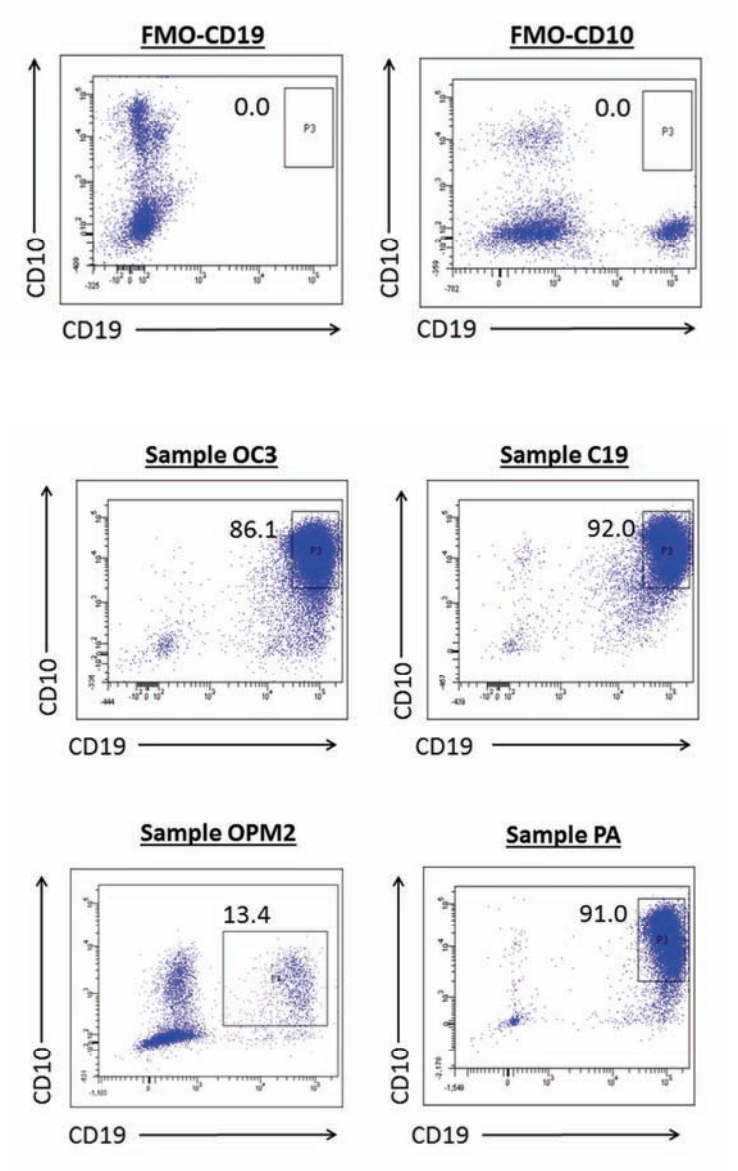

Figure 24 FACS gating approach taken for the isolation of iPS-derived B cell populations.
$CD34^+$ cells were generated following co-culture of iPS colonies (C19, OPM2, OC3 and PA iPS cell lines) with OP9 stroma. $CD34^+$ cells were enriched by MACS and seeded into co-culture with MS-5 cells and cultures were supplemented with IL-7, IL-3, SCF and Flt3L. Cultures were maintained for 21/22 days and harvested by collagenase IV/trypsin incubation. Cells were then enriched by MACS using CD19-PE and anti-PE microbeads before being stained with mAbs to CD10 for FACS isolation. FMO controls were run using whole cell fractions as MACS enrichment involved the usage of fluorescently labeled antibodies (CD19-PE and anti-PE microbeads). FMO controls for the OPM2 sample can be seen in Figure 26. $CD19^+CD10^+$ cells were isolated from iPS-derived B cell populations using the gates shown.

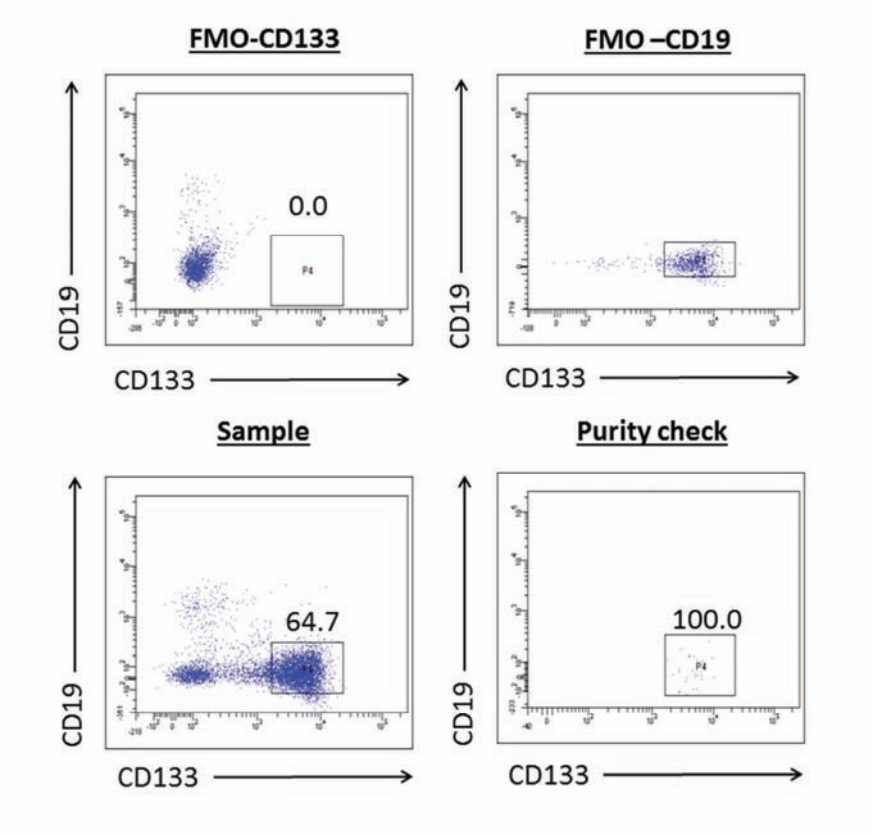

Figure 25 FACS gating approach taken for the isolation of CD133^{+}CD19^{-} cells from UCB MNCs.
The MNC fraction was isolated from UCB, CD133^{+} HSC/HPCs were enriched by MACS. Cells were then FACS isolated to eliminate CD19+ B cells. CD133^{+}CD19^{-} cells were seeded into co-culture with MS-5 stroma supplemented with IL-7, IL-3, SCF and Flt3L to promote B cell differentiation. Sorted cells were checked for purity and were demonstrated to be 100% pure. Representative image from 4 different donor samples.

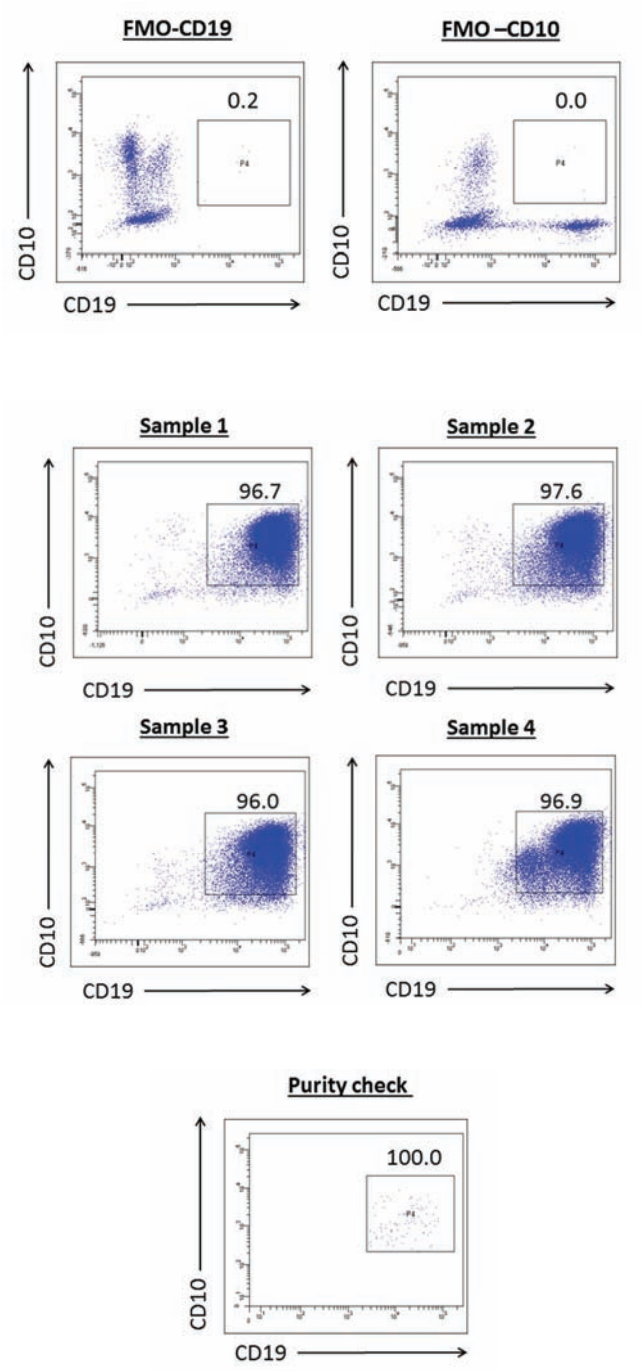

Figure 26 FACS gating approach taken for the isolation of UCB- derived B cell populations. $CD133^{+}CD19^{-}$ cells were FACS isolated from UCB MNCs and seeded into co-culture with MS-5 cells, cultures were supplemented with IL-7, IL-3, SCF and Flt3L. Cultures were maintained for 21/22 days and harvested by collagenase IV/trypsin incubation. Cells were then enriched by MACS using CD19-PE and anti-PE microbeads before being stained with mAbs to CD10 for FACS isolation. FMO controls were run using whole cell fractions as MACS enrichment involved the usage of fluorescently labeled antibodies (CD19-PE and anti-PE microbeads). $CD19^{+}CD10^{+}$ cells were isolated from UCB-derived B cell populations using the gates shown. A purity check was run, a representative sample of cells were 100% $CD19^{+}CD10^{+}$.

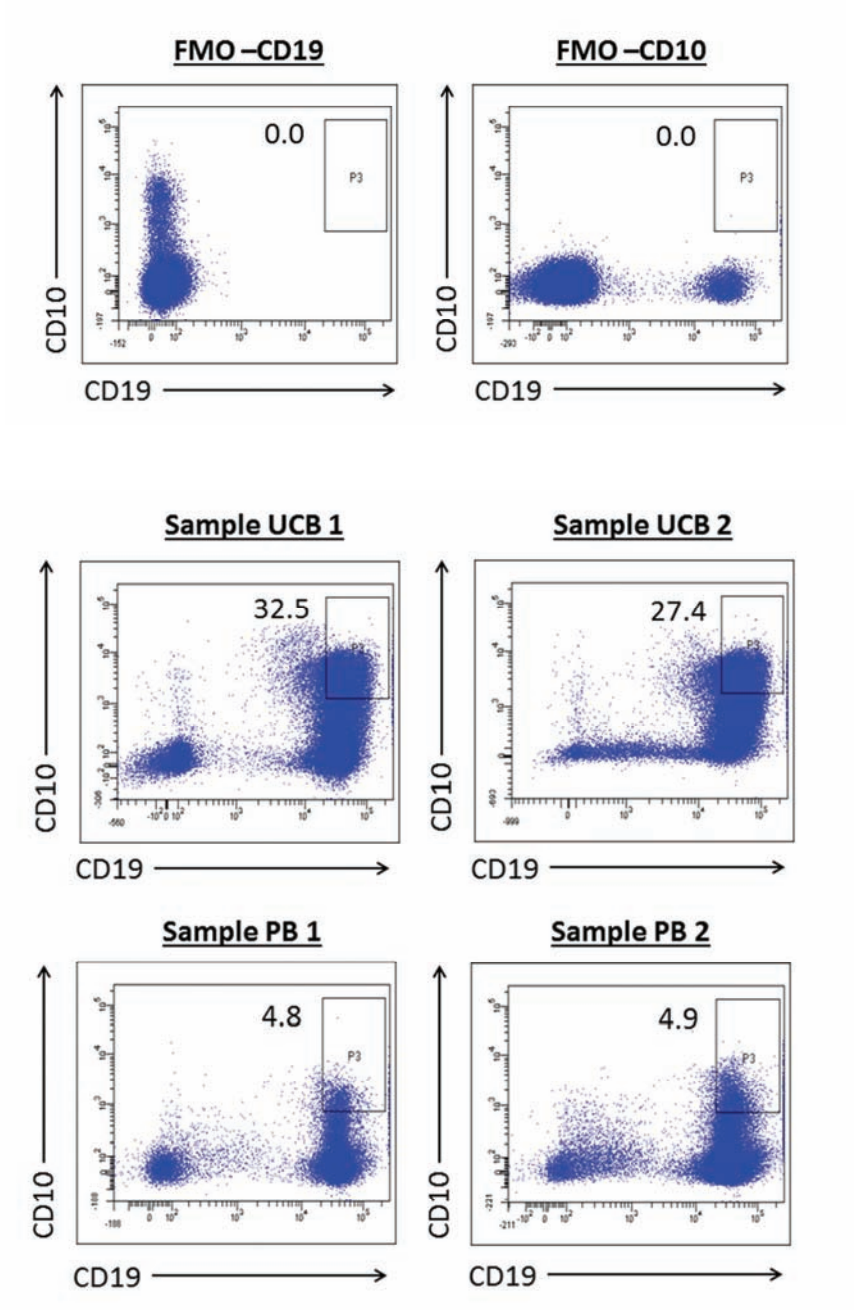

Figure 27 FACS isolation of UCB and PB B cell populations.
MNCs were isolated from 4 UCB and 4 PB donors. Cells were then enriched by MACS using CD19-PE and anti-PE microbeads before being stained with mAbs to CD10 for FACS isolation. FMO controls were run using whole cell fractions as MACS enrichment involved the usage of fluorescently labeled antibodies (CD19-PE and anti-PE microbeads).$CD19^{+}CD10^{+}$ cells were isolated from UCB and PB B cell populations using the gates shown. Four UCB and PB samples from different donors were isolated, figures are representative of two UCB and PB donors.

3.3.3.2 iPS-B cells demonstrate high levels of similarity in gene expression with UCB HSC/HPC- derived B cells

RNA from iPS cells, iPS-derived B cells (iPS-B), UCB HSC/HPC-derived B cells (HSC-B), UCB B cells (UCB) and PB B cells (PB), as described in 3.3.3.1, was taken for gene array profiling using the Illumina Human-HT-12v4 expression BeadChip system. Briefly, quality controls were analysed and RNA was converted to biotin-labelled cRNA for hybridisation. Samples were loaded, scanned and analysed. Sample number 3 of the PB group failed in the assay and was therefore not included in further analysis. Data were then normalised using the lumi bioconductor package and the 767 statistically significant differentially expressed genes were analysed by SAM (Significance Analysis of Microarrays) using MeV software (Du et al., 2008). Data were visualised as a heat map with hierarchical clustering (Figure 28). All biological replicates clustered within sample type/cell source. Within biological groups, strong similarity in gene expression could be observed. One sample (HSC-B 1) showed observable differences within the group and variation within the PB group appeared to be higher than within other biological cell type groups. As expected the greatest difference could be observed between undifferentiated iPS and the four B cell groups. Broadly the heat map could be seen to be made up of three regions: 1) high expression in iPS samples and low in all B cell samples 2) high expression in B cell samples and predominantly low expression in iPS samples and 3) high expression in iPS samples, generally low expression in UCB and PB samples and intermediate expression in iPS-B and HSC-B (Figure 28). To look at relatedness between groups, Principal Component Analysis (PCA) was run using the same 767 gene data set. PCA simplifies complex data sets, reducing dimensionality by analysing covariance. The majority of the variance in

expression was described by principal component 1 (PC1) which accounted for 44.9% of the variation within the data described. PC2 contained 30.1% and PC3 11.6% of the spread of data. Summary of expression data by PCA, plotted by with each sample as a single point, demonstrated close similarity between samples in a group. In the dimensions of PC1, iPS-B, PB and HSC-B were positioned most closely with overlap of iPS-B and PB (Figure 29 A). MNC samples are then the next most closely plotted points, with iPS samples showing the highest separation in PC1. When PC2 is considered, iPS-B, HSC-B and PB sub segmented, with iPS-B and HSC-B being more closely positioned (Figure 29 B). Of the three PB samples, one sample demonstrated large differences in PC2 as well as PC3 and can potentially be considered to be an anomaly. In PC2, PB and iPS were closely clustered with marginally more distant positioning of UCB. Analysis of PC3 revealed the close relatedness of iPS-B (with one sample showing more diffuse positioning in this parameter) and HSC-B (Figure 29 C). In PC3, iPS samples were more closely related to iPS-B than UCB. When PC1, PC2 and PC3 were considered in conjunction, iPS-B and HSC-B clustered most closely. Two of the PB samples then had the most similarity to iPS-B and HSC-B samples with greater differences in UCB. Of all five groups, undifferentiated iPS cells demonstrated the greatest differences, as would be expected.

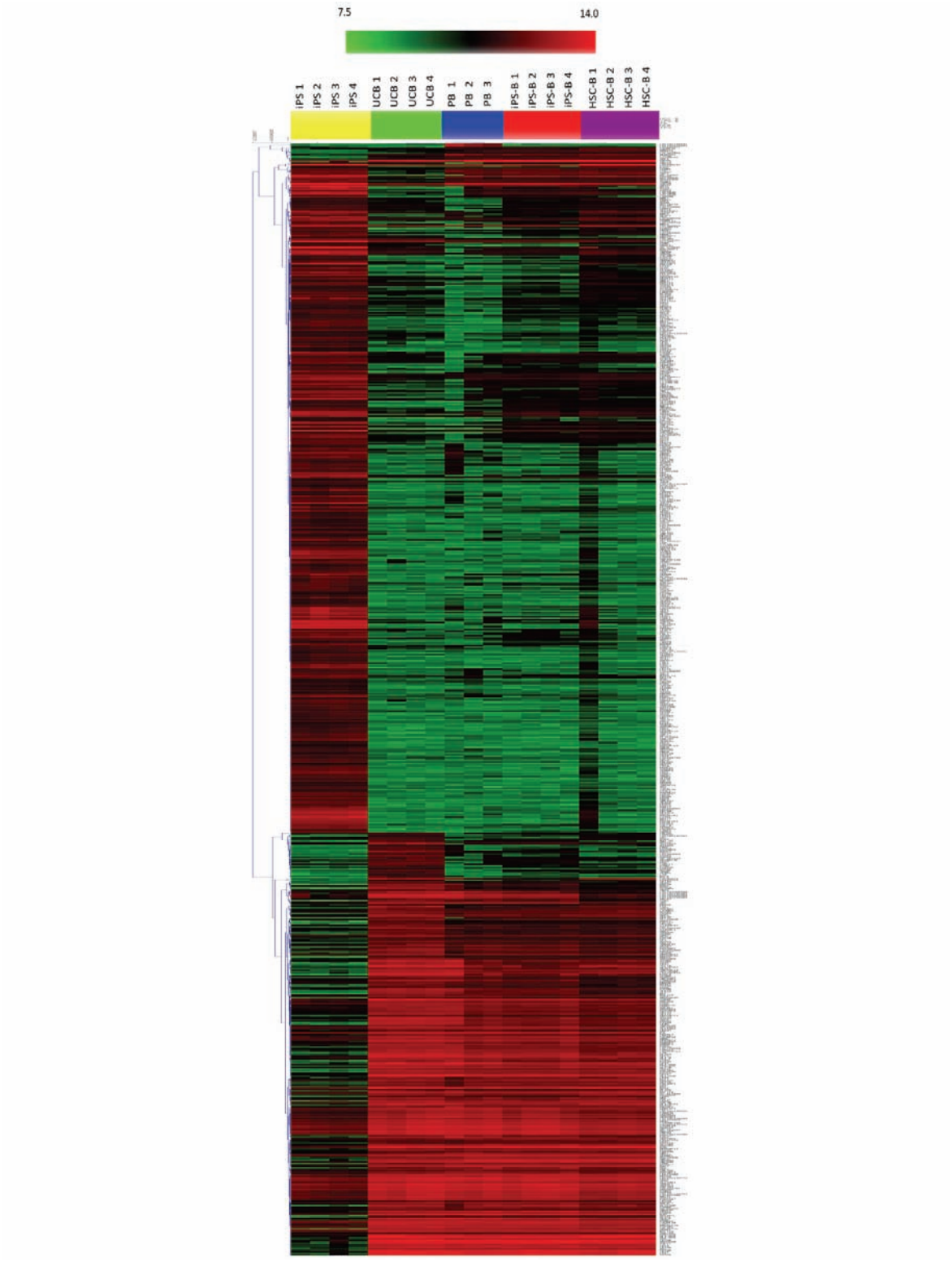

Figure 28 Heat map representation of 767 significantly expressed genes.
Gene array data was normalised and then analysed by SAM (Significance Analysis of Microarrays). Columns represent array comparisons between different samples and replicates. 4 biological replicates of iPS, iPS-B, HSC-B and UCB with 3 biological replicates of PB are shown. Rows represent genes. Red indicates a high expression level with green indicating low expression levels.

A

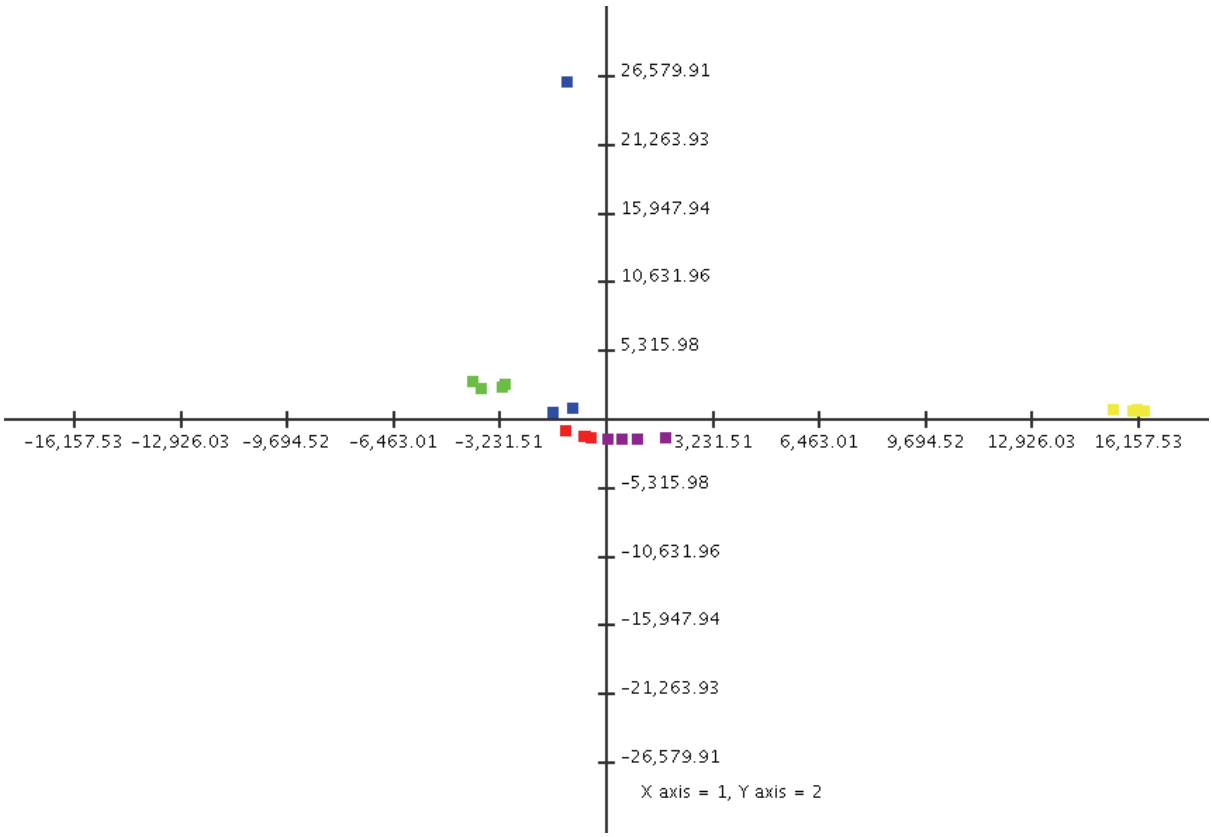
26,579.91
21,263.93
15,947.94
10,631.96
5,315.98
-16,157.53 -12,926.03 -9,694.52 -6,463.01 -3,231.51 3,231.51 6,463.01 9,694.52 12,926.03 16,157.53
-5,315.98
-10,631.96
-15,947.94
-21,263.93
-26,579.91
X axis = 1, Y axis = 2

B

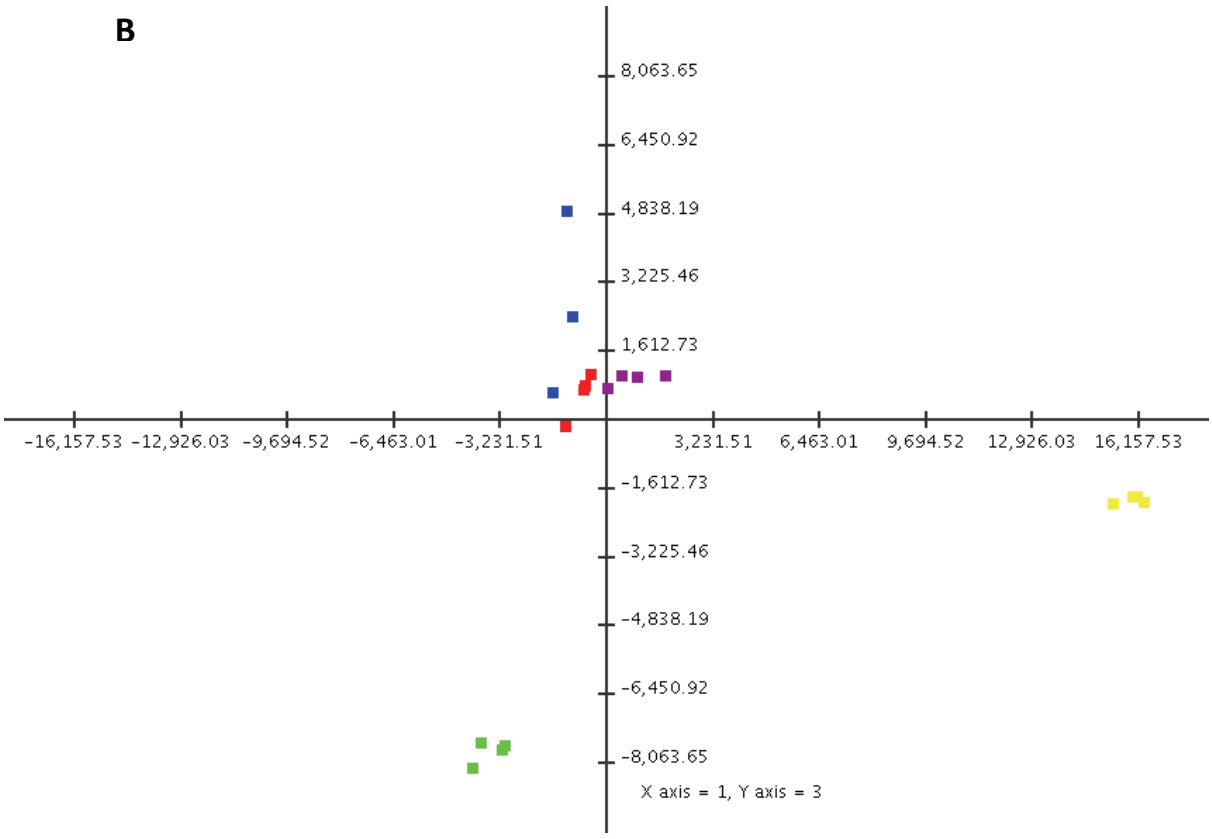
8,063.65
6,450.92
4,838.19
3,225.46
1,612.73
-16,157.53 -12,926.03 -9,694.52 -6,463.01 -3,231.51 3,231.51 6,463.01 9,694.52 12,926.03 16,157.53
-1,612.73
-3,225.46
-4,838.19
-6,450.92
-8,063.65
X axis = 1, Y axis = 3

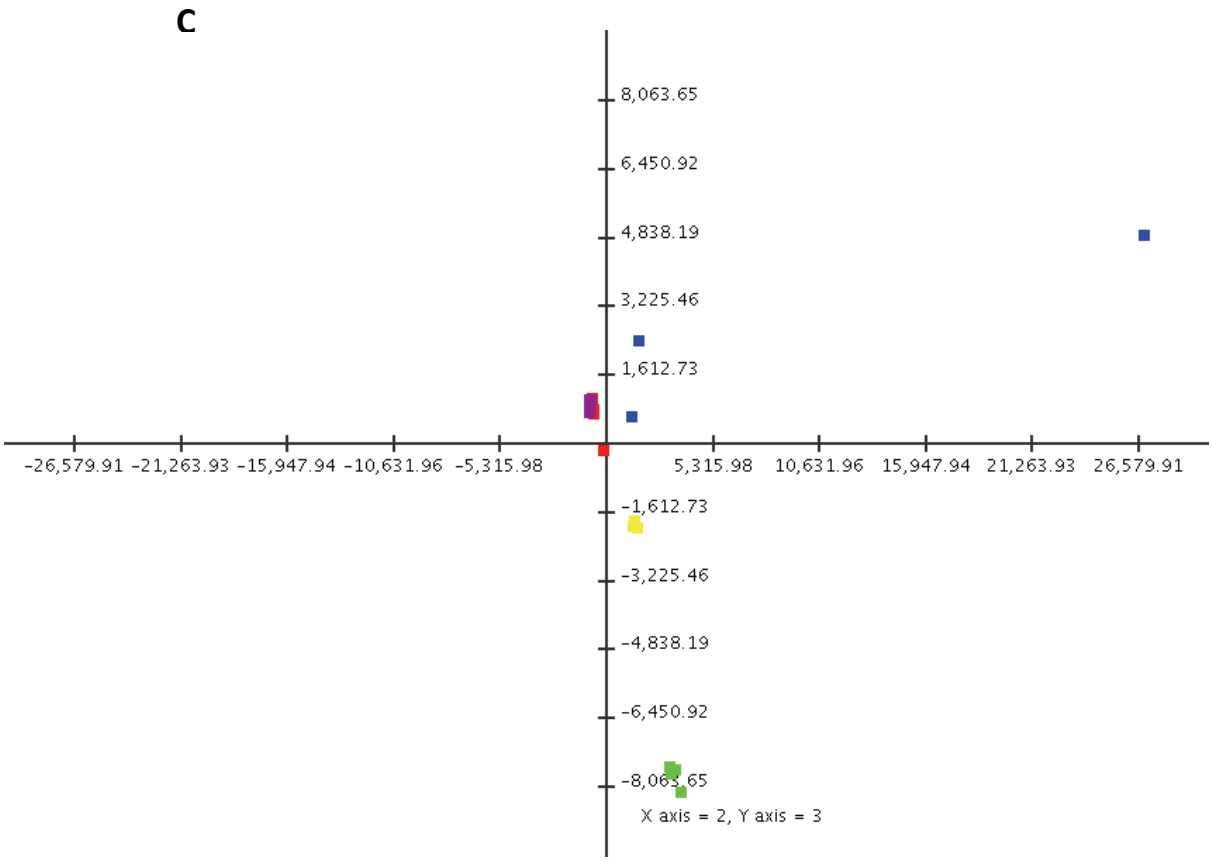

Figure 29 Correlation of 767 significantly expressed genes mapped onto the first three principal components.
PC1 accounts for 44.9% of the variance in the data described, PC2 for 30.1% and PC3 11.6%. (A) X axis= PC1, Y axis = PC2 (B) X axis= PC1, Y axis = PC3 (C) X axis= PC2, Y axis = PC3. Overall samples in biological groups cluster together. Within the 3 PB samples that passed the quality control assessment, 1 sample demonstrates large differences in PC2 and can be considered to be anomalous. iPS-B clusters most closely with HSC-B, with overlap between these two groups in PC3 and proximal positioning in PC1 and PC2. In PC1, the PB samples overlap with the outer iPS-B value. iPS cells are clustered away from in PC1 as well as PC2 and PC3. PC3 positions UCB far from iPS-B, HSC-B and PB. PC1 and PC2 show a smaller degree of difference in PC1 and PC2 of UCB in relation to the remainder of the groups than with iPS. Red= iPS-B, Purple= HSC-B, Blue= PB, Green= UCB, Yellow= iPS.

To assess the small number of differences between iPS-B and HSC-B at the single gene level, expression profiles were directly compared. Normalised genes were filtered based on significance with adjusted P values of <0.05 and empirical Bayes log odds of differential expression >3. Genes with a logF fold change of >1.0 (Table 9) or <-1.0 (Table 10) were considered. In a comparison of iPS-B and HSC-B samples, there were 52 genes fitting these criteria (21 genes logF >1.0 and 31 logF <-1.0). The number of genes described by these parameters in a comparison of HSC-B and UCB was 544 (251 genes logF >1.0 and 293 logF <-1.0).

The group of 21 genes that were upregulated in iPS-B cells in relation to HSB-B cells included PDGFRA, Lin28B, and CCR7 (Table 9). The differential expression of Lin28b is of interest due to recent data supporting a role for this RNA-binding protein in conveying a fetal-like potential to adult HSCs (Yuan et al., 2012). The potential relevance of the differential expression of Lin28b and PDGFRA are discussed further in section 3.4. CCR7 expression levels were higher in iPS-B than HSC-B. CCR7 is a chemokine receptor that binds CCL21 and CCL19, having a role in lymphocyte migration (Copley et al., 2013). CCR7 has been reported to be expressed at low levels in human B cells until they reach the IgM^+ immature cell stage (Honczarenko et al., 2006). It is therefore possible that iPS-B cells are more mature than HSC-B cells in this assay. Notably, CCR7 was differentially expressed in UCB B cells, with higher expression observed in comparison to HSC-B cells.

When the 20 genes upregulated in iPS-B (in comparison to HSC-B) were analysed using DAVID (Database for Annotation, Visualization and Integrated Discovery) (Table 9), 10 of the genes encoded membrane proteins (P=0.065), 11 were phosphoproteins (P=0.064) and 9 were glycoproteins (P=0.022). The list also included 5 genes involved in nucleotide-

binding (P=0.056), specifically, purine ribonucleotide binding. 4 of the enriched genes are known to be involved in the immune response (P=0.028) (Huang da et al., 2009b, Huang da et al., 2009a).

Analysis, using DAVID, of the 27 genes downregulated in iPS-B in relation to HSC-B (Table 10) revealed the following associations: 4 genes involved in the positive regulation of (macromolecular) biosynthesis (P= 0.053), 4 genes that are positive regulators of molecular function (P= 0.041), 3 genes involved in the regulation of protein modification (P=0.058) and 2 transcription elongation factors (P= 0.0086). (Huang da et al., 2009b, Huang da et al., 2009a). This suggests that HSC-B cells are more metabolically active than iPS-B cells. Of interest, the differential expression of the myosin light chain regulatory gene, MYL10/PLRLC, has been demonstrated to distinguish fetal from adult pre-B cells (Oltz et al., 1992). MYL4, a structural myosin light chain but not MYL10 was differentially expressed. Previously MYL4 has been associated with expression in embryonic muscle and adult cardiac tissue (Price et al., 1980, Kurabayashi et al., 1988).

544 genes were significantly differentially expressed between HSC-B and UCB. Of these genes, the 20 with the greatest and lowest expression values within the pair-wise comparison were analysed further. Of the 20 genes that showed the greatest positive differential expression between HSC-B and UCB (Table 11), 9 genes are involved in cell cycle/cell division (P= 0.0000049). Of these 9, 7 genes are involved in M phase (P= 0.0000041), 4 genes are involved in the regulation of apoptosis (3 anti-apoptotic) (P=0.033). HSC-derived B cells therefore appear to be undergoing a greater rate of proliferation than isolated UCB B cells. This could be due to differences in heterogeneity as well as extent of differentiation in the two populations. IgLL1, which encodes λ5, a

surrogate light-chain was highly expressed in HSC-B cells in comparison to UCB. This gene is part of the pre-BCR that is expressed on pre-B cells and does not contribute to the antibody structure (Herzog et al., 2009).

Of the 20 genes that showed the greatest negative differential expression between HSC-B and UCB (Table 12), 14 genes are associated with polymorphism (P=0.066)- proteins that are variant within the population. 6 genes are membrane proteins (P=0.093), 4 are involved in chemokine signalling (P=0.0024) and 3 are Immunoglobulin-like genes (P=0.082). This could suggest that the isolated UCB B cell population is more mature than the HSC-derived B cell population.

Table 9 Genes upregulated in iPS-B cells relative to HSC-B cells.

logFC	P.Value	adj.P.Val	B	PROBE_ID	SYMBOL	CHROMOSOME	DEFINITION
3.456159	2.91E-06	0.000463	4.894123	ILMN_3251587	LOC100008589		Homo sapiens 28S ribosomal RNA (LOC100008589), non-coding RNA.
2.157481	3.72E-06	0.000557	4.656703	ILMN_1733559	LOC100008589		Homo sapiens 28S ribosomal RNA (LOC100008589), non-coding RNA.
1.964523	2.07E-06	0.000362	5.228263	ILMN_2086470	PDGFRA	4	Homo sapiens platelet-derived growth factor receptor, alpha polypeptide (PDGFRA), mRNA.
1.739929	1.83E-05	0.001614	3.091279	ILMN_2115862	ESPNL	2	Homo sapiens espin-like (ESPNL), mRNA.
1.683171	3.68E-09	5.89E-06	11.20305	ILMN_1662358	MX1	21	Homo sapiens myxovirus (influenza virus) resistance 1, interferon-inducible protein p78 (mouse) (MX1), mRNA.
1.631937	8.08E-07	0.000198	6.139794	ILMN_1715131	CCR7	17	Homo sapiens chemokine (C-C motif) receptor 7 (CCR7), mRNA.
1.626654	1.47E-05	0.001448	3.308951	ILMN_1795429	VCL	10	Homo sapiens vinculin (VCL), transcript variant 1, mRNA.
1.543455	2.37E-06	0.000407	5.094144	ILMN_2386790	KLRC3	12	Homo sapiens killer cell lectin-like receptor subfamily C, member 3 (KLRC3), transcript variant 1, mRNA.
1.491172	6.57E-07	0.000174	6.34014	ILMN_1743205	ABCA7	19	Homo sapiens ATP-binding cassette, sub-family A (ABC1), member 7 (ABCA7), mRNA.
1.303125	4.00E-08	3.31E-05	9.005695	ILMN_1668277	BLK	8	Homo sapiens B lymphoid tyrosine kinase (BLK), mRNA.
1.285123	1.91E-05	0.001655	3.053555	ILMN_2129505	CYBASC3	11	Homo sapiens cytochrome b, ascorbate dependent 3 (CYBASC3), mRNA.
1.24946	1.45E-05	0.001446	3.324628	ILMN_1768505	IL13RA1	X	Homo sapiens interleukin 13 receptor, alpha 1 (IL13RA1), mRNA.
1.22099	9.00E-07	0.000213	6.035435	ILMN_2414762	TLR10	4	Homo sapiens toll-like receptor 10 (TLR10), transcript variant 1, mRNA.
1.20158	6.00E-08	4.19E-05	8.624517	ILMN_1784300	TUBA4A	2	Homo sapiens tubulin, alpha 4a (TUBA4A), mRNA.
1.166454	7.96E-06	0.000974	3.911464	ILMN_1797822	SEL1L3	4	Homo sapiens sel-1 suppressor of lin-12-like 3 (C. elegans) (SEL1L3), mRNA.
1.109582	3.89E-08	3.31E-05	9.032013	ILMN_1748697	LIN28B	6	Homo sapiens lin-28 homolog B (C. elegans) (LIN28B), mRNA.
1.10723	9.66E-06	0.001109	3.721205	ILMN_1770290	CNN2	19	Homo sapiens calponin 2 (CNN2), transcript variant 2, mRNA.

1.064689	7.72E-08	4.52E-05	8.386704	ILMN_1695404	LY6E	8	Homo sapiens lymphocyte antigen 6 complex, locus E (LY6E), mRNA.
1.032722	7.49E-07	0.000189	6.213286	ILMN_2311537	HMGA1	6	Homo sapiens high mobility group AT-hook 1 (HMGA1), transcript variant 1, mRNA.

Data from Illumina Human-HT-12v4 expression array were normalised and the expression of iPS-B and HSC-B genes was compared. Significantly upregulated genes in iPS-B cells were filtered based on; adj. P value $P<0.05$, $B>3.0$ log FC >1.0. Based on these criteria 20 known genes were identified.

Table 10 Genes downregulated in iPS-B cells relative to HSC-B cells.

logFC	P.Value	adj.P.Val	B	PROBE_ID	SYMBOL	CHROMOSOME	DEFINITION
-3.21467	5.48E-07	0.000158	6.515172	ILMN_1794927	LOC90925		Homo sapiens hypothetical protein LOC90925 (LOC90925), mRNA.
-2.162	8.55E-12	1.88E-07	16.32902	ILMN_2201596	CYTL1	4	Homo sapiens cytokine-like 1 (CYTL1), mRNA.
-2.06868	3.62E-07	0.000126	6.912718	ILMN_1684255	MYL4	17	Homo sapiens myosin, light chain 4, alkali; atrial, embryonic (MYL4), transcript variant 2, mRNA.
-1.88424	1.57E-05	0.001508	3.245392	ILMN_1655595	SERPINE2	2	Homo sapiens serpin peptidase inhibitor, clade E (nexin, plasminogen activator inhibitor type 1), member 2 (SERPINE2), mRNA.
-1.71713	1.83E-05	0.001614	3.091087	ILMN_3308961	MIR1974		Homo sapiens microRNA 1974 (MIR1974), microRNA.
-1.57511	3.02E-08	3.02E-05	9.268396	ILMN_1748625	TCEAL4	X	Homo sapiens transcription elongation factor A (SII)-like 4 (TCEAL4), transcript variant 4, mRNA.
-1.54485	5.30E-06	0.000722	4.309865	ILMN_2370091	NGFRAP1	X	Homo sapiens nerve growth factor receptor (TNFRSF16) associated protein 1 (NGFRAP1), transcript variant 1, mRNA.
-1.46865	1.06E-07	5.30E-05	8.085697	ILMN_2103761	TLE4	9	Homo sapiens transducin-like enhancer of split 4 (E(sp1) homolog, Drosophila) (TLE4), mRNA.
-1.4292	4.63E-11	2.78E-07	14.98313	ILMN_1691476	MYLK	3	Homo sapiens myosin light chain kinase (MYLK), transcript variant 8, mRNA.
-1.41958	1.19E-10	4.32E-07	14.20414	ILMN_1707491	KIAA0125	14	Homo sapiens KIAA0125 (KIAA0125), mRNA.
-1.38804	5.33E-07	0.000156	6.54165	ILMN_1734190	TCEAL3	X	Homo sapiens transcription elongation factor A (SII)-like 3 (TCEAL3), transcript variant 1, mRNA.
-1.37639	1.51E-06	0.000302	5.532312	ILMN_1752199	LHPP	10	Homo sapiens phospholysine phosphohistidine inorganic pyrophosphate phosphatase (LHPP), mRNA.
-1.34356	1.46E-05	0.001448	3.318446	ILMN_2352097	GPR56	16	Homo sapiens G protein-coupled receptor 56 (GPR56), transcript variant 2, mRNA.
-1.29862	2.64E-11	2.11E-07	15.4373	ILMN_1795715	DPYD	1	Homo sapiens dihydropyrimidine dehydrogenase (DPYD), transcript variant 1, mRNA.
-1.22773	1.26E-05	0.001331	3.458412	ILMN_3197097	TSTD1	1	Homo sapiens thiosulfate sulfurtransferase (rhodanese)-like domain containing 1 (TSTD1), transcript variant 2, mRNA.

-1.21065	5.09E-08	3.94E-05	8.77929	ILMN_1768110	ZAK	2	Homo sapiens sterile alpha motif and leucine zipper containing kinase AZK (ZAK), transcript variant 2, mRNA.
-1.19232	1.88E-07	8.06E-05	7.539998	ILMN_1700257	C4orf32	4	Homo sapiens chromosome 4 open reading frame 32 (C4orf32), mRNA.
-1.16152	3.92E-08	3.31E-05	9.025336	ILMN_1757074	GNG10	9	Homo sapiens guanine nucleotide binding protein (G protein), gamma 10 (GNG10), mRNA.
-1.13081	1.08E-10	4.32E-07	14.27842	ILMN_1662795	CA2	8	Homo sapiens carbonic anhydrase II (CA2), mRNA.
-1.10287	5.22E-06	0.00072	4.324224	ILMN_2384122	GPR56	16	Homo sapiens G protein-coupled receptor 56 (GPR56), transcript variant 3, mRNA.
-1.09511	1.40E-09	2.58E-06	12.07045	ILMN_1737972	TSPYL5	8	Homo sapiens TSPY-like 5 (TSPYL5), mRNA.
-1.05809	6.17E-07	0.000168	6.400483	ILMN_1667966	C1orf24	1	Homo sapiens chromosome 1 open reading frame 24 (C1orf24), transcript variant 2, mRNA.
-1.03978	3.26E-08	3.13E-05	9.196196	ILMN_2157240	MNS1	15	Homo sapiens meiosis-specific nuclear structural 1 (MNS1), mRNA.
-1.0328	1.84E-05	0.001614	3.090066	ILMN_1771385	GBP4	1	Homo sapiens guanylate binding protein 4 (GBP4), mRNA.
-1.02361	1.04E-05	0.001145	3.652633	ILMN_1715886	CNOT7	8	Homo sapiens CCR4-NOT transcription complex, subunit 7 (CNOT7), transcript variant 1, mRNA.
-1.00786	1.43E-05	0.001443	3.335855	ILMN_1762436	UBB	17	Homo sapiens ubiquitin B (UBB), mRNA.

Data from Illumina Human-HT-12v4 expression array were normalised and the expression of iPS-B and HSC-B genes was compared. Significantly downregulated genes in iPS-B cells were filtered based on; adj. P value $P<0.05$, $B>3.0$ log FC <-1.0. Based on these criteria 27 known genes were identified.

Table 11 Genes upregulated in HSC-B cells relative to UCB B cells.

logFC	P.Value	adj.P.Val	B	PROBE_ID	SYMBOL	CHROMOSOME	DEFINITION
3.670653	8.84E-08	5.25E-06	8.195126	ILMN_1669113	ATF5	19	Homo sapiens activating transcription factor 5 (ATF5), mRNA.
3.047503	1.73E-07	8.75E-06	7.513907	ILMN_1757467	H1F0	22	Homo sapiens H1 histone family, member 0 (H1F0), mRNA.
3.01602	7.08E-06	0.000136	3.720437	ILMN_1683450	CDCA5	11	Homo sapiens cell division cycle associated 5 (CDCA5), mRNA.
2.965309	8.83E-07	2.83E-05	5.84837	ILMN_1656713	IGLL1	22	Homo sapiens immunoglobulin lambda-like polypeptide 1 (IGLL1), transcript variant 2, mRNA.
2.851152	1.55E-13	3.71E-10	21.03359	ILMN_1747911	CDC2	10	Homo sapiens cell division cycle 2, G1 to S and G2 to M (CDC2), transcript variant 1, mRNA.
2.712681	1.79E-06	4.80E-05	5.127974	ILMN_2409298	NUSAP1	15	Homo sapiens nucleolar and spindle associated protein 1 (NUSAP1), transcript variant 2, mRNA.
2.70175	3.69E-06	8.34E-05	4.386956	ILMN_1737184	CDCA7	2	Homo sapiens cell division cycle associated 7 (CDCA7), transcript variant 1, mRNA.
2.690958	4.75E-10	1.08E-07	13.44498	ILMN_1711988	KCNK12	2	Homo sapiens potassium channel, subfamily K, member 12 (KCNK12), mRNA.
2.629683	7.10E-08	4.48E-06	8.417829	ILMN_1704537	PHGDH	1	Homo sapiens phosphoglycerate dehydrogenase (PHGDH), mRNA.
2.579075	5.32E-06	0.00011	4.012848	ILMN_1777564	MAD2L1	4	Homo sapiens MAD2 mitotic arrest deficient-like 1 (yeast) (MAD2L1), mRNA.
2.516354	3.25E-06	7.63E-05	4.515231	ILMN_1790508	KCNA5	12	Homo sapiens potassium voltage-gated channel, shaker-related subfamily, member 5 (KCNA5), mRNA.
2.490984	1.45E-06	4.09E-05	5.342947	ILMN_1756326	CKS2	9	Homo sapiens CDC28 protein kinase regulatory subunit 2 (CKS2), mRNA.
2.471775	1.15E-05	0.000198	3.224101	ILMN_2327860	MAL	2	Homo sapiens mal, T-cell differentiation protein (MAL), transcript variant d, mRNA.
2.450673	1.29E-06	3.78E-05	5.461609	ILMN_1724658	BNIP3	10	Homo sapiens BCL2/adenovirus E1B 19kDa interacting protein 3 (BNIP3), nuclear gene encoding mitochondrial protein, mRNA.
2.444912	1.16E-10	4.49E-08	14.83129	ILMN_1786125	CCNA2	4	Homo sapiens cyclin A2 (CCNA2), mRNA.
2.412507	3.68E-07	1.49E-05	6.742835	ILMN_1708778	ASS1	9	Homo sapiens argininosuccinate synthetase 1 (ASS1), transcript variant 1,

							mRNA.
2.399692	3.63E-07	1.49E-05	6.754565	ILMN_1666305	CDKN3	14	Homo sapiens cyclin-dependent kinase inhibitor 3 (CDK2-associated dual specificity phosphatase) (CDKN3), mRNA.
2.380364	5.69E-08	3.86E-06	8.642304	ILMN_1684255	MYL4	17	ALC1; AMLC; GT1; PRO1957
2.378078	1.38E-05	0.000228	3.037646	ILMN_2219712	HMGB2	4	HMG2
2.33777	3.00E-06	7.19E-05	4.59953	ILMN_2143155	KIF11	10	KNSL1; EG5; HKSP; TRIP5

Data from Illumina Human-HT-12v4 expression array were normalised and the expression of HSC-B and UCB B genes was compared. Significantly upregulated genes in HSC-B cells were filtered based on; adj. P value $P<0.05$, $B>3.0$ log FC >1.0. Based on these criteria 251 genes were identified, the 20 known genes with the greatest logFC values that were statistically significant are included.

Table 12 Genes downregulated in HSC-B cells relative to UCB B cells.

logFC	P.Value	adj.P.Val	B	PROBE_ID	SYMBOL	CHROMOSOME	DEFINITION
-3.92023	6.09E-07	2.16E-05	6.227281	ILMN_3251587	LOC100008589		Homo sapiens 28S ribosomal RNA (LOC100008589), non-coding RNA.
-3.53644	1.09E-08	1.13E-06	10.31294	ILMN_1776181	BIRC3	11	Homo sapiens baculoviral IAP repeat-containing 3 (BIRC3), transcript variant 1, mRNA.
-3.238	1.38E-08	1.33E-06	10.07329	ILMN_2109416	NAPSB	19	Homo sapiens napsin B aspartic peptidase pseudogene (NAPSB), non-coding RNA. XR_001413
-3.07279	2.88E-10	7.58E-08	13.94097	ILMN_2196078	SLAMF6	1	Homo sapiens SLAM family member 6 (SLAMF6), mRNA.
-3.02396	6.50E-15	5.20E-11	23.73907	ILMN_2337928	CXCR5	11	Homo sapiens chemokine (C-X-C motif) receptor 5 (CXCR5), transcript variant 2, mRNA.
-2.99285	7.85E-08	4.82E-06	8.3153	ILMN_3243593	LOC100008588		Homo sapiens 18S ribosomal RNA (LOC100008588), non-coding RNA.
-2.95617	1.09E-05	0.000189	3.279615	ILMN_2374352	DBNDD1	16	Homo sapiens dysbindin (dystrobrevin binding protein 1) domain containing 1 (DBNDD1), transcript variant 1, mRNA.
-2.94339	3.98E-12	4.15E-09	18.06577	ILMN_2368318	FGR	1	Homo sapiens Gardner-Rasheed feline sarcoma viral (v-fgr) oncogene homolog (FGR), transcript variant 3, mRNA.
-2.88217	8.27E-10	1.58E-07	12.89594	ILMN_2376403	TSC22D3	X	Homo sapiens TSC22 domain family, member 3 (TSC22D3), transcript variant 2, mRNA.
-2.8126	1.37E-07	7.24E-06	7.747611	ILMN_1785424	ABLIM1	10	Homo sapiens actin binding LIM protein 1 (ABLIM1), transcript variant 4, mRNA.
-2.75075	2.05E-06	5.38E-05	4.98675	ILMN_1700428	HLA-DOB	6	Homo sapiens major histocompatibility complex, class II, DO beta (HLA-DOB), mRNA.
-2.72061	1.16E-15	1.84E-11	25.11618	ILMN_2099528	BTLA	3	Homo sapiens B and T lymphocyte associated (BTLA), mRNA.
-2.69163	5.87E-08	3.93E-06	8.610463	ILMN_1714567	AHNAK	11	Homo sapiens AHNAK nucleoprotein (AHNAK), transcript variant 1, mRNA.
-2.66438	1.08E-07	6.12E-06	7.987013	ILMN_2112988	NCF1C	7	Homo sapiens neutrophil cytosolic factor 1C pseudogene (NCF1C), non-coding RNA.
-2.65047	6.43E-07	2.25E-05	6.171962	ILMN_1767509	DEF8	16	Homo sapiens differentially expressed in FDCP 8 homolog (mouse) (DEF8),

							transcript variant 1, mRNA.
-2.6308	3.03E-06	7.23E-05	4.588988	ILMN_1751607	FOSB	19	Homo sapiens FBJ murine osteosarcoma viral oncogene homolog B (FOSB), mRNA.
-2.57912	2.27E-09	3.41E-07	11.89035	ILMN_1765994	ZBP1	20	Homo sapiens Z-DNA binding protein 1 (ZBP1), mRNA.
-2.56288	1.82E-09	2.86E-07	12.10915	ILMN_1715131	CCR7	17	Homo sapiens chemokine (C-C motif) receptor 7 (CCR7), mRNA.

Data from Illumina Human-HT-12v4 expression array were normalised and the expression of HSC-B and UCB B genes was compared. Significantly downregulated genes in HSC-B cells were filtered based on; adj. P value $P<0.05$, $B>3.0$ log $FC<-1.0$. Based on these criteria 293 genes were identified, the 20 known genes with the lowest logFC values that were statistically significant are included.

3.3.4 Serum and feeder- free assays for promoting haemato-endothelial differentiation of iPS cells.

3.3.4.1 Defining conditions to promote haematopoietic differentiation of iPS cells in the absence of feeder cells or serum.

Co-culture of iPS colonies with OP9 stroma in the presence of serum-containing media robustly and efficiently promotes haemato-endothelial differentiation. However, as a system to understand the mechanism of haematopoietic development and identify critical factors, the OP9 co-culture is limited. Mouse stromal cells express a whole range of cell surface molecules and secreted soluble factors that have not been defined. Furthermore, the range of components within serum is both variable and not fully defined. In addition to the restrictions that such a assay places on a precise understanding of mechanisms, it is also true that for the differentiated cells to be used clinically protocols must be cGMP (current Good Manufacturing Practices) compliant. Therefore, the aim of this section of research was to describe a serum and feeder-free system which promotes haematopoietic differentiation of iPS cells.

Work within the laboratory has built on the findings of both Keller and colleages and Murray and colleages to demonstrate that AA, BMP-4 and bFGF are able to drive the formation of beating cardiomyocytes from iPS cells under serum and feeder-free conditions (Laflamme et al., 2007, Carpenter et al., 2012, Yang et al., 2008). As both cardiomyocytes and haematopoietic progenitors are of mesodermal orgin, it seemed likely that the initial stages of the iPS- cardiomyocyte protocol might be relevant for

haematopoietic differentiation. Other factors that have been identified to play a role in haematopoietic differentiation include VEGF, SCF, Flt3L and TPO, cytokines known to play a critical role in ontogeny of the blood system (Fina et al., 1990, Kabrun et al., 1997, Murray, 1932, Sabin, 1920, Young et al., 1995, McKenna et al., 2000, Solar et al., 1997, Besmer et al., 1993). The starting point therefore was to introduce these seven factors in different combinations and stages to determine whether haematopoietic progenitors could be generated from iPS cell colonies. To change from 'maintenance' to 'differentiation' conditions, C18 or C19 iPS colonies that had been allowed to grow maximally (without spontanous differentiation) were switched from mTeSR medium to supplemented Stem Pro-34 media containing cytokines as described in Table 13 and this time point was thus designated day 0. Cultures were then fed every two days with supplementation as described in Table 13 before being harvested on day 10 of culture by incubation with accutase. The total population was then stained with mAbs to haematopoietic and endothelial markers and analysed by flow cytometry. The protocol is shown schematically in Figure 30.

In preliminary experiments, all six protocols tested generated $CD34^+CD43^+$ cells indicative of successful haematopoieitc differentiation, however the percentage of cells produced within the total population ranged from 0.1- 1.1%. Conditions 1 and 4 protocols resulted in the highest number of $CD43^+$ cells, these differentiation protocols were therefore repeated. The condition 1 protocol generated the highest but overall very low proportion of $CD43^+$ cells (0.67% ± 0.3 mean ± SD) (Figure 31). Similarly, $CD41a^+$ cells could be detected, in the absence of $CD45^+$ cells (Figure 31). $CD34^+CD43^-$, $CD144^+CD41a^-$ and $CD31^+CD45^-$ cells could be detected, which may represent an endothelial-like population,

with a higher differentiation efficiency than CD43/CD41a^{+} haematopoietic cells (Figure 31). Morphologically, endothelial-like cells, phase dark sac-like and cord-like structures could all be observed (Figure 32).

Table 13 Cytokine regime included in serum and feeder-free defined cultures to promote haemato-endothelial differentiation of iPS colonies.

Condition number	Day 0 - 2	Day 2 - 4	Day 4 - 6	Day 6 - 8	Day 8 - 10
1	High AA, BMP4, bFGF	AA, BMP-4, bFGF	VEGF, SCF, TPO, Flt3L	VEGF, SCF, TPO, Flt3L	VEGF, SCF, TPO, Flt3L
2	AA, BMP4, bFGF	AA, BMP4, bFGF	VEGF, SCF, TPO, Flt3L	VEGF, SCF, TPO, Flt3L	VEGF, SCF, TPO, Flt3L
3	High AA, BMP4, bFGF	VEGF, AA, BMP-4, bFGF	VEGF	Flt3L, SCF, TPO	Flt3L, SCF, TPO
4	High AA, BMP4, bFGF	VEGF	Flt3L, SCF, TPO, VEGF	Flt3L, SCF, TPO	Flt3L, SCF, TPO
5	High AA, BMP4, bFGF	VEGF, AA, BMP-4, bFGF	VEGF, AA, BMP-4, bFGF	VEGF, AA, BMP-4, bFGF	Flt3L, SCF, TPO
6	High AA, BMP4, bFGF	VEGF	VEGF	VEGF	VEGF

iPS colonies were cultured in Stempro-34^{+} supplemented with recombinant cytokines as indicated at the following concentrations- High AA= 50ng/ml, Low AA= 5ng/ml, BMP-4= 10ng/ml, bFGF= 5ng/ml, SCF= 100ng/ml, Flt3L= 100ng/ml, TPO= 20ng/ml, VEGF= 10ng/ml. High AA was included where indicated for 4 hours and then replaced with medium containing Low AA plus indicated cytokines.

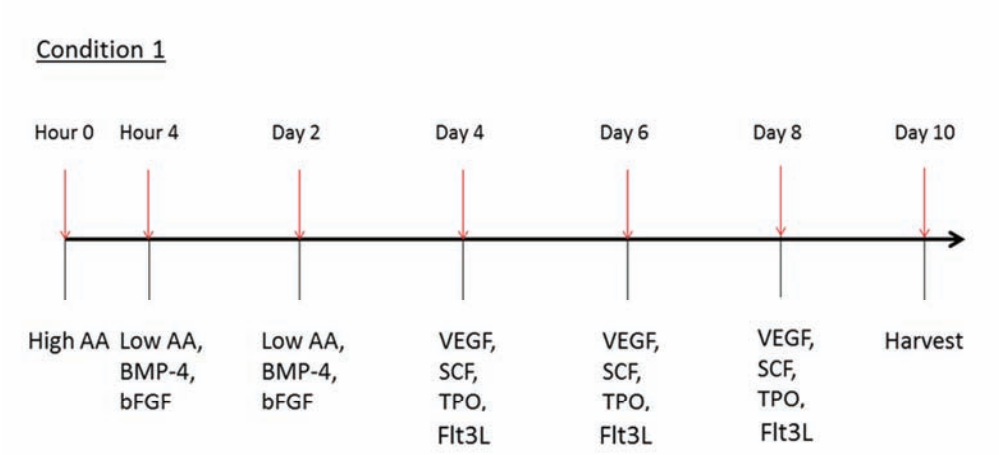

Figure 30 Schematic representation of the feeding regime in serum-free and feeder-free defined differentiation cultures.
Representation of condition 1 protocol. High concentrations (50ng/ml) of Activin A (AA) was added for 4 hours before total replacement with media containing low (5ng/ml) AA, BMP-4 (10ng/ml) and bFGF (5ng/ml). Cultures were then fed every two days. On day 4, the cytokine regime was changed and cells were cultures in VEGF (10ng/ml), Flt3L (100ng/ml), SCF (100ng/ml) and TPO (20ng/ml). On day 10 cells were harvested and analysed by flow cytometry.

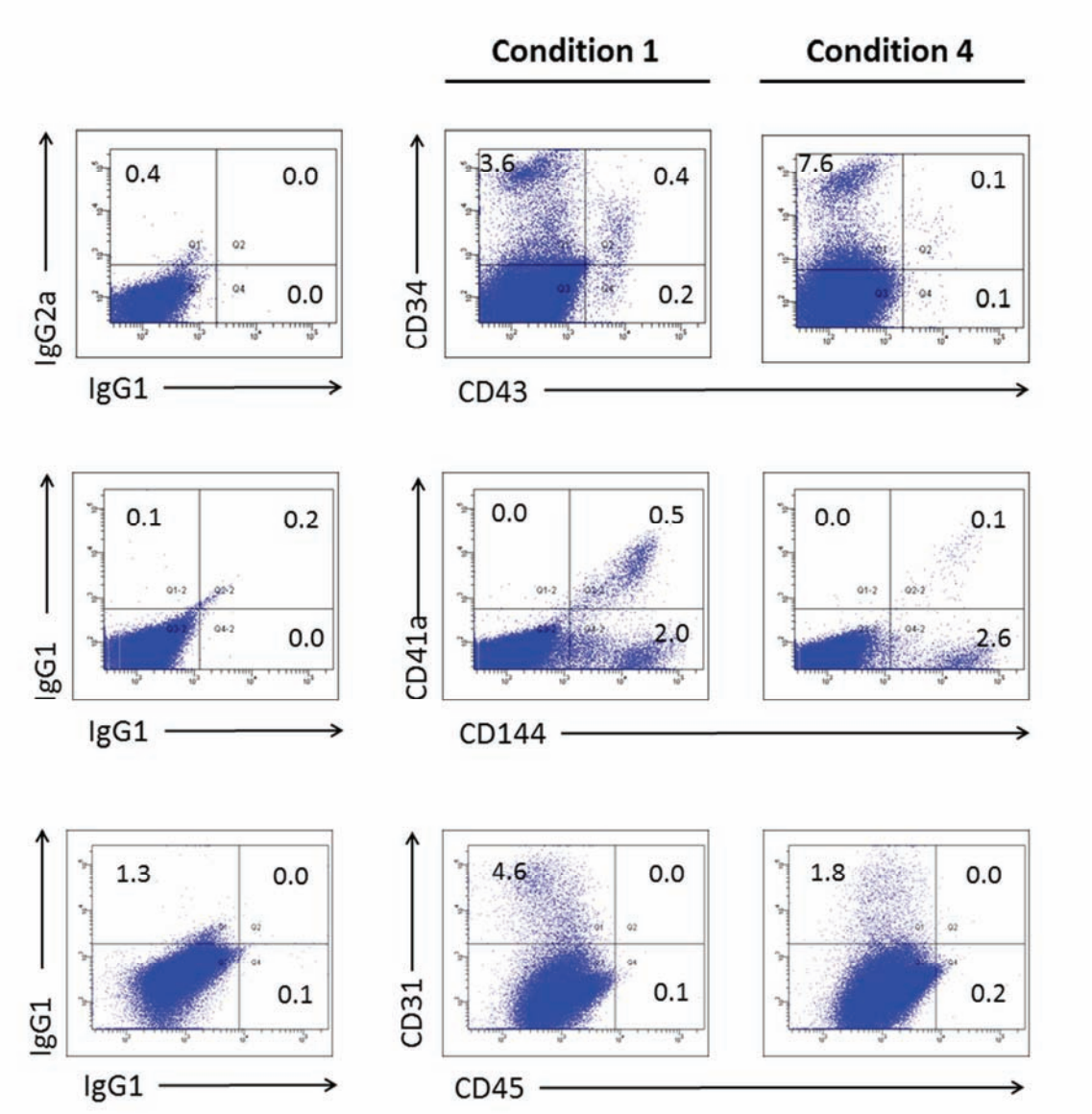

Figure 31 Haematopoietic differentiation from iPS colonies in the absence of feeder cells and serum.

C19 or C18 iPS colonies grown on matrigel in mTesR were switched to Stempro-34^{+} media, supplemented with cytokines as described in Table 13. Cultures were maintained for 10 days and were harvested, stained with mAbs and analysed by flow cytometry. Condition 1 protocol generated CD43^{+} and CD41a^{+} with the highest, albeit low, efficiency (0.7% ± 0.3, mean ± SD). CD34^{+}, CD31^{+} and CD144^{+} cells were also generated, in the absence of CD45^{+} cells. Representative image n=3 independent experiments.

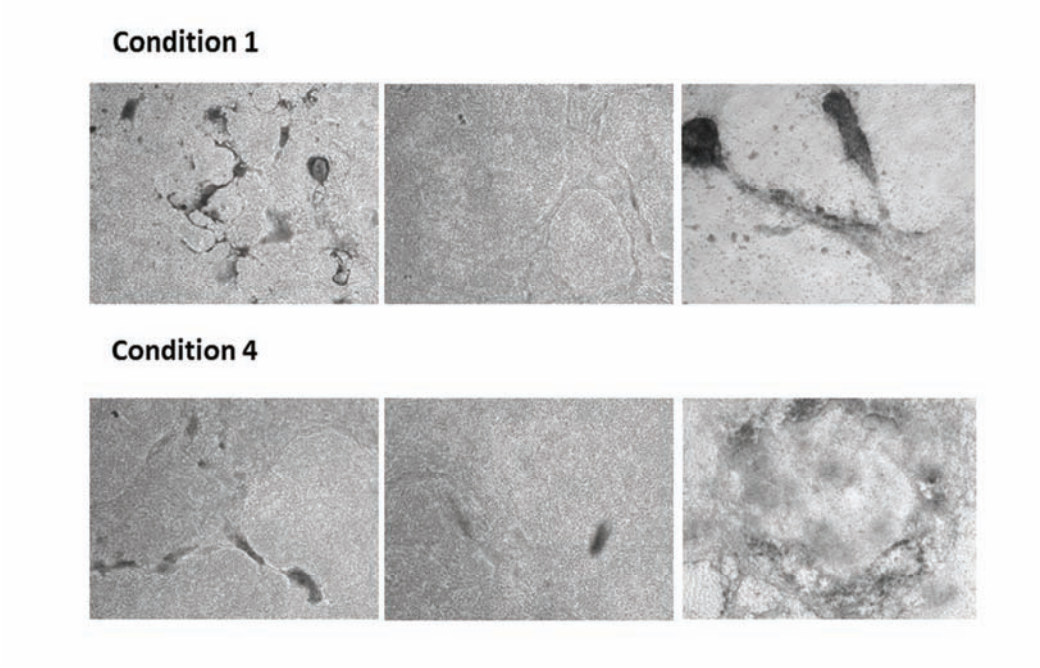

Figure 32 Day 8 brightfield images of C19 cultures differentiated as monolayers in the presence of cytokine cocktails condition 1 and 4.
Representative images of cord-like structures could be observed which may be indicative of haematopoietic differentiation. Cells with a pebblestone morphology were also present that are typically associated with an endothelial identity (x4 magnification). Representative images n=3 independent experiments.

To determine whether haematopoietic progenitor cells generated from iPS colonies as a monolayer culture with serum-free media were functional, MACS enriched $CD34^+$ cells were seeded into the CFU assay as previously described (2.6.4). CFU-G/GM colonies were observed, demonstrating that this population had myeloid potential, but no other colony types could be detected (Figure 33). The potential of $CD34^+$ cells to produce endothelial-like cells was also addressed by morphology and live cell staining. $CD34^+$ cells cultured in EGM-2 media on collagen differentiating into $CD31^+$ passagable cells, although further phenotypic and functional assays would have been required to ascribe endothelial identity (Figure 33).

Overall, haematopoietic differentiation was achieved in the absence of feeder cells and serum-containing media, however, differentiation efficiencies were extremely low and not amenable for downstream applications. Therefore, these experiments were not considered further.

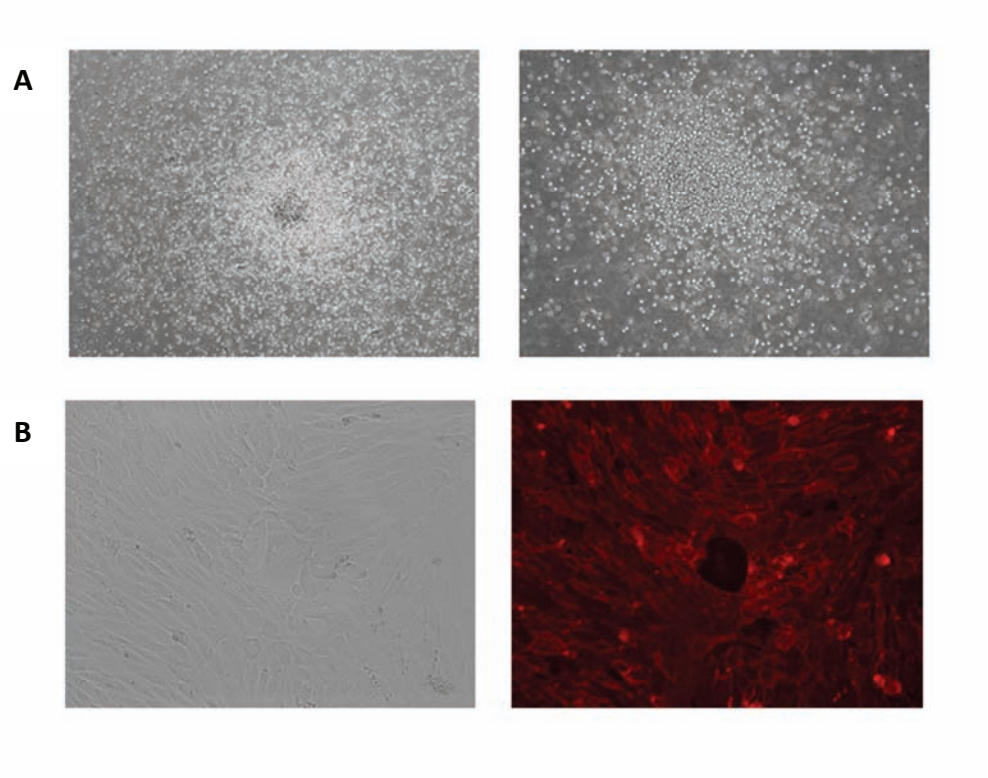

Figure 33 CD34$^+$ cells harvested from iPS directed differentiation cultures demonstrate restricted haematopoietic potential.
CD34$^+$ cells were enriched from day 10 C19 iPS cell cultures differentiated in the presence of condition 4 cytokine regime. Cells were seeded into a CFU assay to assess haematopoietic (myeloid) potential (A, x4 magnification). CFU-G/GM colonies could be observed in the absence of all other colony morphologies. CD34$^+$ cells were also cultured in EGM-2 on collagen-I coated plates (B, x20 magnification). Cells with a endothelial-like morphology that stained CD31$^+$ could be detected, live cell staining with CD31 PE. n=2 independent experiments.

3.4 Discussion

In establishing the iPS/OP9 co-culture system it was apparent that the media components and splitting regime were highly important to ensure efficient differentiation of HPCs capable of lymphopoiesis. In 'sub-optimal' conditions, OP9 stroma was observed to become increasingly undergo adipogenesis. This is in agreement with a reported negative impact on haematopoiesis of increasing numbers of adipocytes in the bone marrow (Naveiras et al., 2009).

The first haematopoietic cells identified in iPS/OP9 co-cultures express CD41a and CD43. Analysis of the CD43 population revealed $CD41a^+$ and $CD41a^-$ populations. It has been suggested that $CD43^+CD41a^-$ cells may have a broader myeloid potential with the $CD43^+CD41a^+$ population being erythro-megakaryocyte restricted (Rafii et al., 2013, Vodyanik et al., 2006).

Co-culture of iPS-$CD34^+$ cells with MS-5 stroma, and to a lesser extent with OP9 cells, supplemented with either IL-7, IL-3, SCF and Flt3L or VEGF resulted in the production of B lymphocytes as well as monocyte/macrophages and endothelial-like cells. B cell differentiation from pluripotent stem cells has typically proven difficult to achieve, possibly because of the greater transcriptional differences between B cells and the remainder of the hematopoietic pool (Laurenti et al., 2013b, Wada et al., 2011, Martin et al., 2008). The ability of the pre-circulation YS to generate B cells has been described, this potential therefore cannot be used to as a readout for HSC capacity (Sugiyama et al., 2007, Yoshimoto et al., 2011). An *in vitro* assay to investigate multilineage potential in haematopoietic progenitors, such as that described here, is an informative and accessible laboratory tool. Indeed, if cell types that broadly represent the haematopoietic repertoire

can be generated simultaneously then questions of lineage potential can be asked more rigorously than when the clonogenic expansion of a cell is required to permit parallel assays of different lineage potentials. The observation that a bipotent B cell/macrophage progenitor is present in the mouse indicated that the simultaneous demonstration of T cell capacity might also be valuable to assay for multilineage potential (Montecino-Rodriguez et al., 2001). Furthermore, whether such a mouse-human hydrid culture system is biologically relevant and/or whether cells are experiencing near-physiological levels of soluble and membrane factors is debatable.

As OP9 co-culture continued towards the day 22 time point, a large number, but not all, of $CD45^+$ cells began to acquire myeloid lineage markers such as CD14. The CFU assay however revealed a gain in haematopoietic multipotentiality following continued culture as demonstrated by CFU-GEMM potential. This bears resemblance with the yolk sac where multilineage potential is detected at E8.25 in the mouse embryo, following the emergence of first emergence of blood cells at E7.0 (Palis et al., 1999, Palis et al., 2001). The CFU frequency described here was low at ~100 colonies/$1x10^5$ cells. In an iPS/OP9 co-culture system, Slukvin and colleagues assessed the CFU potential of numerous iPS cells lines and demonstrated the production of ~100-2500 colonies/$1x10^5$ cells (Choi et al., 2009). The findings in this thesis therefore are at the very lower end of this diverse range. Choi *et. al.,* reported no correlation with the reprogramming strategy, or tissue of origin, with haematopoietic differentiation efficiency (Choi et al., 2009). The iPS lines used in the CFU study described here were derived using retroviral introduction of the reprogramming factors, is it possible that integration may impact upon differentiation efficiency and therefore CFU potential.

Analysis by SAM and PCA of gene array data revealed a close similarity between iPS-B and HSC-B. Both B cell types were generated using the same co-culture assay over the same time period. Whilst haematopoietic progenitor cells from iPS cells (iPS-$CD34^+$ cells) and those isolated from UCB (UCB-$CD133^+$ cells) were generated in different conditions, the signals experienced during subsequent differentiation to the B cell lineage had great similarity. One limitation of this is that human progenitors with endothelial potential, and reported mesenchymal potential were included in the iPS-$CD34^+$ cultures (Vodyanik et al., 2006). This diversity was most likely lacking in UCB-$CD133^+$ cultures. Purification on day 10 of iPS/OP9 co-cultures for $CD43^+$ cells would have addressed this problem, however the required scale for generating $CD19^+$ cells from FACS isolated $CD43^+$ cells was prohibitory. Other than the potential effect arising from the heterogeneity of iPS progenitors, the conditions and factors used to promote B cell lymphopoiesis in iPS-B and HSC-B cultures were identical. A difference in the efficiency of iPS differentiation to the B cell lineage, in comparison to populations derived from UCB HSC/HPCs, was observed. iPS cell cultures yielded fewer and lower proportions of B cells but this difference in $CD19^+$ cell number was also observed in long term cultures, as described in Chapter 5. The data described here may suggest that the differential expression of a small number of genes distinguish iPS-derived B cells from HSC-derived B cells. Of particular interest was the high expression levels of PDGFRA and Lin28b in iPS-B when compared to HSC-B. PDGFRA encodes a transmembrane receptor tyrosine kinase which is activated by the binding of its ligand, PDGF (Andrae et al., 2008). PDGFR-α is expressed in a broad range of normal and cancer cell types (Andrae et al., 2008). Deletion of this receptor results in embryonic lethality in half of the embryos, with survivors having major defects in connective tissues (Schatteman et al., 1992). PDGFR-α is expressed in the mesoderm, absent in endoderm

and expressed in ectoderm at late stages (Schatteman et al., 1992). In pluripotent stem cell cultures, PDGFR-α has been reported to be expressed on paraxial mesoderm progenitors which form connective tissue, skeletal muscle and endothelium (Sakurai et al., 2006, Sakurai et al., 2012). Flk-1^{+}PDGR-α^{+} primitive mesoderm differentiated to Flk-1^{+}PDGR-α^{-} and Flk-1^{-}PDGR-α^{+} populations which possess vascular mesoderm and paraxial mesoderm potential respectively (Sakurai et al., 2006, Kataoka et al., 1997). However, a number of reports in both mouse and human have demonstrated the presence of PDGR-α on cardiac progenitors, which suggests a border expression profile of this receptor within mesodermal tissues than just the primitive mesoderm (Kattman et al., 2011, Evseenko et al., 2010). In one report, Keller and colleagues distinguished cardiac and haematopoietic progenitors in a mouse ES cell system with a Flk-1^{+}PRDGR-α^{+} (cardiac) and a Flk-1^{+}PRDGR-α^{-} (haematopoietic) phenotype (Kattman et al., 2011). Moreover, the capacity of PDGFRα^{+} cells to give rise to haemato-endothelial lineages, including HE and fetal liver B cells has been recently described in a transgenic mouse embryo (Ding et al., 2013). PDGFRα^{+} cells from human ES cells were also described to have haematopoietic potential (Davis et al., 2008, Choi et al., 2012). High expression of PDGFR-α has been reported in hES-derived progenitors with primitive haematopoietic potential and low or negative expression on HE precursors (Choi et al., 2012). Of note, some pre-B acute lymphocytic leukaemia (ALL) cell lines have been described to express PDGFR-α (Tsai et al., 1994b).

Interestingly, iPS-B cells showed a higher expression of Lin28b than HSC-B cells. Lin28 was used as part of the reprogramming cocktail to generate OPM2 and OC3 iPS cell lines. However, loss of transgenes was demonstrated and lines were characterise as *bona fide*

iPS cells. Therefore, this observation of high Lin28b expression is likely to be independent of the introduction of the exogenous factor. Lin-28 proteins are RNA binding proteins that repress let-7 microRNAs and influence translation (Van Wynsberghe et al., 2011, Winter et al., 2009). A role for Lin28 in the regulation of ES cell self-renewal has been described, which was supported by the use of Lin28 as a reprogramming factor for the generation of iPS cells (Yu et al., 2007). Notably, Lin28b knockout mice are viable and fertile. Work by Muljo and colleagues demonstrated that Lin28b mRNA was abundant in mouse fetal liver B cells and HPCs but not in the adult bone marrow equivalents (Yuan et al., 2012). This difference was also observed in human tissues (Yuan et al., 2012). The authors went on to demonstrate that adult mouse HSC/HPCs transduced with Lin28b switched potential to a fetal B cell program, preferentially generating B-1a B cells and MZ B cells (Yuan et al., 2012). Knockdown of Lin28b has also been described to reduce the expression of fetal globins in UCB red blood cells (Lee et al., 2013). Furthermore, a role for Lin28b in the self-renewal potential of fetal HSCs, which exceeds that of adult HSCs, has been reported (Copley et al., 2013). Interestingly, Sox17, that has been described as a fetal-adult haematopoietic switch (Kim et al., 2007), was not differentially expressed between iPS-B and HSC-B cells (logFC <0.01, adj.p value=0.99). Low expression of *SOX17* in human ES-derived HPCs has however been described (Nakajima-Takagi et al., 2013).

A large volume of evidence supports the concept that HSCs are generated intra-embryonically (Medvinsky and Dzierzak, 1996, Kumaravelu et al., 2002). It is however possible that yolk sac-derived progenitors may also be found in the bone marrow of the adult, a concept that has been indirectly supported by Nishikawa and colleagues (Samokhvalov et al., 2007). CD133 expression defines a population that includes HSCs,

however the frequency of HSCs defined by this criteria is low. No unique marker has been found, or indeed is perhaps likely to be found that can be used to identify an HSC with the exclusion of all other cells. A cell surface phenotype of $Lin^{-}CD34^{+}CD38^{-}CD45RA^{-}Thy1^{+}Rho^{lo}CD49f^{+}$ has been described by Dick and colleagues and was used to demonstrate the reconstitution ability of single UCB cells with frequencies of 14-28% (Notta et al., 2011). Suggesting that up to 1 in 4 cells isolated by this criteria may be true HSCs. As expected, after freeze thawing UCB, (using media with high FCS content) cells with this phenotype could not be easily detected and therefore this level of stringency was not achievable for the experiments described herein. An alternative explanation for the close similarity between iPS-B and HSC-B cells could be that UCB-$CD133^{+}$/HSC-B cells were not derived from an HSC-like population. In these cultures, B cells could have been produced from more differentiated populations. It is possible that the MS-5 co-culture system may preferentially promote B cell lymphopoiesis from the non-HSC compartment in the $CD133^{+}$ pool.

$CD19^{+}CD10^{+}$ B cells were also isolated from peripheral blood and umbilical cord blood. Analysis of gene array data revealed greater differences between these two populations than was seen with iPS-B and HSC-B, obtained by *in vitro* co-culture with MS-5 cells. Furthermore, greater similarity was generally observed between PB and iPS-B than UCB and iPS-B. This could however be due to experimental design. CD10 is known to be expressed on the CLP in human haematopoiesis, with cell surface CD19 expression occuring from the early-B/pro-B cell stage (Galy et al., 1995, LeBien, 2000). In the MS-5 co-culture system, B cell development from either iPS or UCB HSC/HPCs appears to be relatively synchronous. By day 21, the majority of $CD19^{+}$cells express CD10 and lack CD34

or IgM expression, thus the population resembles pre-B cells. Isolation of B cells based purely on CD19 and CD10 expression however would, in general include, pro-B, pre-B and immature B cells. The lower fluorescent intensity of CD10 in UCB and PB B cells than iPS-B and HSC-B indicates that the isolated B cells from blood sources are likely to be more developmentally mature. B cells isolated from UCB will have been a heterogeneous mix of pro-B, pre-B and immature B cells. As B cell development from the HSC to the immature B cell stage occurs in the bone marrow, the likelihood of these cell types being present in non-mobilised peripheral blood is low. As described here, $CD10^{+}CD19^{+}$ cells have been reported in non-mobilised peripheral blood (Hoffkes et al., 1996). Peripheral blood $CD10^{+}CD19^{+}$ cells are likely to be immature B cells that express cell surface antibodies. This experiment could therefore have been improved by including $CD34^{-}$ and IgM^{-} in the FACS isolation strategy. Indeed, UCB B cells differentially expressed immunoglobulin-related genes and had a lower rate of cell division than HSC-B cells. It is well known that pre-B cells go through a highly proliferative stage, pre-B I, before cell division rates are reduced in the pre-B II population (Hess et al., 2001, Hardy et al., 1991). Therefore, it would be expected that $CD19^{+}CD10^{+}$ B cells from UCB would contain an immature B cell population which could account for these differences.

Whilst the defined serum and feeder-free differentiation system described generated haematopoietic cells, this assay was inefficient and showed large variability that impacted upon reproducibility. Furthermore, as research in the field has failed to demonstrate lymphocyte development in such defined systems, it was deemed prudent to move forward with the OP9 co-culture system to promote the generation of iPS-HPCs with B cell potential.

In conclusion, iPS cells can be differentiated to produce haematopoietic progenitor cells with B lymphocyte potential. iPS-derived B cells and HSC-derived B cells demonstrated a high number of similarities at the transcriptional level.

Chapter 4.

Identifying iPS-derived haemogenic endothelium with B cell potential.

4.1 Aims and objectives

The aim of this chapter was to establish whether haemogenic endothelium (HE), arising from iPS co-cultures, was capable of differentiating into B lymphocytes. The main objectives were to:

1) Understand the temporal dynamics and identity of haematopoietic and endothelial progenitors arising in an iPS/OP9 co-culture system and their relationship therein.

2) Assess the capacity and possible dichotomy of endothelial-like and haematopoietic populations to generate B cells prior to, during and after the emergence of haematopoietic cells in iPS/OP9 co-culture.

3) Determine the potential of FACS purified iPS-derived HE to produce B cells.

4) Assess the potential of iPS-derived haemato-endothelial progenitors to generate functional endothelium.

4.2 Background

The observation of cells, that label with haematopoietic markers, budding from the endothelium of the dorsal aorta in both chick and mouse embryos gave support to the principle of haemogenic endothelium (Jordan, 1917, Jaffredo et al., 1998, Pardanaud et al., 1987). Haemogenic endothelium (HE) is described as a cell that is characteristically endothelial but capable of differentiating to generate haematopoietic progeny. Additional support came from studies where endothelial cells were labelled with Dil-AcLDL which subsequently marked haematopoietic cells (Jaffredo et al., 1998, Sugiyama et al., 2003). It was also demonstrated that (pre)-HSCs in the AGM co-express CD144 and CD45 prior to the downregulation of CD144 (North et al., 2002, Taoudi et al., 2008). This $CD144^{+}CD45^{+}$ population was also transiently observed in the fetal liver (Kim et al., 2005). How HE cells relate to the remainder of the phenotypically similar endothelial cell pool (that lack haematopoietic potential) is relevant to the understanding of haematopoietic ontogeny. Elegant studies in the chick demonstrated the independent origin of cells in the dorsal aorta wall, those cells of splanchnopleural origin exclusively possessing haematopoietic potential (Pardanaud et al., 1996). Interestingly, a remodelling phase may occur during development in which the haemogenic cells of the aorta are replaced by the endothelium lacking this potential (Pouget et al., 2006). Additional data in line with this concept was demonstrated by a reduction in the diameter of the dorsal aorta following haematopoietic differentiation (Kissa and Herbomel, 2010). Support for the presence of HE in the developing human embryo has also been described with the visualisation of intra-aortic clusters and by *ex vivo* culture methods (Oberlin et al., 2002, Tavian et al., 1996).

Whilst the data supporting the existence of HE was strong, conclusive evidence was not demonstrated until 2009/2010 when the use of timelapse imaging technologies enabled the direct visualisation of haematopoietic cells budding from endothelium, both *in vitro* and *in vivo* (Eilken et al., 2009, Boisset et al., 2010, Bertrand et al., 2010, Kissa and Herbomel, 2010). Here, the authors illustrated that haematopoietic emergence from endothelium occurred via an endothelial to haematopoietic transition (EHT). EHT describes a process where, in contrast to differentiation by asymmetric cell division, a cell directly changes identity. This process was demonstrated to require Runx1 expression, a transcription factor that is necessary for definitive haematopoiesis (Chen et al., 2009, Okuda et al., 1996, Wang et al., 1996, Kissa and Herbomel, 2010, North et al.,1999). Inversely, a role for HoxA3 in the maintenance of the endothelial programme has also been described (Iacovino et al., 2011).

During ontogeny multiple, potentially autonomous waves of haematopoiesis occur. A primitive wave that generates erythro-megakaryocyte restricted progenitors is initially observed followed by successive waves of definitive haematopoiesis. The first that produces a multilineage progenitor and the second the HSC (Lassila et al., 1978, Muller et al., 1994, Medvinsky and Dzierzak, 1996, Tavian et al., 2001, Dieterlen-Lievre, 1975). If these populations do indeed have independent origins, and if they both develop via a haemogenic endothelial intermediate, it would seem logical that there are multiple subtypes of HE in the developing embryo. Support for such a concept was described by Speck and colleagues, who reported two independent populations of endothelium which generated the erythoid/myeloid progenitor and HSC respectively (Chen et al., 2011, Miller et al., 2002). Additionally, Yoder and colleagues demonstrated that YS-derived HE

preferentially generated B-1 B cells, which may be reminiscent of the first wave of definitive haematopoiesis (Yoshimoto et al., 2011). Suggestions of distinct populations of HE with erythro-megakaryocyte and erythroid/myeloid potentials from human ES cells have also been proposed (Rafii et al., 2012).

As demonstrated by Schroeder and colleagues in the context of HE, and by numerous other groups in the field, pluripotent stem cells are an accessible and adaptable system to interrogate biologically relevant developmental questions (Eilken et al., 2009, Nishikawa et al., 1998a). This is even more poignant in the context of human ontogeny due to the inaccessibility of human embryos. Once such question that may be advanced with *in vitro* pluripotent stem cell cultures is whether a unique marker for haemogenic endothelium can be identified. Such a cell surface marker has eluded the scientific community thus far. HE can be distinguished from endothelium by the expression of the transcription factor Runx1 (North et al., 1999). However, the identification of cell surface markers that can be monitored in live cells, without the need for the genetic modification of the population of interest, is desirable for multiple applications. CD144 is an adhesion molecule that is required for vascular integrity that is expressed on endothelial cells and haematopoietic progenitors (Kim et al., 2005, Oberlin et al., 2010a). Expression of CD144 in the absence of haematopoietic markers therefore should identify endothelium and HE. It was hypothesised that the presence of $CD144^{+}haem^{+}$ cells would mark a haematopoietic population that has recently emerged from HE. However, by the time $CD144^{+}$ cells express haematopoietic markers this population has become committed to the haematopoietic lineage. Recently, and as this research was being completed, Slukvin and colleagues used the absence of CD73 expression to distinguish HE from endothelium in a

human PSC/OP9 co-culture system (Choi et al., 2012). There have been multiple reports of HE generation from human PSCs however, evidence relating to whether these cells are able to contribute to the lymphoid lineages has frequently been lacking (Rafii et al., 2012, Choi et al., 2012). Keller and colleagues did recently demonstrate that hPSC-derived $CD34^+$ cells lacking CD43 and CD45, that expressed high levels of Sox17, were capable of differentiating to the T cell lineage, the first such demonstration of this kind (Kennedy et al., 2012). B lymphocytes represent one of the main cell types of the differentiated haematopoietic system and therefore serve as an important readout for multilineage potential. Whether B cell potential is possessed by hPSC-derived HE has not been demonstrated.

Despite numerous attempts to expand HSCs *in vitro*, this has not been successfully achieved. Indeed it is plausible that such an accomplishment might be unachievable when considering the 'normal' biological behaviour of this population. Whilst it is true that HSC expansion in the AGM and fetal liver is rapid and large scale, once HSCs have homed to the bone marrow, and have passed the post-natal period, they are found to be relatively quiescent (Yahata et al., 2008, Oguro et al., 2013, Bowie et al., 2007). To generate HSCs for clinical transplantation, an alternative strategy may be to expand HE cells or their progenitors, derived from pluripotent stem cells. The generation of hPSC-derived HE with lymphocyte potential moves the field one step closer to attaining this endeavour.

The generation of stable, expandable and functional endothelium from pluripotent stem cells also has numerous applications. Clinically, endothelium could be used for improving revascularisation and aiding haematopoietic engraftment. As $CD144^+CD45^-$ cells could be detected in long term cultures seeded with iPS-$CD34^+$ cells (Chapter 3), it seems probable

that endothelial progenitors cells might be present. Endothelial cell colonies have been succesfully cultured from umblical cord and peripheral blood using VEGF containing media. At the time when this aspect of the project was being undertaken, a limited number of studies had described efficient endothelial generation from human pluripotent stem cells (Li et al., 2007, Taura et al., 2009, Yamashita et al., 2000). Functional assessment of endothelial cells is typically undertaken using *in vitro* tubule-forming cultures such as the matrigel and stromal co-culture assay, as well as the *in vivo* hindlimb ischaemia or matrigel implantation models (Ponce, 2009, Limbourg et al., 2009, Roubelakis et al., 2013).

4.3 Results

4.3.1 B lymphocyte potential is transiently observed in the CD144^{+}haem^{neg} population.

4.3.1.1 Mapping the co-expression of cell surface VE-cadherin (CD144) and haematopoietic markers during iPS/OP9 co-culture.

It was hypothesised that haematopoietic progenitors generated from differentiating iPS cells arise via a haemogenic endothelial (HE) intermediate, such has been identified for some haematopoieitic cells *in vivo* and, *in vitro* from murine ES cells (Boisset et al., 2010, Bertrand et al., 2010, Eilken et al., 2009). To demonstrate this *in vitro,* the precursor population must be characterised as HE and then, either by direct visualisation or by single cell assays, should be demonstrated to produce haematopoieitic cells. The aim was therefore to get closer to such an understanding by identifying a time window for EHT and to identify the phenotype of emerging haematopoietic cells. The transient observation of cells co-expressing endothelial-associated and haematopoietic markers could be indictive of recent EHT events and could be used as a temporal signpost for the possible presence or absence of HE as has been described for emerging pre-HSCs in the AGM (Taoudi et al., 2008).

To this end, and following on from the observations made in Chapter 3, the expression of the endothelial-associated CD144 and haematopoieitic marker CD41a was assessed over time in the iPS/OP9 co-culture (Figure 34B). C18 or C19 iPS colonies were seeded onto overconfluent OP9 cells and maintained as previously described without the addition of cytokines (as described in 2.6.1). The whole cell fraction, both adherent and non-adherent cells, was harvested daily from day 5-10 and then on alternate days from day

10-22 of co-culture. The first $CD41a^+$ cells arising, observed from day 6 were $CD144^+$. By day 7, $CD41a^+CD144^-$ cells were present with a progressively large increase in cell number (Figure 34B). By day 12, the number of double positive ($CD41a^+CD144^+$) cells had reduced dramatically, with both $CD41a^+CD144^-$ and $CD41a^-CD144^+$ populations still present (Figure 34B). This pattern of population change was also reflected when the expression of CD34 and CD43 was compared, although $CD34^+CD43^+$ cells were detected throughout the timeperiod assessed (Figure 35A). CD34 is a molecule that is expressed on a more diverse range of cell types than CD144 (De Francesco et al., 2009, Vodyanik et al., 2006, Drew et al., 2005, Oberlin et al., 2010b, Kim et al., 2005). $CD34^+CD43^+$ cells were detectable on day 6. By day 8, $CD43^+CD34^-$ cells could be observed (Figure 35A).

As has been described above and by others, CD45 is a haematopoietic marker that is expressed later on in PSC/OP9 co-cultures than both CD41a and CD43 (Vodyanik et al., 2006). Interestingly, the first $CD45^+$ cells, observed on day 10, were $CD41a^-$ (Figure 36). In contrast, whilst $CD45^+CD43^{-/low}$ cells were present on day 12, a $CD45^+CD43^+$ populations was also observed (Figure 36). The analysis of CD144 and CD45 expression revealed an interesting sub-segmentation of populations. Whilst both $CD144^{low}CD45^+$ and $CD144^-CD45^+$ cells were present, this may not be a sequential acquisition. On day 10, when $CD45^+$ cells were first observed, a significant $CD45^+CD144^-$ population was already apparent (Figure 35). This is potentially of interest as pre-HSCs arising in the AGM have a $CD144^+CD45^+$ phenotype (Rybtsov et al., 2011).

In summary, the first cells expressing haematopoietic markers co-expressed endothelial-associated molecules such as CD144 and CD34. At later time points, the number of double positive cells was reduced and cells expressing haematopoietic markers in the

absence of endothelial-associated makers were present. This suggests, but does not prove, that haematopoietic cells might be arising, and then diverging from a population with an endothelial-like phenotype. A hypothesis driven by these data is that EHT might be occurring between day 5-6.

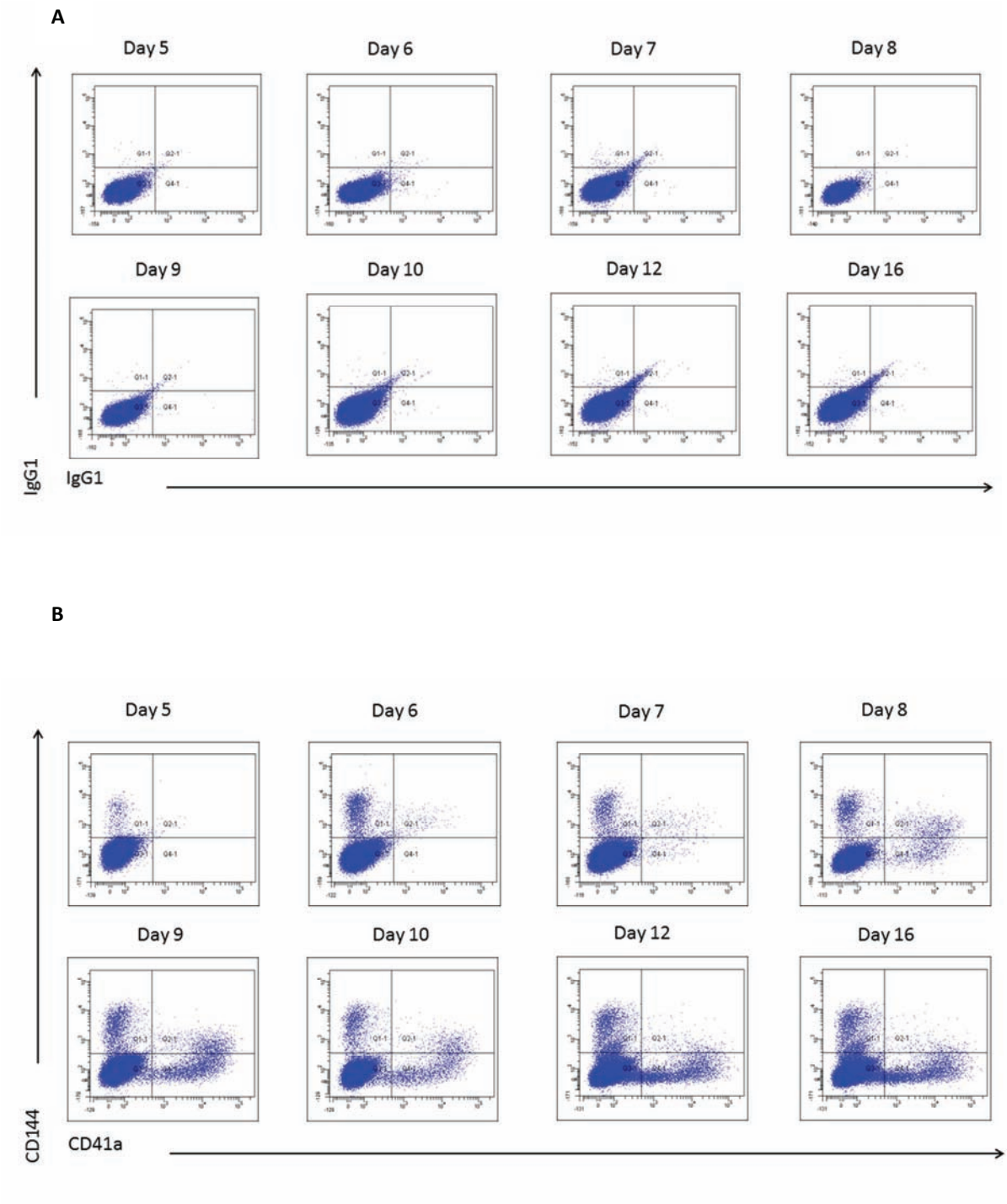

Figure 34 Mapping the temporal expression of haematopoietic and endothelial cell surface markers.

C18 or C19 iPS colonies were co-cultured with OP9 stroma and harvested at indicated time points where whole cell fractions were stained with mAbs and analysed by flow cytometry. (A) Representative isotype control staining of co-cultures throughout iPS/OP9 timecourse. (B) $CD41a^+$ cells arising in culture initially co-expressed CD144 before $CD41a^+CD144^-$ populations could be observed. At later timepoints $CD144^+CD41a^+$ cells were predominantly absent. (Statistical analysis of key populations and timepoints is described in Appendix Table 18). Representative images n=3.

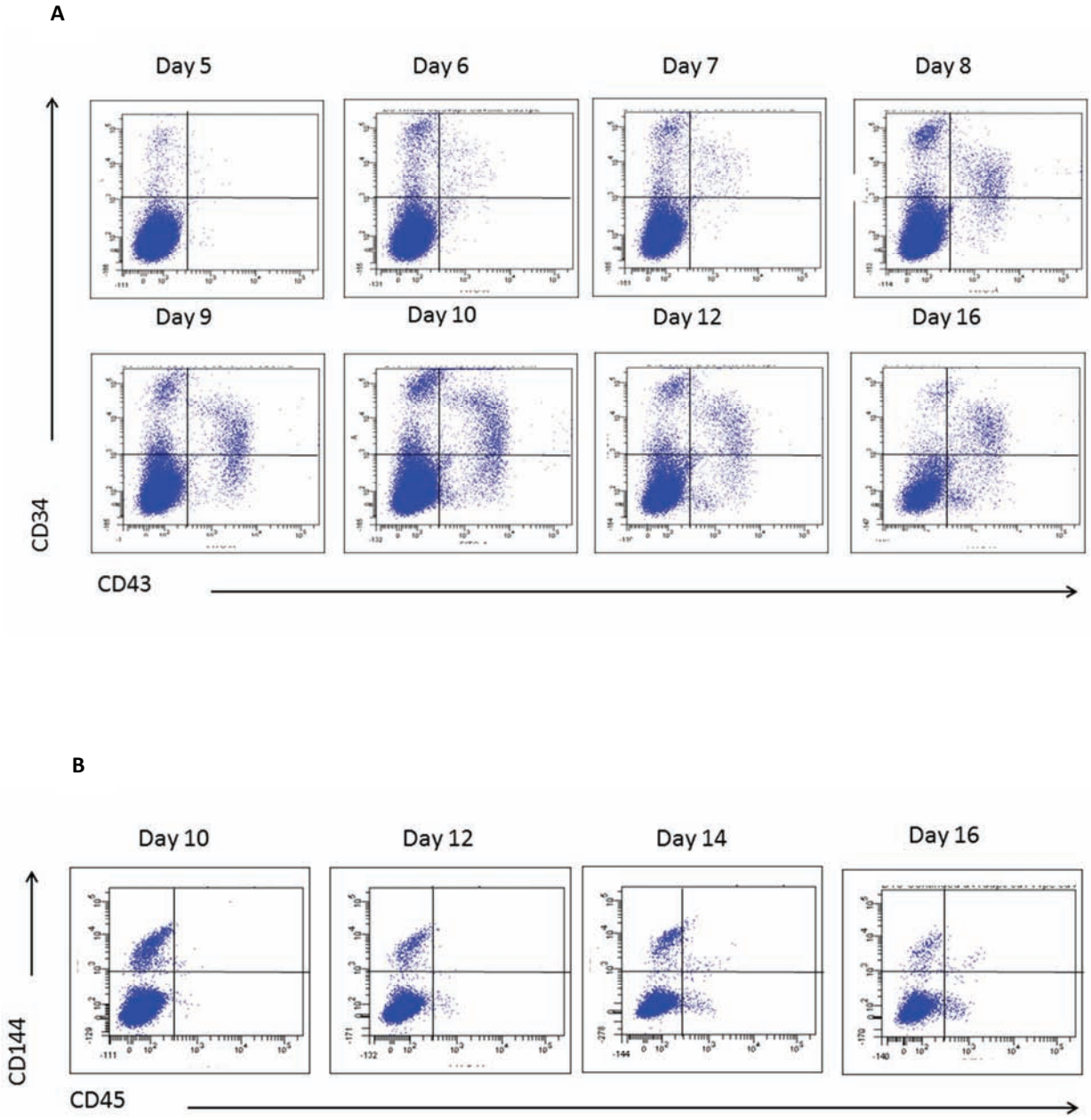

Figure 35 Mapping the temporal expression of haematopoietic and endothelial cell surface markers.

C18 or C19 iPS colonies were co-cultured with OP9 stroma and harvested at indicated time points where whole cell fractions were stained with mAbs and analysed by flow cytometry. (A) $CD34^{+}CD43^{-}$ cells were observed prior to a $CD34^{+}CD43^{+}$ population. From day 8, a $CD34^{+}CD43^{-}$ fraction was also detectable. (B) When CD45 expression was assessed in conjunction with CD144, $CD45^{+}CD144^{-}$ cells were present prior to, and at the same timepoints as $CD144^{+}CD45^{+}$ cells. (Statistical analysis of key populations and timepoints is described in Appendix Table 18).Representative images n=3.

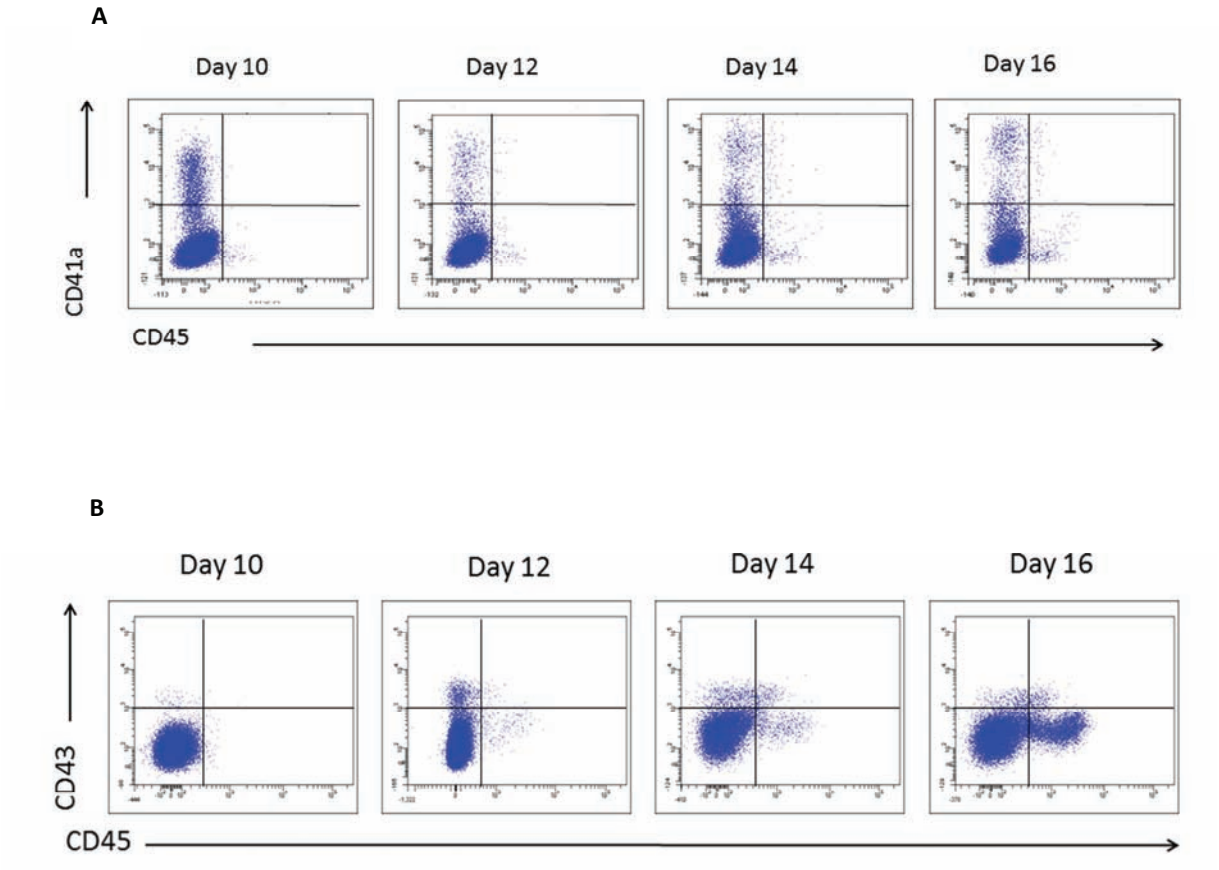

Figure 36 Mapping the temporal expression of early and late haematopoietic cell surface markers.

C18 or C19 iPS colonies were co-cultured with OP9 stroma and harvested at indicated time points where whole cell fractions were stained with mAbs and analysed by flow cytometry. (A) The earliest detectable $CD45^{+}$ cells were $CD41a^{-}$, with the majority of the population remaining negative for CD41a over the time assayed. (B) Both $CD43^{+}CD45^{+}$ and $CD43^{int}CD45^{+}$ cells were observed. (Statistical analysis of key populations and timepoints is described in Appendix Table 19).Representative images n=3 with the exception of (B) where n=1.

4.3.1.2 Day 10 B cell potential in iPS/OP9 co-cultures is restricted to the CD43$^+$ fraction.

The day 10 CD34$^+$ population isolated from C18 or C19 iPS/OP9 co-cultures, as described in Chapter 3, were capable of generating B cells, red blood cells (RBCs), monocyte/macrophages and an endothelial-like population. The CD34$^+$ population however was heterogeneous when analysed for cell surface expression. The CD34$^+$ fraction included cells that were positive for haematopoietic markers (CD43 and CD41a) as well as CD43/CD41a$^-$ cells. The CD43 cell surface marker has previously been used to discriminate haematopoietic (haem) from endothelial (endo) cells in a hES/OP9 co-culture setting (Vodyanik et al., 2006). The first question addressed here was whether B cell potential is restricted to CD34$^+$CD43$^+$ haem and/or CD34$^+$CD43$^-$ endo populations in day 10 cultures. C18 or C19 iPS colonies were differentiated on OP9 stroma for 10 days, as previously described, and then harvested. CD34 and CD43 populations were enriched by MACS using CD34 and CD43 microbeads respectively (Figure 37 A). The CD34$^+$CD43$^-$ enriched population was generated using a CD34 multisort kit. Briefly, cells were initially isolated using CD34 multisort beads, the microbeads were then released using the Multisort Release Reagent and then cells were selected with CD43 microbeads (Figure 37 A). Due to the limitations of the MACS technique CD34$^+$CD43$^-$ fractions contained a small population (<1%) CD43$^+$ cells (Figure 37 A). Cells were then seeded onto MS-5 stroma with IL-7, IL-3, SCF and Flt3L to promote B cell differentiation. Pebblestone-like colonies that have been associated with B cell development were observed in CD34$^+$ and CD43$^+$ but not CD34$^+$CD43$^-$ cultures (Figure 37 B). After 21 days, cultures were harvested and stained with mAbs to CD19, CD10 and CD45 for analysis by flow cytometry. B cells could

be identified in the $CD34^+$ and $CD43^+$ but not in $CD34^+CD43^-$ cultures (Figure 37 C). This suggests that by day 10 B cell potential is restricted to the haematopoietic fraction.

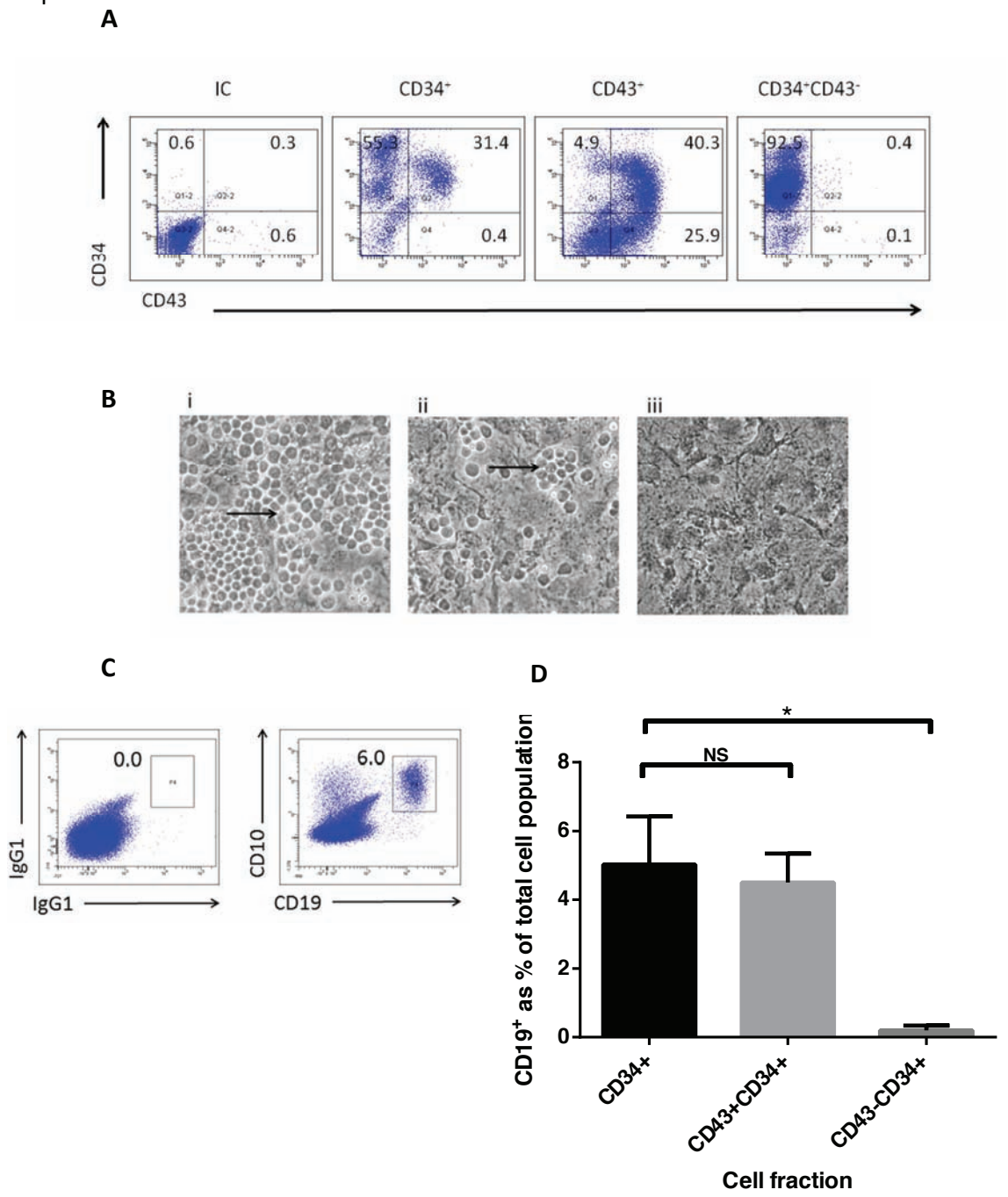

Figure 37 B cell potential in day 10 iPS/OP9 co-cultures is restricted to the CD43$^+$ haematopoietic fraction.

(A) iPS colonies were differentiated in OP9 co-culture for 10 days, cells were then harvested and enriched for the CD34$^+$, CD43$^+$ or CD34$^+$CD43$^-$ fractions by MACS. Cells were seeded into conditions that promote B cell differentiation. (B) In CD34$^+$ and CD43$^+$ cultures, colonies with a pebblestone-morphology that have been associated with B cell development were observed (magnification x40). (C) Cultures were harvested after 21 days and stained with mAbs to CD19 and CD10 for analysis by flow cytometry. (D) CD34$^+$ and CD43$^+$ cultures yielded a significant CD19$^+$ population that was absent in CD34$^+$CD43$^-$ cultures. n=4 (independent experiments), unpaired t-test. *=P <0.05, NS= P >0.05.

4.3.1.3 The CD144^{+}haem^{neg} population transiently demonstrates B cell potential.

In iPS/OP9 co-cultures, the day 10 endothelial-like population lacked B cell potential when assayed by the MS-5 co-culture described. Haematopoietic cells first appeared in this culture system on day 6 when a CD144^{+}haem^{+} phenotype was transiently observed. By day 12, this population was significantly reduced. It was hypothesised that a subpopulation which is phenotypically endothelial (CD144^{+}haem^{neg}), as observed on day 5 of co-culture, may have the potential to either differentiate into haematopoietic cells or to maintain endothelial characteristics. In this hypothesis, whether the HE population is capable of producing B cells may be dependent on the point along the endo→HE→haem continuum at which the cells are assayed and the conditions of the assay itself. It was also hypothesised that once HE had been generated and subsequently differentiated to produce haematopoietic cells that the endothelial-like population would then lack haematopoietic potential. If this hierarchy exists then the smaller the temporal period between the presence of cultures containing an endothelial-like populations, but not haematopoietic cells, and the presence of a cultures containing both endothelial-like and haematopoietic cells, the greater the likelihood of HE being found in cultures.

To assess whether endothelial-like cells, described as a CD144^{+}haem^{neg} population, were capable of yielding B lymphocytes, a pilot study was carried out whereby cells were enriched at three time points during C19 iPS/OP9 co-culture. Days 5, 8 and 22 were selected as, day 5 represents a time point at which haematopoietic cells were predominantly absent. Day 8 was chosen as CD144^{+}CD41a/CD43^{+} cells were present as a significant population and day 22 when CD144^{+}CD41a/CD43^{+} were mainly absent. The

ability of the haematopoietic populations present on day 8 and 22 to generate B cells was also assessed. Following co-culture of iPS cells with OP9 stroma for 5, 8 or 22 days, cells were harvested and enriched by MACS to yield $CD144^{+}CD43/45^{-}$ endothelium or $CD43/45^{+}$ haematopoietic cells (Figure 38). Due to the limitations of MACS day 5 endothelial populations contained 3.8% $CD144^{+}CD43^{+}$ cells, although they lacked $CD144^{-}$ $43/45^{+}$ cells (Figure 38). Day 8 endothelium had 0.6% $CD43^{+}$ cells and day 22 endothelium around 10% $CD43/CD45^{+}$ cells (Figure 38).

Enriched populations were seeded into MS-5 co-cultures with B cell cytokines and into CFU assays, cultures were maintained as previously described. After 21 days cells were harvested and analysed by flow cytometry. $CD19^{+}$ B cells could be detected in cultures seeded with day 8 and day 22 haematopoietic cells (Figure 39). Day 5 and day 22 endothelial populations did not yield B cells, however, endothelial cells enriched on day 8 were capable of contributing to the B cell lineage (Figure 39). $CD144^{+}haem^{neg}$ cells were present in all day 21 cultures with the exception of those seeded with day 22 haematopoietic populations (Figure 39).

When cells were seeded into the CFU assay, both day 8 and 22 haematopoietic populations generated CFU colonies (Table 14). A limited number of colonies were also detectable in wells seeded with day 8 and day 22 endothelial cells. However, owing to the impurity of MACS enriched samples and the low number of colonies detected, this result was not conclusive (0.33 colonies/well and 1 colony/well respectively) (Table 14).

An alternative explanation for the data described, is that day 8 but not day 5 endothelium can differentiate to form B cells, and that this potential is only found after day 5, and that the contaminating 0.6% of $CD43^{+}$ cells could be responsible for the lymphocytes

produced. It was therefore necessary to FACS isolate the day 8 endothelial population to exclude contaminating cells expressing haematopoietic markers.

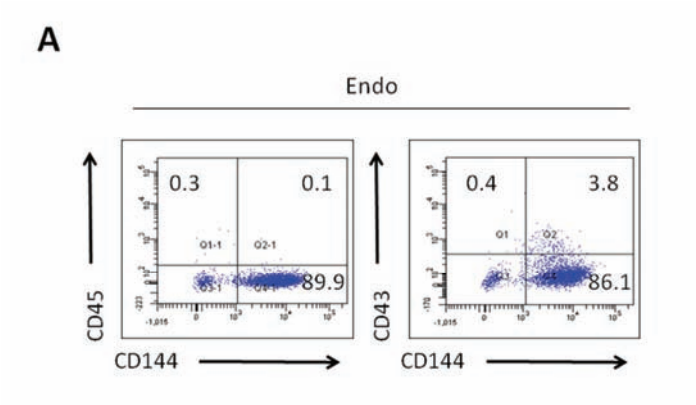
A
Endo
0.3
0.1
89.9
CD45
CD144
0.4
3.8
86.1
CD43
CD144

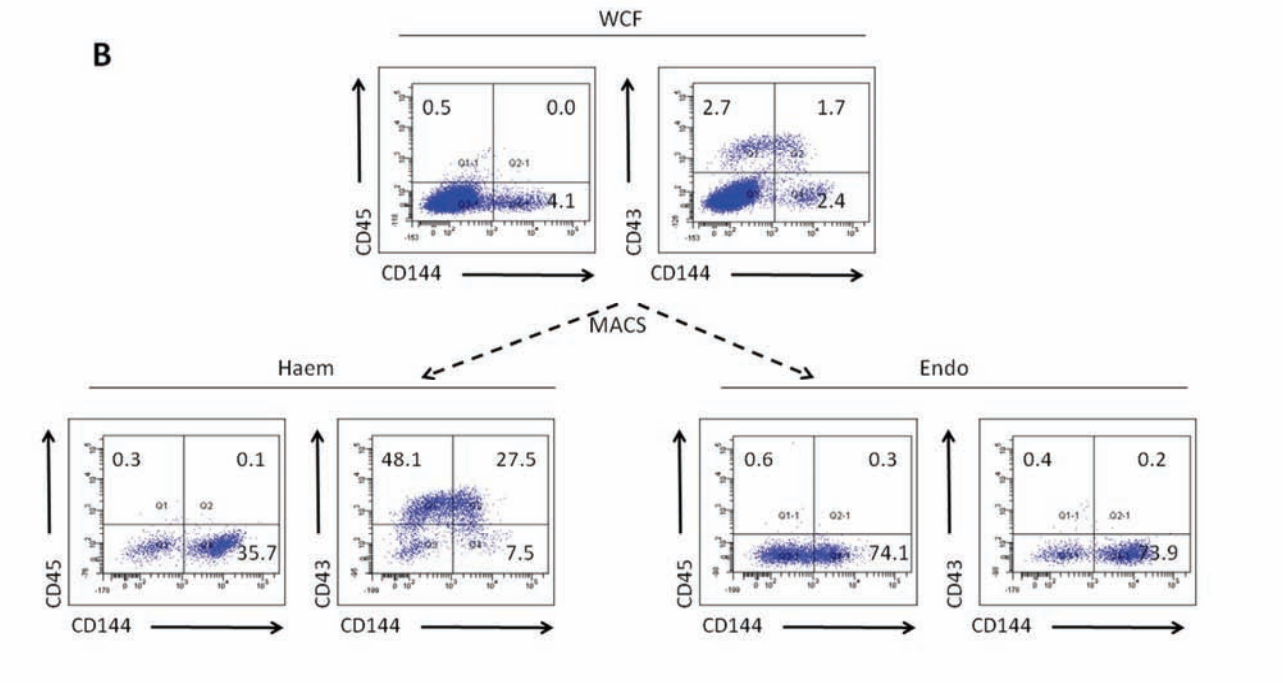
B
WCF
0.5
0.0
4.1
CD45
CD144
2.7
1.7
2.4
CD43
CD144
MACS
Haem
Endo
0.3
0.1
35.7
CD45
CD144
48.1
27.5
7.5
CD43
CD144
0.6
0.3
74.1
CD45
CD144
0.4
0.2
CD43
CD144

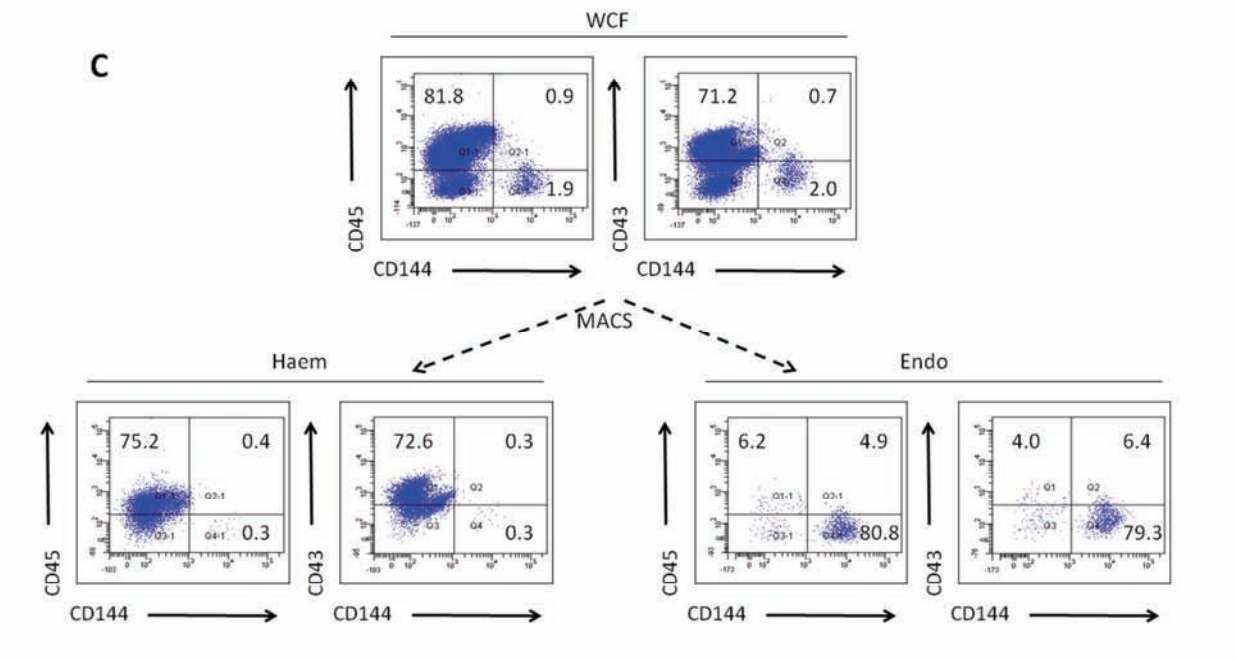

Figure 38 Analysis of MACS enrichment strategy implemented to segregate haematopoietic and endothelial populations on days 5,8 and 22 of iPS/OP9 co-culture.
iPS colonies were differentiated on OP9 stroma for 5 (A),8 (B) and 22 (C) days before being harvested. Cells were then enriched by MACS, haematopoietic cells were initially selected from day 8 and 22 co-cultures using CD43 or CD43/CD45 microbeads. The negative flow through was then enriched for CD144 using CD144-PE and anti-PE beads. Due to the limitations of MACS all endothelial populations contained a small number of contaminating cells. WCF= whole cell fraction, Endo= endothelium and Haem= haematopoietic cells. Pilot study, n=1.

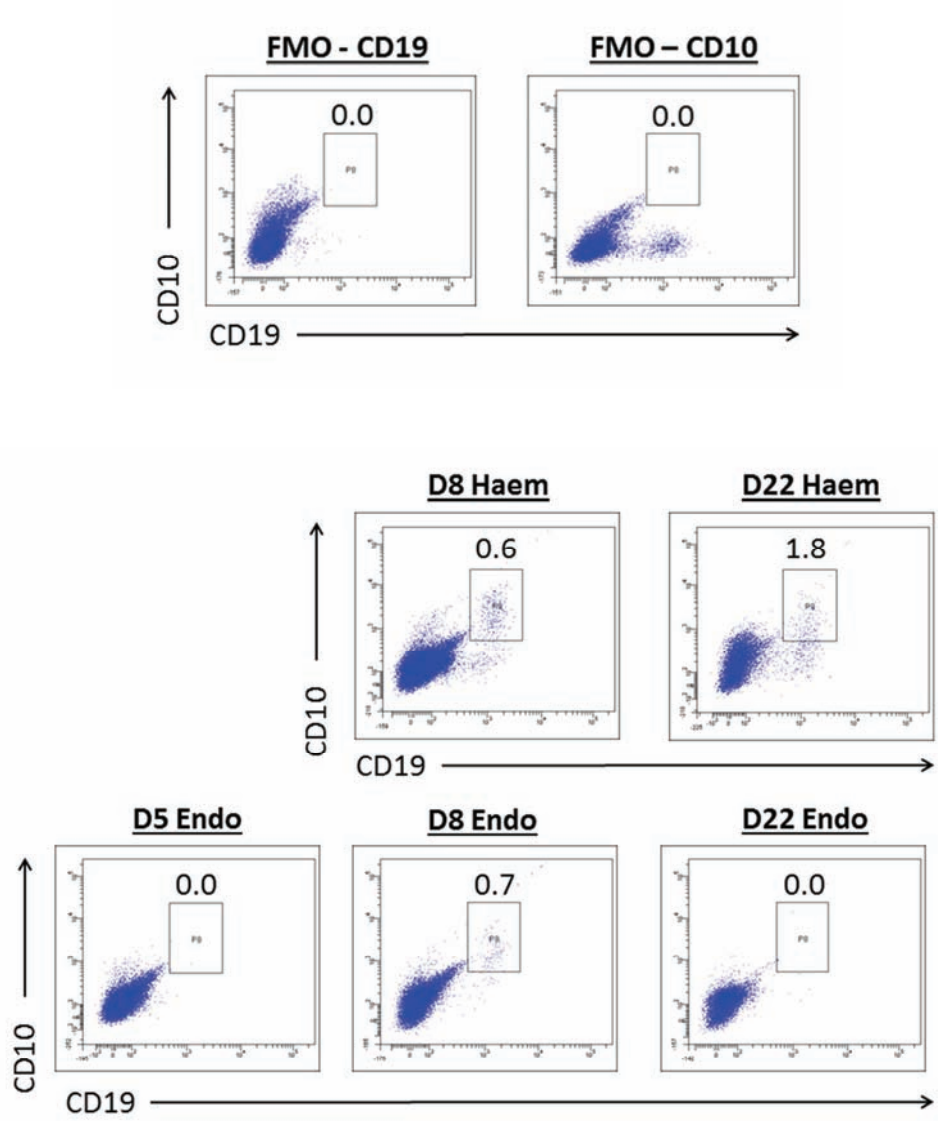

Figure 39 Assessing B cell potential of endothelial and haematopoietic enriched populations from day 5, 8 and 22 of iPS/OP9 co-culture.

Cell fractions were enriched by MACS from harvested populations cultured for 5, 8 and 22 days. Cells were seeded into co-culture with MS-5 stroma and supplemented with IL-7, IL-3, SCF and Flt3L before being harvested after 21 days. Cells were then stained for analysis by flow cytometry. $CD19^{+}$ B cells could be detected in day 8 and 22 haem populations as well as day 8 endothelial cultures but not in day 5 or 22 endothelial cell cultures. Pilot study, n=1.

Table 14 CFU potential of endothelial and haematopoietic populations over time.

Cell Fraction	CFU colonies/1000 cells
D5 endothelium	0
D8 endothelium	0.33
D8 haematopoietic	8.33
D22 endothelium	1
D22 haematopoietic	9.66

Cells were harvested on day 5, 8 and 22 of iPS/OP9 co-culture, MACS enriched for the endothelial or haematopoieitic markers and seeded into the CFU assay. After 14 days colonies were scored. Endothelial populations generated low numbers of colonies with a larger number being detected in wells seeded with haematopoietic cells. Pilot study, n=1.

4.3.2 FACS isolated CD144^{+}haem^{neg} putative haemogenic endothelium is capable of B cell lymphopoiesis

4.3.2.1 Assessing the presence of CD144^{+}CD43/CD235a^{-}CD73^{-} cells during haematopoietic differentiation.

CD144^{+}haem^{neg} describes the phenotype of a population that includes both endothelium and haemogenic endothelium. To date, no cell surface markers has been described that can prospectively identify HE from amongst the endothelial cell pool. Recently, a report by Slukvin and colleagues demonstrated that the absence of CD73 could be used to distinguish endothelium from HE in pluripotent stem cell co-cultures with OP9 stroma (Choi et al., 2012). They demonstrated that a transient CD144^{+}CD43/235a^{-}CD73^{-} population was exclusively capable of producing red blood cells that expressed adult β-globins (Choi et al., 2012). The authors however did not describe the lymphoid potential of this population.

To assess the presence of a CD144^{+}CD43/235a^{-}CD73^{-} population at day 5, 8 and 22 of C19 iPS/OP9 co-culture, cells were harvested and stained with mAbs for flow cytometry. On day 5, CD73^{-} cells were the major population in the CD144^{+}CD43/235a^{-} fraction (Figure 40). By day 8 this population had decreased and was only a minor fraction in the CD144^{+}CD43/235a^{-} population (Figure 40). On day 22 of co-culture, the CD144^{+}CD43/235a^{-}CD73^{-} population was completely absent, whilst the CD144^{+}CD43/235a^{-}CD73^{+} population could still be detected (Figure 40). The aim was to develop this work by FACS isolating prospective HE cells to assay for B cell potential. Although, based on these results, the percentage of the population with a CD144^{+}CD43/235a^{-}CD73^{-} phenotype was low on day 8, in general, cells at this timepoint

were demonstrated to be capable of B cell lymphopoiesis (Figure 39). This potential may not be found prior to day 8. Furthermore, on day 8 the overall number of cells expressing haematopoietic and endothelial markers was much greater than on day 5, which has practical importance for downstream assays.

To exclude OP9 stroma and enrich the haemato-endothelial population prior to FACS isolation, cells were selected on CD34 by MACS. On average, 374,524 ± 75,513 $CD34^+$ cells (mean ± SD) were harvested on day 8 from one 10cm dish culture of iPS colonies differentiated on OP9 stroma. $CD34^+$ cells contained, on average, 19.7% ± 3.4 $CD43/CD235a^+$ haematopoietic cells, 32.3% ± 11.3 $CD43/CD235a^-CD144^+CD73^+$ endothelial cells and 9.1% ± 6.2 $CD43/CD235a^-CD144^+CD73^-$ putative haemogenic endothelial cells (mean ± SD) (Figure 41).

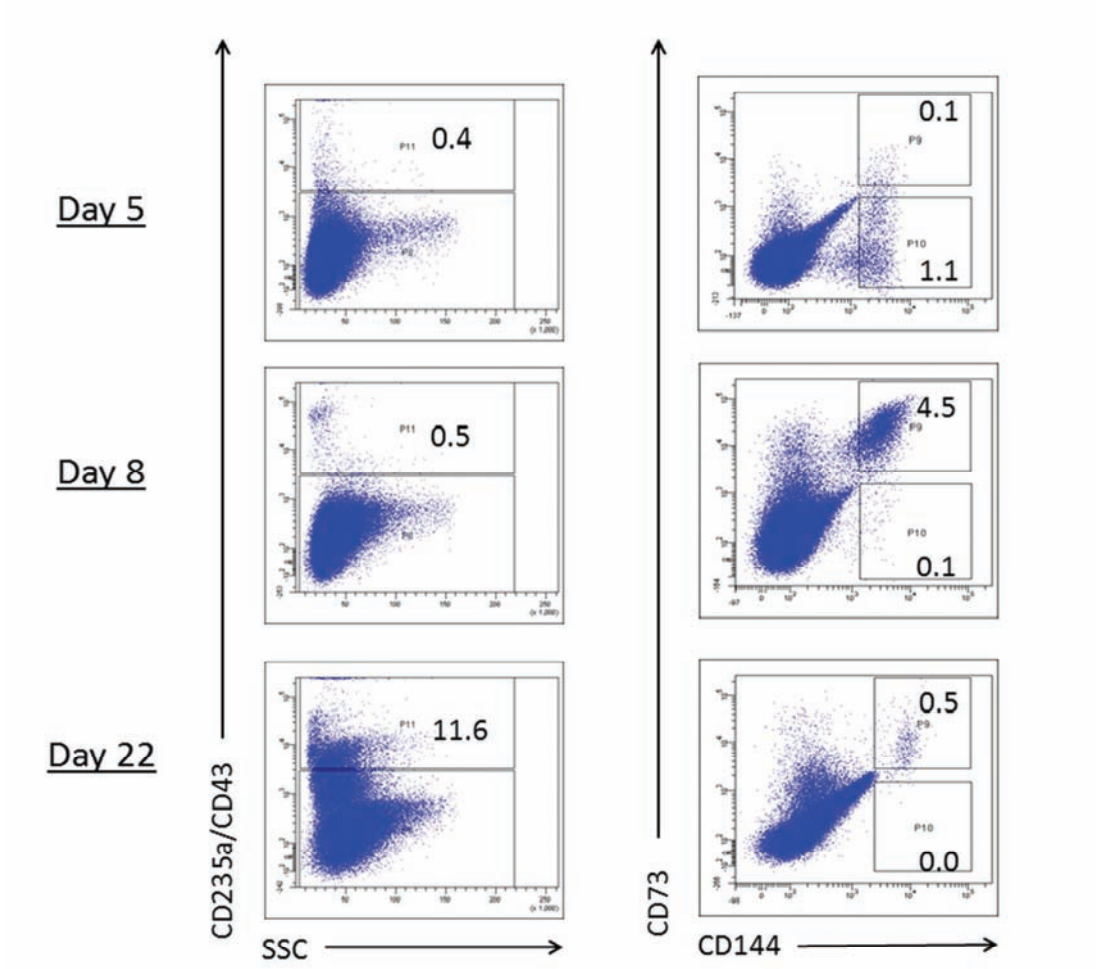

Figure 40 Assessing the presence of a CD144^{+}CD43/CD235a^{-}CD73^{-} population on day 5, 8 and 22 of iPS/OP9 co-culture.

Cells were harvested and analysed by flow cytometry. CD144^{+}CD43/CD235a^{-}CD73^{-} cells have been reported to describe an HE population with CD144^{+}CD43/CD235a^{-} CD73^{+} cells described as endothelium. CD144^{+}CD43/CD235a^{-}CD73^{-} cells were present on day 5, a small population was observed on day 8, with an absence of these cells on day 22.

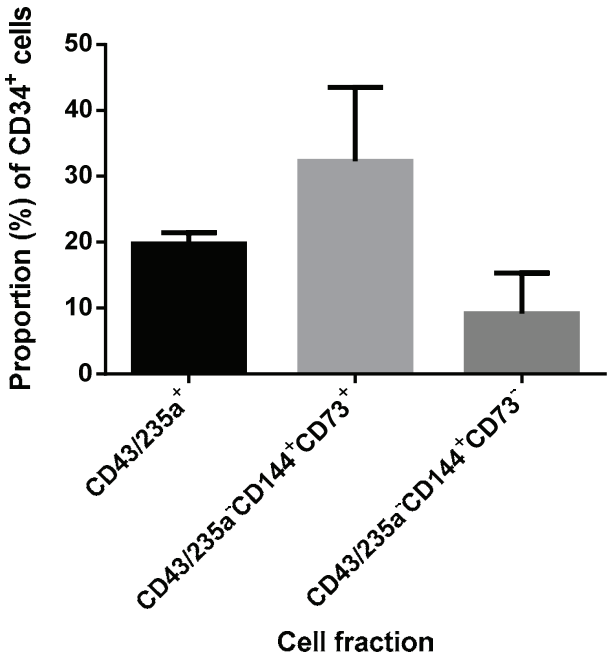

Figure 41 Proportion of day 8 $CD34^+$ cells with a haematopoietic, endothelial or haemogenic endothelial phenotype.

Day 8 iPS/OP9 co-cultures were harvested and enriched by MACS using CD34 microbeads. Analysis of cell surface phenotype was undertaken by flow cytometry. The $CD34^+$ population was composed of, 19.7 ± 3.4 $CD43/CD235a^+$ haematopoietic cells; 32.3 ± 11.3 $CD43/CD235a^-CD144^+CD73^+$ endothelial cells; 9.1 ± 6.2 $CD43/CD235a^-CD144^+CD73^-$ haemogenic endothelial cells. n=4 independent experiments, mean (% of total $CD34^+$ fraction) ± SD.

4.3.2.2 CD144^{+}CD43/CD235a^{-}CD73^{-} haemogenic endothelium gives rise to B lymphocytes.

Initial experiments, described is this thesis using MACS enrichment, suggested that day 8 CD144^{+}haem^{neg} cells may have B cell progenitor potential. This result, however, was not conclusive as cell isolation by MACS does not result in 100% purity. The aim therefore was to demonstrate this potential with FACS purified populations. Experiments described here show that, at the day 8 timepoint, CD45 is not expressed in iPS/OP9 co-cultures (Figure 16). Furthermore, that CD41a^{+} cells co-expressed CD43 (Appendix Figure 74). Therefore, nucleated haematopoietic cells on day 8 homogeneously express CD43. Therefore, to assess the potential of putative iPS-HE to give rise to B lymphocytes, day 8 cells were harvested from C19 iPS/OP9 co-culture and isolated by FACS for the following populations, i) CD43/CD235a^{+} haematopoietic (haem) cells, ii) CD43/CD235a^{-} CD144^{+}CD73^{+} endothelial (endo) cells and iii) CD43/CD235a^{-}CD144^{+}CD73^{-} haemogenic endothelium (HE) (population phenotypes as described in (Choi et al., 2012)). Harvested cells were initially enriched for CD34 by MACS and then stained for FACS. Sorting gates were set using FMO controls (Figure 42).

When purity checks were performed, endo, HE and neg fractions were >99% pure (Figure 43). The haem fraction however, contained up to 5% of CD43/CD235a^{-} cells (Figure 43). Cells were then seeded either to permit B cell differentiation (MS-5 stoma with IL-7, IL-3, SCF and Flt3L) or into the CFU assay. After 21 days, B cell condition cultures were harvested and analysed by flow cytometry. Cultures seeded with endothelial cells did not generate any haematopoietic cells, the expression of CD45 or CD14 could not be detected. CD45^{-}CD144^{+} cells were observed in endothelial-derived cultures (Figure 44).

Both HE and haematopoietic cells generated $CD45^+$ and $CD14^+$ populations in addition to a very low number of $CD45^-CD144^+$ cells (Figure 44). As predicted by the lack of $CD45^+$ cells, endothelial cultures did not generate $CD19^+$ B cells (Figure 45)(Table 15). B cells could be detected in both HE and haem cultures (Figure 45).

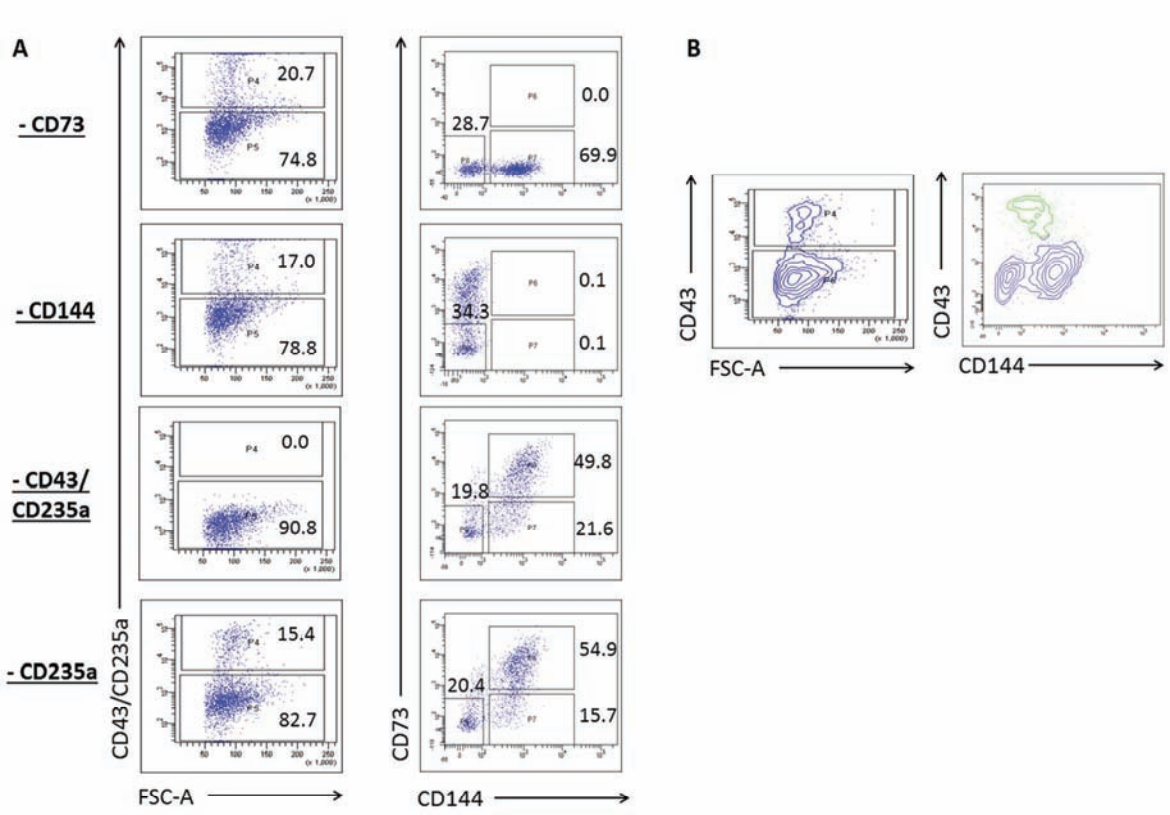

Figure 42 FMO staining controls for FACS sorting of day 8 iPS/OP9 co-cultures.
C19 iPS colonies were differentiated on OP9 stroma for 8 days. Cells were harvested, enriched for the $CD34^+$ fraction by MACS and stained with mAbs for FACS isolation. (A) FMO controls used to set gates for FACS isolation of $CD43/CD235a^+$ (Haem) cells. Additionally, cell gates were also set on the $CD43/CD235a^-$ fraction and then either $CD144^+CD73^+$ (endo), $CD144^+CD73^-$ (HE) or $CD144^-CD73^-$ (neg). (B) Checking the validity of the $CD43/CD235a^+$ vs. $CD43/CD235a^-$ gate. $CD43^+$ cells form a distinct population that is included in the $CD43/CD235a^+$ gate. Representative image, n=4 independent experiments.

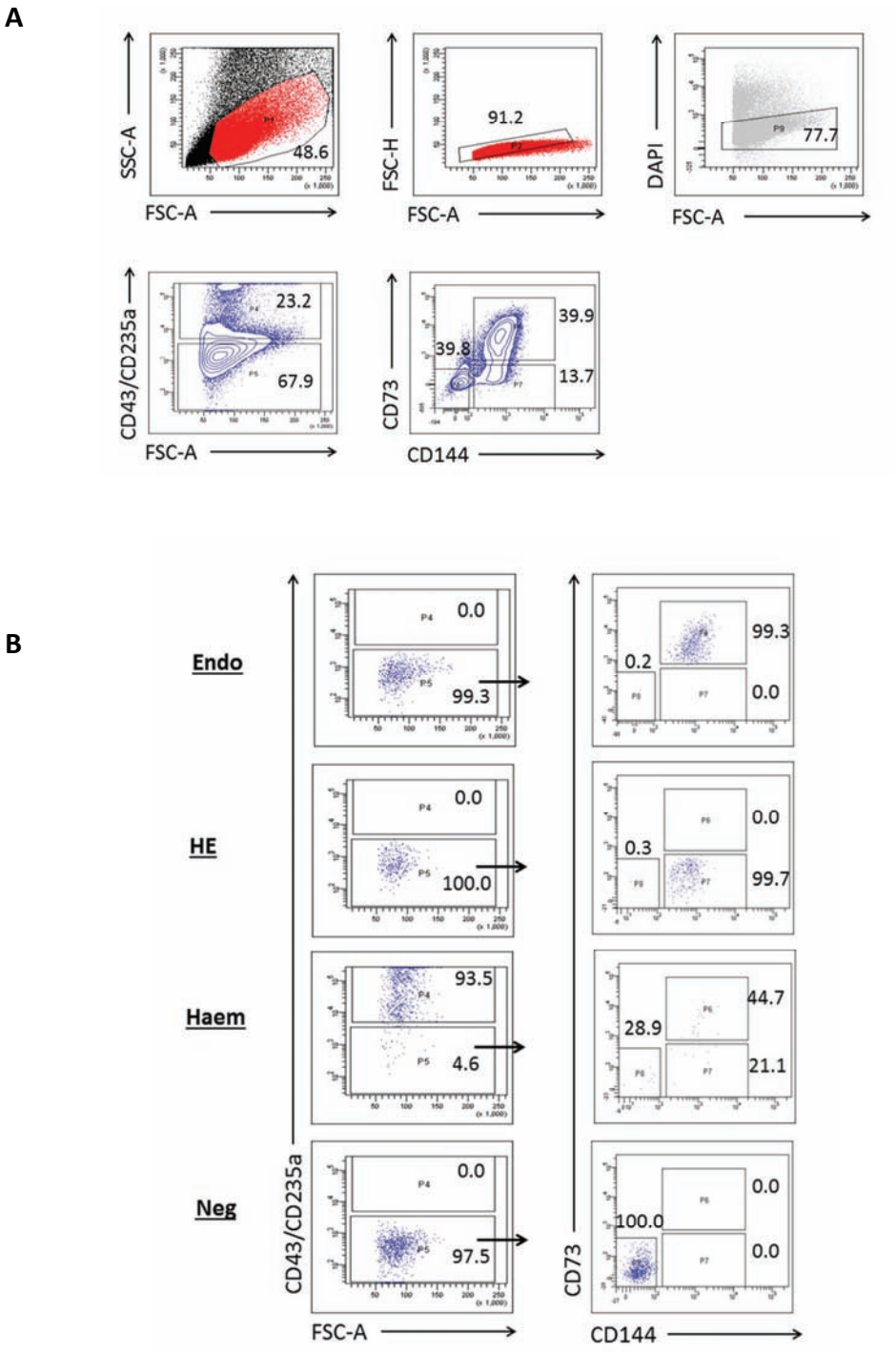

Figure 43 FACS isolation of haem, HE, endo and neg populations from day 8 iPS/OP9 co-cultures.

C19 iPS colonies were differentiated on OP9 stroma for 8 days. Cells were harvested, enriched for the $CD34^+$ fraction by MACS and stained with mAbs for FACS isolation. (A) Gates set for FACS sorting, based on FMO controls (described in Figure 42) for the isolation of haem ($CD43/CD235a^+$), HE ($CD43/CD235a^-CD144^+CD73^-$), endo ($CD43/CD235a^-CD144^+CD73^+$) and neg ($CD43/CD235a^-CD144^-CD73^-$) populations. (B) Purity check of FACS isolated populations, all populations were >99% pure with the exception of the haem fraction. Representative image, n=4 independent experiments.

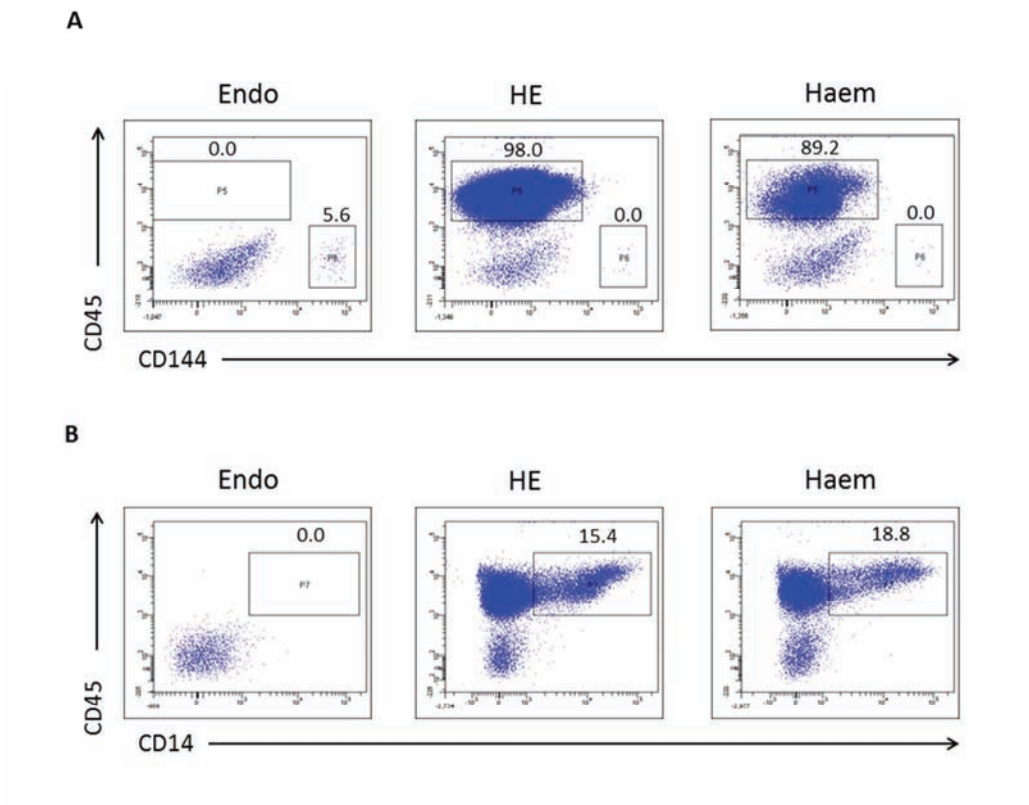

Figure 44 Haematopoietic and endothelial output of day 8 endo, HE and haem cultures.
Day 8 endothelial (endo) (CD43/CD235a$^-$CD144$^+$CD73$^+$), haemogenic endothelium (HE) (CD43/CD235a$^-$CD144$^+$CD73$^-$) and haematopoietic (haem) (CD43/CD235a$^+$) cells, purified by FACS, were cultured for 21 days with MS-5 stroma supplemented with IL-7, IL-3, SCF and Flt3L. Harvested cells were analysed by flow cytometry. HE and haem populations generated CD45$^+$ and CD14$^+$ haematopoietic cells with very low numbers of CD45$^-$CD144$^+$ cells. Conversely, endo populations did not generate haematopoietic cells but did produce larger numbers of CD45$^-$CD144$^+$ cells. Representative images, n=4 independent experiments.

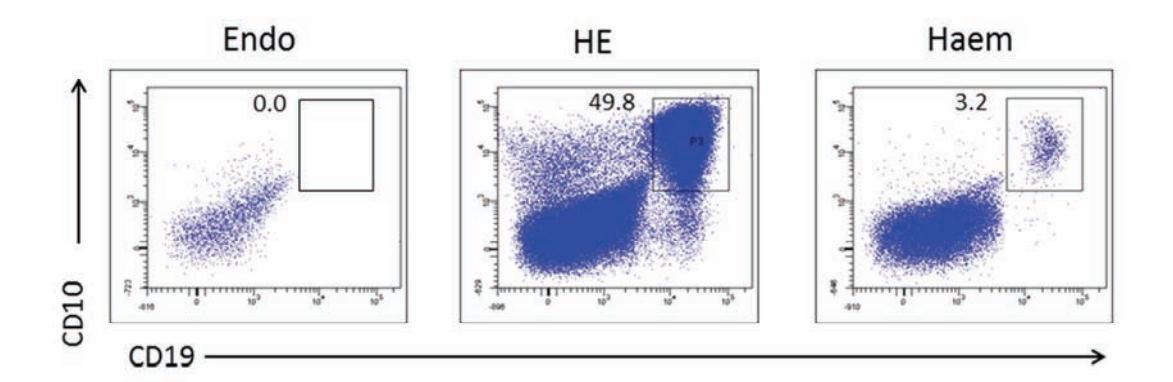

Figure 45 B cell potential of day 8 endothelium, HE and haematopoietic populations.
Day 8 endothelial (endo) (CD43/CD235a$^-$CD144$^+$CD73$^+$), HE (CD43/CD235a$^-$ CD144$^+$CD73$^-$) and haematopoietic (haem) (CD43/CD235a$^+$) cells were cultured for 21 days with MS-5 stroma supplemented with IL-7, IL-3, SCF and Flt3L. Harvested cells were analysed by flow cytometry. Endo populations did not generate B cells. CD19$^+$ B cells were detected in haem-derived cultures. HE populations were also capable of B cell differentiation. Representative images, n=4 independent experiments.

HE cultures generated a greater proportion and total number of $CD19^+$ cells than haematopoietic cultures (HE, 94,748 ± 30,998; Haem, 1,141 ± 567; mean ± SD) respectively when 5,000 cells were seeded (Figure 46). This difference amounted to over a 80-fold enrichment for B cell generation potential in the HE fraction when compared to the potential of the haem population. When day 10 $CD34/43^+$ populations were typically seeded at 50,000 cells per well, the number of B cells generated was of a similar magnitude to the day 8 haematopoietic fraction (16,542 ± 6,023 SD) when accounting for a difference in starting cell number. HE cultures that generated B cells also yielded a greater number of total $CD45^+$ cells than the haematopoietic fractions (Figure 46). 269,435 ± 63,291 (mean ± SD) $CD45^+$ cells were detected in wells seeded with HE cells, over a 6-fold increase in comparison to the $CD45^+$ cells generated in haematopoietic cultures (43,198 ± 9,331 (mean ± SD)) (Figure 46). Whilst the number of B cells generated in HE cultures was many magnitudes higher than observed with any haematopoietic fraction assayed, the frequency of wells in which $CD19^+$ cells could be detected was low (Table 15). This assay was not performed with a single cell input; therefore, the frequency of progenitors with B cell potential could not be accurately determined.

An additional observation made during the course of these experiments was that a proliferative burst of non-adherent cells occurred in a number of, and depending on the population seeded, the majority of cultures. When this proliferative burst was not observed, $CD19^+$ cells were never detected. However, this proliferative burst could be observed in cultures that did not contain $CD19^+$ cells. To investigate this observation further, the number of $CD45^+$ cells generated was compared between HE seeded cultures that did or did not contain B cells. In cultures where B cells could be detected, the

number of $CD45^+$ cells was 272,962 ± 69,091 (mean ± SD) when 5,000 HE cells/well were seeded (Figure 47). In contrast, when B cells were not detected in HE seeded cultures (at 5,000 cells/well), the number of $CD45^+$ cells generated was 45,522 ± 36,655 (mean ± SD) (Figure 47).

The CFU potential of the isolated FACS populations was also assessed. As expected endothelial populations did not generate CFU colonies (0.0 ± 0.0, colonies/1000 cells seeded mean ± SD) (Figure 48). HE populations did generate a limited number of CFU colonies (2.3 ± 0.7, colonies/1000 cells seeded mean ± SD), but a larger number were observed when haematopoietic cells were seeded (11.8 ± 3.2, colonies/1000 cells seeded mean ± SD) (Figure 48). All colonies scored were CFU-GM.

Table 15 Frequency of haematopoietic and B cell potential in day 8 FACS isolated populations.

Population	Experiment number	$CD45^+$	$CD19^+$
HE	1	2/2	1/2
	2	2/4	1/4
	3	3/3	1/3
	4	3/3	0/3
Haem	1	2/2	2/2
	2	4/4	0/4
	3	3/3	0/3
	4	3/3	1/3
Endo	1	0/2	0/2
	2	0/4	0/4
	3	0/3	0/3
	4	0/3*	0/3
Neg	2	0/4	0/4
	3	0/3	0/3
	4	0/3	0/3

Haemogenic endothelium (HE), haematopoietic (haem), endothelial (endo) and negative (neg) cells were FACS sorted from day 8 C19 iPS/OP9 co-cultures. Cells were seeded at 5,000 cells/well in experiment 1, 3 and 4 and 2,500 cells/well in experiment 2, into culture with MS-5 cells, IL-7, IL-3, SCF and Flt3L. After 21 days of culture, cells were harvested, stained with mAbs and analysed by flow cytometry. *<60 cells detected in 2/3 wells. Numbers indicate; wells containing population/total wells seeded.

A

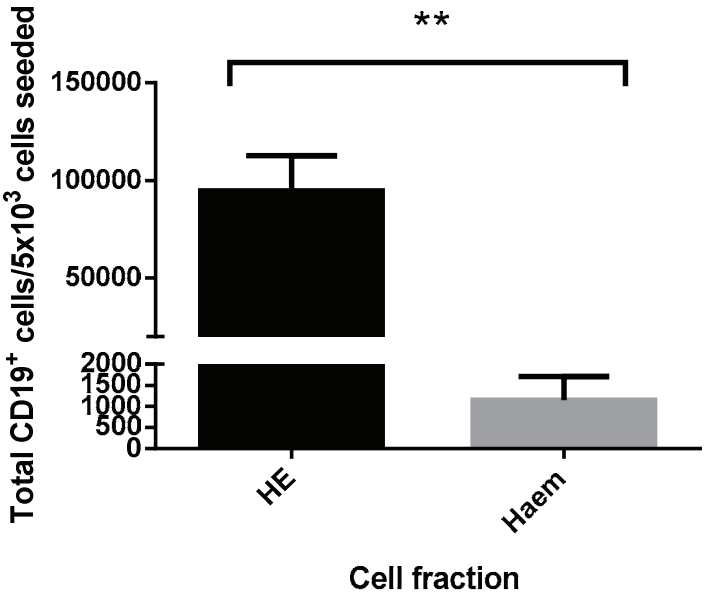

B

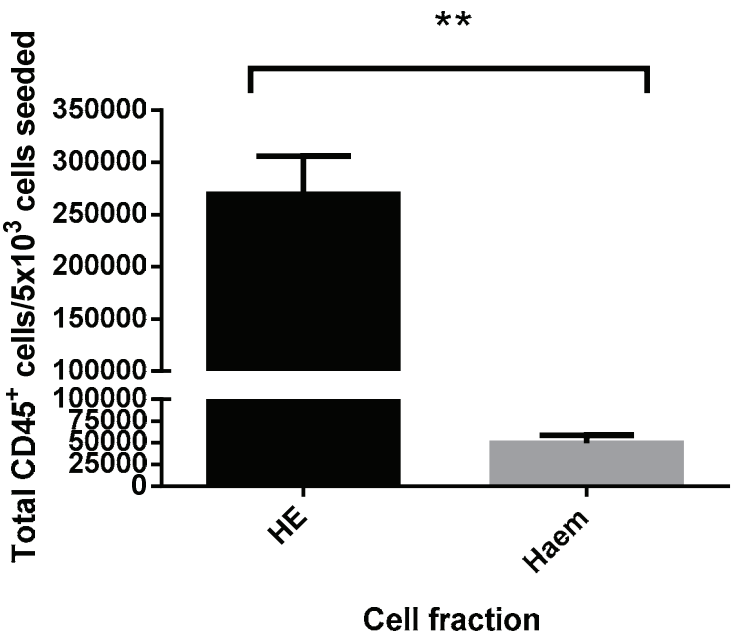

Figure 46 The HE fraction yields a greater number of $CD19^+$ and $CD45^+$ cells than the haematopoietic population.

$CD34^+$ cells from day 8 C19 iPS/OP9 co-cultures were harvested and FACS isolated to generate HE, haem and endothelial populations. After 21 days on MS-5 stroma, $CD45^+$ haematopoietic cells, including $CD19^+$ B cells could be detected in HE and haem cultures. The number of $CD19^+$ and $CD45^+$ cells was determined using the total gated event number by flow cytometry analysis. (A) HE generated over 80-fold more $CD19^+$ cells with a (B) 6-fold increase in total $CD45^+$ cells in comparison to haematopoietic cultures. n=4 independent experiments (HE is data from 3 wells from 3 independent experiments. Haem is 3 wells from 2 independent experiments. Mean ± SD, ** P= ≤0.01

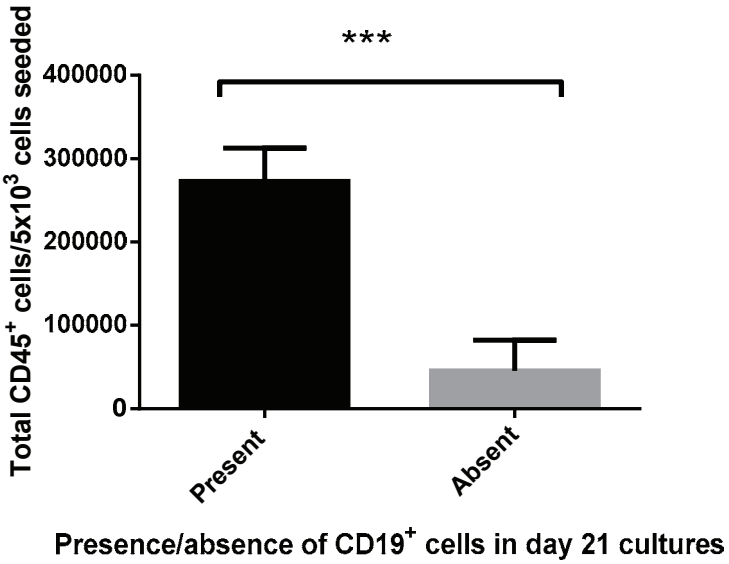

Figure 47 A high number of CD45$^+$ cells correlates with the generation of CD19$^+$ cells from HE. HE cells, FACS isolated from day 8 C19 iPS/OP9 co-cultures, were seeded at 5,000 cells/well into co-culture with MS-5 cells. After 21 days cultures were harvested, stained with mAbs and analysed by flow cytometry. The number of CD45$^+$ cells generated was compared between cultures that also contained CD19$^+$ cells (present) and cultures that lacked this population (absent). Present 272,962 ± 69,091; Absent 45,522 ± 36,655; mean ± SD. n=3 independent experiments. *** P= ≤ 0.001

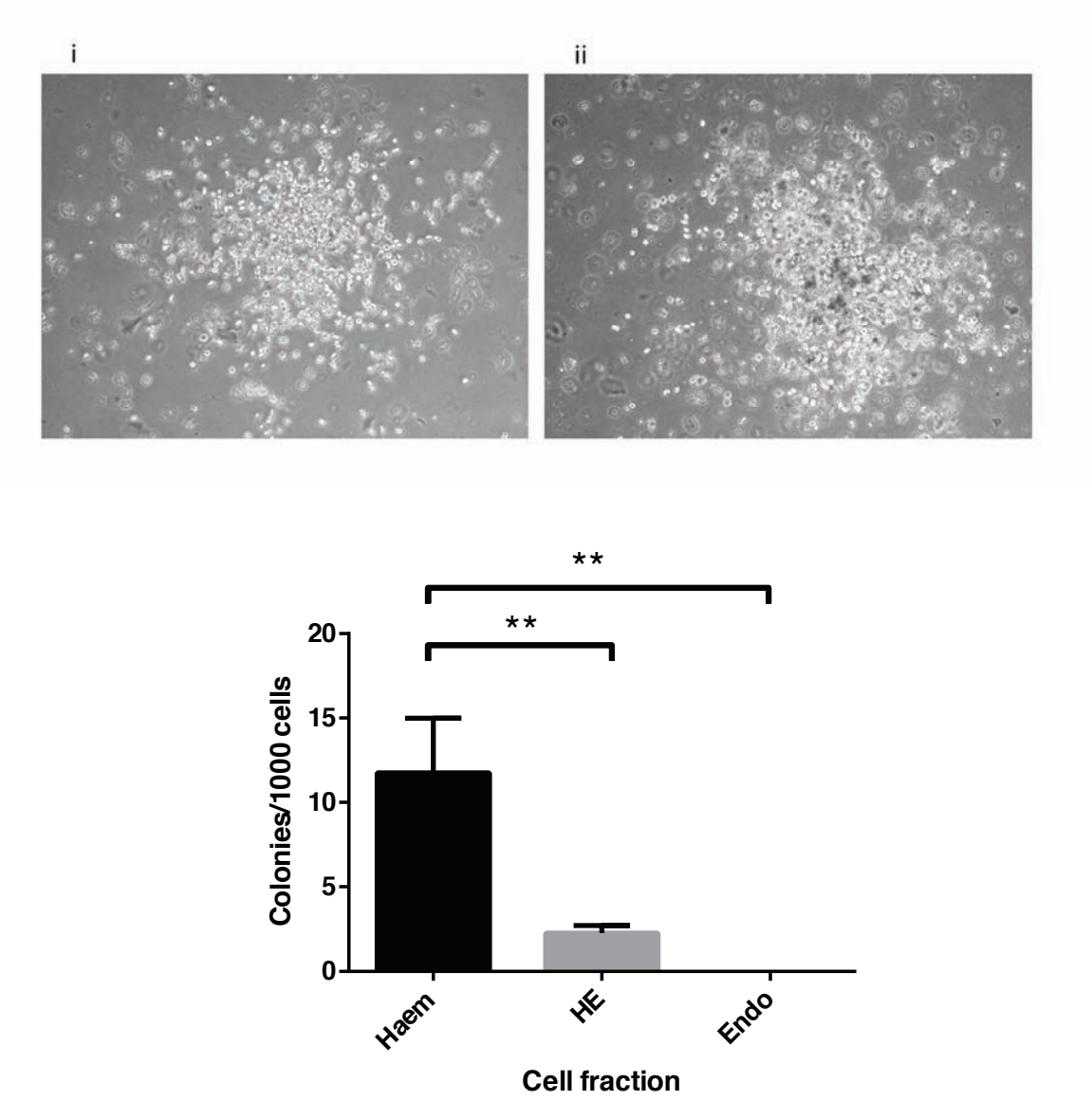

Figure 48 CFU potential of day 8 endothelial, haematopoietic and HE populations.
Day 8 endothelial (endo) (CD43/CD235a$^-$CD144$^+$CD73$^+$), haemogenic endothelium (HE) (CD43/CD235a$^-$CD144$^+$CD73$^-$), haematopoietic (haem) (CD43/CD235a$^+$) cells were seeded into the CFU assay at 1000 cells/well and maintained for 14 days before colonies were scored. (A) Brightfield images of CFU colonies from i) HE and ii) haem populations. B) Scored CFU-G/GM CFU colonies. All colonies detected were CFU-G/GM type. Endothelial cells did not generate colonies (0.0 ± 0.0), HE populations did at a low frequency (2.3 ± 0.4) and a larger number of colonies being produced in haematopoietic cultures (11.8 ± 1.9). n=3 independent experiments, mean ± SD colonies/1000 cells seeded. ** P= ≤0.01

4.3.2.3 The impact of in vitro conditions on perceived cellular potentials.

Co-culture with MS-5 stroma supplemented with appropriate cytokines was exploited as a system to probe B lymphocyte potential of iPS-derived HPCs. This was because $CD19^+$ cell numbers were higher using this co-culture system than when this population was reseeded into OP9 co-culture with the same factors (Figure 21). However, there may be additonal differences between OP9 and MS-5 stroma. Whilst endothelial cells isolated from day 8 iPS/OP9 co-cultures may not display haematopoietic potential on MS-5 cells, this does not necessarily mean that these cells were lacking such a differentiation capacity. Therefore, to assess whether $CD144^+CD43/235a^-CD73^+$ cells were truely lacking haematopoietic protential, cells were isolated from day 8 cultures by FACS as described above and reseeded onto OP9 stroma. After 21 days, cultures were harvested and analysed by flow cytometry. The $CD43/235a^+$ haematopoietic fraction yielded $CD45^+$ cells and less than 1% $CD45^-CD144^+$ cells (Figure 49). The endothelial population consistently generated $CD45^-CD144^+$ cells but also $CD45^+$ cells (Figure 49). This demonstrated that the $CD144^+CD43/235a^-CD73^+$ population may still have haematopoietic potential and therefore is not homogeneously endothelial.

Additionally, the impact of cell seeding density on culture populations was investigated, initially intended to address the finding of low frequency B cell potential in the HE fraction when cells were seeded at 5,000/well. Haem, HE, endo and neg populations were FACS purified, as illustrated in 4.3.2.2, and seeded at 25,000 cells/well in the MS-5 co-culture assay. After 21 days of culture, cells were harvested and stained with mAbs for analysis by flow cytometry. As observed when HE and haem cells were seeded at the lower density, both fractions generated $CD45^+$ cells (Table 16). B cells were also

generated in both HE and haem cultures, although the frequency of B cell detection was much lower in haem than HE cultures. Across two independent experiments B cells could be detected in 5/6 HE cultures, but only 1/6 haem cultures (Table 16). However, in contrast to cultures initiated with the lower seeding density, all endo cultures generated $CD45^+$ cells (Table 16). B cell potential was never detected in endo or neg cultures, even when cells were seeded at a high density (Table 16). In one of two independent experiments, the neg fraction also generated $CD45^+$ haematopoietic cells (Table 16).

Seeding density also had an impact on the number of $CD19^+$ cells generated from the HE fraction. When day 8 HE cells were seeded at 5,000 cells/well, the number of B cells generated was higher (94,748 ± 30,998, mean ± SD) than observed with the haem fraction at any time point assayed. However, when HE cells were seeded at 25,000 cells/well, although the proportion of total culture wells that contained B cells was increased in relation to the lower seeding density (Table 16), the total number of $CD19^+$ cells generated was significantly lower (13,922 ± 14,595, mean ± SD) (Figure 50A). When the number of $CD19^+$ cells detected was expressed as a ratio of B cells generated:HE cells seeded this difference was even more striking. At a low seeding density, 18.9:1 ± 6.2 (mean ± SD) B cells are generated per HE cell seeded (Figure 50B). Comparably, when HE cells were seeded at a high density, the number of B cells generated per HE cell was 0.6:1 ± 0.6 (mean ± SD) (Figure 50B).

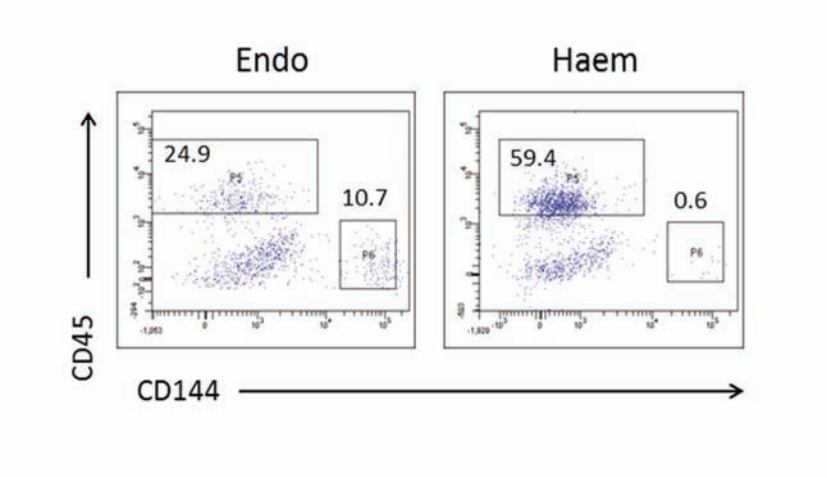

Figure 49 CD144^{+}CD43/235a^{-}CD73^{+} populations seeded onto OP9 stroma generate haematopoietic cells.
Day 8 endo (CD43/235a^{-}CD144^{+}CD73^{+}) and haem (CD43/235a^{+}) cells were reseeded with OP9 stroma and cultured for 21 days. Cells were then harvested and analysed by flow cytometry. Endo populations gave rise to CD45^{+} cells in addition to CD45^{-} CD144^{+} cells. Haem fractions generated CD45^{+} cells but a very low number of CD45^{-} CD144^{+} cells. Representative image, n=3 independent experiments.

Table 16 The effect of seeding density on differentiation potential.

Population	Experiment number	$CD45^+$	$CD19^+$
HE	3	3/3	2/3
	4	3/3	3/3
Haem	3	3/3	0/3
	4	3/3	1/3
Endo	3	3/3	0/3
	4	3/3	0/3
Neg	3	0/3	0/3
	4	3/3	0/3

Haemogenic endothelium (HE), haematopoietic (haem), endothelial (endo) and negative (neg) cells were FACS sorted from day 8 C19 iPS/OP9 co-cultures. Cells were seeded at 25,000 cells/well into culture with MS-5 cells, IL-7, IL-3, SCF and Flt3L. After 21 days of culture, cells were harvested, stained with mAbs and analysed by flow cytometry. Numbers indicate; wells containing population/total wells seeded. n=2 independent experiments.

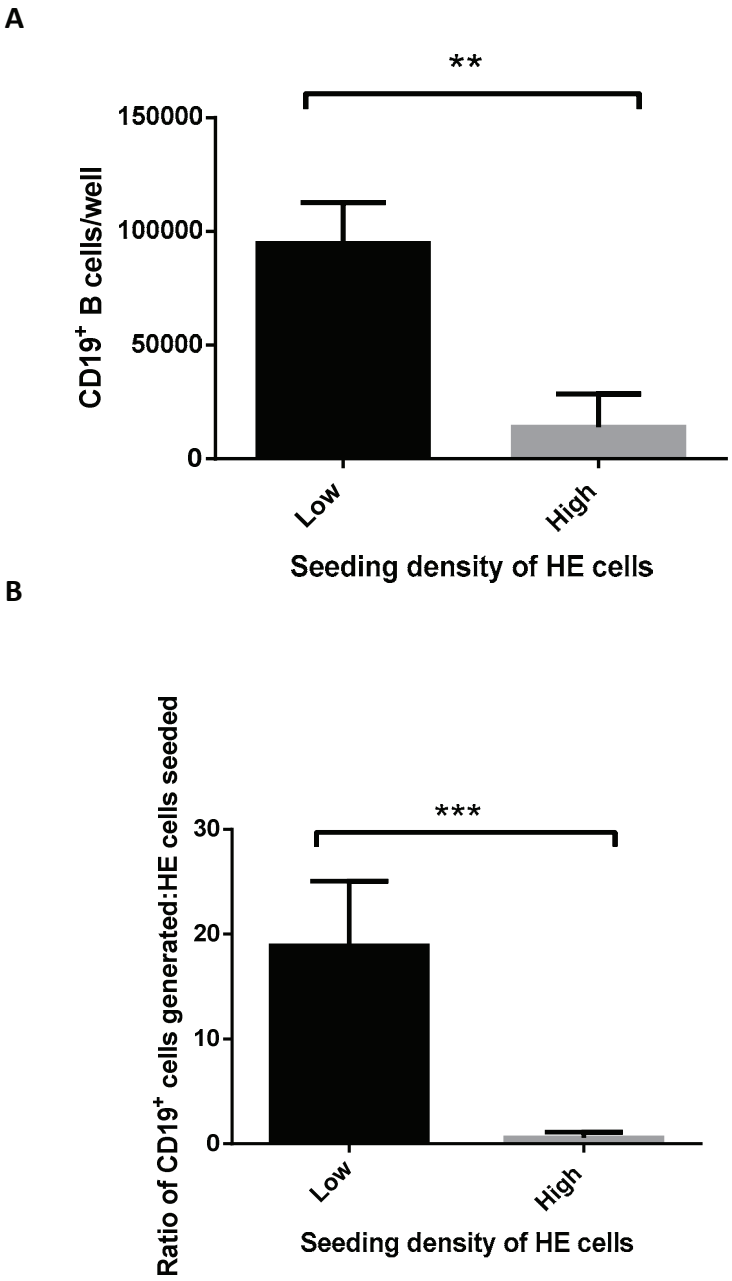

Figure 50 The effect of seeding density on the total number of B cells generated from haemogenic endothelium.

HE cells, FACS isolated from day 8 C19 iPS/OP9 co-cultures, were seeded at 5,000 cells/well (low) or 25,000 cells/well (high) into co-culture with MS-5 cells. After 21 days cultures were harvested, stained with mAbs and analysed by flow cytometry. (A) Cultures seeded with low numbers of HE cells generated a higher total number of $CD19^+$ cells. Low density; 94,748 ± 30,998 and high density 13,922 ± 14,595, mean ± SD. Low density, n=3; high density n=2 independent experiments. (B) Number of $CD19^+$ cells generated in cultures seeded with HE cells at 5,000 cells/well (low) and 25,000 cells/well (high) expressed as a ratio of B cells generated:HE cells seeded. ** P= ≤ 0.01, *** P= ≤ 0.001

4.3.3 Functional assessment of endothelial progenitor cells derived from iPS cells.

4.3.3.1 iPS- derived endothelial-like cells have limited functional capacity to form tubule network and appear to retain a degree of plasticity

The presence of $CD144^+$ cells lacking haematopoietic markers during late stages of culture, established from a heterogenous day 10 $CD34^+$ population, suggests that endothelial progenitor cells may be present. Endothelial cells are involved in vasculogenesis and play a role in haematopoietic engraftment (Gerber et al., 1999, Hooper et al., 2009, Watt et al., 2010). Therefore, endothelial cells could be a valuable tool in a variety of transplantation settings To determine whether functional endothelial cells could be differentiated from iPS colonies, day 10 $CD34^+$ cells were seeded onto collagen-I coated plates in EGM-2 media at $5x10^3$ cells/ml, a culture system optimised for endothelial cell growth within our laboratory (Ingram et al., 2005, Benny et al., 2008, Zhang et al., 2009, Roubelakis et al., 2013). Cultures were then maintained for 14 days and wells were stained for CD31 and CD90; culture wells with a predominant $CD31^+$ population and endothelial-associated morphology that lacked $CD90^+$ fibroblast-like cells were identified (Figure 51). Culture wells that fulfilled this criterion were harvested by trypsinisation and replated in EGM-2 media on collagen-I to expand, and were subsequently referred to as endothelial outgrowth colonies (EOC) (termed P1 at this stage). At P2, a sample of cells was taken for analysis by flow cytometry, >99% of cells were positive for endothelial-associated markers CD31, CD146 and CD105, while being negative for the haematopoietic markers CD45 and CD14, 7.4% of cells expressed CD90 (Figure 52A). Continued expansion of this population, and analysis at P4, revealed that >99% of cells retained the expression of endothelial-associated markers and lacked the expression of haematopoietic markers. However, CD90 positivity had increased

substantially up to 36.0% of the population (Figure 52 B). It is possible that cells with this phenotype were not committed to the endothelial lineage or that a process referred to as endothelial-to-mesenchymal transition (EMT) could be occuring. Alternatively, human cells with this $CD31^{+}CD90^{+}CD45^{-}$ phenotype have been postulated to be activated endothelium or recently proposed to be vascular stem cells (Wetzel et al., 2004, Wandel et al., 2012, Zimmerlin et al., 2010, Lin and Lue, 2013).

A functional readout of endothelial potential is the ability to form tubule networks. One common assay for tubule- forming capacity involves using matrigel (an extracellular matrix) as the support (Khoo et al., 2011). While there are advantages to this functional test, studies suggest that this assay may detect more mature endothelial cells rather than early endothelial precursors. An alternative methodology for assessing vascular tubule potential involves the co-culture of endothelial cells with human dermal fibroblasts, which provide the support and signals for endothelial networks to form (Zhang et al., 2009). $CD34^{+}$ cells from day 10 iPS/OP9 culture, iPS- endothelial outgrowth colony (EOC) cells at passage 4 or primary HUVECS cells at passage 4 were co-cultured with hDFs. After two weeks cultures were fixed and stained with anti-CD31 mAb and then visualised using the HRP system (described in 2.6.6). Both iPS-$CD34^{+}$ cells and iPS-EOC performed poorly in the co-culture tubule assay in comparison to HUVECS (Figure 54). iPS-EOCs cultures showed a small increase in the total number of tubules in comparison to iPS-$CD34^{+}$ cells, but the total tubule length and number of junctions formed was highly similar. Time constraints did not permit this to be investigated further.

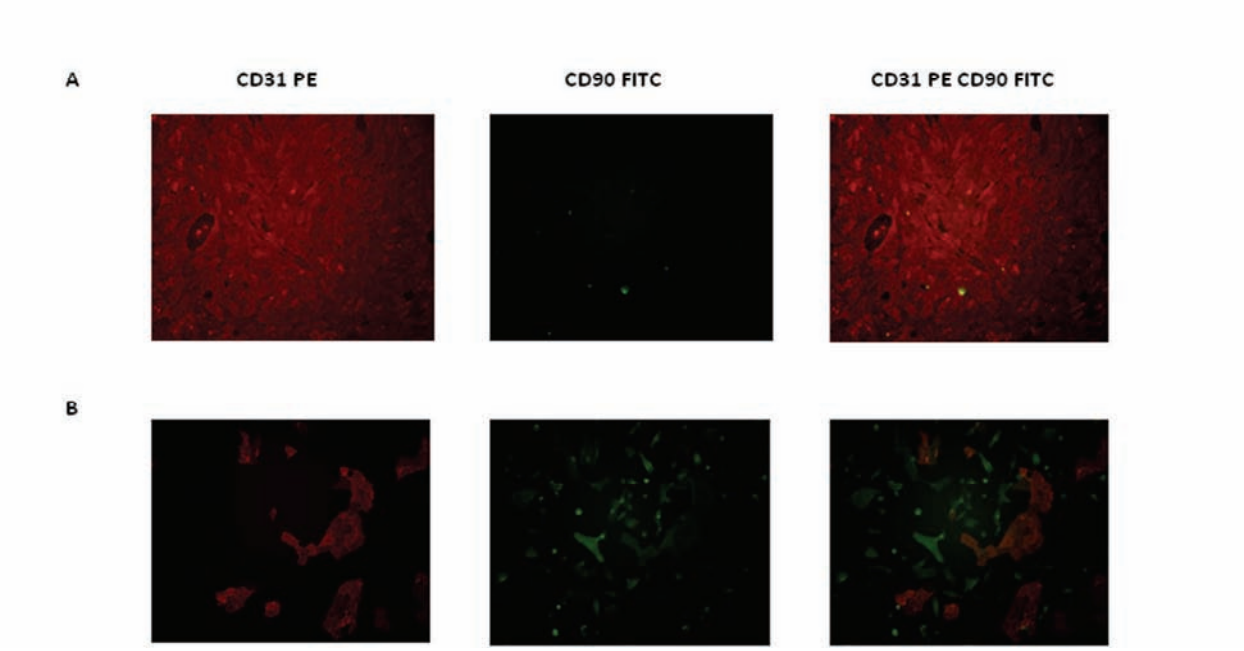

Figure 51 Immunofluorescent live cell staining of day 14 endothelial cultures generated from iPS-CD34$^+$ cells.
iPS-CD34$^+$ cells were seeded onto collagen-I coated plates in EGM-2 media to promote the outgrowth of endothelial cells. After 14 days of cultures cells were stained for CD31 and CD90 to enable the selection of wells with a predominant CD31$^+$CD90$^-$ phenotype. Selected cell populations were then reseeded onto collagen-I coated plates in EGM-2 media for continued growth and expansion. Images at x20 magnification. Representative images.

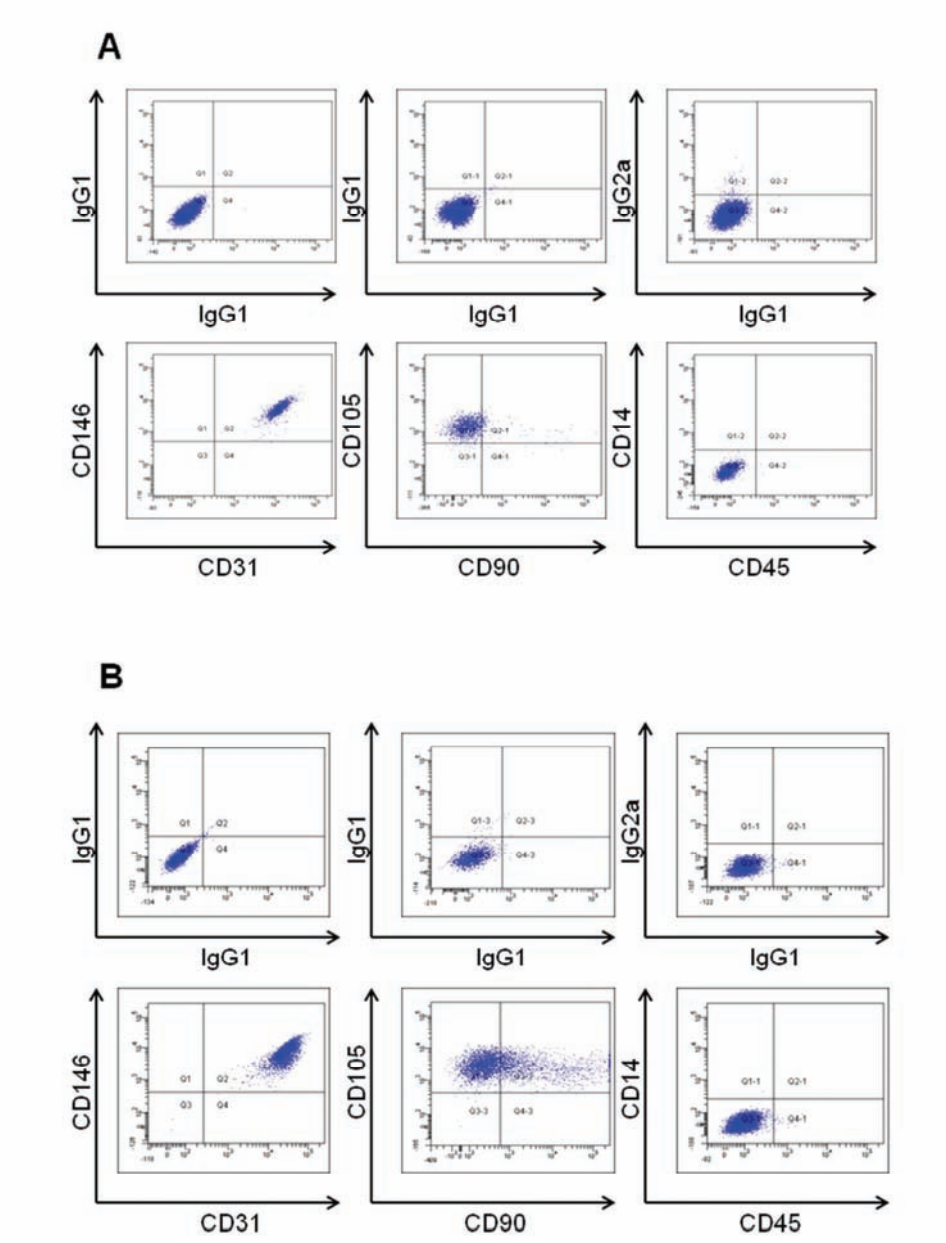

Figure 52 Cell surface phenotype of P2 and P4 endothelial outgrowth colonies.
(A) Cells were expanded in EGM-2 media on collagen-I coated plates and harvested at P2. A sample was taken for analysis by flow cytometry. 99.7% of cells were $CD146^{+}CD31^{+}$, 90.5% $CD105^{+}CD90^{-}$ (7.4% $CD105^{+}CD90^{+}$) and 99.9% $CD14^{-}CD45^{-}$. (B) EOCs cultured to P4 were 99.8% of cells were $CD146^{+}CD31^{+}$, 63.6% $CD105^{+}CD90^{-}$ (36.0% $CD105^{+}CD90^{+}$) and 99.6% $CD14^{-}CD45^{-}$. Representative image, n= 2 independent experiments.

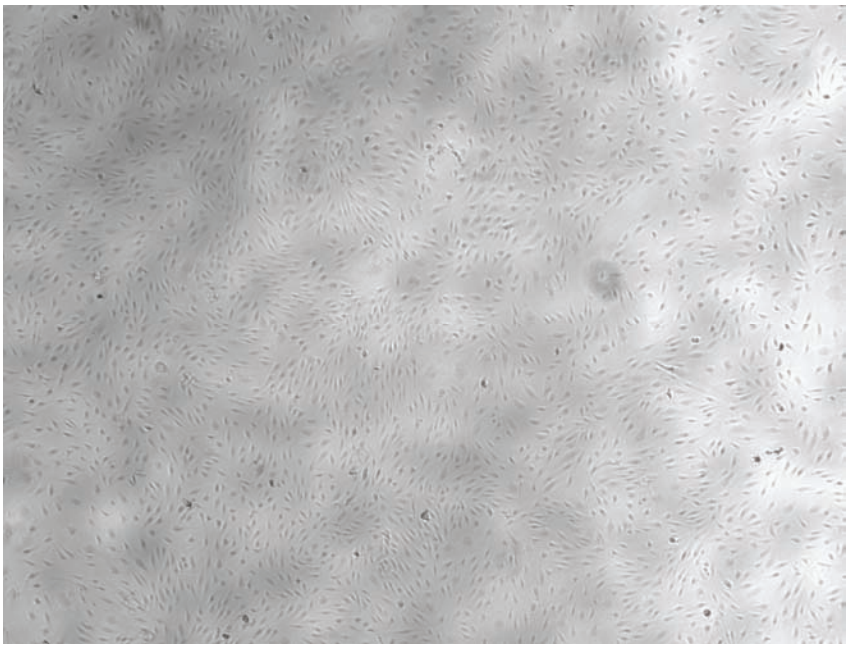

Figure 53 Brightfield image of P2 endothelial outgrowth colony cells.
iPS-CD34^{+} cells were cultured on collagen-coated plates in EGM-2 media. Cultures that stained homogenously CD31^{+}CD90^{-} with a typical endothelial morphology were harvested to expand. Representative image of cultured cells morphologically resembled endothelium. Brightfield image, x10 magnification.

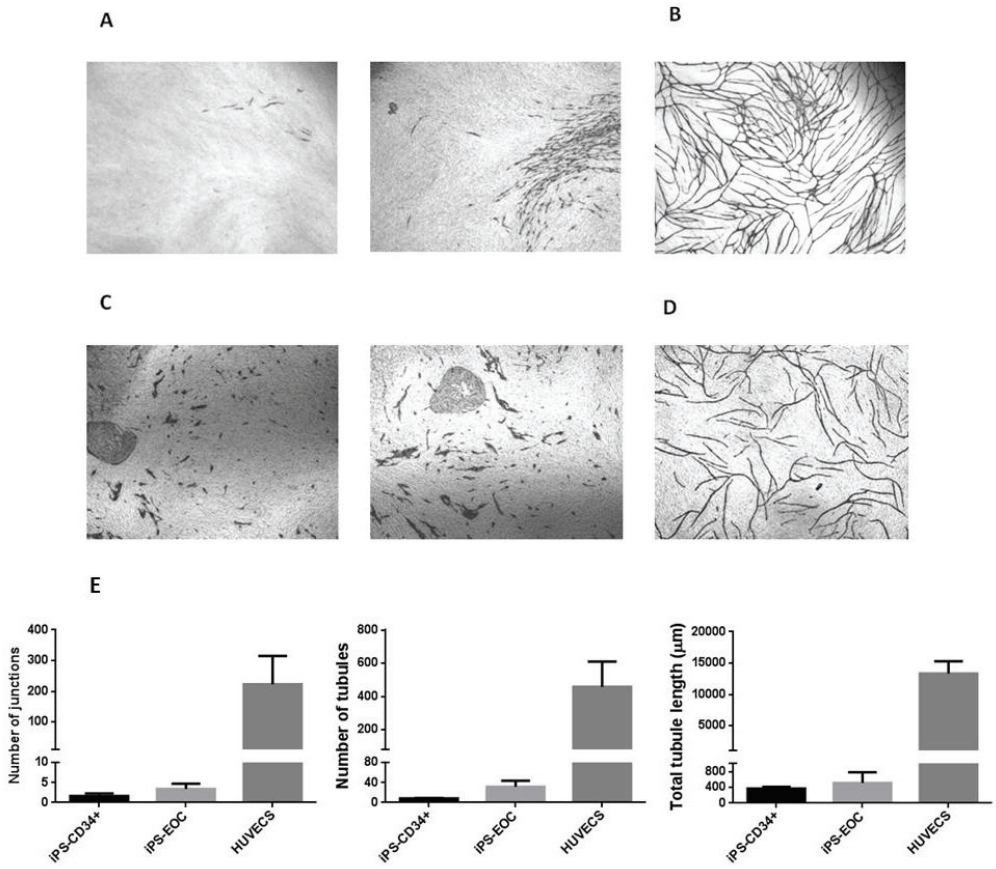

Figure 54 Comparison of the functional capacity of iPS-derived endothelial progenitor cells to form tubule networks *in vitro*.
(A) $CD34^+$ cells from day 10 iPS/OP9 co-culture (ratio cells:hDFs 1:2), (C)iPS-EOCs at P5 (ratio cells:hDFs 1:5) and (B and D) HUVECS (ratio cells:hDFs 1:5) were seeded with hDFs to assess tubule forming potential. After 14 days cultures were fixed and stained with CD31 and visualised using avidin/biotin labeling and horseradish peroxidase activity. Analysis of tubule network formation was performed using Angiosys software (TCS Cellworks). (E)HUVECS outperformed iPS-$CD34^+$ and iPS-EOC cells in all parameters measured. iPS-EOC formed a greater number of tubules than iPS-$CD34^+$ but demonstrated little improvement in the number of junctions formed and the total tubule length measured. Values are mean ± SEM, n=2 independent experiments

4.4 Discussion

The first haematopoietic cells identified in iPS/OP9 co-cultures expressed CD41a and CD43. Analysis of the CD43 population revealed $CD41a^+$ and $CD41a^-$ populations. Expression of CD41 has been identified prior to CD45 expression in budding intra-aortic cultures of the dorsal aorta as well as on multilineage progenitors in the yolk sac (Boisset et al., 2010, Mikkola et al., 2003, Ferkowicz et al., 2003). The T cell potential of $CD41^+$ cells arising in the zebrafish AGM has also been described (Bertrand et al., 2008). It has, however, been suggested that $CD43^+CD41a^-$ cells may have a broad myeloid potential, with the $CD43^+CD41a^+$ population being erythro-megakaryocyte restricted (Rafii et al., 2013, Vodyanik et al., 2006). Indeed, the data here demonstrates that the first emerging $CD45^+$ were uniformly $CD41a^-$ with at least a fraction of CD45 cells emerging via a $CD45^+CD43^+$ phenotype. Additionally, cells co-expressing CD144 and CD41a are transiently present in iPS/OP9 co-cultures. Comparisons between this simple co-culture system and population dynamics in the midgestation mouse embryo can be made as $CD144^+CD41^{low}CD45^-$ cells, demonstrated to be precursors of definitive HSCs, are observed transiently in the E11.5 AGM (Rybtsov et al., 2011). However, in the AGM $CD41^+$ cells quickly co-express CD45, with cells even displaying a $CD144^+CD45^+$ phenotype (Rybtsov et al., 2011). This differs from the population dynamics described here in the OP9 co-culture system. E9.5 mouse yolk sac (in circulation deficient mice) may also contain a limited number of cells with this $CD144^+CD45^+$ phenotype (Yoshimoto et al., 2011). Co-expression of CD41a and CD144 was used here to identify hypothetical timepoints before, during and after HE had undergone EHT. Day 5 $CD41^+CD144^+$ cells (from PSC/OP9 co-cultures) have been described as erythroid-megakaryocyte restricted (Choi et al., 2012). The authors described day 5 $CD43^+$ cells as primitive, whilst this

population on day 8 had multipotent myeloid potential (Choi et al., 2011a). Using a different culture system with defined factors and an absence of OP9 cells, Keller and colleagues described the restricted differentiation potential of $CD41a^{+}$ and $CD43^{+}$ that arose at earlier timepoints (Kennedy et al., 2012). At this initial stage, when haematopoietic markers are first detected, T lymphocyte potential was restricted to the $CD34^{+}haem^{-}$ population (Kennedy et al., 2012). Therefore, the analysis of CD41a and CD144 expression may be inappropriate for predicting the generation of progenitors with lymphocyte potential.

By day 10, B cell potential was restricted to the haematopoietic population. However, on day 8 of co-culture the potential to generate B cells could be found in a fraction of the population with a $CD43/235a^{-}CD144^{+}CD73^{-}$ phenotype. This population lacked expression of the haematopoietic marker CD45 (which is not expressed until day 10), CD43 and therefore CD41a, as well the red blood cell marker CD235a. Two main alternative theories that relate to the identity of progenitors which give rise to the haematopoietic lineage are prevelant, one describes the haemangioblast and the other haemogenic endothelium. The haemangioblast is a bipotent progenitor whilst HE is a phenotypically endothelial population with haematopoietic potential. Work by Lacaud and colleagues using a mouse ES cell system demonstrated a progenitor-progeny relationship of these two populations, with the haemangioblast generating HE (Lancrin et al., 2009). The authors described the expression of the mesoderm marker, Brachyury, in the haemangioblast in addition to the lack of c-kit and Tie-2, which discriminates the haemangioblast from HE (Lancrin et al., 2009). Slukvin and colleagues also reported the intracellular expression of CD144 in haemangioblast-like cells, whilst HE cells express cell

surface CD144 (Choi et al., 2012). Therefore, HE can be distinguished from haemangioblast-like cells by the expression of endothelial-associated cell surface markers and from haematopoietic cells by the absence of haematopoietic specific markers. Thus, with the work detailed here and the supporting data in the report described by Slukvin and colleagues, where Dil-AcLDL uptake and the expression of Tie-2 (CD202B) and c-kit (low expression) was assessed, the CD43/235a^{-}CD144^{+}CD73^{-} population can be described as a putative haemogenic endothelium population (Choi et al., 2012).

Although not fully investigated, MS-5 stroma did not appear to be capable of supporting the generation of haematopoietic cells directly from iPS cells. Whether the MS-5 conditions described are capable of supporting EHT and therefore the generation of haematopoietic cells from haemogenic endothelium was also not determined. The impact therefore of transferring cells from the OP9 environment to MS-5 co-culture should be considered. The MS-5 culture system was capable of supporting B cell differentiation from haematopoietic populations that can be isolated from as early as day 8 of OP9 co-culture. B cell differentiation from haematopoietic progenitors isolated from day 22 iPS/OP9 co-cultures was also observed. When cells of a CD144^{+}CD73^{+}CD43/CD235a^{-} phenotype, that has been proposed to describe an endothelial population, were seeded into the MS-5 culture, haematopoietic cells were not generated. However, when this same population was seeded back onto OP9 stroma, a limited number of haematopoietic cells could be observed. This therefore suggests that OP9 cells are capable of revealing haematopoietic potential in a way that MS-5 cells do not. Furthermore, the day 8 CD144^{+}CD73^{+}CD43/CD235a^{-} population is not entirely a homogenous endothelial population devoid of haematopoietic potential. This finding was

confirmed in supplemental figures of the paper published by Slukvin and colleagues (Choi et al., 2012). Whether $CD144^{+}CD73^{+}CD43/CD235a^{-}$ 'endothelial' cells could generate B cells was not assessed as the OP9 cultures were not supplemented with B cell differentiation promoting cytokines. Additionally, while $CD144^{+}CD73^{+}CD43/CD235a^{-}$ 'endothelial' cells did not generate haematopoietic progeny in the MS-5 co-culture when cells were seeded at 5,000 cells/well, haematopoietic progeny was consistently detected when 'endothelial' cells were seeded at a higher density. This implies either that, there are 'contaminating' haematopoietic progenitor cells present in the cells isolated with the $CD144^{+}CD73^{+}CD43/CD235a^{-}$ profile which are only revealed when a sufficient number of cells are present. Alternatively, that factors secreted by the endothelial cells are sufficient to drive haematopoietic differentiation when present at critical levels. It has recently been demonstrated that the underlying aortic mesenchyme controls the expression of *Runx1*, and therefore the generation of haematopoietic cells from the aortic endothelium (Richard et al., 2013). If this control also applies to the MS-5 iPS-derived endothelial cell cultures, then it would be interesting to determine which factors, that, when produced by the endothelium at a sufficient level, stimulate haematopoiesis.

The observation that $CD144^{+}CD73^{-}CD43/CD235a^{-}$ cells, switched from OP9 co-culture on day 8 to MS-5 co-cultures were capable of differentiating to the B cell lineage can be interpreted in a number of different ways. In scenario A), MS-5 cultures are capable of supporting EHT and subsequent B cell differentiation, while in scenario B), MS-5 cultures are not capable of supporting EHT, only the B cell differentiation of a committed haematopoietic population. If scenario A is true, then the data described within this chapter supports the hypothesis that haemogenic endothelium is capable of B cell

differentiation. However, if scenario B is true, then the results from the assay are reliant on a subfraction of $CD144^{+}CD73^{-}CD43/CD235a^{-}$ cells that have already committed to the haematopoietic lineage. This could possibly be dissected by using reportor genes for the expression of haematopoietic-associated genes, perhaps even for CD43, alongside continuous live cell imaging. *Runx1* is a required factor that is expressed during EHT; Runx-1 is also expressed in putative HE (Richard et al., 2013, Chen et al., 2009, North et al., 2002). A reporter for *Runx1* enhancer activity may however be informative within this context (Nottingham et al., 2007). An alternative way in which this experiment could be performed, would involve the replating of the candidate HE population back onto OP9 stroma with B cell-associated cytokines which would permit both EHT and B cell differentiation. The reason that this approach was not initially adopted was because B cell differentiation in OP9 co-culture occurred with lower efficiencies than in MS-5 co-cultures.

The observation that day 21 B cells numbers were 80- fold higher in HE seeded cultures than in haematopoietic cultures, suggests that the B cell potential of the HE population is not caused by a contaminating number of $CD43/CD235a^{+}$ cells. Furthermore, a hypothesis that this finding results from the shorter lag in HE than haem populations of a cell becoming haematopoietic before being switched to B cell conditions, and therefore having a reduced chance for lineage potential to be skewed, is not supported, as day 22 haematopoietic cells have B cell potential.

When HE cells were seeded at a higher density (25,000 cells/well vs. 5,000 cells/well) into the MS-5 co-culture, the total number of $CD19^{+}$ cells generated in any given well was

largely reduced. There are numerous contributors to the pool of cytokines that are present in an assay such as the MS-5 co-culture described. Firstly, recombinant cytokines are added to promote B cells differentiation. Secondly, stromal cells express and secrete a range of factors to which the iPS-derived cells respond. Thirdly, serum, which is a component of the culture media, contains a largely undefined range of factors. A further source of factors is the iPS-derived cells themselves. Endothelial and haematopoietic cells form part of the niche in the bone marrow and express or secrete a host of factors which impact upon haematopoietic differentiation. The identity and impact of inhibitory cells and factors on B cell differentiation should be investigated. A permutation on this hypothesis is that progenitors with B cell potential require a period of time to mature before these cells are able to differentiate to the B cell lineage. If haematopoietic differentiation from the HE pool occurs before these progenitors are able to mature, and if these haematopoietic cells then secrete factors which impact upon maturation, then this potential could be lost.

Irrespective of the potential implications of cell transfer from OP9 to MS-5 co-culture, another factor as to whether HE has B cell potential might relate to maturation state of the HE population. The differentiation of iPS cells in the conditions described, as well as the *in vivo* situation, are that of a developing system; a continuum of cell potentials may be present over a specific time scale. For example, the paired dorsal aorta is formed around E8.0 in the mouse embryo, which fuses to form the dorsal aorta at E9.0 (Drake and Fleming, 2000, Walls et al., 2008, Garcia-Porrero et al., 1995). The endothelial cells that line the paired dorsal aorta are of splanchnopleural origin, and are the endothelial cells with haemogenic capacity (Pouget et al., 2006, Pardanaud et al., 1996). The

splanchnopleural endothelial cells then are partially replaced by somite endothelial cells before the onset of haematopoiesis (Pouget et al., 2006). At E9.5 intraaortic clusters are observed, before HSC activity can be detected at E10.5 (Garcia-Porrero et al., 1995, Rybtsov et al., 2011). As the HE cells of the dorsal aorta endothelium are presumably formed by E8.0/E8.5, the reason for the delay in the formation of intraaortic clusters until E9.5 could relate to new environmental signals, created by cells of the remodelled aorta, or factors carried in the circulation. Alternatively, the time taken could be required for HE cells to be able to respond to such signals. Whether cells characterised with the $CD144^{+}CD73^{-}CD43/CD235a^{-}$ phenotype, that are present before day 8 in the iPS/OP9 co-culture, are able to generate B cells remains to be determined.

The frequency of B cell progenitors in the $CD144^{+}CD73^{-}CD43/CD235a^{-}$ population appears to be low as, when cells were seeded at 5,000 cells/well, only 25% of culture wells (n=4 independent experiments) contained B cells. In comparison, when HE cells were seeded at 25,000 cells/well, 83% of culture wells generated B cells (n=2 independent experiments). This methodology provides a broad insight into B cell progenitor frequency, however if assays are not performed at a single cell level the difference between one or the additive potential of numerous cells can not be distinguished. Due to time constraints, single cell assays were not attempted. This would be an important next series of experiments. The observation that a proliferative burst, which is seen between day 7 and 14 of MS-5 co-culture, correlates with B cell capacity. Inversely, cultures which lacked $CD19^{+}$ cells on day 21 of MS-5 culture, did not appear to have undergone this same cell expansion phase. These observations have implications for a single cell study. Furthermore, there was a high positive correlation between the total number of $CD45^{+}$

cells on day 21 of the MS-5 co-culture, with the presence of B cells within these cultures. If these observational findings are caused by paracrine effects, due to the requirement for a large intermediate population secreting active factors, then it may not be possible to conduct this experiment at a single cell level. Instead a labelling strategy might need to be applied. Alternatively, the generation of a significantly higher number of $CD45^+$ cells in correlation with the presence of B cells could be caused by the presence of different progenitor populations in the two settings that both fall within the HE phenotype. For example, if B cell potential is a readout for the presence of a multipotent progenitor, this progenitor could have the capacity to generate a much larger number of haematopoietic cells than a more lineage-restricted progenitor cell. In the report by Slukvin and colleagues, the investigators followed a single cell approach and assessed the potential of these cells, when reseeded into OP9 co-culture, to form a $CD43^+$ population. Around 15% of the $CD144^+CD73^-CD235a^-$ population had the ability to generate $CD43^+$ cells (Choi et al., 2012). If follow-up experiments support the hypothesis that a limited number of HE cells and their progeny have an extremely high capacity to yield large numbers of B cells, then the identity and multilineage potential of this population would be of great interest to the field. Keller and colleagues also recently demonstrated the capacity of a haemogenic endothelial-like population to generate T lymphocytes, although cells were selected using a less stringent $CD34^+CD43/45^-(CD144^+)$ criteria (Kennedy et al., 2012).

The presence of $CD144^+haem^-$ cells in long term cultures, in addition to the report by Kaufman and colleagues demonstrating the potential of PSC-derived $CD34^+$ cells to form endothelium *in vivo*, suggests that differentiated iPS cells from OP9 co-culture might have endothelial potential (Tian et al., 2009). Attempts to promote endothelial differentiation

from progenitor populations were relatively unsuccessful when assessed for tubule-forming potential. This could be because $CD34^+$ and EOC cells have more lineage plasticity than HUVECs, or that they are potentially differ in maturity. Alternatively, the factors and support produced by hDFs maybe more suitable for supporting tubule formation from HUVECs than from iPS-derived cells. Indeed, tubule-like networks were routinely observed from iPS progenitors when co-cultured with MS-5 stroma by colleagues in the laboratory (personal communication). The increased expression of CD90 in EOC cultures with continued passage, whilst maintaining a highly homogenous $CD31^+CD146^+$ phenotype, may represent plasticity in cell identity. This has been described by others, with the occurrence of EMT in hES-endothelial cultures (James et al., 2010). However, CD90 is expressed highly on the majority of day 10 iPS-$CD34^+$ cells, and has been detected on multiple cell types including HSCs, activated endothelium and MSCs. Expression levels of CD90, therefore, may be an inappropriate indicator in this context. The derivation of endothelium, including identified subtypes such as blood-brain barrier endothelium, from PSCs has progressed with improved differentiation efficiencies (Lippmann et al., 2012, Kusuma et al., 2013, James et al., 2010, Prado-Lopez et al., 2010). More recently, the capacity for these PSC-derived endothelial cells to self-organise into 3D vessel structures revealed functional potential with a number of similarities to *in vivo* vasculogenesis (Kusuma et al., 2013).

In conclusion, the data described here demonstrates, for the first time, that putative haemogenic endothelium, as described with the most stringent current criteria, is capable of undergoing B cell lymphopoiesis.

Chapter 5.

Assessing the capacity of iPS- B cells to express cell surface antibodies in vitro and in vivo.

5.1 Aims and objectives

The purpose of this chapter was to determine whether iPS pre-B cells could mature to express cell surface IgM, a developmental process that requires DNA recombination of V,D and J gene segments. The specific aims were to:

1) Define *in vitro* conditions for the differentiation of iPS pre-B cells to an IgM^+ phenotype.

2) Confirm VDJ recombination in iPS-IgM^+ cells derived *in vitro*.

3) Assess the capacity of iPS pre-B cells to differentiate and expand *in vivo.*

5.2 Background

During development, haematopoiesis is thought to occur in distinct waves, initially from haematopoietic precursors and subsequently from the HSC (reviewed in (Cumano and Godin, 2007)). Postnatally, HSCs are multipotent, giving rise to a broad range of lymphoid and myeloid cells. However, T, B and myeloid cells have been detected prior to the generation of HSCs (Yoder et al., 1997a, Yoder et al., 1997b). In the mouse, developmentally and functionally distinct B cell populations have been described, termed B-1 and B-2 B cells (reviewed in (Montecino-Rodriguez and Dorshkind, 2012)). Evidence thus far, from mouse models, has described a possible HSC autonomous production of B-1a and MZ cells (Ghosn et al., 2012). However, B-2 B cells, the major B cell population that is found in the spleen and peripheral blood, are generated continuously from HSCs that reside in the bone marrow (Ghosn et al., 2012). B-2 B cells play an important role in the adaptive immune response (reviewed in (Allman and Pillai, 2008).

Stages of B cell differentiation, typically described in relation to HSC-derived (B-2) B cells, have been distinguished using a panel of cell surface markers, the expression of stage-restricted genes and the configuration of the immunoglobulin heavy and light chain loci (Hardy et al., 1991). Cell surface expression of immunoglobulins is first observed in immature B cells (reviewed in (Hardy and Hayakawa, 2001, Ikuta et al., 1992). The pro-B to immature B cell stage can be dissected in mouse B cell populations by assessing CD34, CD43 and IgM expression. $CD19^{+}CD34^{+}$ cells are pro-B cells, CD34 is then downregulated in the subsequent pre-B cell stage, with continued expression of CD43 (Hardy et al., 1991). As B cells transit from pre-B-I to pre-B-II cells, proposed sub-stages of the pre-B cell, cell surface CD43 is no longer detected (Hardy et al., 1991). In human B cell

development, CD34 and CD10 expression has been used to order differentiation (Ghia et al., 1996, Davi et al., 1997, Blom and Spits, 2006). CD10 is expressed from the CLP to the immature B cell stage and continues to be detected until B cells leave the bone marrow to develop further in the periphery, when cell surface CD10 expression is predominantly downregulated (Loken et al., 1987). CD34 is expressed in human pro-B cells and is downregulated by the pre-B-II stage (Ghia et al., 1996). However, whether CD43 expression patterns in the early stages of human B cell differentiation mimic patterns in the mouse, has not been determined.

In vivo studies in the mouse have revealed the identity of numerous critical factors in B cell lymphopoiesis. For example, Flt3L is required for lymphoid progenitor development and SDF-1/CXCL12 is necessary for the commitment of $CD19^-$ progenitors to the B cell lineage (Sitnicka et al., 2002) (Egawa et al., 2001). Stimuli that promote B cell development from committed $CD19^+IgM^-$ cells to immature B cells (IgM^+) have been difficult to identify *in vivo*. Whilst B cell lymphopoiesis displays many commonalities between mouse and human, there are notable differences. A disparity in the expression of markers such as CD10, CD45RA and CD38 between human and mouse B cells highlight phenotypic differences (Kee et al., 1992, Hao et al., 2001). Therefore, an *in vitro* model of human B cell development from lymphoid progenitor to immature B cell, or even plasma B cell, would have wide ranging applications. *In vitro* culture systems to promote human B cell development (from bone marrow HSC or UCB-HSC) to the immature B cell stage have been infrequently described. This has been achieved in a limited number of reports using murine stromal cells, MS-5, AFT024, S17 or transfected fibroblastic-L cells, to support the generation of human IgM^+ cells (Ohkawara et al., 1998, Fluckiger et al., 1998,

Barker and Verfaillie, 2000). Sekiguchi and colleagues generated IgM^+ cells from human UCB-$CD34^+$ cells using a co-culture system with MS-5 stroma supplemented with G-CSF and SCF (Ohkawara et al., 1998). In this system, $CD19^+IgM^+$ cells could be observed after 4 weeks of culture (Ohkawara et al., 1998). UCB-$CD34^+$ cells cultured on S17 stroma yielded IgM^+ cells between week 6 and 8 of culture, at 3-10% of the $CD19^+$ population (Fluckiger et al., 1998). Subsequent isolation of $CD19^+$ cells from week 8 $CD34^+$/S17 cultures, and transfer onto murine fibroblasts transfected with CD40L in the presence of IL-4, resulted in a large increase in the proportion of B cells expressing IgM (Fluckiger et al., 1998). Verfaillie and colleagues differentiated human pro-B cells to the immature IgM^+ cell stage over a 3 week period in co-culture with AFT024 cells (Barker and Verfaillie, 2000). In the work by Verfaillie and colleagues, cells were cultured for two weeks with a cocktail of cytokines, including IL-7 and Flt3L, prior to the addition of CD40 antibody, IL-4, IL-5, IL-6 and IL-10 for the remaining 7 days (Barker and Verfaillie, 2000). In addition to CD40L, lipopolysaccharide (LPS), phosphorylcholine (PC), BAFF (B cell activating factor), APRIL (a proliferation inducing ligand), poke-weed mitogen (PWM), CpG DNA, heparan sulphates, TSLP (thymic stromal lymphopoietin) and a wide range of interleukins (IL-4, IL-5, IL-10, IL-13) have all been described to promote B cell differentiation *in vitro* (Fluckiger et al., 1998, Andersson et al., 1972, Ray et al., 1998, Haas et al., 2005, Claudio et al., 2002, Belnoue et al., 2008, Bekeredjian-Ding et al., 2012, Krieg et al., 1995, Reijmers et al., 2011). B-1 B cells, which are thought to be the major source of natural antibodies, have been demonstrated to react to common bacterial antigens that include PC and LPS (Haas et al., 2005, Seidl et al., 1999, Andersson et al., 1972). The capacity of APRIL (a proliferation-inducing ligand) to promote expansion of the B-1 B cell pool has also been reported (Planelles et al., 2004).

For B cell development to progress to the IgM^+ stage, where cell surface antibodies are first expressed, cells must undergo VDJ recombination. This is a process that requires the expression of RAG (Recombination Activating Gene) recombinase, which uniquely occurs in T and B lymphocytes (Oettinger et al., 1990). In B cells, V,D and J gene segments at the IgH locus and, V and J segments at the IgK and IgL loci, are rearranged to generate antibody diversity. Recombination at the IgH locus occurs first, which results in the expression of the pre-BCR. Light chain loci are then rearranged prior to the appearance of IgM/BCR on the cell surface (Tonegawa, 1983). The human IgH locus is composed of 56 V, 23 D and 6 J genes, in addition to numerous pseudogenes (Lefranc et al., 2009). Indeed, the greatest contribution to antigen specificity occurs at the IgH locus where VDJ segments form the CDR3 region (complementarity determining region 3) (Ohno et al., 1985). Recent estimates using high throughput screening have suggested that there are 3-9 million unique CDR3s in the blood of an adult human (Arnaout et al., 2011). The total number of B cells found in the body is many magnitudes lower than the hypothetical total number of possible unique antibodies. One research question that has frequently been addressed therefore, is what determines utilisation of specific V, D or J gene segments? Preferential utilisation of segments has been indicated following infection or immunisation (Lucas and Reason, 1999, Throsby et al., 2008, Scheid et al., 2009). Moreover, there have been indications that the propensity for utilisation of specific gene segments may change with developmental age in both mouse and human (Schroeder et al., 1987, Marshall et al., 1997, Perlmutter et al., 1985). Overall, it can be observed that the frequency in which IgH locus genes are found in recombined DNA is not equal (Arnaout et al., 2011, Weinstein et al., 2009). Further investigation is required to elucidate the mechanisms involved in the preferential selection of segments. In addition

to diversity by recombination of individual V, D and J genes, variability in sequence is also increased by the addition of random nucleotides at junctions. This process is at least partially controlled by the expression of TdT (terminal deoxynucleotidyl transferase) which appears to be differentially expressed during haematopoietic ontogeny (Li et al., 1993). Numerous questions remain with regard to the regulation and control of VDJ recombination. An *in vitro* iPS to IgM^+ B cell differentiation system that could be used to compare iPS cells with a germline configuration, to those that retain a rearranged IgH locus, may permit new insights.

In vitro differentiation is limited directly by experimental conditions. The postnatal anatomical location of development from the HSC to immature B cells is the bone marrow. B cells then move into the periphery for further development. Therefore, the *in vitro* culture system required to produce large numbers of immature B cells and their terminally differentiated progeny are likely to be different from the earlier stages of B cell differentiation. The adoptive transfer of populations *in vivo,* as an alternative method for promoting B expansion and maturation, may prove effective. Immunodeficient mice that lack T, B and NK cells have been demonstrated to support both short term repopulation of human lymphocytes, as well as long term reconstitution of the major populations of the human immune system (McCune et al., 1988, Mosier et al., 1988, Shultz et al., 2005, Shultz et al., 2012). These studies indicated that haematopoietic niches in mice have sufficient and at least minimum similarity to human niches to enable the support of human haematopoiesis.

At the time of writing, and to the author's knowledge, there have only been two reports of B cell generation from human ES or iPS cells, one of which originated from this

laboratory (Carpenter et al., 2011, Vodyanik et al., 2005). The differentiation of human ES cells to the B cell lineage *in vitro* has been described; although the $CD19^+$ cells generated were not further characterised and maturation ability was not assessed (Vodyanik et al., 2005). The differentiation of human iPS cells to the B cell lineage, to which work in this thesis contributed, yielded pre-B cells that were positive for Pax5, IL7Rα and VpreB transcripts and had undergone D-J recombination (Carpenter et al., 2011). Whether these iPS-B cells are capable of maturing to stages where cell surface antibodies are expressed, represents an important functional assay. Furthermore, it has been demonstrated that reprogrammed T lymphocytes, that maintain their rearranged genomic VJ configuration at the iPS cell stage, can be differentiated to express their original T cell receptors (TCRs) (Wakao et al., 2013). The technical capability therefore to generate antibody expressing B cells from an iPS cell source would describe a model to investigate rare B cell populations associated with pathologies such as acute lymphoblastic leukemia (ALL). Additionally, if B-1 B cell identity in humans is more convincingly described, the classification of B cells arising from pluripotent stem cells, either as B-1 or B-2 B cells, may provide a readout to discriminate YS-like HPCs from AGM-like HSCs in differentiating pluripotent stem cell populations.

One question addressed within the context of this thesis was, whether iPS-B cells resembled innate B-1 B cells or adaptive B-2 B cells, if indeed these two populations exist in humans. A number of attempts were made to address this question with functional assays, but, due to the lack of convincing controls, this work was not progressed. Another way in which the B-1 versus B-2 B cell question could be addressed is by the preferential reconstitution of B cell compartments *in vivo*. It is known that B-1 B cells are primarily

found in the peritoneal cavity, with a minor fraction in the spleen (Berland and Wortis, 2002, Hardy and Hayakawa, 2001). This propensity to occupy distinct anatomical locations therefore may describe an assay to discriminate human B-1 B cells from B-2 B cells in the absence of unique markers.

5.3 Results

5.3.1 iPS-derived B cells differentiate to express cell surface IgM *in vitro*.

5.3.1.1 iPS-B cells continue to develop with increasing time in culture.

B cell differentiation from C19 iPS cells was described by seeding $CD34^+$ cells, from day 10 iPS/OP9 co-culture, onto MS-5 stroma with IL-3, IL-7, SCF and Flt3L (Figure 37). After 21 days of culture, cells were harvested and stained with mAbs for analysis by flow cytometry. $CD19^+$ cells were gated using the approach outlined in Figure 55. Autofluorescence in the APC channel was observed with both long-term iPS-derived and UCB-derived cultures. Autofluorescent cells also stained positively for CD45. To enable accurate identification of $CD19^+$ B cells, the signal from the CD19-conjugated flurochrome was analysed in conjunction with an APC signal, when APC-labelled antibodies were not included. Alternatively, the CD19 signal could be detected in conjunction with DAPI staining as, autofluorescent cells also demonstrated a high fluorescence intensity in the UV range of the emission spectra. Fidelity of the CD19 signal was determined with FMO and biological controls. Furthermore, $CD19^+$ cells had a low side scatter profile, as expected for lymphocytes, and were observed as a contiguous population (Figure 55).

$CD19^+$ iPS-B cells were predominantly $CD34^-CD43^+CD10^+$ on day 21 (Figure 56A). Work in this laboratory has revealed the identity of this population as a pre-B cell population (Carpenter et al., 2011). When UCB-$CD133/34^+$ cells were cultured for an equivalent duration, in the same conditions, the $CD34^-CD43^+CD10^+$ phenotype was also observed (Figure 56A). In comparison, B cells present in non-cultured UCB MNCs were predominantly $CD43^-$ and contained both $CD10^+$ and $CD10^-$ populations (Figure 56A). This

suggests that the UCB MNC B cell fraction contains populations which are generally more developmentally mature than B cells generated from either iPS or UCB-HSC/HPCs at day 21 of the MS-5 co-culture assay. Statistical analysis of B cell populations demonstrated the lack of variability in the phenotypes described (Appendix Table 20).

iPS-B cell cultures were then maintained for a longer duration. Day 21 iPS-$CD34^+$/MS-5 co-cultures were harvested and selected by MACS for the $CD45^+$ fraction (as outlined in 2.5.2.4). $CD45^+$ cells were reseeded onto new MS-5 stromal cells and maintained as summarised in Figure 57. Cells were harvested after day 42/43 days of co-culture and stained with mAbs for analysis by flow cytometry. $CD19^+$ iPS-B cells had downregulated expression of CD43, but cells remained $CD10^+$ (Figure 56B). This suggests that CD43 may be a marker that is differentially expressed during human B cell differentiation. Furthermore, that iPS-B cells may have matured with continued culture.

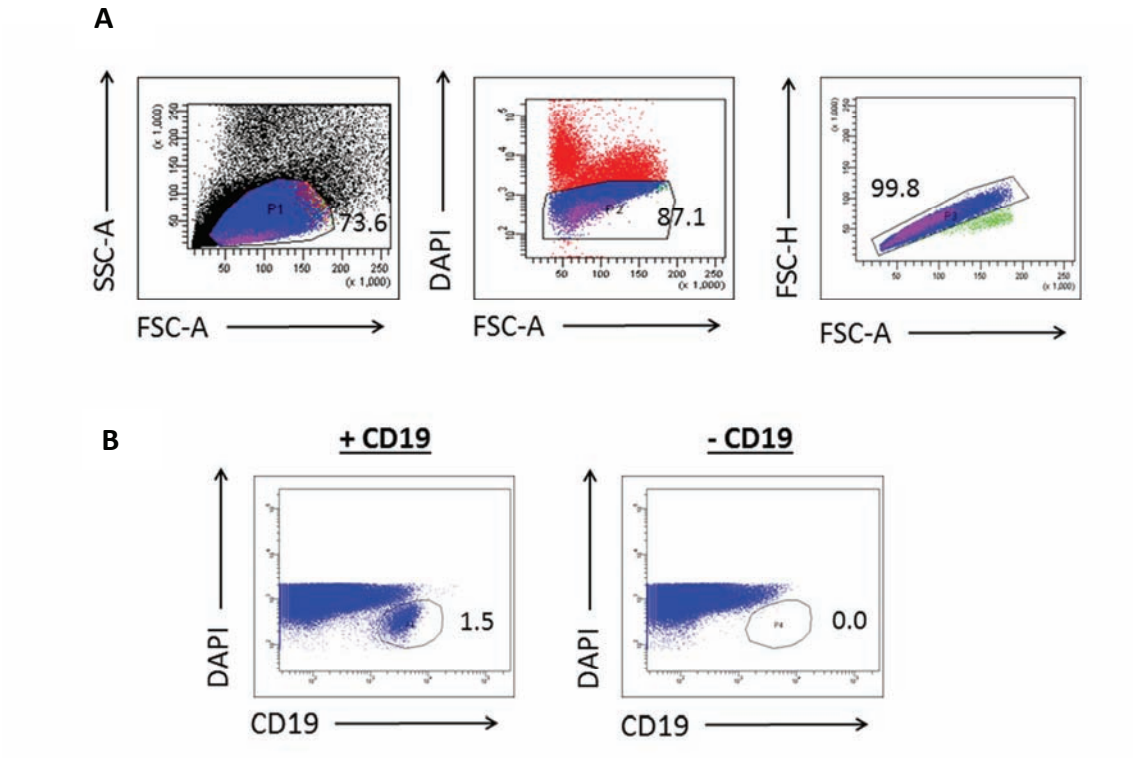

Figure 55 Gating approach and FMO control for analysis of CD19$^+$ cells by flow cytometry.
CD19$^+$ B cell populations were identified and analysed by flow cytometry using the following gating strategy; (A) Viable cells were gated based on low DAPI staining (P2) which were then gated to exclude possible doublets (P3). (B) CD19$^+$ cells were identified using DAPI versus CD19 or APC versus CD19 as appropriate. This approach was required as autofluorescent cells at c. 680-700 nm were frequently observed in long-term co-cultures. FMO control demonstrates fluorescence attributed to the CD19$^+$ population. CD19$^+$ cells (highlighted in pink in panel (A) from positive population in panel (B) have low SSC as expected for lymphocytes and form a contiguous population. The same gating approach was used for all B cell types (depicted are iPS-B cells in MS-5 co-culture). Numbers expressed as a percentage of parent gate.

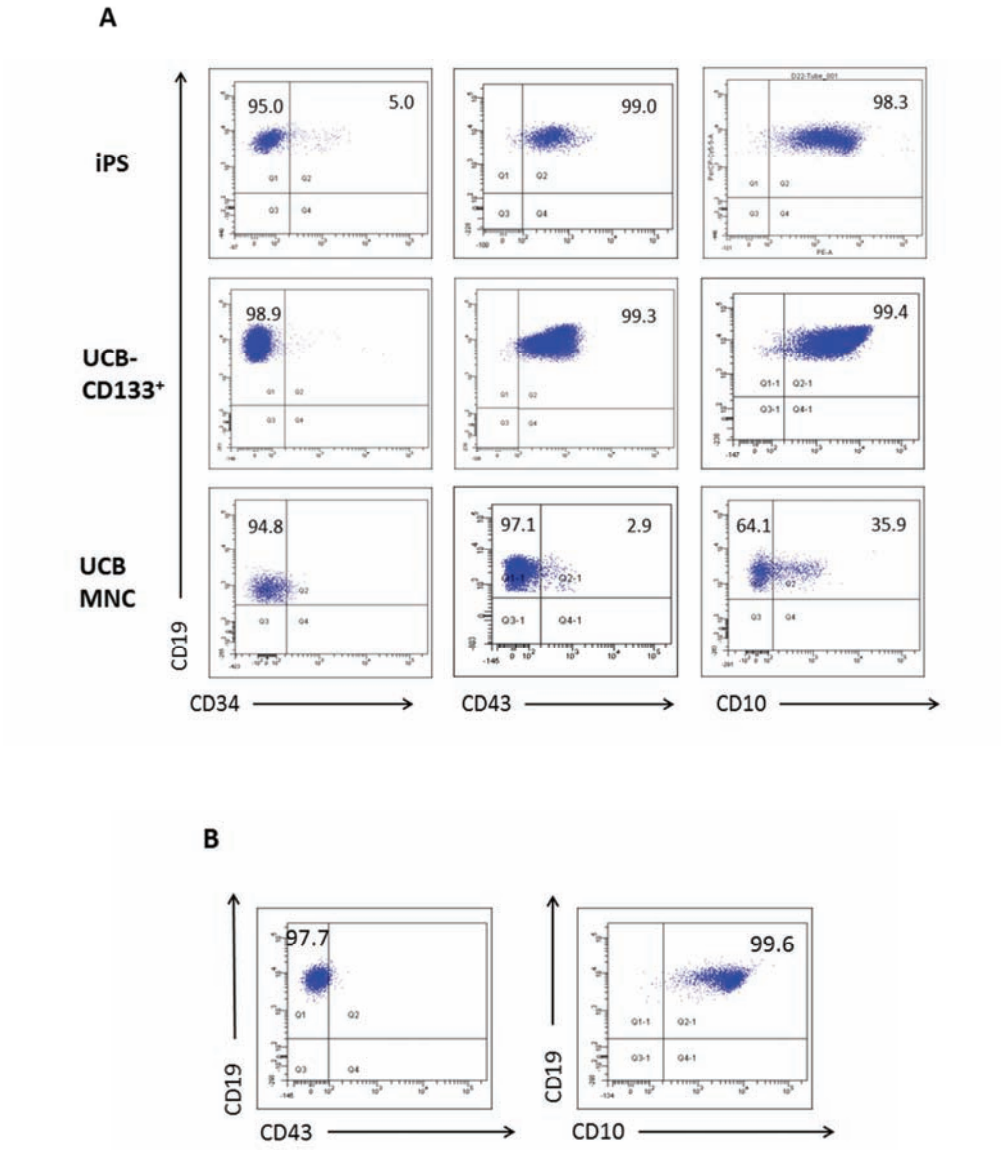

Figure 56 Assessing iPS-B cell development through the expression of CD34, CD43 and CD10. CD34, CD43 and CD10 are cell surface markers that can be used to distinguish stages of human B cell development. Populations shown were gated on $CD19^+$ cells using the approach depicted in Figure 55. (A) Day 21 iPS-B cells were predominantly $CD34^-CD43^+CD10^+$ (>95% of CD19+ cells), describing a pre-B cell identity. UCB-$CD133^+$ cells on day 21 also displayed this $CD34^-CD43^+CD10^+$ phenotype (>90% of $CD19^+$ cells). Comparably, B cells in the UCB MNC fraction were predominantly $CD43^-$ ($CD43^+$ 5.8% ± 3.2) and contained both a $CD10^+$ ($CD10^+$ 27.6% ± 11.9) and $CD10^-$ population. (B) Following a further 3 weeks in culture to day 42, iPS-B cells downregulated CD43 with CD10 expression remaining high. Different intensities of CD19 staining were observed with UCB MNC staining due to the use CD19-FITC antibody, in comparison to the CD19-PerCPCy5.5 antibody, used to stain iPS and UCB-$CD133^+$ B cells. PerCPCy5.5-conjugated antibodies produce a higher fluorescence intensity than FITC-conjugated antibodies. Numbers expressed as a percentage of total $CD19^+$ population. Representative images n=3.

5.3.1.2 In long term cultures iPS- B cells express IgM in the absence of supplementation with additional cytokines

Pre-B cells differentiate in the bone marrow to the immature B cell stage, where they express cell surface IgM (Hardy and Hayakawa, 2001, Ikuta et al., 1992). With the aim of promoting this development from iPS pre-B cells, $CD45^+$ cells, enriched by MACS from day 21 iPS-$CD34^+$/MS-5 co-cultures, were seeded onto fresh MS-5 stroma. The approach taken is summarised in Figure 57. $CD45^+$ cells were cultured in Differentiation media at $5x10^4$ cells/ml either a) without the addition of cytokines or with the inclusion of the following factors, b) IL-7/SCF/Flt3L, c) CD40L/IL-4/IL-5, d) PC or e) APRIL. Cultures were initially seeded into 1ml of media per well (12 well plate format), fed with an additional 1ml/well on day 28 and then a half media change on day 35. Both adherent and non-adherent cells on days 29, 36 and 43 were harvested by incubation with collagenase IV/trypsin and stained with mAbs for flow cytometry analysis.

On day 21, the $CD19^+$ population was negative for IgM (Figure 59). On day 29 and 36 the population remained IgM^- (Figure 59). By day 53, a significant difference could be observed with iPS-B cells that were cultured in the absence of cytokines, an average of 3.74% (mean 3.74% ± 1.47 SD) of $CD19^+$ cell expressed cell surface IgM (Figure 59). This production of IgM was not observed in cultures containing IL-7/SCF/Flt3L (Figure 59). In initial experiments, in the absence of IL-7/SCF/Flt3L but presence of PC or APRIL, similar proportions of the $CD19^+$ population expressed IgM (Appendix Figure 76). Furthermore, when CD40L, IL-5 and IL-4 were added from day 21, in the absence of IL-7/SCF/Flt-3L, a large decrease in total $CD19^+$ cells numbers was observed (Appendix Figure 76). The

assessment of the impact of CD40L/IL-4/IL-5, PC or APRIL on iPS pre-B cell maturation was therefore not continued.

Attempts to expand iPS-B cell or UCB-derived B cells in the absence of MS-5 stroma, either in Differentiation media or in RPMI media containing 10% serum, were unsuccessful. In initial experiments, a vast reduction in $CD19^+$ cells was observed such that meaningful data could not be acquired (UCB B cells: 12.4% $CD19^+$ in the presence of stroma and 0.1% $CD19^+$ in the absence of stroma and iPS-B cells: 2.3% $CD19^+$ in the presence of stroma and 0.4% $CD19^+$ in the absence of stroma) (Appendix Figure 78).

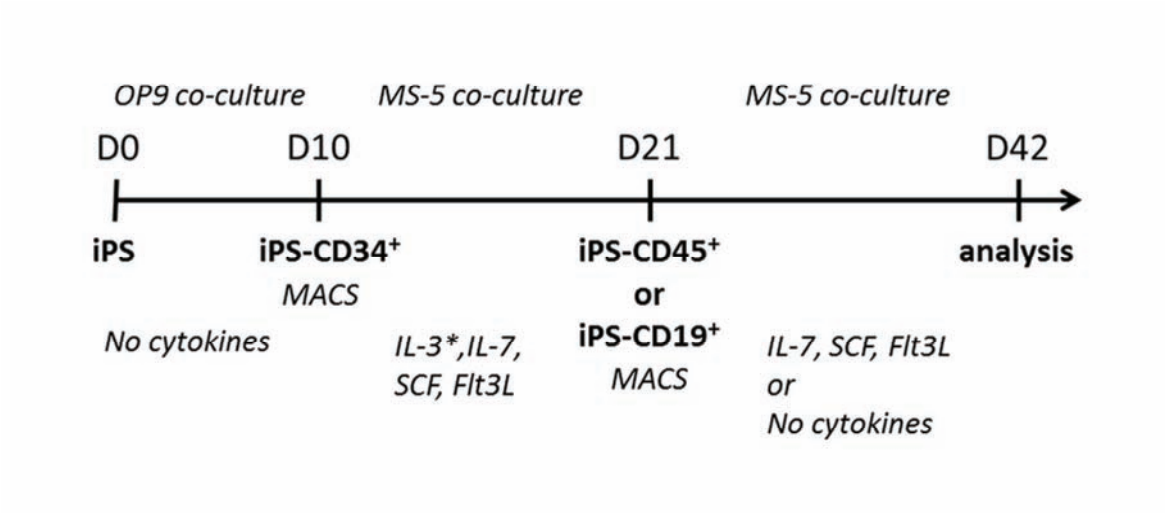

Figure 57 Schematic representation of protocol for long-term B cell cultures.
$CD34^+$ cells were isolated by MACS from day 10 iPS/OP9 co-cultures and seeded onto confluent MS-5 stroma in Differentiation media supplemented with IL-3, IL-7, SCF and Flt3L. Cultures were fed after 7 and 14 days with the same media, excluding IL-3 from this timepoint onwards. On day 21 cells were harvested and enriched by MACS for $CD45^+$ cells or $CD19^+$ cells and then seeded onto new MS-5 stroma. At this point cells were either cultured in Differentiation media without cytokine supplementation or with media plus cytokines. Cultures were then fed after a further 7 or 14 days and generally harvested on day 42/43 of culture.

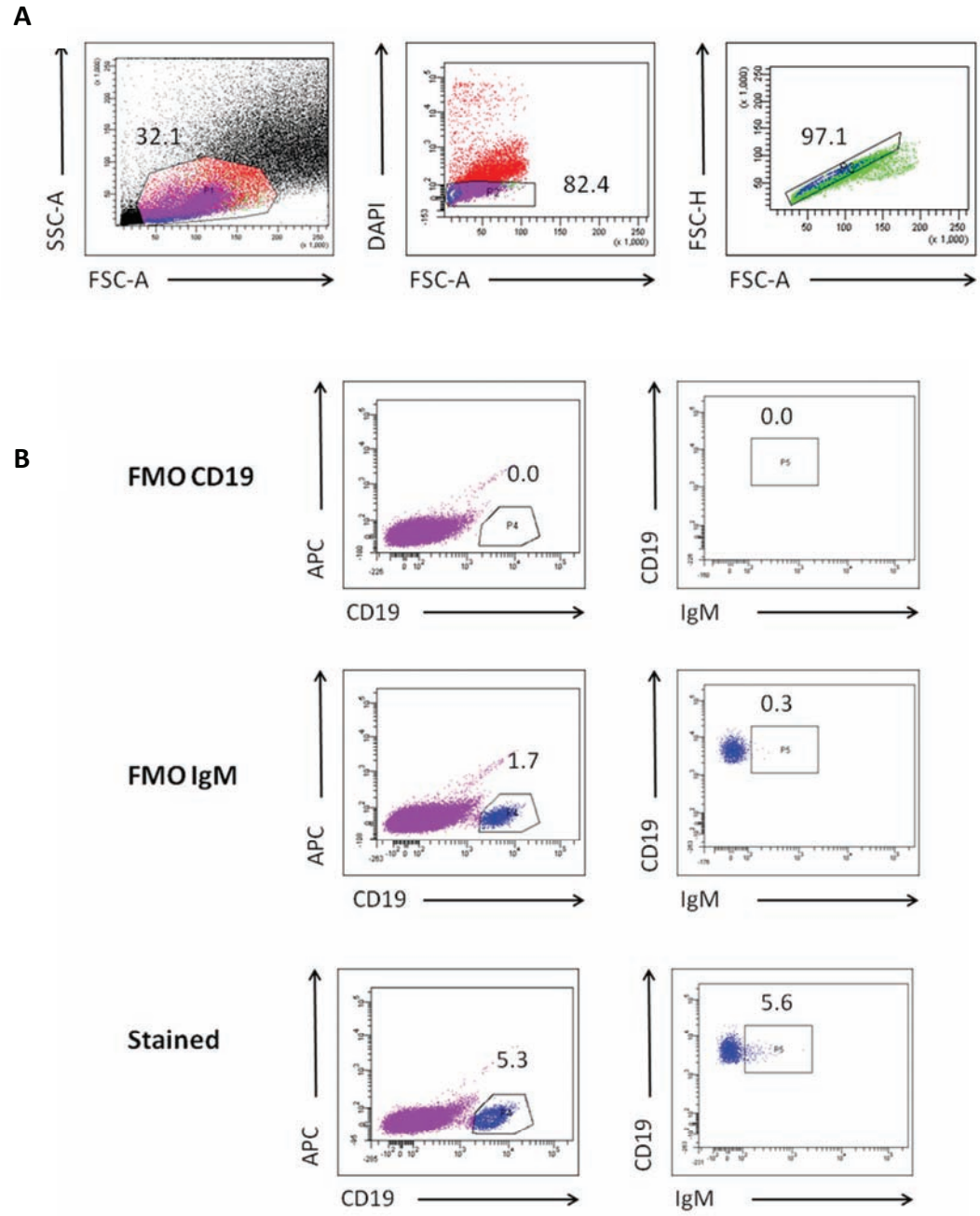

Figure 58 Gating approach for flow cytometry analysis of CD19 and IgM expression.
Analysis of iPS-B cell populations in MS-5 co-culture. (A) Cells were gated based on low FSC and SSC profile, then for the viable cell fraction ($DAPI^{low/-}$). A doublet exclusion gate was also applied. (B) Identification of CD19 and IgM positivity. The $CD19^{+}$ fraction was gated based on negative APC autofluorescence and a positive CD19 signal, which was not present in the relevant FMO control. IgM positivity was also determined with FMO gates set ≤0.3% of the CD19+ population. Numbers expressed as a percentage of the parent gate.

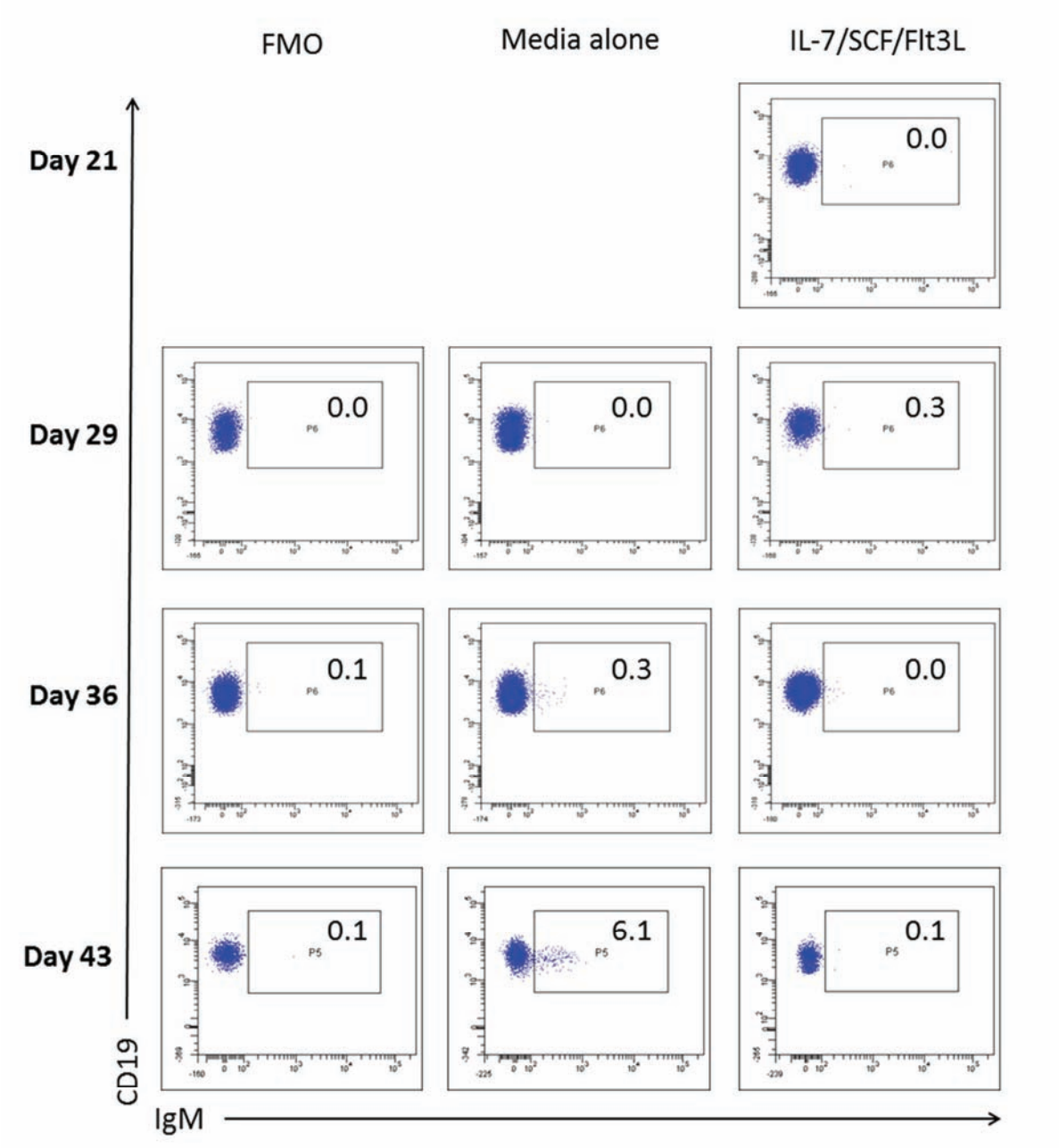

Figure 59 iPS-B cells differentiate to produce $CD19^+IgM^+$ cells with extended co-culture.
Day 21 $CD45^+$ cells, containing a $CD19^+$ subpopulation, were seeded at $5x10^4$ cells/ml onto MS-5 stroma. Cultures were harvested after 29 and 36 days, where upon significant levels (<0.5%) of IgM expression could not be detected by flow cytometry. By day 43, $CD19^+IgM^+$ cells were observed in cultures maintained in the absence of IL-7/SCF/Flt3L. Number are expressed as a percentage of total $CD19^+$ population. Day 29 and 36 timepoints n=2, day 43 and 21 time points n=>3 independent experiments.

5.3.1.3 iPS-B cells do not persist in long-term culture following CD19$^+$ enrichment.

Initial studies described the propensity of iPS-B cells to express cell surface IgM, when enriched for the CD45$^+$ fraction on day 21, and after continued time in culture. Concurrently, CD19$^+$ cells were isolated by MACS from day 21 of CD34$^+$/MS-5 co-culture and reseeded onto fresh MS-5 stroma, in the absence of cytokine supplementation. CD19$^+$ enriched fractions were seeded at 1x10^4 cells/ml, of which cells had a purity of >90% (as described in Table 6). Comparatively, CD45$^+$ fractions were seeded at 5x10^4 cells/ml (>95% purity), of which 5-10% of cells were also CD19$^+$ (2.5.2.4). Therefore, cultures seeded with CD45$^+$-enriched fractions contained around 50% less B cells at seeding than cultures with CD19$^+$-enriched cells. Cultures were maintained as summarised in Figure 57, before cells were harvested on day 42/43 cells and analysed by flow cytometry. Analysis revealed a large reduction of CD19$^+$ cells on day 42/43 from CD19-enriched cultures (Figure 60 A). To quantify this difference, the number of CD19$^+$ cells detected on day 42/43 was expressed as a proportion of CD19$^+$ cells seeded at day 21, either in CD19 or CD45-enriched cultures, onto MS-5 cells. CD45-enriched cultures demonstrated an average ratio of 4.86:1 (mean 4.86 ± 3.02 SD) of CD19$^+$ cells recovered on day 42/43 to CD19$^+$ cells seeded (Figure 60 B). When cells were enriched for CD19, the ratio of CD19$^+$ cells recovered on day 42/43 to CD19$^+$ cells seeded was 0.01:1 (mean 0.01 ± 0.004 SD) (Figure 60). These data revealed that there was, on average, a 4-fold increase in total CD19$^+$ cells with continued culture from CD45 enriched populations but that a large significant decrease in total B cells was observed when cells were enriched by CD19 selection.

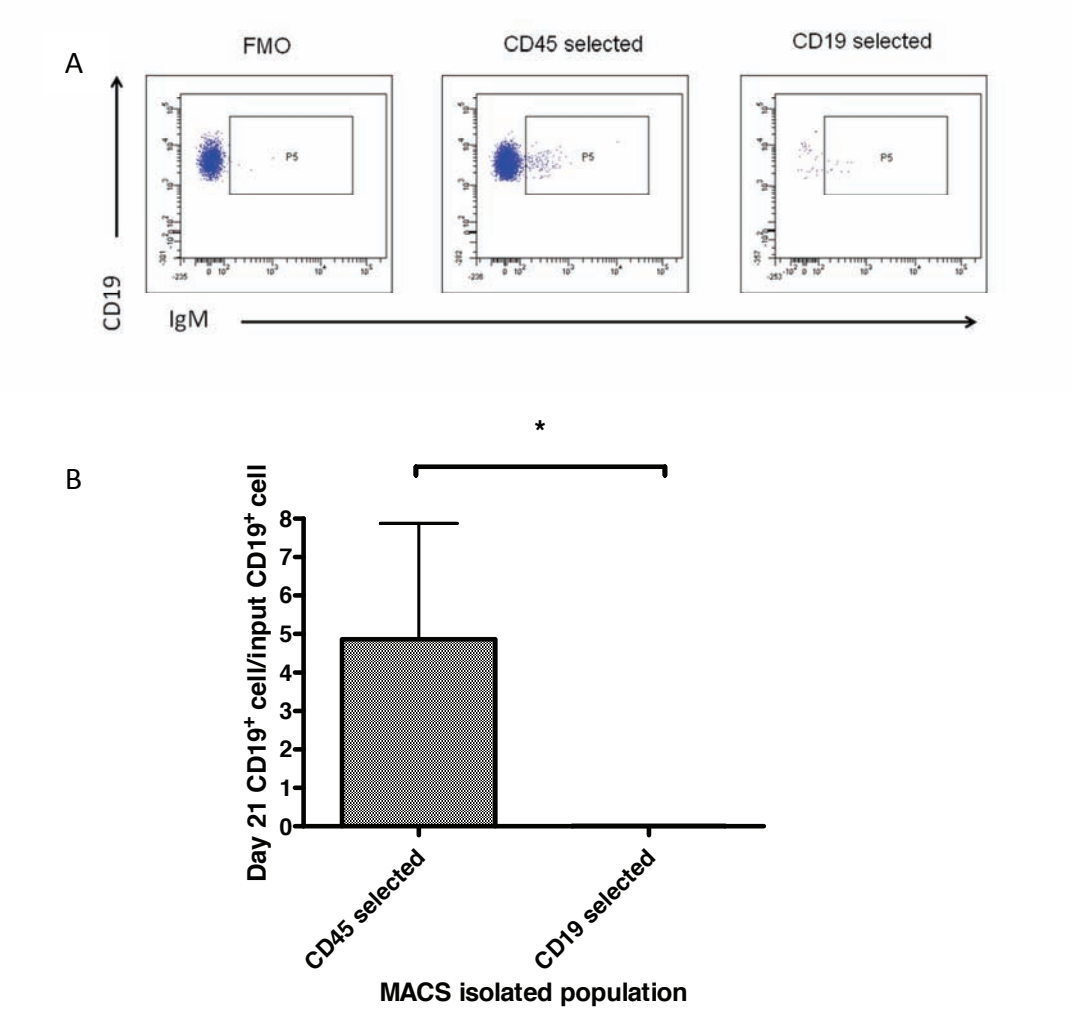

Figure 60 B cells enriched by CD19 selection from day 21 cultures persist in low numbers in long term culture.

On day 21 of iPS-CD34$^+$/MS-5 co-cultures cells were enriched by positive selection for CD45 or CD19 expression. Cells were reseeded with MS-5 stroma in the absence of cytokine supplementation. On day 42/43, cultures were harvested and analysed by flow cytometry (A). Following CD45 enrichment, total CD19$^+$ cells increased from day 21 to day 42/43 at a ratio of 1:4.86 (mean 4.86 ± 3.02 SD) (B). In contrast, when CD19 selection on day 21 was used as a purification step the ratio of CD19$^+$ cells on day 21 to day 42/43 was 1:0.01 (mean 0.01 ± 0.004 SD), demonstrating a large reduction in the B cell pool. P= 0.0248. *= P≤0.05. n=3 independent experiments.

5.3.1.4 The addition of IL-7 to iPS-B cell co-cultures prevents differentiation to the IgM$^+$ stage

IgM$^+$ cells were not produced when day 21 CD45$^+$ cells were cultured in the presence of IL-7,SCF and Flt3L for the duration of the assay. It therefore could be hypothesised that one or multiple of these cytokines were preventing the development of IgM$^+$ cells. To this end, CD45$^+$ cells were selected from day 21 cultures and reseeded as described in Figure 57, in the absence of cytokines, the presence of IL-7, or SCF, or Flt3L, or with all three cytokines. Cultures were maintained until day 42/43, harvested and analysed by flow cytometry for cell surface IgM expression. As previously described, IgM$^+$ cells could be detected in the absence but not presence of IL-7/SCF/Flt3L. The presence of Flt3L had no significant impact upon the percentage of CD19$^+$ cells expressing IgM (media alone 3.7 ± 1.5; Flt-3; 3.0 ± 1.4, mean(%) ± SD. P=0.377). Cultures with IL-7 supplementation showed a vast reduction of IgM$^+$ cells both when the cytokine was included singularly, and in combination with SCF and Flt3L (media alone 3.7 ± 1.5; IL-7 0.4 ± 0.1, mean(%) ± SD. P=0.0005. IL-7/SCF/Flt3L 0.3 ± 0.2, mean(%) ± SD. P=<0.0001) (Figure 61).

Phenotypically, it was observed that cultures maintained in the presence of IL-7 had a larger number of non-adherent cells. Brightfield images demonstrate the lack of colonies with a pebblestone morphology that has been associated with B cell populations in this assay (Figure 63 A). To dissect the role of IL-7 on the production of IgM$^+$ cells, broad analysis of the size of the B cell population, the number of total cells produced and the viability of cultures was undertaken. The total number of CD19$^+$ cells on day 42/43 showed a large degree of variability (media alone 2980 ± 2014; IL-7 2113 ± 1288; Flt3L 4087 ± 2447; IL-7/SCF/Flt3L 2265 ± 1327. Mean ± SD number of CD19$^+$ cells/5x10^4 CD45$^+$

cells seeded) within and between independent experiments but there was no significant difference between any of the culture regimens assessed (Figure 63 C). The addition of IL-7 therefore, did not appear to have a direct effect on B cell numbers. When the viability of the harvested cultures was analysed by the percentage of the population that was DAPI positive, a significant effect of IL-7 was demonstrated (Figure 63 B). Cells cultured in the presence of Flt3L and media alone showed no significant difference in non-viable cells. Cells cultured in the presence of IL-7 alone had a greater proportion of $DAPI^+$ non-viable cells (Media alone 1.2 ± 0.1; IL-7 4.1 ± 0.1, mean(%) ± SD). The viability of cultures with IL-7/SCF/Flt3L was greater than that of IL-7 alone, but still significantly different from media alone (IL-7/SCF/Flt3L 2.7 ± 0.5, mean(%) ± SD) (Figure 63 B). When the total cell number was analysed, there was no significant difference between media alone, IL-7 and Flt3L groups (Figure 63 D). Cultures in the presence of IL-7/SCF/Flt3L had a greater total number of cells in comparison to cultures with media alone, which suggests expansion of a non-B cell haematopoietic population(s) (Media alone 121,627 ± 34,176; IL-7/SCF/Flt3L 226,559 ± 79,095, mean ± SD).

In conclusion, the addition of IL-7 either alone or in combination with SCF and Flt3L resulted in the absence of IgM^+ cells. This was not due to an effect on total B cell numbers. An impact upon the proportion of non-viable cells in culture could be seen when IL-7, either alone or in combination, was added to cultures. However, as a total percentage of the culture population, this difference was minor.

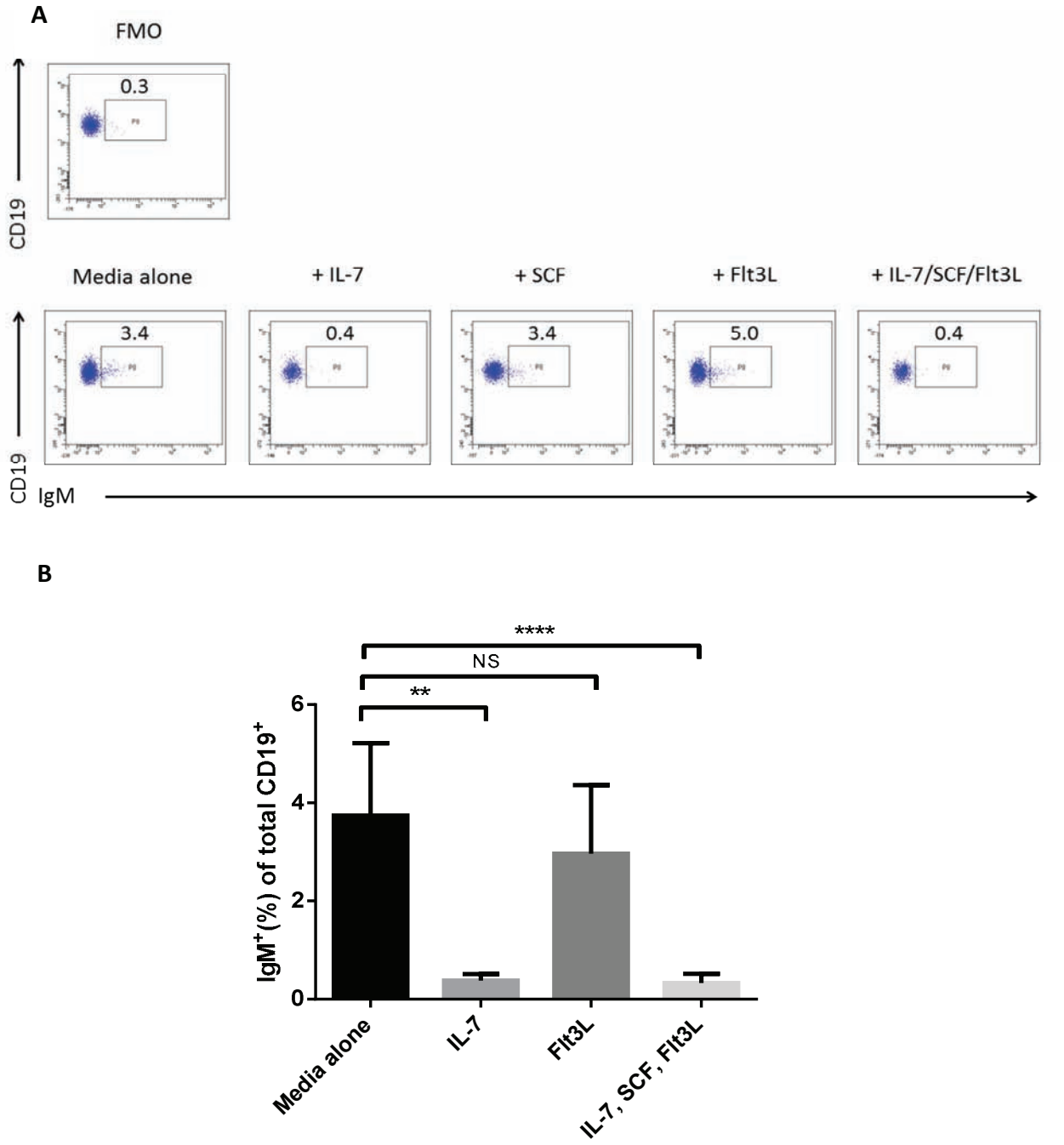

Figure 61 The inclusion of IL-7 results in the absence of $CD19^+IgM^+$ cells.
Cultures seeded with day 21 $CD45^+$ cells on MS-5 stroma in the absence of cytokines (media alone), IL-7, SCF, Flt3L or all three cytokines in combination (IL-7,SCF,Flt3L) were harvested on day 43 of culture and analysed by flow cytometry (A). IgM^+ cells could be detected in media alone cultures, in the presence of SCF and with Flt3L. In both IL-7 and IL-7/SCF/Flt3L cultures, IgM^+ cells were absent (B). NS= P>0.55, *= P≤0.05, **= P≤0.01, ***= P≤0.001, ****= P≤0.0001. Unpaired t-test, mean ± SD. Number expressed as a percentage of total $CD19^+$ population. n= 3 independent experiments.

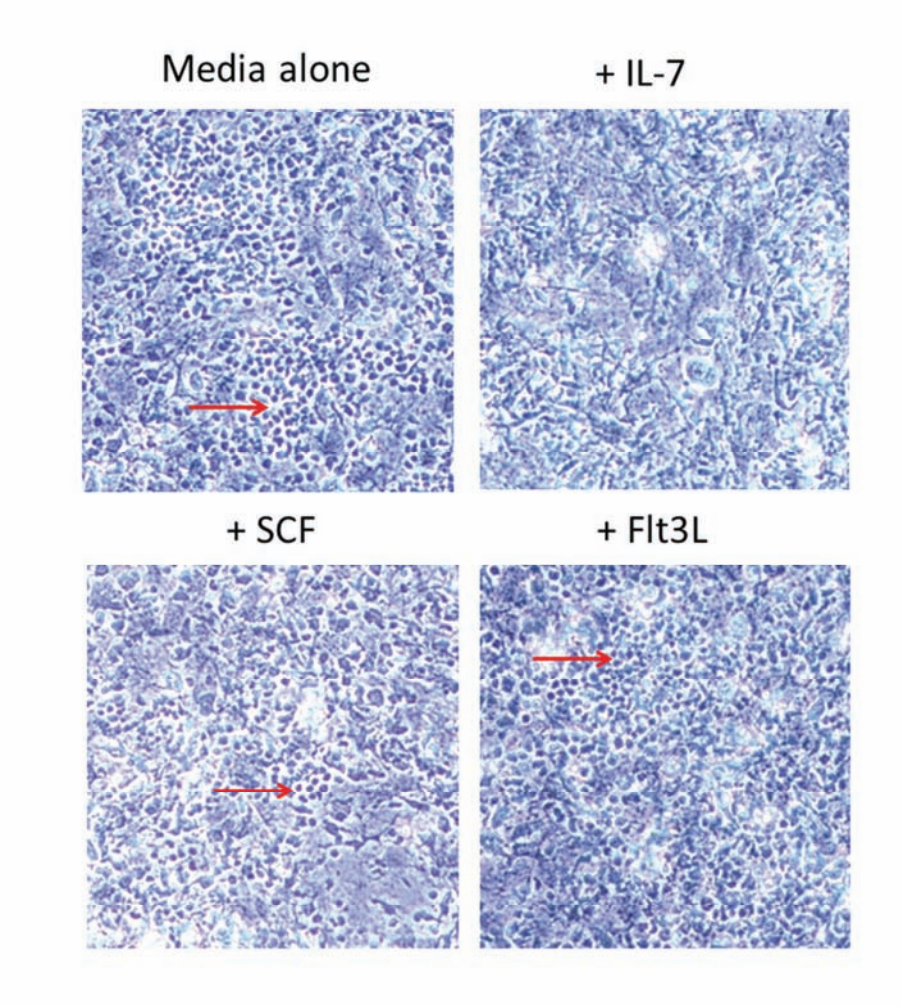

Figure 62 The effect of IL-7 on long-term B cell cultures.
iPS-CD45^{+} cells in co-culture with MS-5 stroma with, or without cytokines as indicated. Brightfield images (x20 magnification) of day 37 cultures. Pebblestone-like colonies can be observed in the absence of IL-7.

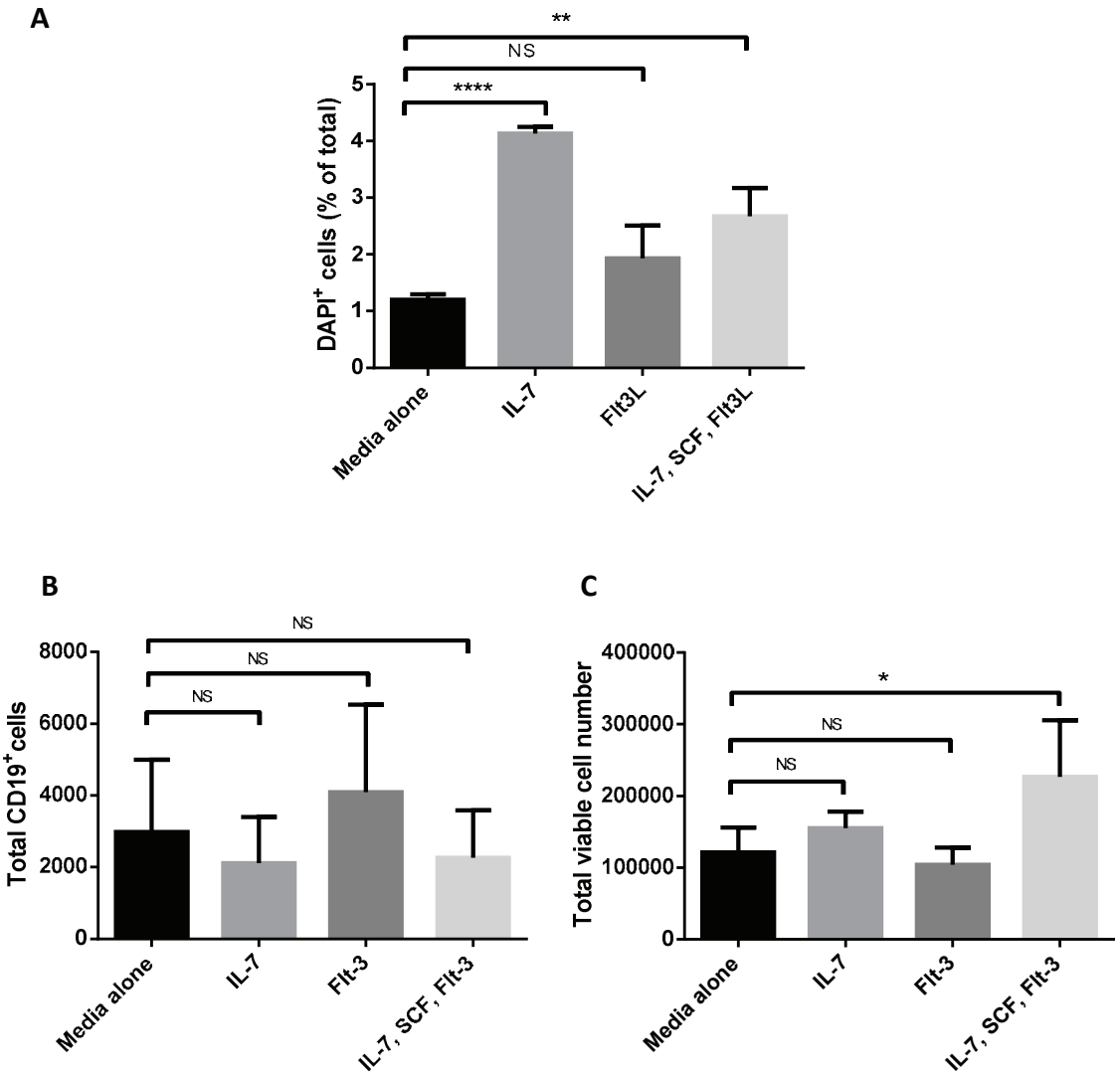

Figure 63 Dissecting the effect of IL-7 on day 42/43 cultures.
Cells were harvested for flow cytometry analysis on day 43 and stained with antibodies to CD19, IgM, and with the viability marker DAPI. (A) The number of $DAPI^+$ non-viable cells is expressed as a percentage of the total cell population. IL-7 and IL-7/SCF/Flt3L have a significant impact on the number of non-viable cells, in comparison to media alone. (B) Total number of $CD19^+$ cells present on day 43 per $5x10^4$ $CD45^+$ cells seeded on day 21. While large variation could be seen between groups; there is no significant difference between different conditions. (C) The total viable cell number was determined by flow cytometry. Both IL-7 and Flt3L showed no significant difference in terms of total cell number in comparison to media alone. An increase in total cell number was observed with the inclusion of IL-7/SCF/Flt3L when compared to media alone. NS= P>0.5, *= P≤0.05, **= P≤0.01, ***= P≤0.001, ****= P≤0.0001. Mean ± SD. n= 3 independent experiments.

5.3.1.5 UCB-B cells derived in the same conditons express IgM with comparable efficiencies and temporal kinetics

iPS-derived B cells, when cultured in the appropriate conditions, were found to express IgM after continued periods in culture. The proportion of the $CD19^+$ population that expressed IgM however was low. To assess whether the efficiency of IgM expression related to the cell of origin or to limitations of the culture conditions, the process was repeated with a non-iPS HSC/HPC population. Human $CD133^+/CD34^+$ cells (UCB-HPCs) that are known to contain HSCs were isolated from fresh UCB by MACS separation. UCB-HPCs were seeded onto MS-5 stroma in the presence of IL-3, IL-7, SCF and Flt3L and maintained for 22 days. The resulting population contained $CD19^+IgM^-$ cells comparable to iPS-derived pre-B cell populations at the same timepoint (Figure 64B). The $CD45^+$ fraction was then enriched and reseeded onto fresh MS-5 stroma in the absence of cytokine supplementation. On day 43, cultures were harvested and stained for CD19 and IgM, and analysed by flow cytometry. Although the total $CD19^+$ fraction was of a greater magnitude than detected in iPS-B cell cultures, the proportion of $CD19^+$ cells expressing IgM was comparable to that observed with iPS-derived cultures (Figure 64B). It can therefore be assumed that the low efficiency of IgM^+ cell generation from iPS cells was due to the culture conditions, rather than to a restriction with iPS-B cells *per se*.

A

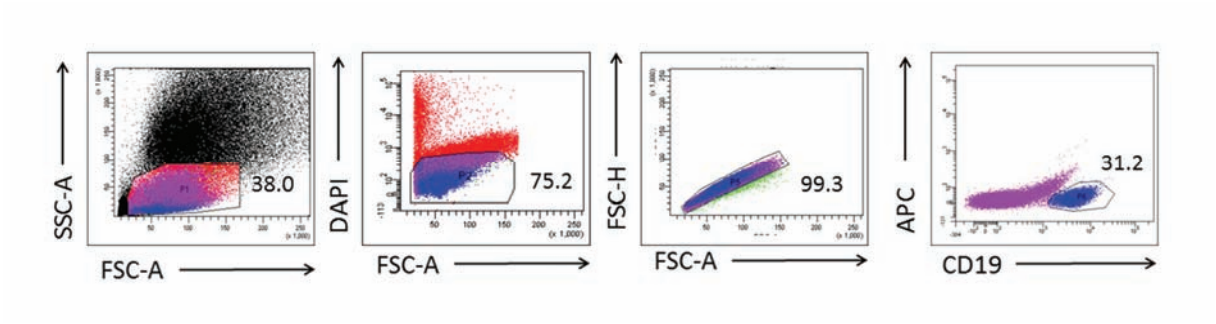

B

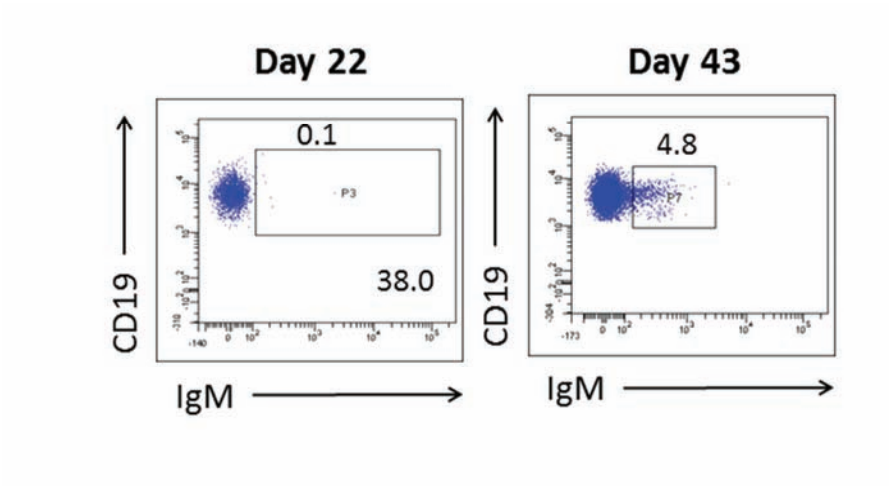

Figure 64 UCB-B cells express IgM at similar efficiencies to iPS-derived B cells.
UCB-CD133^{+} cells were differentiated towards the B cell lineage by co-culture with MS-5 stroma supplemented with IL-3, IL-7, SCF and Flt3L. After 22 days cultures were harvested and enriched based upon CD45 expression and cultured in the absence of cytokine supplementation. (A) Gating strategy in flow cytometry analysis of UCB-derived B cell populations. Cells were gated based on low SSC, viability (DAPI^{-}) and doublets were excluded. CD19^{+} cells were gated based on positive expression and lack of autofluorescence in the APC channel. (B) Day 22 UCB-B cells were negative for cell surface IgM expression. CD45^{+} cells were then seeded at 5x10^{4} cells/ml onto fresh MS-5 cells in the absence of cytokine supplementation. After 43 days cultures were harvested and assessed for the expression of CD19 and IgM by flow cytometry. UCB-B cells expressed IgM at comparable efficiencies to iPS-B cells at the same time points. (A) Numbers expressed as a percentage of the parent gate. (B) Number expressed as a percentage of the total CD19^{+} population. n=2 independent experiments.

5.3.2 Assessment of VDJ status in iPS IgM$^+$ B cells

To demonstrate VDJ recombination in iPS-B cells, genomic DNA (gDNA) was isolated from day 43 CD45$^+$ cells following MS-5 co-culture with iPS-CD34$^+$ cells (as described in 5.3.1.2). For comparison, gDNA was also obtained from day 43 CD45$^+$ cells generated from UCB-CD34/CD133$^+$ cells (designated UCB-B). This UCB-derived population contained B cells that express IgM in similar proportions to iPS-B cells (5.3.1.5). As negative controls, gDNA was isolated from hDFs and undifferentiated iPS cells. Clonal controls from InVivoScribe were also obtained for use as a positive control. The VDJ region was amplified using JH consensus primers, which recognise a conserved sequence in the J gene segment, in addition to three different primers, FR1, FR2 and FR3, that anneal in the V gene region (depicted in Figure 65). PCR products were then separated by electrophoresis on a 2% agarose gel in TBE buffer with gel red to visualise DNA bands using UV lights.

Using FR1 and FR2 primers, recombination of VDJ regions at the IgH locus was demonstrated in both iPS-derived B cells and UCB HSC/HPC-derived B cells (Figure 66 and Figure 67). This was validated by the absence of bands of the relevant size in hDF and undifferentiated iPS samples (Figure 66 and Figure 67). Bands within the 69-129 base pairs (bp) range could also be identified in PCR products from iPS and UCB HSC/HPC-derived B cells when FR3 primers were used (Appendix Figure 79). However, although hDF samples did not produce a band within this region, this was observed in undifferentiated iPS cell samples (Appendix Figure 79). However, the production of non-specific flanking PCR products at 69 and 130 bp when the FR3 primer is used is detailed in the manufacturer's guide. Furthermore, as relevant bands had not been produced from

undifferentiated iPS cells when FR1 and FR2 primers were used, which produced longer products, it is unlikely that this band is representative of a recombined IgH gene.

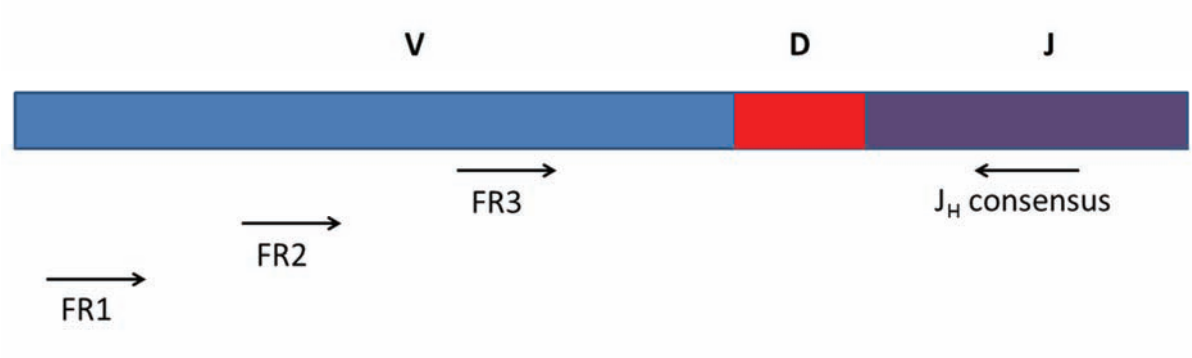

Figure 65 Schematic of PCR approach to VDJ recombination analysis.
Following recombination V, D and J gene segments are brought into proximity at the heavy chain locus. V(D)J configuration status can be assessed using the FR1, FR2 and FR3 primers which bind to the V segment, recognising a conserved sequence. The JH consensus primer binds to the J segment and the intervening DNA is amplified.

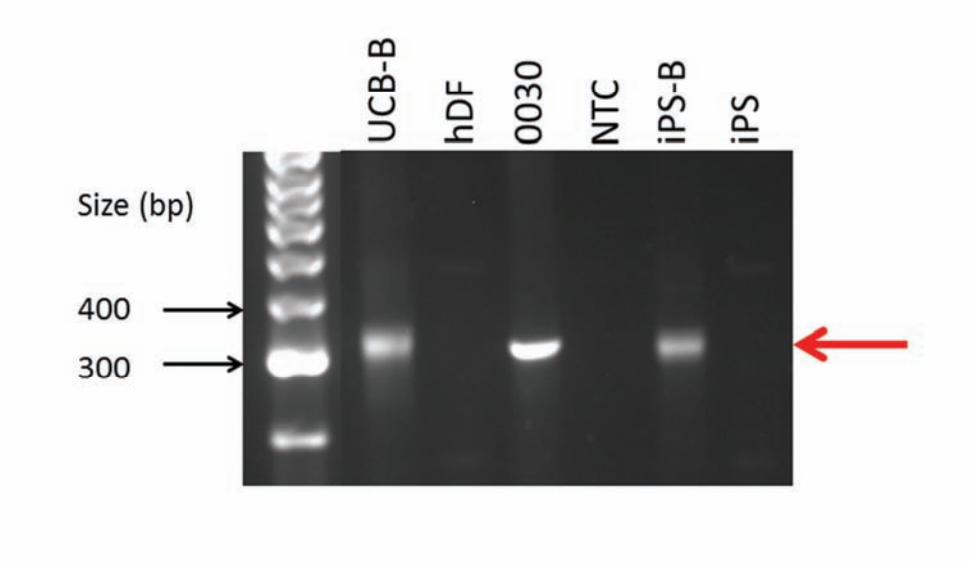

Figure 66 iPS-B cells have a recombined VDJ region at the IgH loci, as assessed using FR1 primers.
Genomic DNA was isolated from day 43 iPS-CD34^{+}/MS-5 co-cultures (iPS-B) and day 43 UCB-CD34^{+}/MS-5 co-cultures (UCB-B) that contained IgM^{+} cells. hDFs and undifferentiated iPS cells (iPS) were also included in addition to the no template control (NTC).The 0030 clonal control was also included which should produce a 317 bp product when FR1 primers are used for amplification. PCR reactions were run using FR1 and JH consensus primers for 37 cycles. PCR products were run on a 2% agarose-TBE gel with gel red and visualised with UV light. Recombined VDJ regions are expected to produce 290-360 bp products. Bands within this region could be observed in both iPS-B and UCB-B, as well as the 0030 positive control. hDF and undifferentiated iPS (iPS) samples, as expected, did not produce a band in this region.

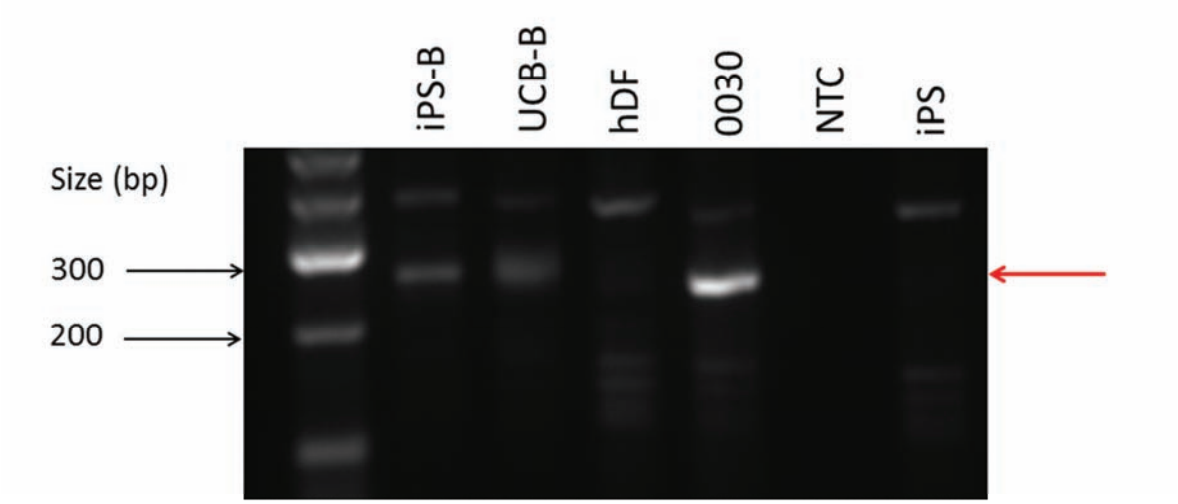

Figure 67 iPS-B cells have a recombined VDJ region at the IgH loci, as assessed using FR2 primers.
Genomic DNA was isolated from day 43 iPS-CD34^{+}/MS-5 co-cultures (iPS-B) and day 43 UCB-CD34^{+}/MS-5 co-cultures (UCB-B) that contained IgM^{+} cells. hDFs and undifferentiated iPS cells (iPS) were also included in addition to the no template control (NTC).The 0030 clonal control was also included which should produce a 258 bp product when FR2 primers are used for amplification. PCR reactions were run using FR2 and JH consensus primers for 37 cycles. PCR products were run on a 2% agarose-TBE gel with gel red and visualised with UV light. Recombined VDJ regions are expected to produce 235-295 bp products. Bands within this region could be observed in both iPS-B and UCB-B, as well as the 0030 positive control. hDF and undifferentiated iPS (iPS) samples, as expected, did not produce a band in this region.

5.3.3 iPS-B cells when injected into neonatal immunodeficient mice do not expand *in vivo, a pilot study.*

5.3.3.1 iPS-B cells when injected intrahepatically or intra-peritoneal into neonatal BALB/c Rag2$^{-/-}$cγ$^{-/-}$ mice are not detectable at week 12

Previous attempts to perform reconstitution assays with HPCs derived from pluripotent stem cells in OP9 co-culture have proven ineffective (Tian et al., 2009). It therefore seemed unlikely that iPS-HPCs derived with the methodologies described herein would differentiate *in vivo* to produce B cell populations. Recent work in mice lacking circulation (Ncx1$^{-/-}$) demonstrated that YS B-1 cell progenitors, that were generated following co-culture with OP9 stroma, could repopulate the peritoneal cavity (Yoshimoto et al., 2011). This experimental set up involved injecting progenitors into the peritoneal cavity of sub-lethally irradiated neonatal mice, an assay which Yoder and colleagues have also employed to ask similar developmental questions (Yoshimoto et al., 2012, Yoder et al., 1997b). In the absence of a more equivalent model, this strategy was adopted to assess the maturation and repopulation capabilities of iPS-B cells.

iPS-CD34^{+} cells were differentiated on MS-5 stroma with IL-3, IL-7, SCF and Flt3L to generate CD19^{+}CD10^{+} pre-B cells. On day 23 of culture, cells were harvested by collagenase IV/trypsin incubation and enriched for CD45^{+} cells by MACS. A CD19 enrichment was not performed as previous *in vitro* results could not exclude an apoptotic effect of CD19 engagement. BALB/c Rag2$^{-/-}$cγ$^{-/-}$ that are deficient in T, B and NK cells were irradiated within 24 hours of birth, with 2 doses of 2 Gy separated by 4 hours. Neonates were then injected 6-12 hours later with 5x10^{5} CD45^{+} cells, in 50µl of PBS-1% (w/v) BSA.

2 mice were injected intrahepatically and 2 mice intraperitoneally, as it was not known whether the cells would be able to home from the circulation. Intrahepatic injection was undertaken to permit comparison with UCB-HSCs as a positive control for reconstitution. The injected $CD45^+$ population contained 7.8% $CD19^+$ B cells, as well as 1.7% $CD56^+$ NK cells, and 37.1% $CD14^+$ monocyte/macrophages (Figure 68).

After 4 and 8 weeks, 20-25µl of blood was obtained from the tail vein. The red blood cells were lysed using Red Blood Cell Lysis Buffer and the MNC fraction was blocked (blocking buffer) prior to incubation with mAbs. No human $CD45^+$ cells were detected in the peripheral blood at week 4 or 8 (Figure 70). At 12 weeks, when the mice were sacrificed, cells were extracted from the peritoneal cavity and splenocytes were harvested by mashing spleens. To harvest bone marrow cells, the muscular and fibrous tissue was dissected from the femur, the femoral heads were removed using surgical scissors and the bone marrow flushed using a 26g needle and PBS-5% BSA at 4°C. Red blood cells in all harvested fractions were lysed, cells were filtered and a sample was taken to assess the total cell number. $2x10^6$ splenocytes, $2x10^6$ peritoneal cavity cells and $5x10^6$ bone marrow cells per individual were taken for analysis by flow cytometry. Human $CD45^+$ cells could not be detected in the spleen, peritoneal cavity or bone marrow (Figure 70).

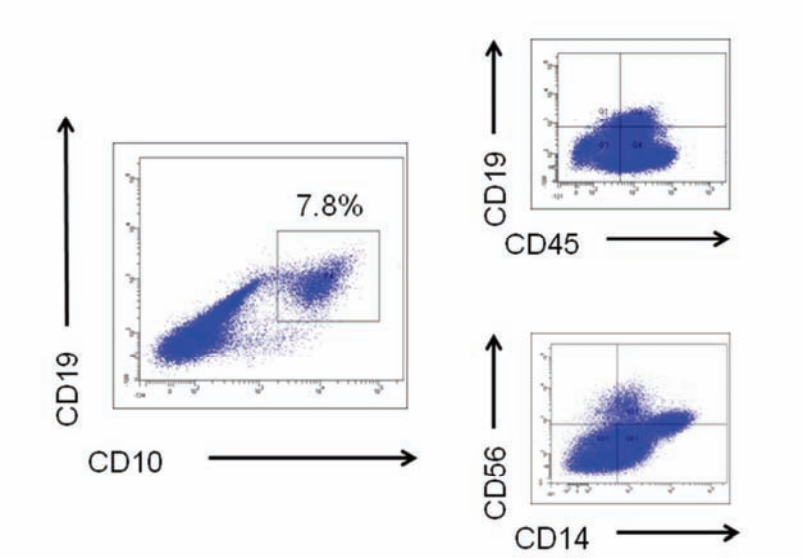

Figure 68 Phenotype of iPS-CD45$^+$ population injected into neonatal immunodeficient mice.
iPS-CD34$^+$ cells were cultured with MS-5 stroma and IL-3,IL-7,SCF and Flt3L for 23 days. Harvested cultures were enriched for CD45 expression and 5x10^5 cells were introduced via an intraperitoneal or intrahepatic injection into sublethally irradiated neonatal BALB/c Rag2$^{-/-}$cγ$^{-/-}$ mice. CD19$^+$ B cells made up 7.8% of the CD45$^+$ population with NK cells (1.7% CD56$^+$) and monocytes/macrophages (37.4% CD14$^+$) also detected. n=4 mice, injected with the aliquots of the same cell population.

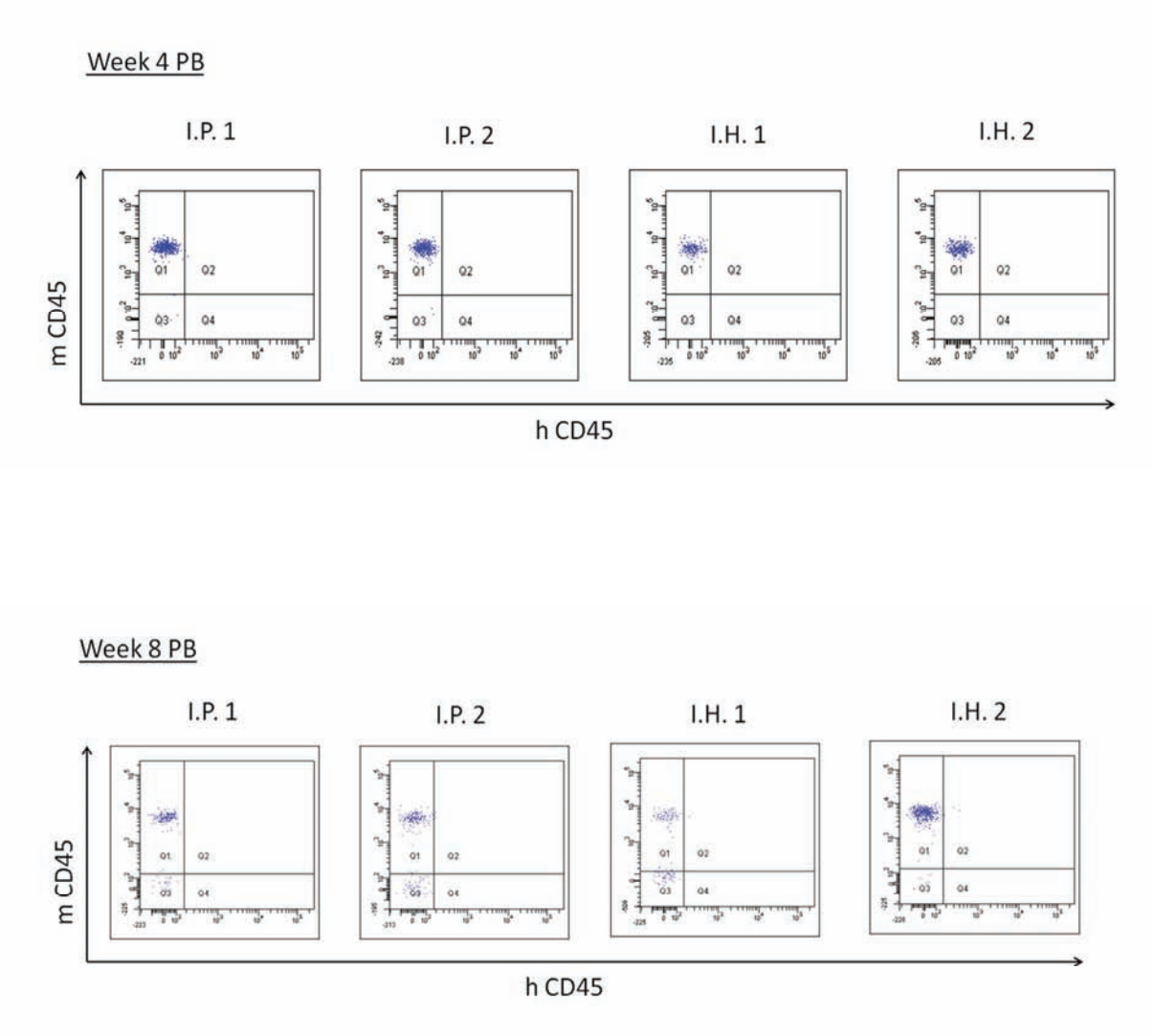

Figure 69 Analysis of week 4 and 8 peripheral blood reveals the lack of human CD45$^+$ cells.
Neonatal BALB/c Rag2$^{-/-}$cγ$^{-/-}$ mice were injected with iPS-CD45$^+$ cells and peripheral blood samples were taken via the tail vein after 4 and 8 weeks. Red blood cells were lysed, cells were blocked and then incubated with antibodies to mouse and human antigens. Human CD45$^+$ cells could not be detected. I.P= intraperitoneal injection I.H= intrahepatic injection. n=4.

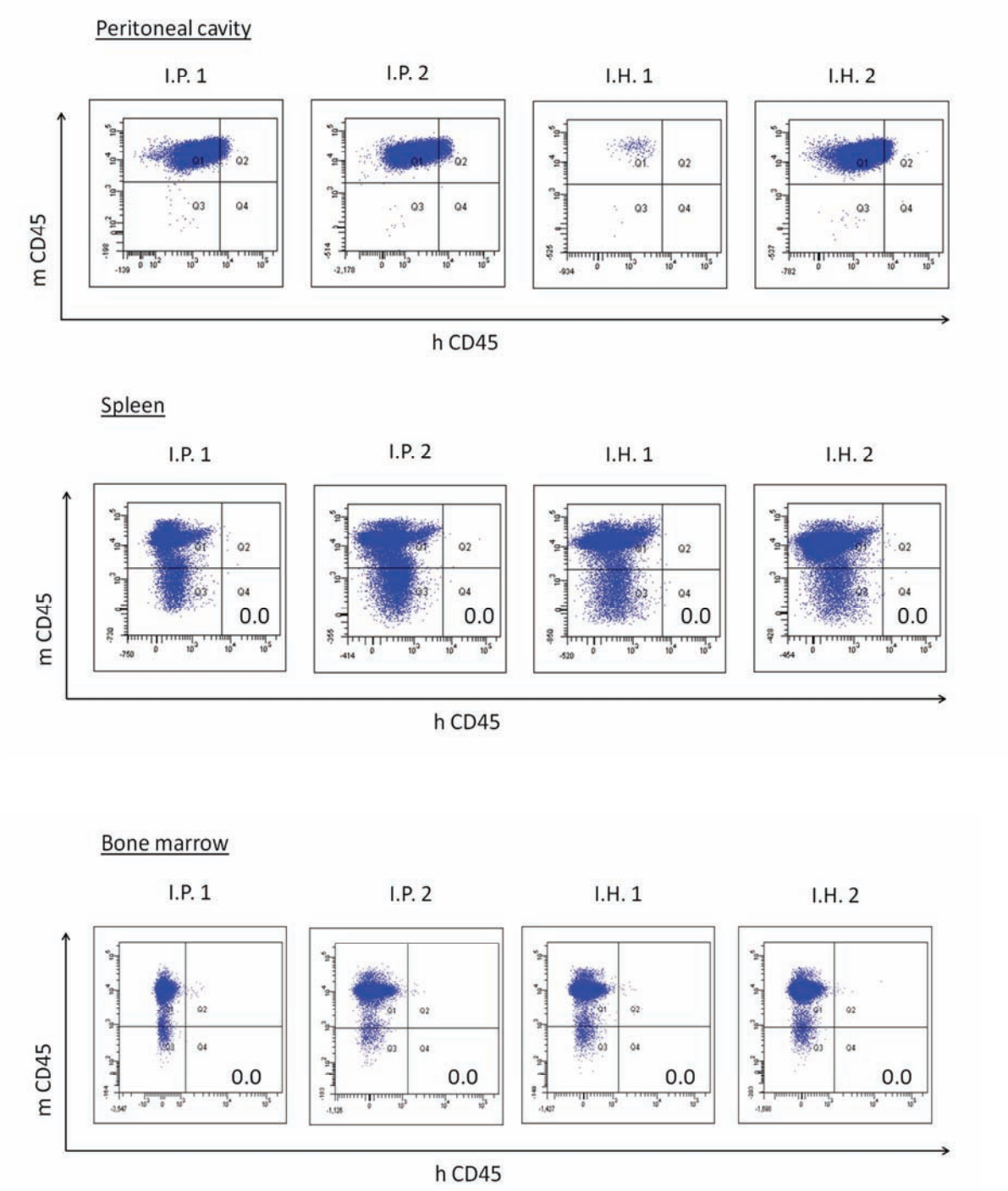

Figure 70 Analysis of week 12 peritoneal cavity cells, splenocytes and bone marrow cells in mice injected with iPS-CD45$^+$ cells reveals a lack of a detectable human cell population.
Neonatal BALB/c Rag2$^{-/-}$cγ$^{-/-}$ were injected with iPS-CD45$^+$ cells and mice were sacrificed after 12 weeks. Peritoneal cavity cells, splenocytes and bone marrow cell preparations were prepared for flow cytometry by lysing red blood cells, blocking non-specific binding and were then incubated with antibodies to human and mouse antigens. Human CD45$^+$ cells could not be detected in any anatomical compartment. n=4, mice depicted.

5.3.3.2 UCB-HSC/HPCs when injected intrahepatically into neonatal BALB/c Rag2$^{-/-}$cγ$^{-/-}$ mice result in low levels of reconstitution at week 12

An appropriate comparison was required for iPS-B cell injected mice. For the research questions being investigated, a) whether iPS-B cells would expand/differentiate *in vivo* and b) whether this model could be used to ascribe B-1 or B-2 B cell identity, an ideal comparison would be the repopulation of B cell compartments by non-iPS B cells. However, there are very few reports on the outcome of injecting B cells into mice, with suggestions that I.V. injected B cells do not home to the bone marrow (Johnson, 2008). Furthermore, it is not currently possible to accurately discriminate human B-1 from B-2 cells, if indeed these populations do exist in humans (Griffin et al., 2011, Covens et al., 2013). The most reliable comparison therefore was the repopulation of B cell compartments by UCB HSC/HPCs. I.P administration of UCB-HSCs has been demonstrated to result in extremely low levels of engraftment (Liu et al., 2012). To generate meaningful data, the inclusion of intrahepatic administration to permit engraftment, and I.P injection as a comparison for iPS-B cell administration, seemed appropriate. Intravenous and intrafemoral injections could not be attempted due to the small size of newborn mice.

UCB CD133^{+} cells that had been frozen on the day of isolation from fresh blood were thawed and cultured overnight in StemSpan media supplemented with SCF, Flt3L, IL-6 and TPO, a cytokine cocktail that has frequently been used to culture HSC/HPCs in the laboratory. Cells were then harvested by gentle aspiration and the CD133^{+} population was re-enriched using CD133 microbeads. A sample of the CD133^{+} population was taken for analysis by flow cytometry and the remaining cells were infused I.P (2 mice) or intrahepatically (1 mouse) at 1x10^{5} cells/mouse. The same irradiation and infusion

strategy was used as for iPS-CD45$^+$ mice. The infused cells were 93.2% positive for CD133 and CD34 (Figure 71).

After 4 and 8 weeks, peripheral blood was harvested via the tail vein. At 4 weeks, human CD45$^+$ cells could not be detected, with rare events being observed after 8 weeks (Figure 72). Mice were sacrificed at 12 weeks and peritoneal cavity cells, splenocytes and bone marrow cells were isolated. Cells were processed as previously described, by lysing red blood cells, enumerating, blocking and staining, for analysis by flow cytometry. Human CD45$^+$ cells were detected in the spleen and bone marrow in the recipient that had received cells intrahepatically (Figure 73). Neither recipient that had received UCB-CD133$^+$ cells via an I.P injection contained detectable human CD45$^+$ cells in the any of the organs analysed at week 12 (Figure 73). It was possible that the UCB unit infused had poor engraftment potential as has been described elsewhere (Ballen et al., 2001). Time constraints did not permit repetition of these experiments.

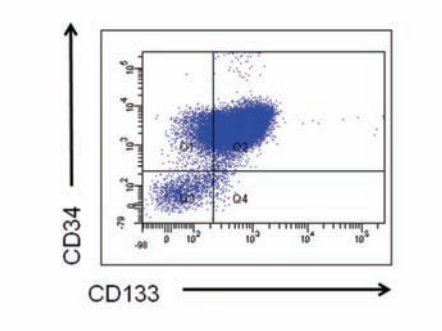

Figure 71 Analysis of UCB-CD133$^+$ cells prior to injection into BALB/c Rag2$^{-/-}$cγ$^{-/-}$ mice.
UCB-CD133$^+$ cells were thawed following cryopreservation and cultured overnight in Stemspan media with SCF, Flt3L, IL-6 and TPO. Cells were then re-enriched using CD133 microbeads by MACS. A sample was taken for FACS analysis, and the remaining cells were injected I.P. or I.H into neonatal immunodeficient mice at 1x10^5 cells/mouse. CD133$^+$ cells were 93.2% CD133$^+$CD34$^+$ and 4.8% CD133$^-$CD34$^+$.

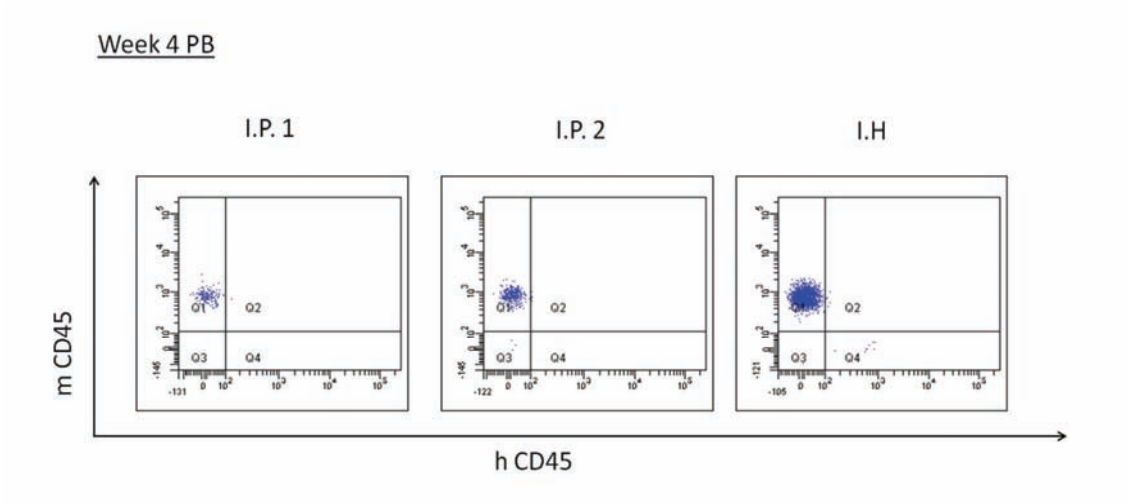

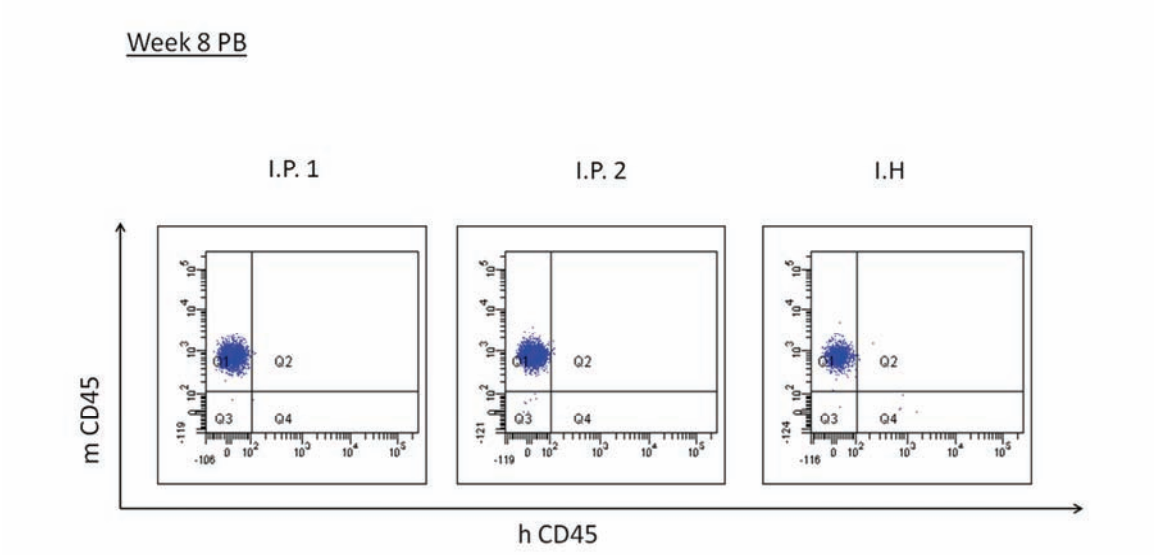

Figure 72 Analysis of week 4 and 8 peripheral blood samples reveals a lack of human CD45$^+$ cells.
BALB/c Rag2$^{-/-}$cγ$^{-/-}$ neonates were injected with 1x10^5 UCB-CD133$^+$ cells following sublethal irradiation. Peripheral blood was taken via the tail vein after 4 and 8 weeks. Red blood cells were lysed, cells were blocked and stained with mAbs for analysis by flow cytometry. At both 4 and 8 weeks only rare events could be observed in the human CD45$^+$ gate.

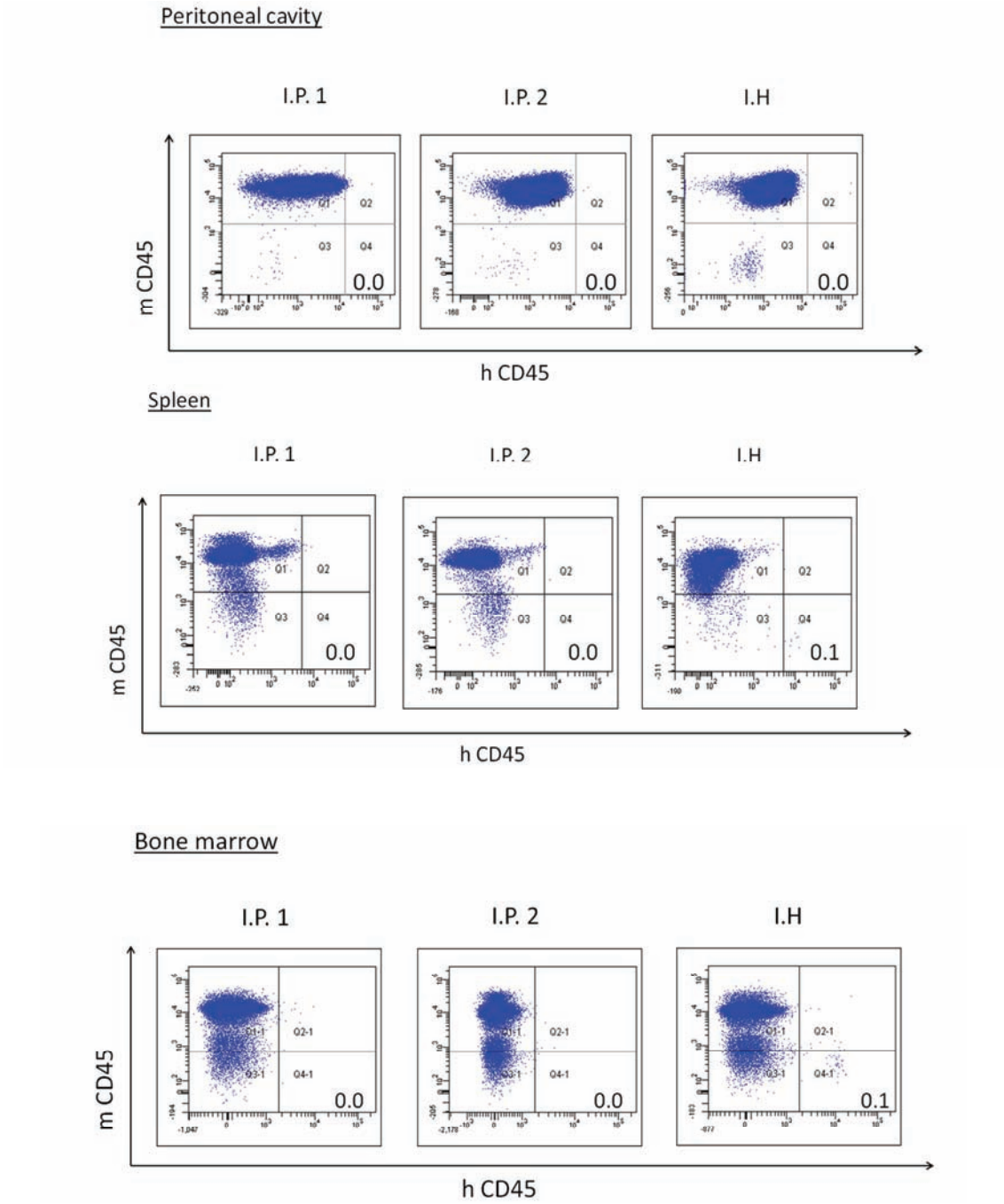

Figure 73 Low levels of human haematopoietic cells were detected at 12 weeks after intrahepatic administration into immunodeficient neonates.
UCB-CD133^{+} cells were injected I.P or intrahepatically (I.H) into sublethally irradiated neonatal immunodeficient mice. After 12 weeks mice were sacrificed and cells were harvested from the peritoneal cavity, spleen and bone marrow. Human CD45^{+} cells could not be detected in mice that had received cells via an I.P injection. In mice that had been injected intrahepatically human CD45^{+} cells were observed in both spleen and bone marrow. Human CD45^{+} cells represented 0.1% of total splenocytes/bone marrow cells.

5.4 Discussion

Here, the *in vitro* development of antibody-expressing iPS-B cells was described for the first time. $CD19^+IgM^+$ cells were generated over a period of 43 days from iPS-$CD34^+$ cells, using a co-culture system with MS-5 stroma in the absence of cytokine supplementation. This assay was robust and cells could easily be detected by flow cytometry, however differentiation efficiencies were low (mean 3.74% ± 1.47 SD). Whether the current assay could be adapted by a further increase in culture time or modification of the feeding regime to promote an increase in the proportion of $CD19^+$ cells expressing IgM was not addressed. However, experiments with UCB-$CD34^+$ cells in co-culture with S17 stromal cells, yielded comparable low proportions of IgM^+ cells (c. 3% after 6-8 weeks of culture) that could only be improved (to c. 12%) upon transfer of B cells to an alternative CD40L-stromal fibroblast environment (Fluckiger et al., 1998). When conditions permissive for the generation of IgM^+ cells were introduced, the immature B cell population could not be detected until week 3 in culture (cells were analysed every 7 days). It is likely that an accumulation of factors and step-wise changes in the development of this population is required for expression of the cell surface immunoglobulin. UCB-B cells, generated from HPCs, yielded IgM^+ cells with comparable efficiencies, in a similar time frame (6 weeks from the CD34/$CD133^+$ cell stage) when the same conditions were implemented. The production of a substantial numbers (between 1-45% of $CD19^+$ cells) of cell surface IgM^+ cells was, in contrast, described by Sekiguchi and colleagues when UCB $CD34^+$ cells were cultured on MS-5 cells in a biphasic culture system (Ohkawara et al., 1998). In the first phase, $CD19^+$ cells were generated, while in the second phase and, after addition of SCF and G-CSF, a significant proportion of $CD19^+$ cells expressed surface IgM (Ohkawara et al., 1998). Our results are consistent with Rawlings *et al.* and Fluckiger *et al.* (Rawlings et al.,

1995b, Fluckiger et al., 1998). These results suggest that immature IgM^+ B lymphocytes are generated from iPS-$CD34^+$ and UCB-$CD34/133^+$ cells in a comparable temporal window.

Alternative explanations for the low efficiency of immature B cell differentiation from both iPS and UCB cells are that factors present in the co-culture are providing inhibitory signals that suppress maturation, that IgM^+ cells which cannot transit out of the bone marrow-like environment undergo apoptosis, or, that earlier stages of B cell development in this culture system generate biologically abnormal progenitors. To eliminate a potentially deleterious impact of MS-5 cells and their secreted factors on iPS-B cell development, initial attempts were made to culture both CD19-selected and CD43-selected day 21 cells in the absence of stroma. By day 14, $CD19^+$ cells could not be detected in the absence of MS-5 support, whilst B cells were observed in parallel cultures with MS-5 cells. Similarly, the co-culture of B cells derived from UCB progenitors in the absence of stroma, resulted in an absence of lymphocytes as described by Sekiguchi and colleagues (Ohkawara et al., 1998). Pro-B cells isolated from human fetal bone marrow could be cultured in the absence of stromal cells, albeit at a reduced frequency when compared to cultures with stromal support (Namikawa et al., 1996). The issues encountered when culturing early stage B cells in the absence of stroma may be due to the requirement for cell-cell interactions. Interestingly, it has been suggested that contacts made between B cells when cultured at high density, may be sufficient to permit the generation of immature B from pro-B cells when stromal cells have been excluded (Ray et al., 1998).

The addition of soluble CD40L, PC and APRIL had no observable effect on the generation of IgM^+ cells at the concentrations described. However, whether iPS-B cells are able to respond to these factors in alternative conditions is unknown. Recent studies suggest that trivalent CD40L is required for B cell activation (Naito et al., 2013). Thus, whether the efficiency of immature B cell generation from iPS-$CD34^+$ cells may be improved by replating onto L cells transfected with CD40L, as described for UCB-B cells, could be investigated (Fluckiger et al., 1998).

When B cells were isolated from day 21 iPS co-cultures using selection of $CD19^+$ cells by MACS, the number of B cells persisting in long term cultures was extremely low. In comparison, when a more heterogeneous $CD45^+$ fraction was enriched, a 4-fold increase in the B cell population was observed. This could either be due to a direct impact of CD19 engagement on B cell viability, or potentially because non-B cells in CD45-enriched cultures are providing positive survival signals. CD19 is a co-receptor of the BCR. Mice deficient in CD19 have a normal bone marrow but abnormal peripheral B cell compartment (Engel et al., 1995). If time had been available for further experiments, this could have been assessed by the addition of the CD19 antibody to CD45 enriched cultures. When B cells were selected from UCB-$CD34^+$/S17 co-cultures by Rawlings and colleagues using CD19 selection and reseeded onto S17 stroma, a reduction in B cell numbers was also observed (Rawlings et al., 1995a). This reduction however appeared to be less dramatic than observed with CD19-selected iPS-derived cells. If, alternatively, this UCB-$CD19^+$ population was cultured with CD40L expressing fibroblasts, the number of B cells increased fivefold (Fluckiger et al., 1998). When mAbs to CD19 were introduced into cultures of mouse fetal liver derived pro-B cells stimulated with LPS, a significant

reduction in IgM secretion was observed (Ray et al., 1998). Here, the authors suggested that antibody binding to CD19 may inhibit cell-cell interactions (Ray et al., 1998). Interestingly, the introduction of a CD19 antibody (1D3) to developing embryos, or to adult mice, resulted in a large reduction of B-1a B cells, but had no significant impact on B-2 B cells (Krop et al., 1996). When the authors assessed the impact of the CD19 antibody on B cells in the presence of BrdUrd, the number of cycling B-1a B cells was affected, with no impact on non-cycling cells (Krop et al., 1996).

When cultures were maintained from day 21 to 43 in the presence of recombinant IL-7, either alone or in combination with Flt3L and SCF, $CD19^{+}IgM^{+}$ cells were not observed. Pilot studies with the addition of neutralising Ab to human and mouse IL-7 resulted in a large reduction in total $CD19^{+}$ cells (Appendix Figure 77). These assays all involved co-culture with murine MS-5 stroma. MS-5 cells have been demonstrated to secrete IL-7 to which human cells are reactive (Johnson et al., 2005, Parrish et al., 2009). These data therefore may suggest a requirement for critical intermediate concentrations of IL-7 for the survival and maturation of iPS-B cells. The role of IL-7 in B cell development has generally been assumed to differ between mice and humans. $IL\text{-}7^{-/-}$ mice have a B-1 and MZ B cell compartment but lack the major B-2 B cell population (Carvalho et al., 2001). Deficiencies in both IL-7 and Flt3L resulted in the complete absence of B cell development (Jensen et al., 2008). In humans, mutations in IL-7Rα are thought to be the third most common cause of SCID; these patients have been described to have an increase in peripheral B cells (Puel et al., 1998). This, however, does not necessarily mean that B cell development is ‘normal’ in humans lacking IL-7Rα.

B cells at various stages of the differentiation pathway appear to differ in their response to IL-7. In murine pro-B and potentially pre-B cells, IL-7 functions to promote proliferation (Claudio et al., 2002, Rolink et al., 2000). Whilst promoting proliferation, high concentrations of IL-7 were described to prevent the differentiation of pre-B cells to immature IgM^+ cells, maturation was observed upon withdrawal of the cytokine (Claudio et al., 2002, Rolink et al., 2000). A role for IL-7 in preventing B cell maturation was also described in B-1 B cells derived from bipotent macrophage-B cell progenitors isolated from the adult mouse bone marrow (Montecino-Rodriguez et al., 2001). In this system, IL-7 was not required for the commitment of bipotent progenitors to the B cell lineage (Kee and Paige, 1996). A mechanism for the role of IL-7 in B cell maturation has been elegantly demonstrated in murine cells. High concentrations of IL-7 prevented rearrangement at the IgK locus due to antagonism of E2A binding, a transcription factor required for light chain recombination (Johnson et al., 2008). The role of IL-7 in the inhibition of *Rag* expression, that may also be E2A-dependent, was also described (Johnson et al., 2008).

IL-7 was required for B cell differentiation from human bone marrow $CD34^+$ cells, but not from UCB-$CD34^+$ cells (Parrish et al., 2009). In agreement with studies in the mouse, IL-7 independent UCB B cells required the presence Flt3L for their generation (Parrish et al., 2009). IL-7 also appeared to stimulate pro-B cell proliferation in humans (Johnson et al., 2005). Interestingly, UCB-$CD34^+$ cultures generated IgM^+ cells in the presence of IL-7, when this cytokine was included at 5ng/ml (Parrish et al., 2009). However, a role for IL-7 in preventing rearrangement at the light chain kappa locus was also described in human B cell populations (Nodland et al., 2011). It is therefore possible that high concentrations of

IL-7 prevent light chain recombination in iPS-B cells and subsequent cell surface expression of IgM.

BALB/c Rag2$^{-/-}$cγ$^{-/-}$ mice were used for *in vivo* studies as, in addition to a deficiency in T and B lymphocytes, these animals lack NK cells (Ito et al., 2002). It has been demonstrated that NK cells can negatively impact upon the reconstitution of human haematopoietic cells (Ito et al., 2002). Whilst being technically difficult, the model that was chosen was the introduction of cells into neonates within 48 hours of birth. The route of administration was either intraperitoneal or intrahepatic. It is generally accepted that the major haematopoietic organs change throughout ontogeny. It has also been demonstrated that YS-derived HPCs can engraft in embryonic but not adult recipients (Yoder et al., 1997b, Yoder et al., 1997a). As iPS-HPCs generated with similar methodologies (to the OP9 co-culture system) had failed to engraft in previous studies, and as RBCs generated from iPS cells predominantly resemble embryonic/fetal erythrocytes, it was hypothesised that haematopoiesis from iPS cells may resemble that occurring in the YS. It was therefore suggested that iPS-B cells might have greater biological similarity with embryonic/fetal B cells than B cells generated from HSCs. With this hypothesis in mind, it seemed appropriate to adopt the approach taken by Yoder and colleagues which described the engraftment of YS-derived B-1 B cells in the peritoneal cavity and spleen of day 1-3 NOG mice (Yoshimoto et al., 2011). As the peritoneal cavity is the major anatomical location for B-1 B cells, intraperitoneal injection was chosen as the route of administration.

iPS-B cells first emerge at around day 12-14 in MS-5 co-cultures, expand, express IgM from day 43 of culture and are then are maintained *in vitro*. For *in vivo* studies, the aim

was to introduce cells that had already become committed to the B cell lineage (assessed by the expression of CD19 and therefore Pax5), but that were early in development and therefore potentially capable of extended continued proliferation (Horcher et al., 2001). The pro-B/pre-B day 21 population was therefore chosen as the $CD19^+$ pool that most accurately fulfilled these criteria. As *in vitro* studies had indicated the potential deleterious effect of isolating iPS-B cells by CD19 enrichment, it seemed prudent to continue with a CD45 enrichment strategy. As $CD19^+$ cells only represented 5-10% of the $CD45^+$ population on day 21, it was therefore desirable to deliver the largest quantity of cells possible, recognising the limitations of injecting into newborn pups. A survey of the literature suggested that $5x10^5$ cells would relate to a safe dose in neonates.

Mice receiving iPS-$CD45^+$ cells did not demonstrate detectable human $CD45^+$ cells in the spleen, bone marrow or peritoneal cavity at week 12. Nor could $CD45^+$ cells be detected in the peripheral blood at weeks 4 or 8. This could have been due to a number of factors. Of the injected population, $CD19^+$ cells were only introduced at 40,000 cells per mouse. iPS-B cells in culture adhere to the stromal layer, making cell-cell contacts. It is possible that when these cells are introduced, either into the circulation or into the volume of the peritoneal cavity, that the lack of these cell-cell contacts might result in loss of viability. If iPS-B cells do indeed resemble murine B-1 B cells, this population would persist by self-renewal. The rate of cell cycling in the B-1 B cell population has been demonstrated to be low, at around 1.3% per day (Deenen and Kroese, 1993, Deenen and Kroese, 1992). If the number of B cells surviving transplantation therefore was low, it is unlikely that a population with a slow self-renewal rate would repopulate the animal with sufficient numbers to be detected using described methodologies. B-2 B cells, excluding memory B-

2 B cells, are also estimated to have low proliferation rates (Macallan et al., 2005). Therefore, if the injected $CD45^+$ population did not include B cell progenitors, the same cell number limitation would also apply. The iPS-$CD45^+$ population included macrophage/monocytes ($CD14^+$) and NK cells ($CD56^+$), neither of which could be detected in week 12 mice. The life span of primitive macrophages is thought to be long as this population is also maintained by self-renewal, whilst monocytes are short-lived (Yona et al., 2013). The ability to detect human myeloid cells on week 12 therefore relates to self-renewal potential, lifespan, *de novo* generation, expansion capacity and viability in the *in vivo* environment. All of which are unknown in this iPS-derived population. Amabile *et al.* recently described the generation of B lymphocytes from human iPS cells *in vivo (Amabile et al., 2012)*. The approach taken involved the introduction of iPS cells, in their pluripotent stem cell state, alongside OP9 stroma which, resulted in teratoma formation (Amabile et al., 2012). B cells could be detected in the teratomas and in haematopoietic tissues, however, $CD19^+$ cells made up c. 1% of $CD45^+$ cells in teratomas, with less than $2x10^4$ $CD19^+$ cells detected in the femoral bone marrow (Amabile et al., 2012). Therefore, whilst B cell lymphopoiesis from iPS cells is possible *in vivo*, the number of cells generated with the teratoma-forming protocol is extremely low. Furthermore, the applications for this approach to model B cell development and disease are limited.

When considering an appropriate cellular comparison for the iPS *in vivo* studies and, considering the technical difficulty of the model described, it seemed appropriate to use a population that is known to reconstitute an animal and therefore repopulate B cell compartments. The gold standard in this regard is the HSC. Umbilical cord blood is a rich source of HSCs that is frequently used in the clinic in the absence of appropriately

matched bone marrow donors. Using UCB as a source of HSCs for research also makes use of a material that is otherwise frequently discarded, whilst the collection of HSCs from bone marrow is an invasive procedure. Therefore, the injection of UCB-HSC/HPCs into sublethally irradiated immunodeficient neonates was chosen as a comparable model for iPS animals, with a particular interest in the repopulation of the B cell pool. As the unpredictable timings of receiving UCB and that of the birth of newborn pups needed to be co-ordinated, transplantations had to be done with UCB cells that had been cryopreserved. I.P was the preferential route of administration for iPS-$CD45^+$ cells, this route of administration was therefore also repeated with UCB-$CD34/CD133^+$ cells. It has been demonstrated that HSC/HPCs, when injected into the peritoneal cavity, did not result in significant levels of engraftment (Liu et al., 2012). An alternative route of administration to permit reconstitution was therefore required. The small size of newborn mice is prohibitory to intravenous or intrafemoral injections so instead, cells were introduced into the liver, a highly vascularised organ.

When UCB-$CD34/CD133^+$ cells were introduced via an intrahepatic injection, human $CD45^+$ cells could be detected on week 12. Human cells however, made up only 0.1% of total splenocytes and bone marrow cells. $1x10^5$ UCB-$CD34/CD133^+$ cells were introduced that had previously been isolated, frozen, thawed and cultured overnight in an appropriate cytokine cocktail. Fewer than $5x10^3$ $CD133^+CD34^+$ cells from uncultured or cultured UCB were required to permit 0.5% reconstitution following intracardiac injection into a similar mouse model (Drake et al., 2011). Similar observations regarding the frequency of repopulating cells in UCB $CD34/133^+$ cells have been made, although engraftment is not 100% effective (McDermott et al., 2010). The limited size of the

experiments described herein prevent the generation of meaningful conclusions. As expected, injection of UCB-CD34/CD133^{+} cells into the peritoneal cavity resulted in a lack of detectable human cells at all timepoints assessed. It has been well reported that some UCB units fail to engraft, whether this was the case for the experiments described herein is unknown (Ballen et al., 2001).

In summary, the research described demonstrated the capacity of iPS-derived B cells to mature and express cell surface IgM. This maturation process appears to be abrogated in the presence of recombinant IL-7, when included at the concentrations described.

Chapter 6.

General Discussion

6.1 Review of the thesis

The aim of this thesis was to investigate the B cell potential of human iPS cells, as well as to determine the origins and potential of the iPS-derived B lymphocytes. The three main questions were: 1) does B cell potential arise from a hemangioblast or haemogenic endothelium-like intermediate population, 2) how do iPS-B cells compare to adult B cells and 3) are iPS-B cells capable of maturing to express cell surface antibodies?

Initially, the establishment of a robust and efficient *in vitro* differentiation system to yield haematopoietic progenitor cells from iPS colonies was required. The OP9 co-culture system has been used by a large number of investigators to promote haematopoietic differentiation from PSCs (Nakano et al., 1994, Vodyanik et al., 2005, Timmermans et al., 2009). Furthermore, Slukvin and colleagues have demonstrated that $CD34^+$ cells from hES/OP9 co-cultures had the capacity to generate B cells when differentiated on MS-5 stroma (Vodyanik et al., 2005). It therefore seemed likely that this culture system would successfully permit B cell differentiation from human iPS cells. This objective was achieved and the work in this thesis contributed to a paper published in 'Blood' which was the first, and currently only, description of *in vitro* human iPS-derived B lymphocytes (Carpenter et al., 2011). Furthermore, iPS-HPCs demonstrated the potential to generate red blood cells and monocyte/macrophages in the co-culture system. Additional

assessment of the functional capacity of iPS-HPCs in the CFU assay demonstrated that continued time in co-culture revealed CFU-GEMM potential, day 9/10 cells lacked this mulitpotentiality which was present in day 22 populations. Both early and late iPS-HPCs generated CFU-G/GM and CFU-E colonies.

Whilst haematopoietic differentiation was robust and efficient using the OP9 co-culture, the factors present, either produced by OP9 cells or present in the supplemented serum, were undefined. Therefore, studies were undertaken to identify a feeder-free and defined culture system to promote haematopoietic differentiation from iPS cell colonies. Research in our laboratory had combined the work of Keller, Murray and colleagues in order to optimise the generation of cardiomyocytes from PSCs in a defined, serum and feeder-free culture (Laflamme et al., 2007, Yang et al., 2008, Carpenter et al., 2012). As cardiomyocytes and haematopoietic cells are both of mesoderm origin, the initial stage of this protocol was adapted and the effect of VEGF, SCF, Flt3L and/or TPO addition was assessed, as these factors are known to be involved in haemato-endothelial differentiation. iPS cells, cultured with Activin A, bFGF and BMP-4 for 4 days, and then for a further 6 days with VEGF, SCF, Flt3L and TPO, generated $CD43^+$ haematopoietic cells. Wnt and Notch signalling are known to be important in haematopoiesis, therefore ligands to stimulate these signalling pathways could also have been assessed (Ruiz-Herguido et al., 2012, Clements et al., 2011, Cerdan and Bhatia, 2010). In the studies described here, $CD34^+$ cells from serum and feeder-free cultures displayed myeloid potential, as demonstrated by the formation of CFU-G/GM colonies in the CFU assay. However, the efficiency of $CD43^+$ cell generation was low, at around 1-2% of the population. Furthermore, in a pilot experiment where both the $CD43^-$ and $CD43^+$ cells were seeded

into the MS-5 co-culture to assay B cell potential, lymphocytes were not generated. As no reports had described PSC-derived lymphocytes in the absence of feeder cells, and, because of time constraints, this work was not progressed. In the remainder of the project, haematopoietic progenitor cells were derived in OP9 co-cultures.

$CD34^+$ cells, isolated from day 10 iPS/OP9 co-cultures, were heterogeneous, subpopulations expressed CD144, tie-2, CD43, KDR and a number of other cell surface markers. To better understand haemato-endothelial differentiation, day 5 to day 22 co-culture populations were analysed. Whilst the proportion of cells expressing a range of haematopoietic and endothelial markers did vary between experimental repeats, the temporal and relative expression patterns were highly reproducible. The expression of CD144, CD34 and CD31 in the absence of haematopoietic markers, was observed first. This was followed by the expression of CD43 and CD41a, before CD45 could be detected. These findings are in accordance with similar analysis performed by Slukvin and colleagues (Choi et al., 2009, Vodyanik et al., 2006). As haematopoietic populations were always observed after the expression of haemato-endothelial markers, it was hypothesised that there might be a direct progenitor-progeny relationship between these two cell types. To assess this further, the expression of haematopoietic markers in relation to haemato-endothelial markers over time was plotted. The presence of $CD144^+CD41a^+$ cells was of interest, as, the expression of CD144 is thought to be restricted to endothelial cells and haematopoietic progenitors. Furthermore, this population was transient and preceded the appearance of $CD144^-CD41a^+$ cells. Of additional interest, emerging $CD45^+$ cells appeared to be largely negative for CD41a and

CD144 which is in contrast to the described phenotype of cells emerging in the AGM (Mikkola et al., 2003, Rybtsov et al., 2011).

As the data described were illustrative and open to multiple interpretations, it was necessary to purify cells to investigate potentiality. $CD34^+$ cells isolated from day 10 co-cultures generated B cells when assayed in the appropriate conditions. The heterogeneous CD34 population was then sub-fractionated based upon CD43 expression, B cell potential was predominantly found in the $CD43^+$ haematopoietic population. Numerous observations suggest that haemogenic endothelium, in mouse, chick, zebrafish and human, may be a transient population (Rafii et al., 2012, Bertrand et al., 2010, Boisset et al., 2010, Kissa and Herbomel, 2010). It was therefore possible that B cell potential may be present in endothelial-like populations that lack haematopoietic markers in co-cultures prior to day 10. The initial pilot experiment to explore this hypothesis was performed by MACS separation due to the inaccessibility of FACS facilities. MACS separation does not yield the 100% cell purities required and therefore the data generated were not conclusive. Day 5, 8 and 22 populations from iPS/OP9 co-cultures were harvested and separated by MACS to generate $CD43/CD45^+$ haematopoietic and $CD43/45^-CD144^+$ endothelial-like populations. Day 5 was selected as a timepoint prior to the observation of a significant $CD144^+haem^+$population, day 8 when $CD144^+haem^+$ cells could be observed and day 22 a timepoint in which $CD144^+haem^+$ cells had been significantly reduced. Populations were then assessed for B cell potential which, after 21 days in MS-5 co-culture, could be identified in both haematopoietic populations but, of the three timepoints assayed, only in the endothelial-like population that had been enriched on day 8.

To build on this observation, it was necessary to FACS purify populations. During the course of these investigations, Slukvin and colleagues published a report describing PSC-derived HE which was distinguished from endothelium based on CD73 expression (Choi et al., 2012). This CD43/CD235a$^-$CD144$^+$CD73$^-$ population was clearly present and was the predominant 'endothelial' population on day 5 of iPS/OP9 co-culture in experiments conducted as part of this research. By day 8, the CD43/CD235a$^-$CD144$^+$CD73$^-$ population was vastly reduced but detectable. When day 22 cultures were assessed, cells with the CD43/CD235a$^-$CD144$^+$CD73$^-$ phenotype were absent. Day 8 cells from iPS/OP9 co-culture were therefore separated into haematopoietic CD43/CD235a$^+$, CD43/CD235a$^-$ CD144$^+$CD73$^+$ endothelial and CD43/CD235a$^-$CD144$^+$CD73$^-$ haemogenic endothelium fractions (Choi et al., 2012). When these populations were assessed for the potential to generate B cells, both the haematopoietic and haemogenic endothelial fractions displayed this capacity. Interestingly, whilst the frequency of B cell potential in wells seeded with HE cells was low, the number of CD19$^+$ cells generated in B cell containing wells was over 80-fold higher for HE than when the equivalent number of haematopoietic cells were seeded. The potential of a haemogenic endothelial-like population to generate T lymphocytes has been recently reported, although the same strict criteria was not applied (Kennedy et al., 2012). This, therefore, represents the first demonstration of B lymphocyte potential from PSC-derived putative haemogenic endothelium. Whilst CD43/CD235a$^-$CD144$^+$CD73$^+$ endothelial cells did not generate haematopoietic progeny in MS-5 co-culture, when cells were alternatively seeded back onto OP9 stroma, a small population of CD45$^+$ cells could be detected. Endothelial cells did generate haematopoietic progeny when seeded at high density into MS-5 co-cultures, however, B cells were never generated from this population.

Another main aim of the thesis was to use B cell potential as a tool to assess the adult vs. fetal similarities of PSC-derived haematopoietic cells, as well as to identify whether iPS-B cells resembled B-1 or B-2 B cells as described in the mouse. Initial attempts were made to profile the controversial human 'B-1' B cell population from UCB using the $CD20^{+}CD43^{+}CD27^{+}$ criteria described (Griffin et al., 2011). Although cells matching this phenotype could be identified, numbers were too low to be used as a comparison to iPS-B cells in the relevant assays. Furthermore, the identity of the B-1 B cell population, based on $CD20^{+}CD43^{+}CD27^{+}$ cell surface phenotype, has frequently been challenged (Covens et al., 2013, Perez-Andres et al., 2011). Therefore, without reliable positive and negative controls for the assays established to probe B-1 B cell associated functionality, this work could not be progressed. An alternative way in which the fetal vs. adult comparison of iPS-B cells could be approached was by the global gene array analysis of the transcriptome. Here, FACS purified $CD19^{+}CD10^{+}$ iPS-B cells were compared to B cells with the same expression profile isolated from adult peripheral blood and umbilical cord blood. Additionally, $CD19^{+}CD10^{+}$ B cells were generated by differentiating UCB-HSC/HPCs ($CD133^{+}CD19^{-}$) in the MS-5 co-culture system for an equivalent period of time. Broadly, this UCB population is also used clinically for transplantation, although some differences in potential have been observed in comparison to bone marrow HSCs. Undifferentiated iPS cells were also included in the gene array. The main conclusion from the analysis of gene array data was that iPS-B cells showed the greatest similarities with UCB-$CD133^{+}$-derived B cells, designated as HSC-B cells, both of which had been generated by co-culture with MS-5 cells. Of the 767 significantly expressed genes, 3 main regions could be observed in the heat map: areas of low expression in iPS cells and high expression in all B cell populations. Secondly, regions of high expression in iPS samples with low expression

in all B cell populations and areas with high expression in iPS cells with a generally low expression in UCB and PB B cell samples. Thirdly, regions of mid to high expression in iPS-B and HSC-B. Although PCA analysis positioned iPS-B and HSC-B samples in close proximity, the populations did not overlap on PC1, the parameter that accounts for the majority of variability. However, overlap of iPS-B and HSC-B samples did occur when PC2 and PC3 were considered. In the comparison of iPS-B and HSC-B there were 52 statistically significant genes with a logFc expression of >1.0 or <-1.0 This was 10-fold lower than when the same criteria were applied in the comparison of HSC-B and UCB B cells. Of the upregulated genes in iPS-B, Lin28b and PDGFRA were notable. Downregulated genes indicated a potentially lower metabolic activity of iPS-B when compared to HSC-B. Differences between HSC-B and UCB B cells revealed numerous genes involved in cell division. As one of the peripheral blood samples failed the quality control assessment, and, the positioning of another by PC1 appeared to show low concordance with the other two samples, the reliability of the PB samples was low. However, both iPS-B and HSC-B clustered more closely to the remaining peripheral blood B cells than to umbilical cord B cells. This however is likely to be an artefact of the experimental design rather than a true biological difference. This is because the sorting strategy employed was insufficient to exclude immature B cells from umbilical cord samples which would not normally be present in the circulation and therefore peripheral blood. Overall, iPS-B cells showed a high level of similarity with UCB-HSC/HPC-derived B cells.

The third major question in the thesis was whether iPS-derived B cells could mature to express cell surface antibodies. This is an important developmental stage in B cell

differentiation as maturation requires the recombination of V, D and J gene segments to form both heavy and light chains. The aim was to assess this both *in vitro* and *in vivo*. On day 21 of iPS-CD34$^+$/MS-5 co-culture, CD19$^+$ cells have a pre-B cell phenotype (Carpenter et al., 2011). As B cell maturation from non-PSC human B cell populations has been infrequently described, there was no obvious culture system to employ. After initial experiments to culture iPS-B cells in the absence of feeder cells resulted in the loss of this population, the approach taken was to add candidate factors to the MS-5 cultures after the generation of pre-B cells. An additional complication that arose during the course of these experiments was that iPS-B cells, when isolated based on CD19 expression by MACS, appeared to be non-viable as assessed after a further 21 days in co-culture (0.007 CD19$^+$ cells were recovered after 21 days of culture per CD19$^+$ cell seeded). When the heterogeneous CD45$^+$ population, that included CD19$^+$ cells was isolated on day 21 of MS-5 co-culture and reseeded onto MS-5, the B cell population persisted and expanded (over 4-fold expansion). IgM is the first antibody to be produced in developing B cells. It is expressed on the cell surface of immature B cells which then, in the adult, leave the bone marrow environment and undergo class-switching to express alternative Ig isotypes. IgM expression was not detected on day 35 of culture, nor was it detected on day 42 when recombinant IL-7 was included in the media. However, when recombinant IL-7 was excluded from the media in the later stages of B cell cultures, IgM expression could be consistently detected on iPS-derived B cells. In an attempt to understand the effect of IL-7 in these cultures various other parameters were assessed. There was no statistically difference in the number of CD19$^+$ cells in the presence of different cytokine regimes. Whilst the inclusion of all three factors appeared to increase the total cell number, this effect was not observed when IL-7 was added alone. A statistical difference was observed

when the number of non-viable cells was assessed, in cultures with IL-7 alone or in combination with SCF and Flt3L the number of non-viable cells increased. This non-viable population however only represented a small proportion (<5%) of the total population. Only 3.74% (mean ± 1.4 SD) of the $CD19^{+}$ population expressed IgM in these conditions. However, this was comparable with efficiencies observed with B cells derived from UCB-HSC/HPCs ($CD133/CD34^{+}$) cells. VDJ recombination was then confirmed by PCR. This was the first demonstration of antibody expression in human PSC-derived cells.

A pilot experiment was run to assess the potential of iPS-B cells to expand and mature in neonatal immunocompromised mice. Previous attempts by other groups to promote haematopoietic engraftment with progenitor cells derived from PSC/OP9 co-culture had been unsuccessful (Tian et al., 2009, Wang et al., 2005a). As the literature describing an *in vivo* model of B cell adoptive transfer was limited, a system described by Yoder and colleagues which demonstrated the capacity of mouse yolk-sac B cells to expand and differentiate was employed (Yoshimoto et al., 2011). Day 21 iPS $CD19^{+}$ B cells in a heterogeneous $CD45^{+}$ population containing $CD14^{+}$ macrophage/monocytes and $CD56^{+}$ NK cells were injected into the peritoneal cavity or liver of sublethally irradiated BALB/c $Rag2^{-/-}c\gamma^{-/-}$ mice within 72 hours of birth. Human cells could not be detected in the peripheral blood or the haematopoietic organs upon sacrifice at week 12. Additionally, when UCB-$CD133^{+}$ cells were introduced by either I.P or intrahepatic injection in the same model, high level reconstitution was not observed. These experiments were carried out with a single UCB CD133/CD34 preparation. Due to time and resource limitations, this work was not progressed.

6.2 Future work

Research and knowledge of the haematopoietic potential of pluripotent stem cells has advanced rapidly over the last decade. However, the generation of a PSC-derived HSC still evades researchers in the field. In this thesis, the capacity of putative haemogenic endothelium (HE), as described by a CD43/CD235a^{-}CD144^{+}CD73^{+} phenotype, to generate B lymphocytes was described for the first time. The questions that arise from these studies are numerous. Firstly, it is important to determine whether a single cell, and/or a single HE cell, has multilineage potential. This would optimally be achieved by demonstrating myeloid, as well as both T and B cell potential. The culture conditions required for the simultaneous generation of both T and B cells may be difficult to achieve. This could be attempted by a brief differentiation phase in which a single HE cell gives rise to a haematopoietic cell that then proliferates before progeny are transferred to separate B cell and T cell permissive conditions. An alternative system may be to seed HE cells onto stroma that is composed of regions of MS-5 stroma and regions of inducible MS-5 stroma that express the Notch ligand Delta-like 1, which has been shown to support T cell differentiation (Calvo et al., 2012, Timmermans et al., 2009, Kennedy et al., 2012). Such a co-culture system could permit the sequential differentiation of both lymphocyte populations, as has recently been described for the differentiation of UCB-derived progenitors (Calvo et al., 2012). The cell surface phenotype and transcriptome of the haematopoietic population immediately after EHT should be assessed. Day 8 HE had the potential to yield B cells, which was also found in the committed CD43/235a^{+} haematopoietic fraction. Whether the entirety of the B cell potential within the culture system can be attributed to an HE population origin should be investigated. A major question arising from this work relates to the frequency of cells within the HE fraction

with B cell potential. If, as these preliminary results suggest, B cell potential frequency in the HE fraction is low, this would suggest a level of heterogeneity in the population. Alternatively, different haematopoietic populations may arise from homogeneous HE populations in relation to the intensity, identity and order of environmental signals. Indeed, numerous EHT events are observed in the dorsal aorta and other haemogenic sites, yet it has been estimated that the E11.5 embryo only contains between 3 and 10 HSCs (Kumaravelu et al., 2002). A level of HSC expansion is thought to arise from continued pre-HSC differentiation; this number therefore may not represent the number of HE cells which are capable of generating HSCs (Rybtsov et al., 2011, Taoudi et al., 2008). Therefore, it would be of interest to determine if, in the *in vivo* situation, a subset of HE has HSC potential or, alternatively, if HE differentiation potentials are equal until haematopoietic cells are generated, which then subsequently become influenced by environmental factors. This experimental question is difficult to investigate. Single cell plating of HE cells from the dorsal aorta or PSC sources, with exposure to the same signals, may help to advance such an understanding. Of equal interest to the frequency of HE cells with B cell potential is the magnitude of the yield of B cells and other haematopoietic cells from a single HE cell. The low frequency of putative HE with B cell potential but high cell numbers produced (greater than 80-fold enrichment in $CD19^+$ cells from HE as compared to haem) suggests that a limited number of progenitor cells may be able to give rise to a large number of B cell progeny. This is most easily assessed at the single cell level, however if paracrine factors are required, a cell labelling approach could be undertaken where a single labelled cell is seeded amongst equivalent non-labelled cells.

Another factor of interest is the point at which a population with an HE phenotype, that has B cell differentiation potential, can be detected and furthermore, how this population differs from cells with the same phenotype that exist earlier on in culture and lack B cell potential. A high level of variability in the proportion of the day 8 HE population within the $CD34^+$ fraction was observed. This may relate to iPS colony seeding density, colony size upon seeding or potentially reflect a difference due to the number of hours of co-culture differentiation prior to harvesting. These parameters could be investigated in turn to elucidate a more robust system for downstream application. As a small number of $CD43/235a^-CD144^+CD73^+$ 'endothelial-like' cells generated $CD45^+$ cells when co-cultured with OP9 stroma, this cell surface phenotype does not completely exclude haematopoietic potential. Whilst the segregation of the endothelial population based on the expression of CD73 was a useful designation to separate cells with B cell potential in the assays described, further investigation is required to define markers which effectively distinguish HE and non-haemogenic endothelium. Furthermore, whether CD73 expression can be detected in the ventral dorsal aorta wall should be assessed.

If additional time had been available, the differential gene expression of PDGFRA and Lin28b should have been confirmed by qRT-PCR. The differential expression of these genes that are upregulated in iPS-B in comparison to HSC-B is of interest. The cell surface expression of PDGFR-α on iPS-B cells should also be assessed by flow cytometry or *in situ* staining. The link between PDGFRA expression, paraxial mesoderm and the cardiac vs. haematopoietic lineage has frequently been disputed in the literature and should be investigated. The expression of Lin28b is also an interesting point of investigation. The levels of Lin28b mRNA in long term iPS cultures, either in iPS-B or of iPS-HPCs should be

measured to determine whether levels are downregulated. Data from mouse *in vivo* developmental models suggest that the first and second definitive waves of haematopoiesis are autonomous, in that multipotent HPCs do not differentiate to form HSCs but that these cells arise *de novo* from an HE population. It is therefore unlikely that iPS-HPCs with B cell, and possibly multipotent potential are able to mature to produce HSCs. The expression of Lin28b in iPS-derived HPCs and differentiated haematopoietic subsets could possibly be used as a marker of fetal haematopoiesis. The absence of high Lin28b levels could be used to screen for the second wave of definitive haematopoiesis, if it is possible to generate such a population. Another approach that could be taken is to decrease Lin28b levels by overexpressing let-7 miRNAs. Whether this may induce a switch in iPS-HPC potential is a hypothesis that could be pursued. Alternative conditions for the culture of these modified iPS-HPCs may also be required such as co-culture with human fetal-liver derived stroma and endothelium.

The question as to whether iPS-B cells can repopulate *in vivo* haematopoietic sites remains to be determined. This approach may represent the most relevant readout for a human B-1 vs. B-2 population in analogy with cells identified in the mouse. Whilst xenogeneic models may be inappropriate for assessing numerous biological questions, the ability of human haematopoietic cells to respond to the mouse environment, such as homing to the bone marrow and spleen, indicates conserved molecules and mechanisms. The restricted viability of mature human B cell populations in immunodeficient mice for a two week period has been reported (Wagar et al., 2000). $CD19^{+}$ cells from human peripheral blood required the addition of recombinant BAFF (B cell activating factor) to enable initial and maintainable B cells numbers in the spleen of NOD/Cg-

Rag1^{tm1Mom}Ppf^{tm1Sclz}/SzJ mice (Schmidt et al., 2008). Intrasplenic, intrafemoural or intraperitoneal injection of iPS-B cells into adult immunodeficient mice may enable long term contribution to haematopoietic sites, but the lack of data supporting such an approach suggests that that this may not be robust, even with a non-iPS B cell populations. Instead, the intrafemoral injection of iPS-derived HPCs may be the more amenable to engraftment, although it is unlikely that the day 10 CD34$^+$ population from iPS/OP9 co-cultures would display such a potential.

The capacity of iPS-B cells to express IgM was explored in Chapter 5. Over long term culture a small fraction (3.74% ± 1.4 SD) of iPS-B cells mature to express cell surface antibodies, with comparable efficiencies to that of B cells generated from UCB-CD133/CD34$^+$ cells. When recombinant IL-7 was added to iPS-B/MS-5 co-cultures from day 21 to 53, IgM$^+$ cells were not detected. MS-5 cells have been demonstrated to produce IL-7 to which human cells are reactive (Johnson et al., 2005, Parrish et al., 2009). Initial experiments, where neutralising antibodies to murine IL-7 were included, resulted in a large reduction in the total CD19$^+$ population, and these experiments should be repeated. Research in both human and mouse B cell populations suggests that high concentrations of IL-7 prevent light chain recombination which is required for the expression of IgM (Nodland et al., 2011, Johnson et al., 2008). It is likely that this mechanism is also relevant in this system and a similar approach could be taken to confirm this, as has been described by such reports. It has been hypothesised that, in the *in vivo* environment, developing B cells will migrate away from the bone marrow stromal cells that produce high levels of IL-7, which subsequently enables maturation (Johnson et al., 2008). The IL-7 concentration could be titrated over time *in vitro* to promote optimal

maturation. A simpler approach may be to analyse the population for heavy chain recombination events and then switch iPS-B cells at this point to an alternative culture system where IL-7 expression is low or absent. This may be similar to the culture system used by Rawlings and colleagues in which the efficiency of UCB-B cell IgM expression was reduced until cells were replated onto fibroblasts expressing CD40L (Rawlings et al., 1995a). A greater yield of iPS IgM^+ B cells would enable investigation into the functionality of more differentiated populations, including whether iPS-B cells are able to respond to T cell help. Alternatively, iPS-B cells may be more responsive to bacterial polysaccharides such as LPS, that do not require co-stimulation. In the fibroblast-CD40L culture, a small proportion of cells were observed to express IgD (Rawlings et al., 1995a). Whether iPS-derived B cells are capable of undergoing class-switching to express alternative isotypes may be an informative assay to investigate a B-1 versus B-2 B cell phenotype. An *in vitro* reconstruction of splenic stroma and, possibly, addition of other haematopoietic subtypes such as macrophages, may enable this. Interestingly, when iPS-B cell populations were selected based on CD19 expression, the number of viable B cells at later timepoints was greatly reduced in comparison to CD45-selected populations. This could be because CD19 engagement is adversely affecting B cell viability or, alternatively, because the accessory haematopoietic cells that are isolated during CD45 enrichment are not present in sufficient number to support B cell populations. This should be investigated by treating CD45-selected cultures with an antibody to CD19. Whereupon, if B cell populations persist, the haematopoietic subpopulation that permits B cell growth in long-term *in vitro* cultures could be investigated. Interestingly, Uckun *et al.* described the apoptotic effect of CD19 ligation in a number of ALL cell lines and primary leukemic cells (Uckun et al., 2011). Whether the selection of UCB-B cells, generated from the HSC/HPC

population in the same conditions, are also adversely affected by CD19 selection could also be investigated.

The generation of antibody-expressing B cells from induced pluripotent stem cells may provide a new route for the production of therapeutic human antibodies. In this context, B cells from patients with rare antibody-mediated immunity to complex diseases could be reprogrammed to generate iPS cells, which can then be expanded exponentially. This technology could offer further benefit as secreted antibodies would have undergone human-specific glycosylation and other post-translational modifications. Initially, mouse B cells were reprogrammed using somatic nuclear transfer (SNT) (Hochedlinger and Jaenisch, 2002). Mature mouse B cells have been successfully reprogrammed using the iPSC method, which generated cells that retained their unique recombined VDJ region (Hanna et al., 2008). This was achieved using an inducible system, initially with cells derived from fibroblast, due to the problems encountered when lymphocytes are a cell source for reprogramming (Hanna et al., 2008). Reprogramming of class-switched mouse B cells has also been described (Wesemann et al., 2012). In contrast, the generation of iPS cells from human B cells has not yet been reported. iPS cells however, have been successful derived from human EBV (Epstein-Barr Virus) immortalised B cell lines (Choi et al., 2011b). Future work should build on the advancement described here, by reprogramming a range of clonal human B cell populations to the iPS cell stage, and then differentiating these iPS cell lines to generate antibody-expressing B cells. Whether B cells generated from these B cell-derived iPS cells would then express the same antibodies as found in the starting cell population, as would be expected, and as described in the mouse SNT experiments, should be assessed (Hochedlinger and Jaenisch, 2002). This

approach has been described with T lymphocytes, initially with mouse cells, and then latterly using human T cell populations (Serwold et al., 2010, Nishimura et al., 2013).

In summary, future work should investigate the frequency and magnitude of B cell potential in iPS-derived putative HE, the relevance of Lin28b expression in iPS-B cells and the capacity of immature B cells to undergo isotype switching and respond to biologically relevant stimuli. Indirect advancement of the findings of this thesis include the generation of iPS lines from patients with pathologies such as ALL and a comparison of B cell development within this *in vitro* system.

6.3 Conclusion

In conclusion, the capacity of B lymphocytes that are derived from human iPS cells to express cell surface antibodies has been described for the first time. This suggests that iPS-B cells follow a similar maturation pathway to that described for human and mouse B cell differentiation. The inhibitory role of IL-7 signalling in the generation of IgM^+ cells suggests further similarities with adult mouse bone marrow B cell and human cord blood B cell development (Nodland et al., 2011, Johnson et al., 2008). The ability to generate antibody expressing B cells from iPS colonies, and therefore from any cell of the body, may provide a system to assess key integral biological processes, such as VDJ recombination, as well as human pathologies such as ALL. Furthermore, when iPS-B cells were compared by global analysis of the transcriptome to B cells derived in the same conditions from an HPC population that typically contains HSCs, gross similarities were observed. Of the 47 genes that were significantly differentially expressed with log Fc > or < 1.0, Lin28b mRNA was detected at high levels in iPS-B and not HSC-B. The expression of this and the other differentially expressed genes may provide an insight into the differences between adult and fetal haematopoiesis or into how haematopoiesis from pluripotent stem cells differs from that of naturally derived progenitors. Additionally, this work describes the capacity of putative haemogenic endothelial, as defined by the strictest current criteria, to generate B lymphocytes. This has not previously been reported. This progresses both understanding of the haematopoietic potential of pluripotent stem cells as well as providing a model system to probe developmental haematopoiesis more broadly.

7 Appendix I

Table 17 Expression of haemato-endothelial markers over time in iPS/OP9 co-cultures.

Cell surface marker	Timepoint (day)	Mean	SD
$CD34^+$	5	1.4	0.7
	12	6.9	1.5
	22	6.0	3.2
$CD43^+$	5	0.0	0.1
	8	3.0	0.6
	22	3.6	1.4
$CD45^+$	8	0.1	0.2
	14	1.9	0.2
	22	17.5	0.9

C18 or C19 iPS cell colonies were seeded onto OP9 stromal cells to promote haemato-endothelial differentiation. Cultures, both adherent and non-adherent cells were harvested at regular time intervals and the expression of cell surface markers was assessed by flow cytometry. The expression of CD34 was observed before CD43 could be detected. Furthermore, the expression of CD43 preceded that of CD45.

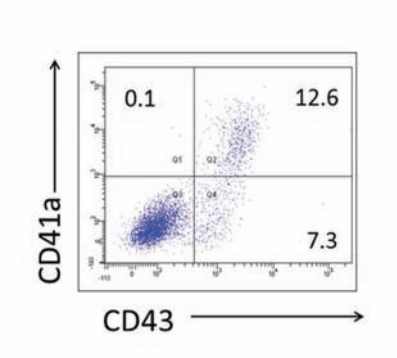

Figure 74 CD41a$^+$ cells on day 8 populations from iPS/OP9 co-cultures are CD43 positive.
C18 or C19 iPS colonies were differentiated on OP9 stromal cells for 8 days before cells were harvested, stained with mAbs and analysed by flow cytometry. CD41a$^+$ cells were homogeneously CD43$^+$. Representative image, n=3.

Table 18 Analysis of the co-expression of haematopoietic and haemato-endothelial markers in iPS cell-derived populations when differentiated on OP9 stromal cells.

Phenotype	Timepoint (day)	Mean	SD
$CD144^{+}CD41a^{-}$	5	2.3	0.5
$CD144^{+}CD41a^{+}$	5	0.0	0.0
$CD144^{-}CD41a^{+}$	5	0.0	0.0
$CD144^{+}CD41a^{-}$	6	3.5	0.9
$CD144^{+}CD41a^{+}$	6	0.1	0.1
$CD144^{-}CD41a^{+}$	6	0.0	0.0
$CD144^{+}CD41a^{-}$	8	4.7	1.1
$CD144^{+}CD41a^{+}$	8	1.2	0.6
$CD144^{-}CD41a^{+}$	8	1.4	0.7
$CD144^{+}CD41a^{-}$	12	3.1	0.2
$CD144^{+}CD41a^{+}$	12	0.4	0.1
$CD144^{-}CD41a^{+}$	12	2.7	1.1

Phenotype	Timepoint (day)	Mean	SD
$CD34^{+}CD43^{-}$	5	1.8	0.8
$CD34^{+}CD43^{+}$	5	0.0	0.0
$CD34^{-}CD43^{+}$	5	0.0	0.0
$CD34^{+}CD43^{-}$	6	3.1	1.1
$CD34^{+}CD43^{+}$	6	0.2	0.2
$CD34^{-}CD43^{+}$	6	0.0	0.0
$CD34^{+}CD43^{-}$	8	6.8	2.8
$CD34^{+}CD43^{+}$	8	1.6	0.9
$CD34^{-}CD43^{+}$	8	0.7	0.3
$CD34^{+}CD43^{-}$	12	8.7	0.8
$CD34^{+}CD43^{+}$	12	2.6	1.0
$CD34^{-}CD43^{+}$	12	2.7	1.6

C18 or C19 iPS cell colonies were seeded onto OP9 stromal cells to promote haemato-endothelial differentiation. Cultures, both adherent and non-adherent cells were harvested at regular time intervals and the expression of cell surface markers was assessed by flow cytometry. The co-expression of haematopoietic cell surface markers, CD41a and CD43 was analysed with respect to the expression of the haemato-endothelial markers CD144 and CD34. $CD144^{+}CD41a^{-}$ cells were detected before $CD144^{+}CD41a^{+}$ cells, which preceded the $CD144^{+}CD41a^{+}$ cell population. Similarly, $CD34^{+}CD43^{-}$ cells were detected before $CD34^{+}CD43^{+}$ cells, which preceded the $CD34^{+}CD43^{+}$ cell population.

Table 19 Analysis of the co-expression of early and late haematopoietic markers in iPS cell-derived populations when differentiated on OP9 stromal cells.

Phenotype	Timepoint (day)	Mean	SD
$CD144^{+}CD45^{-}$	10	4.2	1.9
$CD144^{+}CD45^{+}$	10	0.1	0.1
$CD144^{-}CD45^{+}$	10	0.0	0.1
$CD144^{+}CD45^{-}$	14	2.4	0.6
$CD144^{+}CD45^{+}$	14	0.3	0.2
$CD144^{-}CD45^{+}$	14	1.6	0.5

Phenotype	Timepoint (day)	Mean	SD
$CD41a^{+}CD45^{-}$	10	5.1	0.9
$CD41a^{+}CD45^{+}$	10	0.0	0.0
$CD41a^{-}CD45^{+}$	10	0.0	0.1
$CD41a^{+}CD45^{-}$	14	4.3	3.4
$CD41a^{+}CD45^{+}$	14	0.2	0.1
$CD41a^{-}CD45^{+}$	14	1.6	0.6

C18 or C19 iPS cell colonies were seeded onto OP9 stromal cells to promote haemato-endothelial differentiation. Cultures, both adherent and non-adherent cells were harvested at regular time intervals and the expression of cell surface markers was assessed by flow cytometry. The co-expression of early (CD43, CD41a) and late (CD45) haematopoietic markers was assessed. $CD45^{+}$ cells on day 14 are mainly $CD144^{-}$ and $CD41a^{-}$.

A

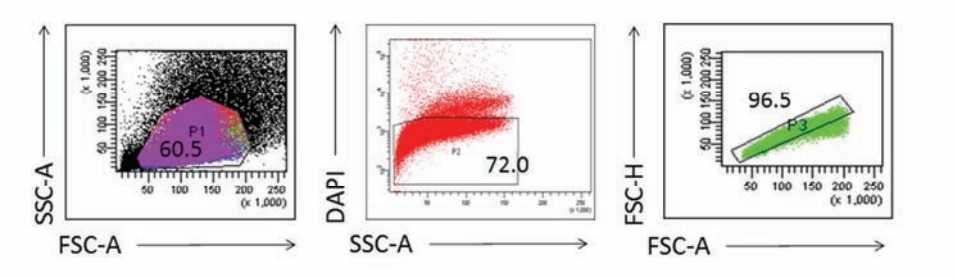

B

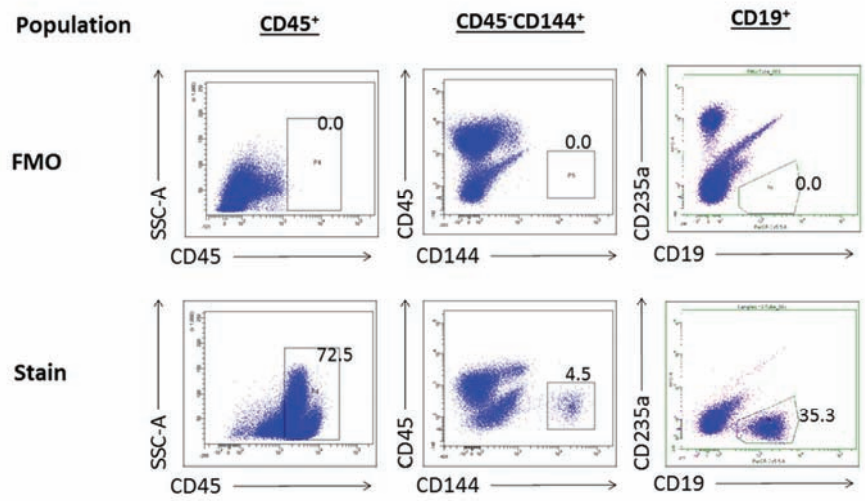

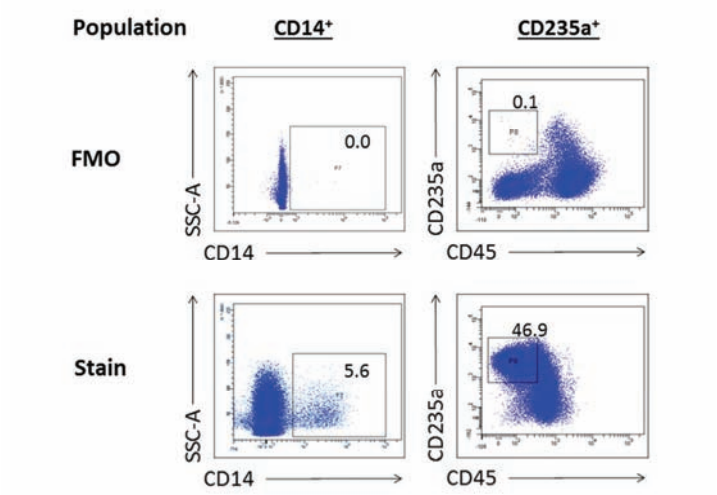

Figure 75 Flow cytometry gating approach for the analysis of haematopoietic and endothelial populations in day 19 iPS-CD34$^+$/MS-5 co-cultures.

CD34$^+$ cells were enriched by MACS from day 10 C19 iPS/OP9 co-cultures and seeded onto confluent MS-5 cells with cytokine supplementation. Cultures were maintained for 19 days, harvested and stained with mAbs for analysis by flow cytometry. (A) Gate setting for the analysis of live, singlet cells. (B) Gates were set using FMO controls to identify CD45$^+$, CD19$^+$, CD45$^-$CD144$^+$, CD14$^+$ and CD235a$^+$ cells.

Table 20 Analysis of the expression of CD34, CD43 and CD10 on diverse B cell populations.

Population	Marker	Mean (%)	SD
iPS-B	$CD34^+$	3.2	2.0
iPS-B	$CD43^+$	98.3	0.7
iPS-B	$CD10^+$	97.2	2.3
UCB-$CD133^+$ B	$CD34^+$	5.6	8.5
UCB-$CD133^+$ B	$CD43^+$	96.4	3.5
UCB-$CD133^+$ B	$CD10^+$	98.0	1.5
UCB B	$CD34^+$	0.5	0.3
UCB B	$CD43^+$	5.8	3.2
UCB B	$CD10^+$	27.6	11.9

B cells were derived from iPS cells (iPS-B) by co-culture with OP9 cells for 10 days, enrichment on $CD34^+$ cells and culture with MS-5 stroma for a further 21 days. B cell populations were also derived from UCB^-CD133^+ cells by a 21 day co-culture with MS-5 stroma (UCB-$CD133^+$ B). $CD19^+$ cells were also isolated from fresh or frozen umbilical cord blood mononuclear cells (UCB B). Cells were stained with mAbs for analysis by flow cytometry. iPS-B cells were predominantly $CD34^-$ $CD43^+CD10^+$, as were UCB-$CD133^+$ B cells. In contrast, UCB B cells were $CD34^-CD43^-$ $CD10^{+/-}$. n=3 independent experiments.

Table 21 iPS-B cells downregulate the expression of CD43 with continued culture.

Population	Marker	Experiment number	Mean (%)
iPS-B	$CD43^+$	n=1	2.7
iPS-B	$CD43^+$	n=2	2.2
iPS-B	$CD10^+$	n=1	99.6
iPS-B	$CD10^+$	n=2	99.7

iPS B cells express a $CD34^-CD43^+CD10^+$phenotype when isolated from day 21 iPS-$CD34^+$/MS-5 co-cultures. When $CD45^+$ cells are reseeded and cultured with MS-5 cells for a further 21/22 days, cells downregulate the expression of CD43. n=2 independent experiments.

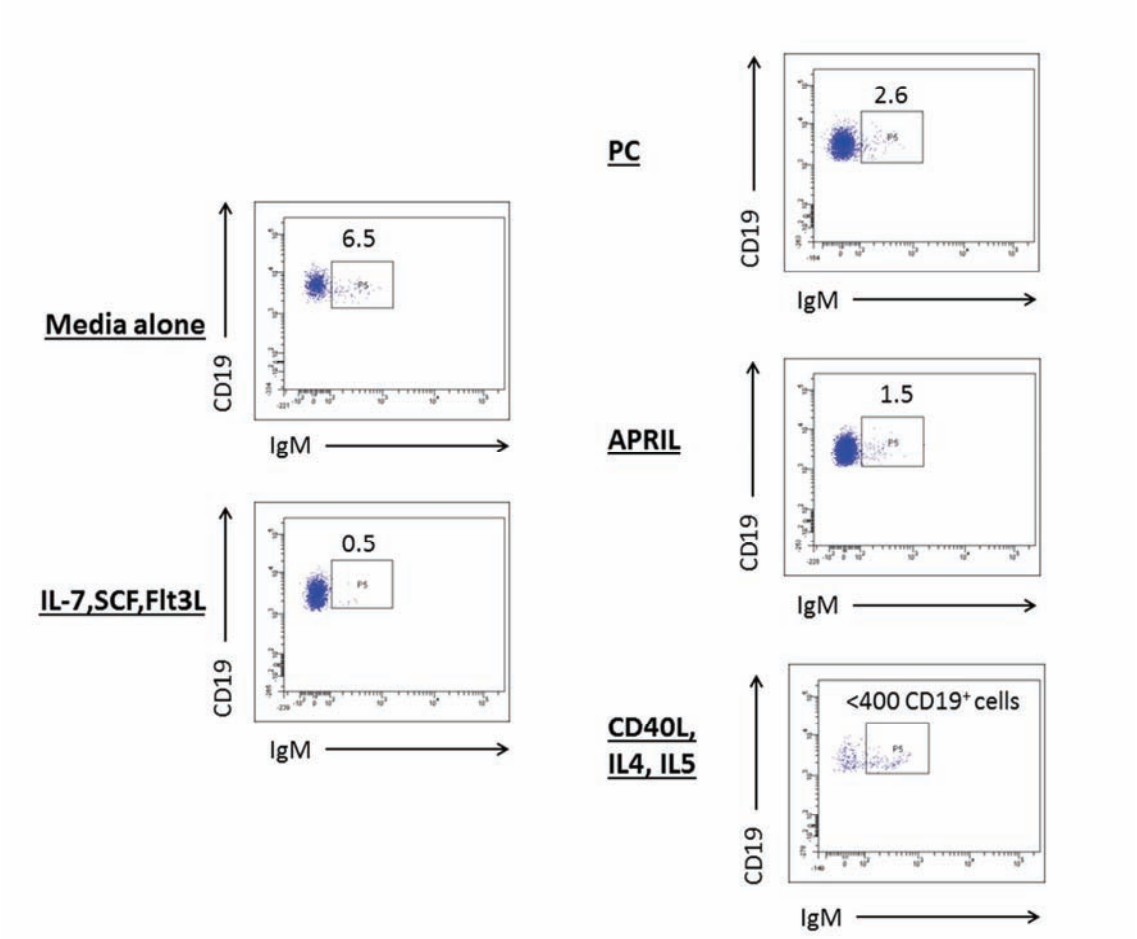

Figure 76 Addition of PC or APRIL does not improve the efficiency of IgM$^+$ cell generation from iPS-derived CD19$^+$IgM$^-$ B cells.

iPS-CD45$^+$ cells, generated after 21 days of iPS-CD34$^+$ culture with MS-5 cells, were seeded onto fresh MS-5 stroma and cultured for an additional 22 days. Media alone or combinations of cytokines were added to cultures from day 21. Day 43 cells were harvested, stained with mAbs and analysed by flow cytometry. The addition of phosphorylcholine (PC) or APRIL did not improve the efficiency of B cell maturation, as assessed by the proportion of CD19+ cells expressing IgM. When CD40L,IL-5 and IL-4 were included in cultures, the number of B cells detected on day 43 was decreased. N=1 for PC, April and CD40L/IL-4/IL-5 experiments.

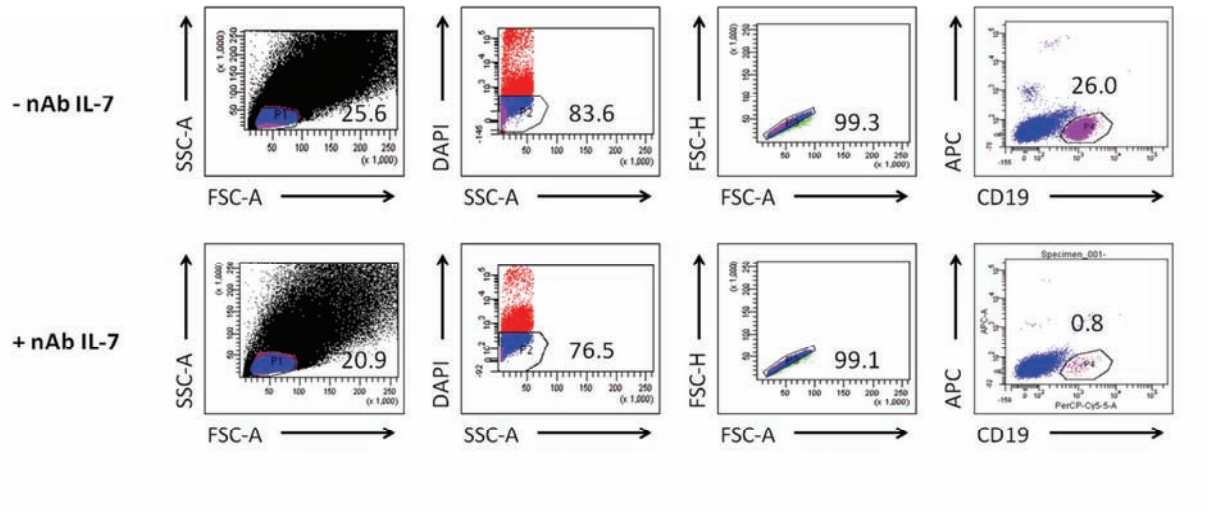

Figure 77 The addition of IL-7 neutralising antibody causes a reduction in total B cell numbers. Neutralising antibodies (nAb) to murine and human IL-7 was added at 10 µg/ml to iPS-CD45^{+}/MS-5 co-cultures. After a further 21/22 days of co-culture, cells were harvested and analysed by flow cytometry. The addition of nAbs caused a large reduction in the percentage of total CD19^{+} cells, when compared to cultures where nAbs were not added. n=2 independent experiments.

A

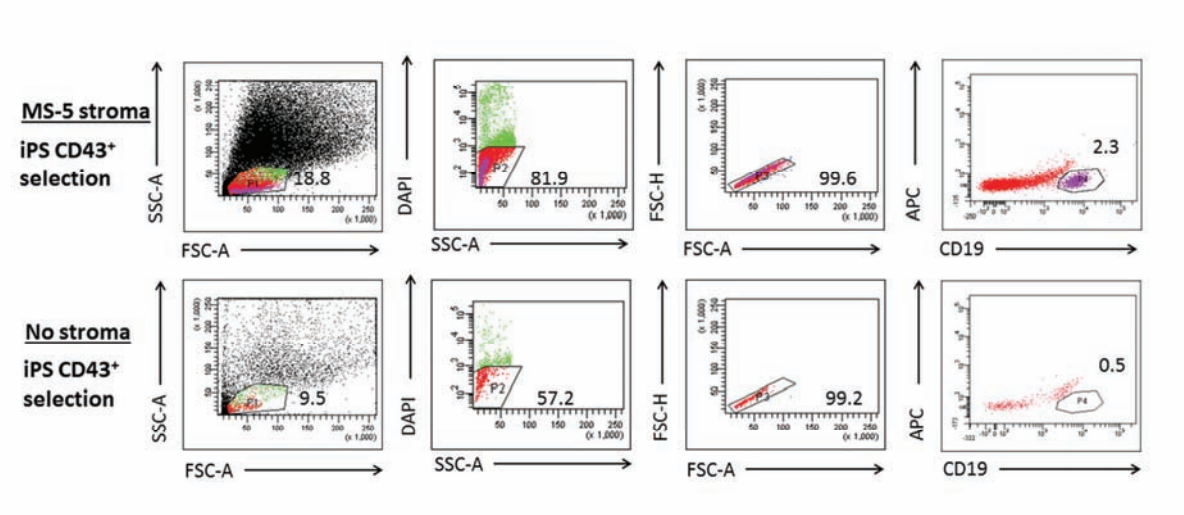

B

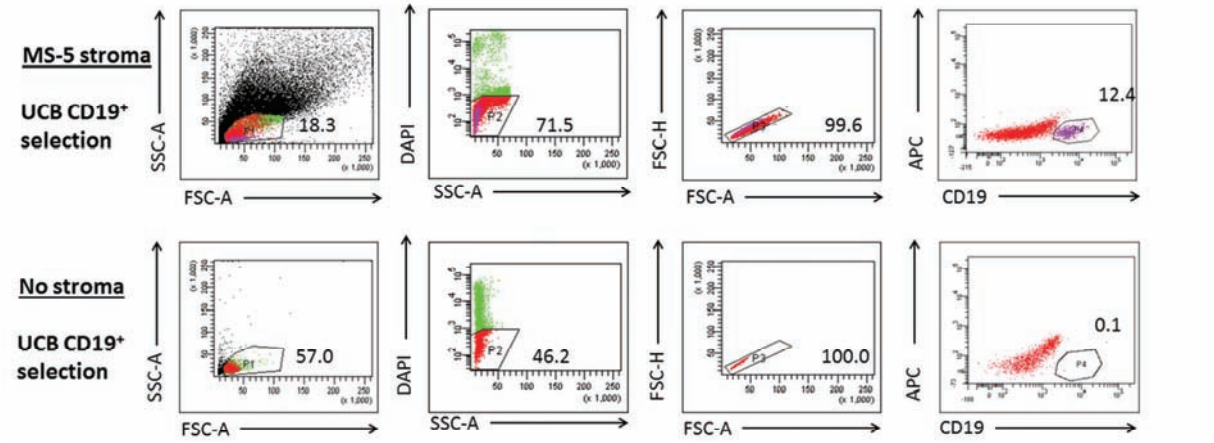

Figure 78 B cells generated on MS-5 stroma from iPS or UCB cell sources are non-viable in stromal-free cultures.

(A) iPS-CD43$^+$ cells, enriched from day 21 iPS-CD34$^+$/MS-5 co-cultures, were seeded in the presence or absence of MS-5 stroma in Differentiation media or RPMI media supplemented with 10% serum. Cultures were maintained for 21/22 days, harvested and analysed by flow cytometry. In the presence of MS-5 stromal cells, CD19$^+$ cells could be detected. The CD19$^+$ population was absent from cultures without MS-5 stromal cells. (B) UCB-derived B cells, enriched from day 21 UCB-CD133$^+$/MS-5 cultures, were seeded in the presence or absence of MS-5 stroma. After 21/22 days of culture, CD19 cells could be detected in cultures containing MS-5 cells but not in stromal-free cultures. (A) n=2 independent experiments, (B) n=1 independent experiment.

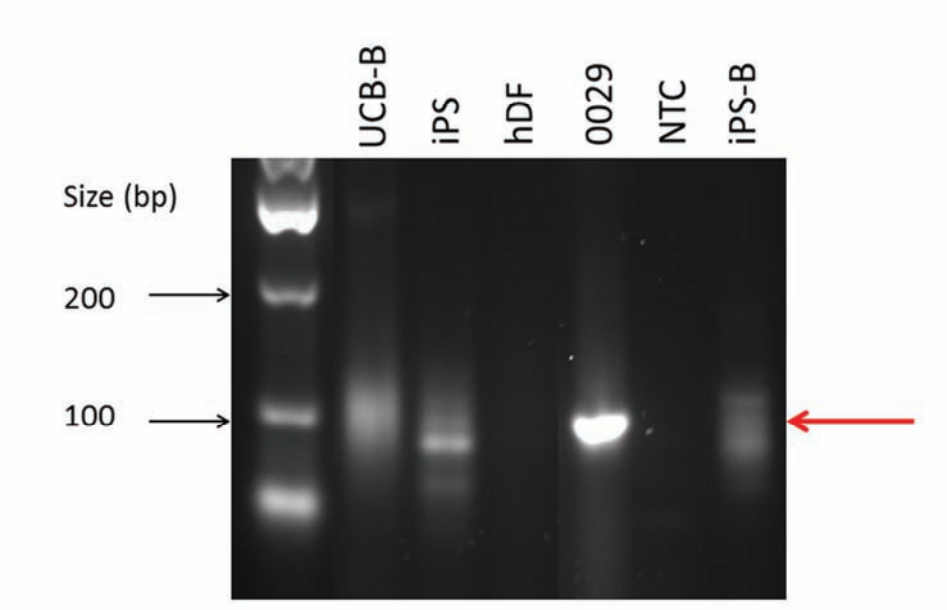

Figure 79 iPS-B cells have a recombined VDJ region at the IgH loci, as assessed using FR3 primers.

Genomic DNA was isolated from day 43 iPS-CD34^{+}/MS-5 co-cultures (iPS-B) and day 43 UCB-CD34^{+}/MS-5 co-cultures (UCB-B) that contained IgM^{+} cells. hDFs and undifferentiated iPS cells (iPS) were also included in addition to the no template control (NTC).The 0029 clonal control was also included which should produce a 104 bp product when FR3 primers are used for amplification. PCR reactions were run using FR3 and JH consensus primers for 37 cycles. PCR products were run on a 2% agarose-TBE gel with gel red and visualised with UV light. Recombined VDJ regions are expected to produce 69-129 bp products. Bands within this region could be observed in both iPS-B and UCB-B, as well as the 0029 positive control. The hDF samples, as expected, did not produce a band in this region. A band could be seen however in undifferentiated iPS (iPS) samples.

7.1 References

ADOLFSSON, J., MANSSON, R., BUZA-VIDAS, N., HULTQUIST, A., LIUBA, K., JENSEN, C. T., BRYDER, D., YANG, L., BORGE, O. J., THOREN, L. A., ANDERSON, K., SITNICKA, E., SASAKI, Y., SIGVARDSSON, M. & JACOBSEN, S. E. 2005. Identification of Flt3+ lympho-myeloid stem cells lacking erythro-megakaryocytic potential a revised road map for adult blood lineage commitment. *Cell,* 121**,** 295-306.

AKASHI, K., TRAVER, D., MIYAMOTO, T. & WEISSMAN, I. L. 2000. A clonogenic common myeloid progenitor that gives rise to all myeloid lineages. *Nature,* 404**,** 193-7.

ALLMAN, D. & PILLAI, S. 2008. Peripheral B cell subsets. *Curr Opin Immunol,* 20**,** 149-57.

ALLSOPP, R. C., CHESHIER, S. & WEISSMAN, I. L. 2001. Telomere shortening accompanies increased cell cycle activity during serial transplantation of hematopoietic stem cells. *J Exp Med,* 193**,** 917-24.

ALVAREZ-SILVA, M., BELO-DIABANGOUAYA, P., SALAUN, J. & DIETERLEN-LIEVRE, F. 2003. Mouse placenta is a major hematopoietic organ. *Development,* 130**,** 5437-44.

AMABILE, G., WELNER, R. S., NOMBELA-ARRIETA, C., D'ALISE, A. M., DI RUSCIO, A., EBRALIDZE, A. K., KRAYTSBERG, Y., YE, M., KOCHER, O., NEUBERG, D. S., KHRAPKO, K., SILBERSTEIN, L. E. & TENEN, D. G. 2012. In vivo generation of transplantable human hematopoietic cells from induced pluripotent stem cells. *Blood*.

AN, M. C., ZHANG, N., SCOTT, G., MONTORO, D., WITTKOP, T., MOONEY, S., MELOV, S. & ELLERBY, L. M. 2012. Genetic correction of Huntington's disease phenotypes in induced pluripotent stem cells. *Cell Stem Cell,* 11**,** 253-63.

ANDERSSON, J., SJOBERG, O. & MOLLER, G. 1972. Induction of immunoglobulin and antibody synthesis in vitro by lipopolysaccharides. *Eur J Immunol,* 2**,** 349-53.

ANDRAE, J., GALLINI, R. & BETSHOLTZ, C. 2008. Role of platelet-derived growth factors in physiology and medicine. *Genes Dev,* 22**,** 1276-312.

ANDREWS, P. W. 1984. Retinoic acid induces neuronal differentiation of a cloned human embryonal carcinoma cell line in vitro. *Dev Biol,* 103**,** 285-93.

ANJOS-AFONSO, F., CURRIE, E., PALMER, H. G., FOSTER, K. E., TAUSSIG, D. C. & BONNET, D. 2013. CD34(-) Cells at the Apex of the Human Hematopoietic Stem Cell Hierarchy Have Distinctive Cellular and Molecular Signatures. *Cell Stem Cell,* 13**,** 161-74.

ANOKYE-DANSO, F., TRIVEDI, C. M., JUHR, D., GUPTA, M., CUI, Z., TIAN, Y., ZHANG, Y., YANG, W., GRUBER, P. J., EPSTEIN, J. A. & MORRISEY, E. E. 2011. Highly efficient miRNA-mediated reprogramming of mouse and human somatic cells to pluripotency. *Cell Stem Cell,* 8**,** 376-88.

ARNAOUT, R., LEE, W., CAHILL, P., HONAN, T., SPARROW, T., WEIAND, M., NUSBAUM, C., RAJEWSKY, K. & KORALOV, S. B. 2011. High-resolution description of antibody heavy-chain repertoires in humans. *PLoS One,* 6**,** e22365.

BAIN, G., MAANDAG, E. C., IZON, D. J., AMSEN, D., KRUISBEEK, A. M., WEINTRAUB, B. C., KROP, I., SCHLISSEL, M. S., FEENEY, A. J., VAN ROON, M. & ET AL. 1994. E2A proteins are required for proper B cell development and initiation of immunoglobulin gene rearrangements. *Cell,* 79**,** 885-92.

BALLEN, K. K., VALINSKI, H., GREINER, D., SHULTZ, L. D., BECKER, P. S., HSIEH, C. C., STEWART, F. M. & QUESENBERRY, P. J. 2001. Variables to predict engraftment of umbilical cord blood into immunodeficient mice: usefulness of the non-obese diabetic--severe combined immunodeficient assay. *Br J Haematol,* 114**,** 211-8.

BARKER, J. & VERFAILLIE, C. M. 2000. A novel in vitro model of early human adult B lymphopoiesis that allows proliferation of pro-B cells and differentiation to mature B lymphocytes. *Leukemia,* 14**,** 1614-20.

BEKEREDJIAN-DING, I., FOERMER, S., KIRSCHNING, C. J., PARCINA, M. & HEEG, K. 2012. Poke weed mitogen requires Toll-like receptor ligands for proliferative activity in human and murine B lymphocytes. *PLoS One,* 7**,** e29806.

BELNOUE, E., PIHLGREN, M., MCGAHA, T. L., TOUGNE, C., ROCHAT, A. F., BOSSEN, C., SCHNEIDER, P., HUARD, B., LAMBERT, P. H. & SIEGRIST, C. A. 2008. APRIL is critical for plasmablast survival in the bone marrow and poorly expressed by early-life bone marrow stromal cells. *Blood,* 111**,** 2755-64.

BENEDICT, C. L. & KEARNEY, J. F. 1999. Increased junctional diversity in fetal B cells results in a loss of protective anti-phosphorylcholine antibodies in adult mice. *Immunity,* 10**,** 607-17.

BENNY, O., FAINARU, O., ADINI, A., CASSIOLA, F., BAZINET, L., ADINI, I., PRAVDA, E., NAHMIAS, Y., KOIRALA, S., CORFAS, G., D'AMATO, R. J. & FOLKMAN, J. 2008. An orally delivered small-molecule formulation with antiangiogenic and anticancer activity. *Nat Biotechnol,* 26**,** 799-807.

BENZ, C., COPLEY, M. R., KENT, D. G., WOHRER, S., CORTES, A., AGHAEEPOUR, N., MA, E., MADER, H., ROWE, K., DAY, C., TRELOAR, D., BRINKMAN, R. R. & EAVES, C. J. 2012. Hematopoietic stem cell subtypes expand differentially during development and display distinct lymphopoietic programs. *Cell Stem Cell,* 10**,** 273-83.

BERARDI, A. C., MEFFRE, E., PFLUMIO, F., KATZ, A., VAINCHENKER, W., SCHIFF, C. & COULOMBEL, L. 1997. Individual CD34+CD38lowCD19-CD10- progenitor cells from human cord blood generate B lymphocytes and granulocytes. *Blood,* 89**,** 3554-64.

BERLAND, R. & WORTIS, H. H. 2002. Origins and functions of B-1 cells with notes on the role of CD5. *Annu Rev Immunol,* 20**,** 253-300.

BERTRAND, J. Y., CHI, N. C., SANTOSO, B., TENG, S., STAINIER, D. Y. & TRAVER, D. 2010. Haematopoietic stem cells derive directly from aortic endothelium during development. *Nature,* 464**,** 108-11.

BERTRAND, J. Y., KIM, A. D., TENG, S. & TRAVER, D. 2008. CD41+ cmyb+ precursors colonize the zebrafish pronephros by a novel migration route to initiate adult hematopoiesis. *Development,* 135**,** 1853-62.

BESMER, P., MANOVA, K., DUTTLINGER, R., HUANG, E. J., PACKER, A., GYSSLER, C. & BACHVAROVA, R. F. 1993. The Kit-Ligand (Steel Factor) and Its Receptor C-Kit/W - Pleiotropic Roles in Gametogenesis and Melanogenesis. *Development***,** 125-137.

BHATIA, M., BONNET, D., MURDOCH, B., GAN, O. I. & DICK, J. E. 1998. A newly discovered class of human hematopoietic cells with SCID-repopulating activity. *Nat Med,* 4**,** 1038-45.

BIANCO, P. 2011. Bone and the hematopoietic niche: a tale of two stem cells. *Blood,* 117**,** 5281-8.

BLOM, B. & SPITS, H. 2006. Development of human lymphoid cells. *Annu Rev Immunol,* 24**,** 287-320.

BLOOM W., B. G. W. 1940. Hematopoiesis in young human embryos. *American Journal of Anatomy,* 67**,** 21-53.

BOCK, C., KISKINIS, E., VERSTAPPEN, G., GU, H., BOULTING, G., SMITH, Z. D., ZILLER, M., CROFT, G. F., AMOROSO, M. W., OAKLEY, D. H., GNIRKE, A., EGGAN, K. &

MEISSNER, A. 2011. Reference Maps of human ES and iPS cell variation enable high-throughput characterization of pluripotent cell lines. *Cell,* 144**,** 439-52.

BOISSET, J. C. & ROBIN, C. 2012. On the origin of hematopoietic stem cells: progress and controversy. *Stem Cell Res,* 8**,** 1-13.

BOISSET, J. C., VAN CAPPELLEN, W., ANDRIEU-SOLER, C., GALJART, N., DZIERZAK, E. & ROBIN, C. 2010. In vivo imaging of haematopoietic cells emerging from the mouse aortic endothelium. *Nature,* 464**,** 116-20.

BOWIE, M. B., KENT, D. G., DYKSTRA, B., MCKNIGHT, K. D., MCCAFFREY, L., HOODLESS, P. A. & EAVES, C. J. 2007. Identification of a new intrinsically timed developmental checkpoint that reprograms key hematopoietic stem cell properties. *Proc Natl Acad Sci U S A,* 104**,** 5878-82.

BOYER, L. A., LEE, T. I., COLE, M. F., JOHNSTONE, S. E., LEVINE, S. S., ZUCKER, J. P., GUENTHER, M. G., KUMAR, R. M., MURRAY, H. L., JENNER, R. G., GIFFORD, D. K., MELTON, D. A., JAENISCH, R. & YOUNG, R. A. 2005. Core transcriptional regulatory circuitry in human embryonic stem cells. *Cell,* 122**,** 947-56.

BROXMEYER, H. E. 1984. Colony assays of hematopoietic progenitor cells and correlations to clinical situations. *Crit Rev Oncol Hematol,* 1**,** 227-57.

BROXMEYER, H. E. 2008. Cord blood hematopoietic stem cell transplantation. *StemBook.* Cambridge (MA).

BROXMEYER, H. E., KURTZBERG, J., GLUCKMAN, E., AUERBACH, A. D., DOUGLAS, G., COOPER, S., FALKENBURG, J. H., BARD, J. & BOYSE, E. A. 1991. Umbilical cord blood hematopoietic stem and repopulating cells in human clinical transplantation. *Blood Cells,* 17**,** 313-29.

CAHAN, P. & DALEY, G. Q. 2013. Origins and implications of pluripotent stem cell variability and heterogeneity. *Nat Rev Mol Cell Biol,* 14**,** 357-68.

CAI, Z., DE BRUIJN, M., MA, X., DORTLAND, B., LUTEIJN, T., DOWNING, R. J. & DZIERZAK, E. 2000. Haploinsufficiency of AML1 affects the temporal and spatial generation of hematopoietic stem cells in the mouse embryo. *Immunity,* 13**,** 423-31.

CALIGARIS-CAPPIO, F. 1996. B-chronic lymphocytic leukemia: a malignancy of anti-self B cells. *Blood,* 87**,** 2615-20.

CALVO, J., BENYOUCEF, A., BAIJER, J., ROUYEZ, M. C. & PFLUMIO, F. 2012. Assessment of human multi-potent hematopoietic stem/progenitor cell potential using a single in vitro screening system. *PLoS One,* 7**,** e50495.

CARPENTER, L., CARR, C., YANG, C. T., STUCKEY, D. J., CLARKE, K. & WATT, S. M. 2012. Efficient differentiation of human induced pluripotent stem cells generates cardiac cells that provide protection following myocardial infarction in the rat. *Stem Cells Dev,* 21**,** 977-86.

CARPENTER, L., MALLADI, R., YANG, C. T., FRENCH, A., PILKINGTON, K. J., FORSEY, R. W., SLOANE-STANLEY, J., SILK, K. M., DAVIES, T. J., FAIRCHILD, P. J., ENVER, T. & WATT, S. M. 2011. Human induced pluripotent stem cells are capable of B-cell lymphopoiesis. *Blood,* 117**,** 4008-11.

CARVALHO, T. L., MOTA-SANTOS, T., CUMANO, A., DEMENGEOT, J. & VIEIRA, P. 2001. Arrested B lymphopoiesis and persistence of activated B cells in adult interleukin 7(-/)- mice. *J Exp Med,* 194**,** 1141-50.

CERDAN, C. & BHATIA, M. 2010. Novel roles for Notch, Wnt and Hedgehog in hematopoesis derived from human pluripotent stem cells. *Int J Dev Biol,* 54**,** 955-63.

CHADWICK, K., WANG, L., LI, L., MENENDEZ, P., MURDOCH, B., ROULEAU, A. & BHATIA, M. 2003. Cytokines and BMP-4 promote hematopoietic differentiation of human embryonic stem cells. *Blood,* 102**,** 906-15.

CHALLEN, G. A., BOLES, N. C., CHAMBERS, S. M. & GOODELL, M. A. 2010. Distinct hematopoietic stem cell subtypes are differentially regulated by TGF-beta1. *Cell Stem Cell,* 6**,** 265-78.

CHEN, M. J., LI, Y., DE OBALDIA, M. E., YANG, Q., YZAGUIRRE, A. D., YAMADA-INAGAWA, T., VINK, C. S., BHANDOOLA, A., DZIERZAK, E. & SPECK, N. A. 2011. Erythroid/myeloid progenitors and hematopoietic stem cells originate from distinct populations of endothelial cells. *Cell Stem Cell,* 9**,** 541-52.

CHEN, M. J., YOKOMIZO, T., ZEIGLER, B. M., DZIERZAK, E. & SPECK, N. A. 2009. Runx1 is required for the endothelial to haematopoietic cell transition but not thereafter. *Nature,* 457**,** 887-91.

CHIANG, P. M. & WONG, P. C. 2011. Differentiation of an embryonic stem cell to hemogenic endothelium by defined factors: essential role of bone morphogenetic protein 4. *Development,* 138**,** 2833-43.

CHO, S. K., WEBBER, T. D., CARLYLE, J. R., NAKANO, T., LEWIS, S. M. & ZUNIGA-PFLUCKER, J. C. 1999. Functional characterization of B lymphocytes generated in vitro from embryonic stem cells. *Proc Natl Acad Sci U S A,* 96**,** 9797-802.

CHOI, K., KENNEDY, M., KAZAROV, A., PAPADIMITRIOU, J. C. & KELLER, G. 1998. A common precursor for hematopoietic and endothelial cells. *Development,* 125**,** 725-32.

CHOI, K. D., VODYANIK, M. & SLUKVIN, II 2011a. Hematopoietic differentiation and production of mature myeloid cells from human pluripotent stem cells. *Nat Protoc,* 6**,** 296-313.

CHOI, K. D., VODYANIK, M. A., TOGARRATI, P. P., SUKNUNTHA, K., KUMAR, A., SAMARJEET, F., PROBASCO, M. D., TIAN, S., STEWART, R., THOMSON, J. A. & SLUKVIN, II 2012. Identification of the hemogenic endothelial progenitor and its direct precursor in human pluripotent stem cell differentiation cultures. *Cell Rep,* 2**,** 553-67.

CHOI, K. D., YU, J., SMUGA-OTTO, K., SALVAGIOTTO, G., REHRAUER, W., VODYANIK, M., THOMSON, J. & SLUKVIN, I. 2009. Hematopoietic and endothelial differentiation of human induced pluripotent stem cells. *Stem Cells,* 27**,** 559-67.

CHOI, S. M., LIU, H., CHAUDHARI, P., KIM, Y., CHENG, L., FENG, J., SHARKIS, S., YE, Z. & JANG, Y. Y. 2011b. Reprogramming of EBV-immortalized B-lymphocyte cell lines into induced pluripotent stem cells. *Blood,* 118**,** 1801-5.

CHOU, B. K., MALI, P., HUANG, X., YE, Z., DOWEY, S. N., RESAR, L. M., ZOU, C., ZHANG, Y. A., TONG, J. & CHENG, L. 2011. Efficient human iPS cell derivation by a non-integrating plasmid from blood cells with unique epigenetic and gene expression signatures. *Cell Res,* 21**,** 518-29.

CIAU-UITZ, A., WALMSLEY, M. & PATIENT, R. 2000. Distinct origins of adult and embryonic blood in Xenopus. *Cell,* 102**,** 787-96.

CLARKE, R. L., YZAGUIRRE, A. D., YASHIRO-OHTANI, Y., BONDUE, A., BLANPAIN, C., PEAR, W. S., SPECK, N. A. & KELLER, G. 2013. The expression of Sox17 identifies and regulates haemogenic endothelium. *Nat Cell Biol,* 15**,** 502-10.

CLAUDIO, E., BROWN, K., PARK, S., WANG, H. & SIEBENLIST, U. 2002. BAFF-induced NEMO-independent processing of NF-kappa B2 in maturing B cells. *Nat Immunol,* 3**,** 958-65.

CLEMENTS, W. K., KIM, A. D., ONG, K. G., MOORE, J. C., LAWSON, N. D. & TRAVER, D. 2011. A somitic Wnt16/Notch pathway specifies haematopoietic stem cells. *Nature,* 474**,** 220-4.

COLLINS, L. S. & DORSHKIND, K. 1987. A stromal cell line from myeloid long-term bone marrow cultures can support myelopoiesis and B lymphopoiesis. *J Immunol,* 138**,** 1082-7.

COPLEY, M. R., BABOVIC, S., BENZ, C., KNAPP, D. J., BEER, P. A., KENT, D. G., WOHRER, S., TRELOAR, D. Q., DAY, C., ROWE, K., MADER, H., KUCHENBAUER, F., HUMPHRIES, R. K. & EAVES, C. J. 2013. The Lin28b-let-7-Hmga2 axis determines the higher self-renewal potential of fetal haematopoietic stem cells. *Nat Cell Biol*.

CORSELLI, M., CHIN, C. J., PAREKH, C., SAHAGHIAN, A., WANG, W., GE, S., EVSEENKO, D., WANG, X., MONTELATICI, E., LAZZARI, L., CROOKS, G. M. & PEAULT, B. 2013. Perivascular support of human hematopoietic stem/progenitor cells. *Blood,* 121**,** 2891-901.

COVENS, K., VERBINNEN, B., GEUKENS, N., MEYTS, I., SCHUIT, F., VAN LOMMEL, L., JACQUEMIN, M. & BOSSUYT, X. 2013. Characterization of proposed human B-1 cells reveals pre-plasmablast phenotype. *Blood,* 121**,** 5176-83.

CROCE, C. M., SHANDER, M., MARTINIS, J., CICUREL, L., D'ANCONA, G. G., DOLBY, T. W. & KOPROWSKI, H. 1979. Chromosomal location of the genes for human immunoglobulin heavy chains. *Proc Natl Acad Sci U S A,* 76**,** 3416-9.

CUMANO, A., DIETERLEN-LIEVRE, F. & GODIN, I. 1996. Lymphoid potential, probed before circulation in mouse, is restricted to caudal intraembryonic splanchnopleura. *Cell,* 86**,** 907-16.

CUMANO, A. & GODIN, I. 2007. Ontogeny of the hematopoietic system. *Annu Rev Immunol,* 25**,** 745-85.

CUMANO, A., PAIGE, C. J., ISCOVE, N. N. & BRADY, G. 1992. Bipotential precursors of B cells and macrophages in murine fetal liver. *Nature,* 356**,** 612-5.

DAKIC, A., METCALF, D., DI RAGO, L., MIFSUD, S., WU, L. & NUTT, S. L. 2005. PU.1 regulates the commitment of adult hematopoietic progenitors and restricts granulopoiesis. *J Exp Med,* 201**,** 1487-502.

DAVI, F., FAILI, A., GRITTI, C., BLANC, C., LAURENT, C., SUTTON, L., SCHMITT, C. & MERLE-BERAL, H. 1997. Early onset of immunoglobulin heavy chain gene rearrangements in normal human bone marrow CD34+ cells. *Blood,* 90**,** 4014-21.

DAVIS, R. P., NG, E. S., COSTA, M., MOSSMAN, A. K., SOURRIS, K., ELEFANTY, A. G. & STANLEY, E. G. 2008. Targeting a GFP reporter gene to the MIXL1 locus of human embryonic stem cells identifies human primitive streak-like cells and enables isolation of primitive hematopoietic precursors. *Blood,* 111**,** 1876-84.

DE BRUIJN, M. F., SPECK, N. A., PEETERS, M. C. & DZIERZAK, E. 2000. Definitive hematopoietic stem cells first develop within the major arterial regions of the mouse embryo. *EMBO J,* 19**,** 2465-74.

DE FRANCESCO, F., TIRINO, V., DESIDERIO, V., FERRARO, G., D'ANDREA, F., GIULIANO, M., LIBONDI, G., PIROZZI, G., DE ROSA, A. & PAPACCIO, G. 2009. Human CD34/CD90 ASCs are capable of growing as sphere clusters, producing high levels of VEGF and forming capillaries. *PLoS One,* 4**,** e6537.

DE VRIES P.A , S. J. B. 1962. *DEVELOPMENT OF THE VENTRICLES & SPIRAL OUTFLOW TRACT IN THE HUMAN HEART,A CONTRIBUTION TO THE DEVELOPMENT OF THE HUMAN HEART FROM AGE GROUP IX TO AGE GROUP XV*.

DE WYNTER, E. A., BUCK, D., HART, C., HEYWOOD, R., COUTINHO, L. H., CLAYTON, A., RAFFERTY, J. A., BURT, D., GUENECHEA, G., BUEREN, J. A., GAGEN, D., FAIRBAIRN, L. J., LORD, B. I. & TESTA, N. G. 1998. CD34+AC133+ cells isolated from cord blood are highly enriched in long-term culture-initiating cells, NOD/SCID-repopulating cells and dendritic cell progenitors. *Stem Cells,* 16**,** 387-96.

DEENEN, G. J. & KROESE, F. G. 1992. Murine peritoneal Ly-1 B cells do not turn over rapidly. *Ann N Y Acad Sci,* 651**,** 70-1.

DEENEN, G. J. & KROESE, F. G. 1993. Kinetics of peritoneal B-1a cells (CD5 B cells) in young adult mice. *Eur J Immunol,* 23**,** 12-6.

DEKOTER, R. P., WALSH, J. C. & SINGH, H. 1998. PU.1 regulates both cytokine-dependent proliferation and differentiation of granulocyte/macrophage progenitors. *EMBO J,* 17**,** 4456-68.

DELASSUS, S., DARCHE, S., KOURILSKY, P. & CUMANO, A. 1998. Ontogeny of the heavy chain immunoglobulin repertoire in fetal liver and bone marrow. *J Immunol,* 160**,** 3274-80.

DIAS, J., GUMENYUK, M., KANG, H., VODYANIK, M., YU, J., THOMSON, J. A. & SLUKVIN, II 2011. Generation of red blood cells from human induced pluripotent stem cells. *Stem Cells Dev,* 20**,** 1639-47.

DICK, J. E. 1996. Normal and leukemic human stem cells assayed in SCID mice. *Semin Immunol,* 8**,** 197-206.

DIETERLEN-LIEVRE, F. 1975. On the origin of haemopoietic stem cells in the avian embryo: an experimental approach. *J Embryol Exp Morphol,* 33**,** 607-19.

DING, G., TANAKA, Y., HAYASHI, M., NISHIKAWA, S. & KATAOKA, H. 2013. PDGF receptor alpha+ mesoderm contributes to endothelial and hematopoietic cells in mice. *Dev Dyn,* 242**,** 254-68.

DING, L., SAUNDERS, T. L., ENIKOLOPOV, G. & MORRISON, S. J. 2012. Endothelial and perivascular cells maintain haematopoietic stem cells. *Nature,* 481**,** 457-62.

DOULATOV, S., NOTTA, F., EPPERT, K., NGUYEN, L. T., OHASHI, P. S. & DICK, J. E. 2010. Revised map of the human progenitor hierarchy shows the origin of macrophages and dendritic cells in early lymphoid development. *Nat Immunol,* 11**,** 585-93.

DRAKE, A. C., KHOURY, M., LESKOV, I., ILIOPOULOU, B. P., FRAGOSO, M., LODISH, H. & CHEN, J. 2011. Human CD34+ CD133+ hematopoietic stem cells cultured with growth factors including Angptl5 efficiently engraft adult NOD-SCID Il2rgamma-/- (NSG) mice. *PLoS One,* 6**,** e18382.

DRAKE, C. J. & FLEMING, P. A. 2000. Vasculogenesis in the day 6.5 to 9.5 mouse embryo. *Blood,* 95**,** 1671-9.

DREW, E., HUETTNER, C. S., TENEN, D. G. & MCNAGNY, K. M. 2005. CD34 expression by mast cells: of mice and men. *Blood,* 106**,** 1885-7.

DU, P., KIBBE, W. A. & LIN, S. M. 2008. lumi: a pipeline for processing Illumina microarray. *Bioinformatics,* 24**,** 1547-8.

DZIERZAK, E. & SPECK, N. A. 2008. Of lineage and legacy: the development of mammalian hematopoietic stem cells. *Nat Immunol,* 9**,** 129-36.

EARLY, P., HUANG, H., DAVIS, M., CALAME, K. & HOOD, L. 1980. An immunoglobulin heavy chain variable region gene is generated from three segments of DNA: VH, D and JH. *Cell,* 19**,** 981-92.

EBERT, A. D., YU, J., ROSE, F. F., JR., MATTIS, V. B., LORSON, C. L., THOMSON, J. A. & SVENDSEN, C. N. 2009. Induced pluripotent stem cells from a spinal muscular atrophy patient. *Nature,* 457**,** 277-80.

EGAWA, T., KAWABATA, K., KAWAMOTO, H., AMADA, K., OKAMOTO, R., FUJII, N., KISHIMOTO, T., KATSURA, Y. & NAGASAWA, T. 2001. The earliest stages of B cell development require a chemokine stromal cell-derived factor/pre-B cell growth-stimulating factor. *Immunity,* 15**,** 323-34.

EILKEN, H. M., NISHIKAWA, S. & SCHROEDER, T. 2009. Continuous single-cell imaging of blood generation from haemogenic endothelium. *Nature,* 457**,** 896-900.

ENGEL, P., ZHOU, L. J., ORD, D. C., SATO, S., KOLLER, B. & TEDDER, T. F. 1995. Abnormal B lymphocyte development, activation, and differentiation in mice that lack or overexpress the CD19 signal transduction molecule. *Immunity,* 3**,** 39-50.

EVANS, M. J. & KAUFMAN, M. H. 1981. Establishment in culture of pluripotential cells from mouse embryos. *Nature,* 292**,** 154-6.

EVSEENKO, D., ZHU, Y., SCHENKE-LAYLAND, K., KUO, J., LATOUR, B., GE, S., SCHOLES, J., DRAVID, G., LI, X., MACLELLAN, W. R. & CROOKS, G. M. 2010. Mapping the first stages of mesoderm commitment during differentiation of human embryonic stem cells. *Proc Natl Acad Sci U S A,* 107**,** 13742-7.

FEHLING, H. J., LACAUD, G., KUBO, A., KENNEDY, M., ROBERTSON, S., KELLER, G. & KOUSKOFF, V. 2003. Tracking mesoderm induction and its specification to the hemangioblast during embryonic stem cell differentiation. *Development,* 130**,** 4217-27.

FERKOWICZ, M. J., STARR, M., XIE, X., LI, W., JOHNSON, S. A., SHELLEY, W. C., MORRISON, P. R. & YODER, M. C. 2003. CD41 expression defines the onset of primitive and definitive hematopoiesis in the murine embryo. *Development,* 130**,** 4393-403.

FINA, L., MOLGAARD, H. V., ROBERTSON, D., BRADLEY, N. J., MONAGHAN, P., DELIA, D., SUTHERLAND, D. R., BAKER, M. A. & GREAVES, M. F. 1990. Expression of the CD34 gene in vascular endothelial cells. *Blood,* 75**,** 2417-26.

FLUCKIGER, A. C., SANZ, E., GARCIA-LLORET, M., SU, T., HAO, Q. L., KATO, R., QUAN, S., DE LA HERA, A., CROOKS, G. M., WITTE, O. N. & RAWLINGS, D. J. 1998. In vitro reconstitution of human B-cell ontogeny: from CD34(+) multipotent progenitors to Ig-secreting cells. *Blood,* 92**,** 4509-20.

FRASER, S. T., ISERN, J. & BARON, M. H. 2007. Maturation and enucleation of primitive erythroblasts during mouse embryogenesis is accompanied by changes in cell-surface antigen expression. *Blood,* 109**,** 343-52.

FREEDMAN, A. S., BOYD, A. W., BIEBER, F. R., DALEY, J., ROSEN, K., HOROWITZ, J. C., LEVY, D. N. & NADLER, L. M. 1987. Normal cellular counterparts of B cell chronic lymphocytic leukemia. *Blood,* 70**,** 418-27.

GADUE, P., HUBER, T. L., NOSTRO, M. C., KATTMAN, S. & KELLER, G. M. 2005. Germ layer induction from embryonic stem cells. *Exp Hematol,* 33**,** 955-64.

GADUE, P., HUBER, T. L., PADDISON, P. J. & KELLER, G. M. 2006. Wnt and TGF-beta signaling are required for the induction of an in vitro model of primitive streak formation using embryonic stem cells. *Proc Natl Acad Sci U S A,* 103**,** 16806-11.

GALLACHER, L., MURDOCH, B., WU, D. M., KARANU, F. N., KEENEY, M. & BHATIA, M. 2000. Isolation and characterization of human CD34(-)Lin(-) and CD34(+)Lin(-) hematopoietic stem cells using cell surface markers AC133 and CD7. *Blood,* 95**,** 2813-20.

GALY, A., TRAVIS, M., CEN, D. & CHEN, B. 1995. Human T, B, natural killer, and dendritic cells arise from a common bone marrow progenitor cell subset. *Immunity,* 3**,** 459-73.

GARCIA-PORRERO, J. A., GODIN, I. E. & DIETERLEN-LIEVRE, F. 1995. Potential intraembryonic hemogenic sites at pre-liver stages in the mouse. *Anat Embryol (Berl),* 192**,** 425-35.

GEKAS, C., DIETERLEN-LIEVRE, F., ORKIN, S. H. & MIKKOLA, H. K. 2005. The placenta is a niche for hematopoietic stem cells. *Dev Cell,* 8**,** 365-75.

GELLERT, M. 2002. V(D)J recombination: RAG proteins, repair factors, and regulation. *Annu Rev Biochem,* 71**,** 101-32.

GERBER, H. P., HILLAN, K. J., RYAN, A. M., KOWALSKI, J., KELLER, G. A., RANGELL, L., WRIGHT, B. D., RADTKE, F., AGUET, M. & FERRARA, N. 1999. VEGF is required for growth and survival in neonatal mice. *Development,* 126**,** 1149-1159.

GHIA, P., TEN BOEKEL, E., SANZ, E., DE LA HERA, A., ROLINK, A. & MELCHERS, F. 1996. Ordering of human bone marrow B lymphocyte precursors by single-cell polymerase chain reaction analyses of the rearrangement status of the immunoglobulin H and L chain gene loci. *J Exp Med,* 184**,** 2217-29.

GHOSN, E. E., SADATE-NGATCHOU, P., YANG, Y. & HERZENBERG, L. A. 2011. Distinct progenitors for B-1 and B-2 cells are present in adult mouse spleen. *Proc Natl Acad Sci U S A,* 108**,** 2879-84.

GHOSN, E. E., YAMAMOTO, R., HAMANAKA, S., YANG, Y., HERZENBERG, L. A. & NAKAUCHI, H. 2012. Distinct B-cell lineage commitment distinguishes adult bone marrow hematopoietic stem cells. *Proc Natl Acad Sci U S A,* 109**,** 5394-8.

GLUCKMAN, E., BROXMEYER, H. A., AUERBACH, A. D., FRIEDMAN, H. S., DOUGLAS, G. W., DEVERGIE, A., ESPEROU, H., THIERRY, D., SOCIE, G., LEHN, P. & ET AL. 1989. Hematopoietic reconstitution in a patient with Fanconi's anemia by means of umbilical-cord blood from an HLA-identical sibling. *N Engl J Med,* 321**,** 1174-8.

GODIN, I. E., GARCIA-PORRERO, J. A., COUTINHO, A., DIETERLEN-LIEVRE, F. & MARCOS, M. A. 1993. Para-aortic splanchnopleura from early mouse embryos contains B1a cell progenitors. *Nature,* 364**,** 67-70.

GORDON-KEYLOCK, S. & MEDVINSKY, A. 2011. Endothelio-hematopoietic relationship: getting closer to the beginnings. *BMC Biol,* 9**,** 88.

GORDON-KEYLOCK, S., SOBIESIAK, M., RYBTSOV, S., MOORE, K. & MEDVINSKY, A. 2013. Mouse extra-embryonic arterial vessels harbor precursors capable of maturing into definitive HSCs. *Blood*.

GORGENS, A., RADTKE, S., MOLLMANN, M., CROSS, M., DURIG, J., HORN, P. A. & GIEBEL, B. 2013. Revision of the human hematopoietic tree: granulocyte subtypes derive from distinct hematopoietic lineages. *Cell Rep,* 3**,** 1539-52.

GRAF, T. & STADTFELD, M. 2008. Heterogeneity of embryonic and adult stem cells. *Cell Stem Cell,* 3**,** 480-3.

GRIFFIN, D. O., HOLODICK, N. E. & ROTHSTEIN, T. L. 2011. Human B1 cells in umbilical cord and adult peripheral blood express the novel phenotype CD20+ CD27+ CD43+ CD70. *J Exp Med,* 208**,** 67-80.

GUEZGUEZ, B., CAMPBELL, C. J., BOYD, A. L., KARANU, F., CASADO, F. L., DI CRESCE, C., COLLINS, T. J., SHAPOVALOVA, Z., XENOCOSTAS, A. & BHATIA, M. 2013. Regional Localization within the Bone Marrow Influences the Functional Capacity of Human HSCs. *Cell Stem Cell,* 13**,** 175-89.

GUHA, P., MORGAN, J. W., MOSTOSLAVSKY, G., RODRIGUES, N. P. & BOYD, A. S. 2013. Lack of Immune Response to Differentiated Cells Derived from Syngeneic Induced Pluripotent Stem Cells. *Cell Stem Cell*.

HAAS, K. M., POE, J. C., STEEBER, D. A. & TEDDER, T. F. 2005. B-1a and B-1b cells exhibit distinct developmental requirements and have unique functional roles in innate and adaptive immunity to S. pneumoniae. *Immunity,* 23**,** 7-18.

HAASE, A., OLMER, R., SCHWANKE, K., WUNDERLICH, S., MERKERT, S., HESS, C., ZWEIGERDT, R., GRUH, I., MEYER, J., WAGNER, S., MAIER, L. S., HAN, D. W., GLAGE, S., MILLER, K., FISCHER, P., SCHOLER, H. R. & MARTIN, U. 2009. Generation of induced pluripotent stem cells from human cord blood. *Cell Stem Cell,* 5**,** 434-41.

HANNA, J., MARKOULAKI, S., SCHORDERET, P., CAREY, B. W., BEARD, C., WERNIG, M., CREYGHTON, M. P., STEINE, E. J., CASSADY, J. P., FOREMAN, R., LENGNER, C. J., DAUSMAN, J. A. & JAENISCH, R. 2008. Direct reprogramming of terminally differentiated mature B lymphocytes to pluripotency. *Cell,* 133**,** 250-64.

HAO, Q. L., ZHU, J., PRICE, M. A., PAYNE, K. J., BARSKY, L. W. & CROOKS, G. M. 2001. Identification of a novel, human multilymphoid progenitor in cord blood. *Blood,* 97**,** 3683-90.

HARDY, R. R. 2006. B-1 B cell development. *J Immunol,* 177**,** 2749-54.

HARDY, R. R., CARMACK, C. E., SHINTON, S. A., KEMP, J. D. & HAYAKAWA, K. 1991. Resolution and characterization of pro-B and pre-pro-B cell stages in normal mouse bone marrow. *J Exp Med,* 173**,** 1213-25.

HARDY, R. R. & HAYAKAWA, K. 1991. A developmental switch in B lymphopoiesis. *Proc Natl Acad Sci U S A,* 88**,** 11550-4.

HARDY, R. R. & HAYAKAWA, K. 2001. B cell development pathways. *Annu Rev Immunol,* 19**,** 595-621.

HARVEY, K. & DZIERZAK, E. 2004. Cell-cell contact and anatomical compatibility in stromal cell-mediated HSC support during development. *Stem Cells,* 22**,** 253-258.

HAVRAN, W. L. & ALLISON, J. P. 1988. Developmentally ordered appearance of thymocytes expressing different T-cell antigen receptors. *Nature,* 335**,** 443-5.

HAYAKAWA, K., HARDY, R. R. & HERZENBERG, L. A. 1985. Progenitors for Ly-1 B cells are distinct from progenitors for other B cells. *J Exp Med,* 161**,** 1554-68.

HAYAKAWA, K., HARDY, R. R., HONDA, M., HERZENBERG, L. A. & STEINBERG, A. D. 1984. Ly-1 B cells: functionally distinct lymphocytes that secrete IgM autoantibodies. *Proc Natl Acad Sci U S A,* 81**,** 2494-8.

HAYAKAWA, K., HARDY, R. R., PARKS, D. R. & HERZENBERG, L. A. 1983. The "Ly-1 B" cell subpopulation in normal immunodefective, and autoimmune mice. *J Exp Med,* 157**,** 202-18.

HAYASHI, K., LOPES, S. M., TANG, F. & SURANI, M. A. 2008. Dynamic equilibrium and heterogeneity of mouse pluripotent stem cells with distinct functional and epigenetic states. *Cell Stem Cell,* 3**,** 391-401.

HAYLOCK, D. N., WILLIAMS, B., JOHNSTON, H. M., LIU, M. C., RUTHERFORD, K. E., WHITTY, G. A., SIMMONS, P. J., BERTONCELLO, I. & NILSSON, S. K. 2007. Hemopoietic stem

cells with higher hemopoietic potential reside at the bone marrow endosteum. *Stem Cells,* 25**,** 1062-9.

HERZOG, S., RETH, M. & JUMAA, H. 2009. Regulation of B-cell proliferation and differentiation by pre-B-cell receptor signalling. *Nat Rev Immunol,* 9**,** 195-205.

HESS, J., WERNER, A., WIRTH, T., MELCHERS, F., JACK, H. M. & WINKLER, T. H. 2001. Induction of pre-B cell proliferation after de novo synthesis of the pre-B cell receptor. *Proc Natl Acad Sci U S A,* 98**,** 1745-50.

HOCHEDLINGER, K. & JAENISCH, R. 2002. Monoclonal mice generated by nuclear transfer from mature B and T donor cells. *Nature,* 415**,** 1035-8.

HOFFKES, H. G., SCHMIDTKE, G., UPPENKAMP, M. & SCHMUCKER, U. 1996. Multiparametric immunophenotyping of B cells in peripheral blood of healthy adults by flow cytometry. *Clin Diagn Lab Immunol,* 3**,** 30-6.

HONCZARENKO, M., GLODEK, A. M., SWIERKOWSKI, M., NA, I. K. & SILBERSTEIN, L. E. 2006. Developmental stage-specific shift in responsiveness to chemokines during human B-cell development. *Exp Hematol,* 34**,** 1093-100.

HOOPER, A. T., BUTLER, J. M., NOLAN, D. J., KRANZ, A., IIDA, K., KOBAYASHI, M., KOPP, H. G., SHIDO, K., PETIT, I., YANGER, K., JAMES, D., WITTE, L., ZHU, Z. P., WU, Y., PYTOWSKI, B., ROSENWAKS, Z., MITTAL, V., SATO, T. N. & RAFII, S. 2009. Engraftment and Reconstitution of Hematopoiesis Is Dependent on VEGFR2-Mediated Regeneration of Sinusoidal Endothelial Cells. *Cell Stem Cell,* 4**,** 263-274.

HORCHER, M., SOUABNI, A. & BUSSLINGER, M. 2001. Pax5/BSAP maintains the identity of B cells in late B lymphopoiesis. *Immunity,* 14**,** 779-90.

HOU, P., LI, Y., ZHANG, X., LIU, C., GUAN, J., LI, H., ZHAO, T., YE, J., YANG, W., LIU, K., GE, J., XU, J., ZHANG, Q., ZHAO, Y. & DENG, H. 2013. Pluripotent Stem Cells Induced from Mouse Somatic Cells by Small-Molecule Compounds. *Science*.

HUANG DA, W., SHERMAN, B. T. & LEMPICKI, R. A. 2009a. Bioinformatics enrichment tools: paths toward the comprehensive functional analysis of large gene lists. *Nucleic Acids Res,* 37**,** 1-13.

HUANG DA, W., SHERMAN, B. T. & LEMPICKI, R. A. 2009b. Systematic and integrative analysis of large gene lists using DAVID bioinformatics resources. *Nat Protoc,* 4**,** 44-57.

HUBER, T. L., KOUSKOFF, V., FEHLING, H. J., PALIS, J. & KELLER, G. 2004. Haemangioblast commitment is initiated in the primitive streak of the mouse embryo. *Nature,* 432**,** 625-30.

IACOVINO, M., CHONG, D., SZATMARI, I., HARTWECK, L., RUX, D., CAPRIOLI, A., CLEAVER, O. & KYBA, M. 2011. HoxA3 is an apical regulator of haemogenic endothelium. *Nat Cell Biol,* 13**,** 72-8.

IKUTA, K., UCHIDA, N., FRIEDMAN, J. & WEISSMAN, I. L. 1992. Lymphocyte development from stem cells. *Annu Rev Immunol,* 10**,** 759-83.

INGRAM, D. A., MEAD, L. E., MOORE, D. B., WOODARD, W., FENOGLIO, A. & YODER, M. C. 2005. Vessel wall-derived endothelial cells rapidly proliferate because they contain a complete hierarchy of endothelial progenitor cells. *Blood,* 105**,** 2783-2786.

INGRAM, V. M. 1972. Embryonic red blood cell formation. *Nature,* 235**,** 338-9.

IRION, S., CLARKE, R. L., LUCHE, H., KIM, I., MORRISON, S. J., FEHLING, H. J. & KELLER, G. M. 2010. Temporal specification of blood progenitors from mouse embryonic stem cells and induced pluripotent stem cells. *Development,* 137**,** 2829-39.

ISCOVE, N. N. & NAWA, K. 1997. Hematopoietic stem cells expand during serial transplantation in vivo without apparent exhaustion. *Curr Biol,* 7**,** 805-8.

ISRAEL, M. A., YUAN, S. H., BARDY, C., REYNA, S. M., MU, Y., HERRERA, C., HEFFERAN, M. P., VAN GORP, S., NAZOR, K. L., BOSCOLO, F. S., CARSON, C. T., LAURENT, L. C., MARSALA, M., GAGE, F. H., REMES, A. M., KOO, E. H. & GOLDSTEIN, L. S. 2012. Probing sporadic and familial Alzheimer's disease using induced pluripotent stem cells. *Nature,* 482**,** 216-20.

ITO, C. Y., KIROUAC, D. C., MADLAMBAYAN, G. J., YU, M., ROGERS, I. & ZANDSTRA, P. W. 2010. The AC133+CD38-, but not the rhodamine-low, phenotype tracks LTC-IC and SRC function in human cord blood ex vivo expansion cultures. *Blood,* 115**,** 257-60.

ITO, M., HIRAMATSU, H., KOBAYASHI, K., SUZUE, K., KAWAHATA, M., HIOKI, K., UEYAMA, Y., KOYANAGI, Y., SUGAMURA, K., TSUJI, K., HEIKE, T. & NAKAHATA, T. 2002. NOD/SCID/gamma(c)(null) mouse: an excellent recipient mouse model for engraftment of human cells. *Blood,* 100**,** 3175-82.

ITOH, K., TEZUKA, H., SAKODA, H., KONNO, M., NAGATA, K., UCHIYAMA, T., UCHINO, H. & MORI, K. J. 1989. Reproducible establishment of hemopoietic supportive stromal cell lines from murine bone marrow. *Exp Hematol,* 17**,** 145-53.

IVANOVS, A., RYBTSOV, S., WELCH, L., ANDERSON, R. A., TURNER, M. L. & MEDVINSKY, A. 2011. Highly potent human hematopoietic stem cells first emerge in the intraembryonic aorta-gonad-mesonephros region. *J Exp Med,* 208**,** 2417-27.

JAFFREDO, T., GAUTIER, R., EICHMANN, A. & DIETERLEN-LIEVRE, F. 1998. Intraaortic hemopoietic cells are derived from endothelial cells during ontogeny. *Development,* 125**,** 4575-83.

JAMES, D., NAM, H. S., SEANDEL, M., NOLAN, D., JANOVITZ, T., TOMISHIMA, M., STUDER, L., LEE, G., LYDEN, D., BENEZRA, R., ZANINOVIC, N., ROSENWAKS, Z., RABBANY, S. Y. & RAFII, S. 2010. Expansion and maintenance of human embryonic stem cell-derived endothelial cells by TGFbeta inhibition is Id1 dependent. *Nat Biotechnol,* 28**,** 161-6.

JENSEN, C. T., KHARAZI, S., BOIERS, C., CHENG, M., LUBKING, A., SITNICKA, E. & JACOBSEN, S. E. 2008. FLT3 ligand and not TSLP is the key regulator of IL-7-independent B-1 and B-2 B lymphopoiesis. *Blood,* 112**,** 2297-304.

JEONG, H. D. & TEALE, J. M. 1988. Comparison of the fetal and adult functional B cell repertoires by analysis of VH gene family expression. *J Exp Med,* 168**,** 589-603.

JOHNSON, K., HASHIMSHONY, T., SAWAI, C. M., PONGUBALA, J. M., SKOK, J. A., AIFANTIS, I. & SINGH, H. 2008. Regulation of immunoglobulin light-chain recombination by the transcription factor IRF-4 and the attenuation of interleukin-7 signaling. *Immunity,* 28**,** 335-45.

JOHNSON, S., E. 2008. The Role of Interleukin-7 in the Regulation of Normal Human B Lymphopoiesis. *In:* PROQUEST, U. D. P. (ed.).

JOHNSON, S. E., SHAH, N., PANOSKALTSIS-MORTARI, A. & LEBIEN, T. W. 2005. Murine and human IL-7 activate STAT5 and induce proliferation of normal human pro-B cells. *J Immunol,* 175**,** 7325-31.

JONES, R. J., WAGNER, J. E., CELANO, P., ZICHA, M. S. & SHARKIS, S. J. 1990. Separation of pluripotent haematopoietic stem cells from spleen colony-forming cells. *Nature,* 347**,** 188-9.

JORDAN, H. E. 1917. Aortic Cell Clusters in Vertebrate Embryos. *Proc Natl Acad Sci U S A,* 3**,** 149-56.

JUNG, D. & ALT, F. W. 2004. Unraveling V(D)J recombination; insights into gene regulation. *Cell,* 116**,** 299-311.

JUNG, D., GIALLOURAKIS, C., MOSTOSLAVSKY, R. & ALT, F. W. 2006. Mechanism and control of V(D)J recombination at the immunoglobulin heavy chain locus. *Annu Rev Immunol,* 24**,** 541-70.

KABRUN, N., BUHRING, H. J., CHOI, K., ULLRICH, A., RISAU, W. & KELLER, G. 1997. Flk-1 expression defines a population of early embryonic hematopoietic precursors. *Development,* 124**,** 2039-48.

KAJI, K., NORRBY, K., PACA, A., MILEIKOVSKY, M., MOHSENI, P. & WOLTJEN, K. 2009. Virus-free induction of pluripotency and subsequent excision of reprogramming factors. *Nature,* 458**,** 771-5.

KAMEL-REID, S. & DICK, J. E. 1988. Engraftment of immune-deficient mice with human hematopoietic stem cells. *Science,* 242**,** 1706-9.

KANTOR, A. 1991a. A new nomenclature for B cells. *Immunol Today,* 12**,** 388.

KANTOR, A. B. 1991b. The development and repertoire of B-1 cells (CD5 B cells). *Immunol Today,* 12**,** 389-91.

KANTOR, A. B., STALL, A. M., ADAMS, S. & HERZENBERG, L. A. 1992. Differential development of progenitor activity for three B-cell lineages. *Proc Natl Acad Sci U S A,* 89**,** 3320-4.

KATAOKA, H., TAKAKURA, N., NISHIKAWA, S., TSUCHIDA, K., KODAMA, H., KUNISADA, T., RISAU, W., KITA, T. & NISHIKAWA, S. I. 1997. Expressions of PDGF receptor alpha, c-Kit and Flk1 genes clustering in mouse chromosome 5 define distinct subsets of nascent mesodermal cells. *Dev Growth Differ,* 39**,** 729-40.

KATTMAN, S. J., WITTY, A. D., GAGLIARDI, M., DUBOIS, N. C., NIAPOUR, M., HOTTA, A., ELLIS, J. & KELLER, G. 2011. Stage-specific optimization of activin/nodal and BMP signaling promotes cardiac differentiation of mouse and human pluripotent stem cell lines. *Cell Stem Cell,* 8**,** 228-40.

KAUFMAN, D. S., HANSON, E. T., LEWIS, R. L., AUERBACH, R. & THOMSON, J. A. 2001. Hematopoietic colony-forming cells derived from human embryonic stem cells. *Proc Natl Acad Sci U S A,* 98**,** 10716-21.

KEE, B. L. & PAIGE, C. J. 1996. In vitro tracking of IL-7 responsiveness and gene expression during commitment of bipotent B-cell/macrophage progenitors. *Curr Biol,* 6**,** 1159-69.

KEE, B. L., PAIGE, C. J. & LETARTE, M. 1992. Characterization of murine CD10, an endopeptidase expressed on bone marrow adherent cells. *Int Immunol,* 4**,** 1041-7.

KELEMEN, E. 1979. *Atlas of human hemopoietic development* Berlin ; New York, Springer-Verlag.

KENNEDY, M., AWONG, G., STURGEON, C. M., DITADI, A., LAMOTTE-MOHS, R., ZUNIGA-PFLUCKER, J. C. & KELLER, G. 2012. T Lymphocyte Potential Marks the Emergence of Definitive Hematopoietic Progenitors in Human Pluripotent Stem Cell Differentiation Cultures. *Cell Rep*.

KENNEDY, M., D'SOUZA, S. L., LYNCH-KATTMAN, M., SCHWANTZ, S. & KELLER, G. 2007. Development of the hemangioblast defines the onset of hematopoiesis in human ES cell differentiation cultures. *Blood,* 109**,** 2679-87.

KHOO, C. P., MICKLEM, K. & WATT, S. M. 2011. A comparison of methods for quantifying angiogenesis in the Matrigel assay in vitro. *Tissue Eng Part C Methods,* 17**,** 895-906.

KIEL, M. J. & MORRISON, S. J. 2008. Uncertainty in the niches that maintain haematopoietic stem cells. *Nat Rev Immunol,* 8**,** 290-301.

KIEL, M. J., YILMAZ, O. H., IWASHITA, T., TERHORST, C. & MORRISON, S. J. 2005. SLAM family receptors distinguish hematopoietic stem and progenitor cells and reveal endothelial niches for stem cells. *Cell,* 121**,** 1109-21.

KIKUCHI, K. & KONDO, M. 2006. Developmental switch of mouse hematopoietic stem cells from fetal to adult type occurs in bone marrow after birth. *Proc Natl Acad Sci U S A,* 103**,** 17852-7.

KIM, D., KIM, C. H., MOON, J. I., CHUNG, Y. G., CHANG, M. Y., HAN, B. S., KO, S., YANG, E., CHA, K. Y., LANZA, R. & KIM, K. S. 2009. Generation of human induced pluripotent stem cells by direct delivery of reprogramming proteins. *Cell Stem Cell,* 4**,** 472-6.

KIM, I., SAUNDERS, T. L. & MORRISON, S. J. 2007. Sox17 dependence distinguishes the transcriptional regulation of fetal from adult hematopoietic stem cells. *Cell,* 130**,** 470-83.

KIM, I., YILMAZ, O. H. & MORRISON, S. J. 2005. CD144 (VE-cadherin) is transiently expressed by fetal liver hematopoietic stem cells. *Blood,* 106**,** 903-5.

KIM, K., DOI, A., WEN, B., NG, K., ZHAO, R., CAHAN, P., KIM, J., ARYEE, M. J., JI, H., EHRLICH, L. I., YABUUCHI, A., TAKEUCHI, A., CUNNIFF, K. C., HONGGUANG, H., MCKINNEY-FREEMAN, S., NAVEIRAS, O., YOON, T. J., IRIZARRY, R. A., JUNG, N., SEITA, J., HANNA, J., MURAKAMI, P., JAENISCH, R., WEISSLEDER, R., ORKIN, S. H., WEISSMAN, I. L., FEINBERG, A. P. & DALEY, G. Q. 2010. Epigenetic memory in induced pluripotent stem cells. *Nature,* 467**,** 285-90.

KINGSLEY, P. D., MALIK, J., FANTAUZZO, K. A. & PALIS, J. 2004. Yolk sac-derived primitive erythroblasts enucleate during mammalian embryogenesis. *Blood,* 104**,** 19-25.

KIRSTETTER, P., THOMAS, M., DIERICH, A., KASTNER, P. & CHAN, S. 2002. Ikaros is critical for B cell differentiation and function. *Eur J Immunol,* 32**,** 720-30.

KISSA, K. & HERBOMEL, P. 2010. Blood stem cells emerge from aortic endothelium by a novel type of cell transition. *Nature,* 464**,** 112-5.

KOHN, L. A., HAO, Q. L., SASIDHARAN, R., PAREKH, C., GE, S., ZHU, Y., MIKKOLA, H. K. & CROOKS, G. M. 2012. Lymphoid priming in human bone marrow begins before expression of CD10 with upregulation of L-selectin. *Nat Immunol,* 13**,** 963-71.

KONDO, M., TAKESHITA, T., HIGUCHI, M., NAKAMURA, M., SUDO, T., NISHIKAWA, S. & SUGAMURA, K. 1994. Functional participation of the IL-2 receptor gamma chain in IL-7 receptor complexes. *Science,* 263**,** 1453-4.

KONDO, M., WEISSMAN, I. L. & AKASHI, K. 1997. Identification of clonogenic common lymphoid progenitors in mouse bone marrow. *Cell,* 91**,** 661-72.

KONDO, T., ASAI, M., TSUKITA, K., KUTOKU, Y., OHSAWA, Y., SUNADA, Y., IMAMURA, K., EGAWA, N., YAHATA, N., OKITA, K., TAKAHASHI, K., ASAKA, I., AOI, T., WATANABE, A., WATANABE, K., KADOYA, C., NAKANO, R., WATANABE, D., MARUYAMA, K., HORI, O., HIBINO, S., CHOSHI, T., NAKAHATA, T., HIOKI, H., KANEKO, T., NAITOH, M., YOSHIKAWA, K., YAMAWAKI, S., SUZUKI, S., HATA, R., UENO, S., SEKI, T., KOBAYASHI, K., TODA, T., MURAKAMI, K., IRIE, K., KLEIN, W. L., MORI, H., ASADA, T., TAKAHASHI, R., IWATA, N., YAMANAKA, S. & INOUE, H. 2013. Modeling Alzheimer's disease with iPSCs reveals stress phenotypes associated with intracellular Abeta and differential drug responsiveness. *Cell Stem Cell,* 12**,** 487-96.

KOZMIK, Z., WANG, S., DORFLER, P., ADAMS, B. & BUSSLINGER, M. 1992. The promoter of the CD19 gene is a target for the B-cell-specific transcription factor BSAP. *Mol Cell Biol,* 12**,** 2662-72.

KRIEG, A. M., YI, A. K., MATSON, S., WALDSCHMIDT, T. J., BISHOP, G. A., TEASDALE, R., KORETZKY, G. A. & KLINMAN, D. M. 1995. CpG motifs in bacterial DNA trigger direct B-cell activation. *Nature,* 374**,** 546-9.

KROP, I., DE FOUGEROLLES, A. R., HARDY, R. R., ALLISON, M., SCHLISSEL, M. S. & FEARON, D. T. 1996. Self-renewal of B-1 lymphocytes is dependent on CD19. *Eur J Immunol,* 26**,** 238-42.

KUMARAVELU, P., HOOK, L., MORRISON, A. M., URE, J., ZHAO, S., ZUYEV, S., ANSELL, J. & MEDVINSKY, A. 2002. Quantitative developmental anatomy of definitive haematopoietic stem cells/long-term repopulating units (HSC/RUs): role of the aorta-gonad-mesonephros (AGM) region and the yolk sac in colonisation of the mouse embryonic liver. *Development,* 129**,** 4891-9.

KURABAYASHI, M., KOMURO, I., TSUCHIMOCHI, H., TAKAKU, F. & YAZAKI, Y. 1988. Molecular cloning and characterization of human atrial and ventricular myosin alkali light chain cDNA clones. *J Biol Chem,* 263**,** 13930-6.

KUSUMA, S., SHEN, Y. I., HANJAYA-PUTRA, D., MALI, P., CHENG, L. & GERECHT, S. 2013. Self-organized vascular networks from human pluripotent stem cells in a synthetic matrix. *Proc Natl Acad Sci U S A*.

KYBA, M., PERLINGEIRO, R. C. & DALEY, G. Q. 2002. HoxB4 confers definitive lymphoid-myeloid engraftment potential on embryonic stem cell and yolk sac hematopoietic progenitors. *Cell,* 109**,** 29-37.

LADEWIG, J., KOCH, P. & BRUSTLE, O. 2013. Leveling Waddington: the emergence of direct programming and the loss of cell fate hierarchies. *Nature Reviews Molecular Cell Biology,* 14**,** 225-236.

LAFLAMME, M. A., CHEN, K. Y., NAUMOVA, A. V., MUSKHELI, V., FUGATE, J. A., DUPRAS, S. K., REINECKE, H., XU, C., HASSANIPOUR, M., POLICE, S., O'SULLIVAN, C., COLLINS, L., CHEN, Y., MINAMI, E., GILL, E. A., UENO, S., YUAN, C., GOLD, J. & MURRY, C. E. 2007. Cardiomyocytes derived from human embryonic stem cells in pro-survival factors enhance function of infarcted rat hearts. *Nat Biotechnol,* 25**,** 1015-24.

LANCRIN, C., SROCZYNSKA, P., STEPHENSON, C., ALLEN, T., KOUSKOFF, V. & LACAUD, G. 2009. The haemangioblast generates haematopoietic cells through a haemogenic endothelium stage. *Nature,* 457**,** 892-5.

LASSILA, O., ESKOLA, J., TOIVANEN, P., MARTIN, C. & DIETERLEN-LIEVRE, F. 1978. The origin of lymphoid stem cells studied in chick yold sac-embryo chimaeras. *Nature,* 272**,** 353-4.

LAURENTI, E., DOULATOV, S., ZANDI, S., PLUMB, I., CHEN, J., APRIL, C., FAN, J. B. & DICK, J. E. 2013a. The transcriptional architecture of early human hematopoiesis identifies multilevel control of lymphoid commitment. *Nat Immunol,* 14**,** 756-63.

LAURENTI, E., DOULATOV, S., ZANDI, S., PLUMB, I., CHEN, J., APRIL, C., FAN, J. B. & DICK, J. E. 2013b. The transcriptional architecture of early human hematopoiesis identifies multilevel control of lymphoid commitment. *Nat Immunol*.

LE DOUARIN, N. M. & JOTEREAU, F. V. 1975. Tracing of cells of the avian thymus through embryonic life in interspecific chimeras. *J Exp Med,* 142**,** 17-40.

LEBIEN, T. W. 1989. Growing human B-cell precursors in vitro: the continuing challenge. *Immunol Today,* 10**,** 296-8.

LEBIEN, T. W. 2000. Fates of human B-cell precursors. *Blood,* 96**,** 9-23.

LEDRAN, M. H., KRASSOWSKA, A., ARMSTRONG, L., DIMMICK, I., RENSTROM, J., LANG, R., YUNG, S., SANTIBANEZ-COREF, M., DZIERZAK, E., STOJKOVIC, M., OOSTENDORP, R. A., FORRESTER, L. & LAKO, M. 2008. Efficient hematopoietic differentiation of human embryonic stem cells on stromal cells derived from hematopoietic niches. *Cell Stem Cell,* 3**,** 85-98.

LEE, Y. T., DE VASCONCELLOS, J. F., YUAN, J., BYRNES, C., NOH, S. J., MEIER, E. R., KIM, K. S., RABEL, A., KAUSHAL, M., MULJO, S. A. & MILLER, J. L. 2013. LIN28B-mediated expression of fetal hemoglobin and production of fetal-like erythrocytes from adult human erythroblasts ex vivo. *Blood*.

LEFRANC, M. P. 2001. Nomenclature of the human immunoglobulin genes. *Curr Protoc Immunol,* Appendix 1**,** Appendix 1P.

LEFRANC, M. P., GIUDICELLI, V., GINESTOUX, C., JABADO-MICHALOUD, J., FOLCH, G., BELLAHCENE, F., WU, Y., GEMROT, E., BROCHET, X., LANE, J., REGNIER, L., EHRENMANN, F., LEFRANC, G. & DUROUX, P. 2009. IMGT, the international ImMunoGeneTics information system. *Nucleic Acids Res,* 37**,** D1006-12.

LI, C. L. & JOHNSON, G. R. 1995. Murine hematopoietic stem and progenitor cells: I. Enrichment and biologic characterization. *Blood,* 85**,** 1472-9.

LI, H. W. & SYKES, M. 2012. Emerging concepts in haematopoietic cell transplantation. *Nat Rev Immunol,* 12**,** 403-16.

LI, Y. S., HAYAKAWA, K. & HARDY, R. R. 1993. The regulated expression of B lineage associated genes during B cell differentiation in bone marrow and fetal liver. *J Exp Med,* 178**,** 951-60.

LI, Z., WU, J. C., SHEIKH, A. Y., KRAFT, D., CAO, F., XIE, X., PATEL, M., GAMBHIR, S. S., ROBBINS, R. C. & COOKE, J. P. 2007. Differentiation, survival, and function of embryonic stem cell derived endothelial cells for ischemic heart disease. *Circulation,* 116**,** I46-54.

LIAO, Y., GEYER, M. B., YANG, A. J. & CAIRO, M. S. 2011. Cord blood transplantation and stem cell regenerative potential. *Exp Hematol,* 39**,** 393-412.

LIMBOURG, A., KORFF, T., NAPP, L. C., SCHAPER, W., DREXLER, H. & LIMBOURG, F. P. 2009. Evaluation of postnatal arteriogenesis and angiogenesis in a mouse model of hind-limb ischemia. *Nat Protoc,* 4**,** 1737-46.

LIN, C. S. & LUE, T. F. 2013. Defining vascular stem cells. *Stem Cells Dev,* 22**,** 1018-26.

LIN, H. & GROSSCHEDL, R. 1995. Failure of B-cell differentiation in mice lacking the transcription factor EBF. *Nature,* 376**,** 263-7.

LIPPMANN, E. S., AZARIN, S. M., KAY, J. E., NESSLER, R. A., WILSON, H. K., AL-AHMAD, A., PALECEK, S. P. & SHUSTA, E. V. 2012. Derivation of blood-brain barrier endothelial cells from human pluripotent stem cells. *Nat Biotechnol,* 30**,** 783-91.

LIU, L., PAPA, E. F., DOONER, M. S., MACHAN, J. T., JOHNSON, K. W., GOLDBERG, L. R., QUESENBERRY, P. J. & COLVIN, G. A. 2012. Homing and long-term engraftment of long- and short-term renewal hematopoietic stem cells. *PLoS One,* 7**,** e31300.

LO CELSO, C. & SCADDEN, D. T. 2011. The haematopoietic stem cell niche at a glance. *J Cell Sci,* 124**,** 3529-35.

LOKEN, M. R., SHAH, V. O., DATTILIO, K. L. & CIVIN, C. I. 1987. Flow cytometric analysis of human bone marrow. II. Normal B lymphocyte development. *Blood,* 70**,** 1316-24.

LU, L., CHAUDHURY, P. & OSMOND, D. G. 1999. Regulation of cell survival during B lymphopoiesis: apoptosis and Bcl-2/Bax content of precursor B cells in bone marrow of mice with altered expression of IL-7 and recombinase-activating gene-2. *J Immunol,* 162**,** 1931-40.

LUC, S., ANDERSON, K., KHARAZI, S., BUZA-VIDAS, N., BOIERS, C., JENSEN, C. T., MA, Z., WITTMANN, L. & JACOBSEN, S. E. 2008. Down-regulation of Mpl marks the transition to lymphoid-primed multipotent progenitors with gradual loss of granulocyte-monocyte potential. *Blood,* 111**,** 3424-34.

LUC, S., LUIS, T. C., BOUKARABILA, H., MACAULAY, I. C., BUZA-VIDAS, N., BOURIEZ-JONES, T., LUTTEROPP, M., WOLL, P. S., LOUGHRAN, S. J., MEAD, A. J., HULTQUIST, A., BROWN, J., MIZUKAMI, T., MATSUOKA, S., FERRY, H., ANDERSON, K., DUARTE, S., ATKINSON, D., SONEJI, S., DOMANSKI, A., FARLEY, A., SANJUAN-PLA, A., CARELLA, C., PATIENT, R., DE BRUIJN, M., ENVER, T., NERLOV, C., BLACKBURN, C., GODIN, I. & JACOBSEN, S. E. 2012. The earliest thymic T cell progenitors sustain B cell and myeloid lineage potential. *Nat Immunol,* 13**,** 412-9.

LUCAS, A. H. & REASON, D. C. 1999. Polysaccharide vaccines as probes of antibody repertoires in man. *Immunol Rev,* 171**,** 89-104.

LUDWIG, T. E., BERGENDAHL, V., LEVENSTEIN, M. E., YU, J., PROBASCO, M. D. & THOMSON, J. A. 2006. Feeder-independent culture of human embryonic stem cells. *Nat Methods,* 3**,** 637-46.

MACALLAN, D. C., WALLACE, D. L., ZHANG, Y., GHATTAS, H., ASQUITH, B., DE LARA, C., WORTH, A., PANAYIOTAKOPOULOS, G., GRIFFIN, G. E., TOUGH, D. F. & BEVERLEY, P. C. 2005. B-cell kinetics in humans: rapid turnover of peripheral blood memory cells. *Blood,* 105**,** 3633-40.

MACLENNAN, I. C., GRAY, D., KUMARARATNE, D.S., BAZIN, H. 1982. The lymphocytes of splenic marginal zones; a distinct B cell lineage. *Immunology Today,* 3**,** 305-7.

MAEHR, R., CHEN, S., SNITOW, M., LUDWIG, T., YAGASAKI, L., GOLAND, R., LEIBEL, R. L. & MELTON, D. A. 2009. Generation of pluripotent stem cells from patients with type 1 diabetes. *Proc Natl Acad Sci U S A,* 106**,** 15768-73.

MALYNN, B. A., YANCOPOULOS, G. D., BARTH, J. E., BONA, C. A. & ALT, F. W. 1990. Biased expression of JH-proximal VH genes occurs in the newly generated repertoire of neonatal and adult mice. *J Exp Med,* 171**,** 843-59.

MARCHETTO, M. C., CARROMEU, C., ACAB, A., YU, D., YEO, G. W., MU, Y., CHEN, G., GAGE, F. H. & MUOTRI, A. R. 2010. A model for neural development and treatment of Rett syndrome using human induced pluripotent stem cells. *Cell,* 143**,** 527-39.

MARKS-BLUTH, J. & PIMANDA, J. E. 2012. Cell signalling pathways that mediate haematopoietic stem cell specification. *Int J Biochem Cell Biol,* 44**,** 2175-84.

MARKS, H., KALKAN, T., MENAFRA, R., DENISSOV, S., JONES, K., HOFEMEISTER, H., NICHOLS, J., KRANZ, A., STEWART, A. F., SMITH, A. & STUNNENBERG, H. G. 2012. The transcriptional and epigenomic foundations of ground state pluripotency. *Cell,* 149**,** 590-604.

MARSHALL, A. J., PAIGE, C. J. & WU, G. E. 1997. V(H) repertoire maturation during B cell development in vitro: differential selection of Ig heavy chains by fetal and adult B cell progenitors. *J Immunol,* 158**,** 4282-91.

MARTELLO, G., SUGIMOTO, T., DIAMANTI, E., JOSHI, A., HANNAH, R., OHTSUKA, S., GOTTGENS, B., NIWA, H. & SMITH, A. 2012. Esrrb is a pivotal target of the

Gsk3/Tcf3 axis regulating embryonic stem cell self-renewal. *Cell Stem Cell,* 11**,** 491-504.

MARTIN, C. H., WOLL, P. S., NI, Z., ZUNIGA-PFLUCKER, J. C. & KAUFMAN, D. S. 2008. Differences in lymphocyte developmental potential between human embryonic stem cell and umbilical cord blood-derived hematopoietic progenitor cells. *Blood,* 112**,** 2730-7.

MARTIN, G. R. 1981. Isolation of a pluripotent cell line from early mouse embryos cultured in medium conditioned by teratocarcinoma stem cells. *Proc Natl Acad Sci U S A,* 78**,** 7634-8.

MASUI, S., NAKATAKE, Y., TOYOOKA, Y., SHIMOSATO, D., YAGI, R., TAKAHASHI, K., OKOCHI, H., OKUDA, A., MATOBA, R., SHAROV, A. A., KO, M. S. & NIWA, H. 2007. Pluripotency governed by Sox2 via regulation of Oct3/4 expression in mouse embryonic stem cells. *Nat Cell Biol,* 9**,** 625-35.

MAYSHAR, Y., BEN-DAVID, U., LAVON, N., BIANCOTTI, J. C., YAKIR, B., CLARK, A. T., PLATH, K., LOWRY, W. E. & BENVENISTY, N. 2010. Identification and classification of chromosomal aberrations in human induced pluripotent stem cells. *Cell Stem Cell,* 7**,** 521-31.

MCBRIDE, O. W., HIETER, P. A., HOLLIS, G. F., SWAN, D., OTEY, M. C. & LEDER, P. 1982. Chromosomal location of human kappa and lambda immunoglobulin light chain constant region genes. *J Exp Med,* 155**,** 1480-90.

MCCULLOCH, E. A. & TILL, J. E. 1960. The radiation sensitivity of normal mouse bone marrow cells, determined by quantitative marrow transplantation into irradiated mice. *Radiat Res,* 13**,** 115-25.

MCCUNE, J. M., NAMIKAWA, R., KANESHIMA, H., SHULTZ, L. D., LIEBERMAN, M. & WEISSMAN, I. L. 1988. The SCID-hu mouse: murine model for the analysis of human hematolymphoid differentiation and function. *Science,* 241**,** 1632-9.

MCDERMOTT, S. P., EPPERT, K., LECHMAN, E. R., DOEDENS, M. & DICK, J. E. 2010. Comparison of human cord blood engraftment between immunocompromised mouse strains. *Blood,* 116**,** 193-200.

MCGRATH, K. E., KONISKI, A. D., MALIK, J. & PALIS, J. 2003. Circulation is established in a stepwise pattern in the mammalian embryo. *Blood,* 101**,** 1669-76.

MCKENNA, H. J., STOCKING, K. L., MILLER, R. E., BRASEL, K., DE SMEDT, T., MARASKOVSKY, E., MALISZEWSKI, C. R., LYNCH, D. H., SMITH, J., PULENDRAN, B., ROUX, E. R., TEEPE, M., LYMAN, S. D. & PESCHON, J. J. 2000. Mice lacking flt3 ligand have deficient hematopoiesis affecting hematopoietic progenitor cells, dendritic cells, and natural killer cells. *Blood,* 95**,** 3489-3497.

MEDVINSKY, A. & DZIERZAK, E. 1996. Definitive hematopoiesis is autonomously initiated by the AGM region. *Cell,* 86**,** 897-906.

MEDVINSKY, A., RYBTSOV, S. & TAOUDI, S. 2011. Embryonic origin of the adult hematopoietic system: advances and questions. *Development,* 138**,** 1017-31.

MEEK, K. 1990. Analysis of junctional diversity during B lymphocyte development. *Science,* 250**,** 820-3.

MIKKOLA, H. K., FUJIWARA, Y., SCHLAEGER, T. M., TRAVER, D. & ORKIN, S. H. 2003. Expression of CD41 marks the initiation of definitive hematopoiesis in the mouse embryo. *Blood,* 101**,** 508-16.

MIKKOLA, I., HEAVEY, B., HORCHER, M. & BUSSLINGER, M. 2002. Reversion of B cell commitment upon loss of Pax5 expression. *Science,* 297**,** 110-3.

MILLER, C. L. & EAVES, C. J. 1997. Expansion in vitro of adult murine hematopoietic stem cells with transplantable lympho-myeloid reconstituting ability. *Proc Natl Acad Sci U S A,* 94**,** 13648-53.

MILLER, J., HORNER, A., STACY, T., LOWREY, C., LIAN, J. B., STEIN, G., NUCKOLLS, G. H. & SPECK, N. A. 2002. The core-binding factor beta subunit is required for bone formation and hematopoietic maturation. *Nat Genet,* 32**,** 645-9.

MILNE, C. D., FLEMING, H. E. & PAIGE, C. J. 2004. IL-7 does not prevent pro-B/pre-B cell maturation to the immature/sIgM(+) stage. *Eur J Immunol,* 34**,** 2647-55.

MIZUOCHI, C., FRASER, S. T., BIASCH, K., HORIO, Y., KIKUSHIGE, Y., TANI, K., AKASHI, K., TAVIAN, M. & SUGIYAMA, D. 2012. Intra-aortic clusters undergo endothelial to hematopoietic phenotypic transition during early embryogenesis. *PLoS One,* 7**,** e35763.

MOIGNARD, V., MACAULAY, I. C., SWIERS, G., BUETTNER, F., SCHUTTE, J., CALERO-NIETO, F. J., KINSTON, S., JOSHI, A., HANNAH, R., THEIS, F. J., JACOBSEN, S. E., DE BRUIJN, M. F. & GOTTGENS, B. 2013. Characterization of transcriptional networks in blood stem and progenitor cells using high-throughput single-cell gene expression analysis. *Nat Cell Biol,* 15**,** 363-72.

MOLD, J. E., VENKATASUBRAHMANYAM, S., BURT, T. D., MICHAELSSON, J., RIVERA, J. M., GALKINA, S. A., WEINBERG, K., STODDART, C. A. & MCCUNE, J. M. 2010. Fetal and adult hematopoietic stem cells give rise to distinct T cell lineages in humans. *Science,* 330**,** 1695-9.

MONTECINO-RODRIGUEZ, E. & DORSHKIND, K. 2012. B-1 B cell development in the fetus and adult. *Immunity,* 36**,** 13-21.

MONTECINO-RODRIGUEZ, E., LEATHERS, H. & DORSHKIND, K. 2001. Bipotential B-macrophage progenitors are present in adult bone marrow. *Nat Immunol,* 2**,** 83-8.

MONTECINO-RODRIGUEZ, E., LEATHERS, H. & DORSHKIND, K. 2006. Identification of a B-1 B cell-specified progenitor. *Nat Immunol,* 7**,** 293-301.

MOREAU, I., DUVERT, V., BANCHEREAU, J. & SAELAND, S. 1993. Culture of human fetal B-cell precursors on bone marrow stroma maintains highly proliferative CD20dim cells. *Blood,* 81**,** 1170-8.

MORETTI, A., BELLIN, M., WELLING, A., JUNG, C. B., LAM, J. T., BOTT-FLUGEL, L., DORN, T., GOEDEL, A., HOHNKE, C., HOFMANN, F., SEYFARTH, M., SINNECKER, D., SCHOMIG, A. & LAUGWITZ, K. L. 2010. Patient-specific induced pluripotent stem-cell models for long-QT syndrome. *N Engl J Med,* 363**,** 1397-409.

MORRISON, S. J. & WEISSMAN, I. L. 1994. The long-term repopulating subset of hematopoietic stem cells is deterministic and isolatable by phenotype. *Immunity,* 1**,** 661-73.

MOSIER, D. E., GULIZIA, R. J., BAIRD, S. M. & WILSON, D. B. 1988. Transfer of a functional human immune system to mice with severe combined immunodeficiency. *Nature,* 335**,** 256-9.

MUCENSKI, M. L., MCLAIN, K., KIER, A. B., SWERDLOW, S. H., SCHREINER, C. M., MILLER, T. A., PIETRYGA, D. W., SCOTT, W. J., JR. & POTTER, S. S. 1991. A functional c-myb gene is required for normal murine fetal hepatic hematopoiesis. *Cell,* 65**,** 677-89.

MULLER-SIEBURG, C. E., WHITLOCK, C. A. & WEISSMAN, I. L. 1986. Isolation of two early B lymphocyte progenitors from mouse marrow: a committed pre-pre-B cell and a clonogenic Thy-1-lo hematopoietic stem cell. *Cell,* 44**,** 653-62.

MULLER, A. M., MEDVINSKY, A., STROUBOULIS, J., GROSVELD, F. & DZIERZAK, E. 1994. Development of hematopoietic stem cell activity in the mouse embryo. *Immunity,* 1**,** 291-301.

MURRAY, P. D. F. 1932. The Development in vitro of the Blood of the Early Chick Embryo. *Proc R Soc Lond,* 111**,** 497-521.

NAGY, A., GOCZA, E., DIAZ, E. M., PRIDEAUX, V. R., IVANYI, E., MARKKULA, M. & ROSSANT, J. 1990. Embryonic stem cells alone are able to support fetal development in the mouse. *Development,* 110**,** 815-21.

NAITO, M., HAINZ, U., BURKHARDT, U. E., FU, B., AHOVE, D., STEVENSON, K. E., RAJASAGI, M., ZHU, B., ALONSO, A., WITTEN, E., MATSUOKA, K., NEUBERG, D., DUKE-COHAN, J. S., WU, C. J. & FREEMAN, G. J. 2013. CD40L-Tri, a novel formulation of recombinant human CD40L that effectively activates B cells. *Cancer Immunol Immunother,* 62**,** 347-57.

NAKAJIMA-TAKAGI, Y., OSAWA, M., OSHIMA, M., TAKAGI, H., MIYAGI, S., ENDOH, M., ENDO, T. A., TAKAYAMA, N., ETO, K., TOYODA, T., KOSEKI, H., NAKAUCHI, H. & IWAMA, A. 2013. Role of SOX17 in hematopoietic development from human embryonic stem cells. *Blood,* 121**,** 447-58.

NAKAMURA, Y., ANDO, K., CHARGUI, J., KAWADA, H., SATO, T., TSUJI, T., HOTTA, T. & KATO, S. 1999. Ex vivo generation of CD34(+) cells from CD34(-) hematopoietic cells. *Blood,* 94**,** 4053-9.

NAKANO, T., KODAMA, H. & HONJO, T. 1994. Generation of lymphohematopoietic cells from embryonic stem cells in culture. *Science,* 265**,** 1098-101.

NAMIKAWA, R., MUENCH, M. O., DE VRIES, J. E. & RONCAROLO, M. G. 1996. The FLK2/FLT3 ligand synergizes with interleukin-7 in promoting stromal-cell-independent expansion and differentiation of human fetal pro-B cells in vitro. *Blood,* 87**,** 1881-90.

NAVEIRAS, O., NARDI, V., WENZEL, P. L., HAUSCHKA, P. V., FAHEY, F. & DALEY, G. Q. 2009. Bone-marrow adipocytes as negative regulators of the haematopoietic microenvironment. *Nature,* 460**,** 259-U124.

NISHIKAWA, S. I., NISHIKAWA, S., HIRASHIMA, M., MATSUYOSHI, N. & KODAMA, H. 1998a. Progressive lineage analysis by cell sorting and culture identifies FLK1+VE-cadherin+ cells at a diverging point of endothelial and hemopoietic lineages. *Development,* 125**,** 1747-57.

NISHIKAWA, S. I., NISHIKAWA, S., KAWAMOTO, H., YOSHIDA, H., KIZUMOTO, M., KATAOKA, H. & KATSURA, Y. 1998b. In vitro generation of lymphohematopoietic cells from endothelial cells purified from murine embryos. *Immunity,* 8**,** 761-9.

NISHIMURA, T., KANEKO, S., KAWANA-TACHIKAWA, A., TAJIMA, Y., GOTO, H., ZHU, D., NAKAYAMA-HOSOYA, K., IRIGUCHI, S., UEMURA, Y., SHIMIZU, T., TAKAYAMA, N., YAMADA, D., NISHIMURA, K., OHTAKA, M., WATANABE, N., TAKAHASHI, S., IWAMOTO, A., KOSEKI, H., NAKANISHI, M., ETO, K. & NAKAUCHI, H. 2013. Generation of rejuvenated antigen-specific T cells by reprogramming to pluripotency and redifferentiation. *Cell Stem Cell,* 12**,** 114-26.

NIWA, A., HEIKE, T., UMEDA, K., OSHIMA, K., KATO, I., SAKAI, H., SUEMORI, H., NAKAHATA, T. & SAITO, M. K. 2011. A novel serum-free monolayer culture for orderly hematopoietic differentiation of human pluripotent cells via mesodermal progenitors. *PLoS One,* 6**,** e22261.

NIWA, H., MIYAZAKI, J. & SMITH, A. G. 2000. Quantitative expression of Oct-3/4 defines differentiation, dedifferentiation or self-renewal of ES cells. *Nat Genet,* 24**,** 372-6.

NODLAND, S. E., BERKOWSKA, M. A., BAJER, A. A., SHAH, N., DE RIDDER, D., VAN DONGEN, J. J., LEBIEN, T. W. & VAN ZELM, M. C. 2011. IL-7R expression and IL-7 signaling confer a distinct phenotype on developing human B-lineage cells. *Blood,* 118**,** 2116-27.

NOGUCHI, M., NAKAMURA, Y., RUSSELL, S. M., ZIEGLER, S. F., TSANG, M., CAO, X. & LEONARD, W. J. 1993. Interleukin-2 receptor gamma chain: a functional component of the interleukin-7 receptor. *Science,* 262**,** 1877-80.

NORTH, T., GU, T. L., STACY, T., WANG, Q., HOWARD, L., BINDER, M., MARIN-PADILLA, M. & SPECK, N. A. 1999. Cbfa2 is required for the formation of intra-aortic hematopoietic clusters. *Development,* 126**,** 2563-75.

NORTH, T. E., DE BRUIJN, M. F., STACY, T., TALEBIAN, L., LIND, E., ROBIN, C., BINDER, M., DZIERZAK, E. & SPECK, N. A. 2002. Runx1 expression marks long-term repopulating hematopoietic stem cells in the midgestation mouse embryo. *Immunity,* 16**,** 661-72.

NOSTRO, M. C., CHENG, X., KELLER, G. M. & GADUE, P. 2008. Wnt, activin, and BMP signaling regulate distinct stages in the developmental pathway from embryonic stem cells to blood. *Cell Stem Cell,* 2**,** 60-71.

NOTTA, F., DOULATOV, S., LAURENTI, E., POEPPL, A., JURISICA, I. & DICK, J. E. 2011. Isolation of single human hematopoietic stem cells capable of long-term multilineage engraftment. *Science,* 333**,** 218-21.

NOTTINGHAM, W. T., JARRATT, A., BURGESS, M., SPECK, C. L., CHENG, J. F., PRABHAKAR, S., RUBIN, E. M., LI, P. S., SLOANE-STANLEY, J., KONG, A. S. J. & DE BRUIJN, M. F. 2007. Runx1-mediated hematopoietic stem-cell emergence is controlled by a Gata/Ets/SCL-regulated enhancer. *Blood,* 110**,** 4188-97.

NOURRIT, F., DOYEN, N., KOURILSKY, P., ROUGEON, F. & CUMANO, A. 1998. Extensive junctional diversity of Ig heavy chain rearrangements generated in the progeny of single fetal multipotent hematopoietic cells in the absence of selection. *J Immunol,* 160**,** 4254-61.

NUTT, S. L., HEAVEY, B., ROLINK, A. G. & BUSSLINGER, M. 1999. Commitment to the B-lymphoid lineage depends on the transcription factor Pax5. *Nature,* 401**,** 556-62.

OBERLIN, E., EL HAFNY, B., PETIT-COCAULT, L. & SOUYRI, M. 2010a. Definitive human and mouse hematopoiesis originates from the embryonic endothelium: a new class of HSCs based on VE-cadherin expression. *Int J Dev Biol,* 54**,** 1165-73.

OBERLIN, E., FLEURY, M., CLAY, D., PETIT-COCAULT, L., CANDELIER, J. J., MENNESSON, B., JAFFREDO, T. & SOUYRI, M. 2010b. VE-cadherin expression allows identification of a new class of hematopoietic stem cells within human embryonic liver. *Blood,* 116**,** 4444-55.

OBERLIN, E., TAVIAN, M., BLAZSEK, I. & PEAULT, B. 2002. Blood-forming potential of vascular endothelium in the human embryo. *Development,* 129**,** 4147-57.

OETTINGER, M. A., SCHATZ, D. G., GORKA, C. & BALTIMORE, D. 1990. RAG-1 and RAG-2, adjacent genes that synergistically activate V(D)J recombination. *Science,* 248**,** 1517-23.

OGURO, H., DING, L. & MORRISON, S. J. 2013. SLAM Family Markers Resolve Functionally Distinct Subpopulations of Hematopoietic Stem Cells and Multipotent Progenitors. *Cell Stem Cell,* 13**,** 102-16.

OHGUSHI, M., MATSUMURA, M., EIRAKU, M., MURAKAMI, K., ARAMAKI, T., NISHIYAMA, A., MUGURUMA, K., NAKANO, T., SUGA, H., UENO, M., ISHIZAKI, T., SUEMORI, H., NARUMIYA, S., NIWA, H. & SASAI, Y. 2010. Molecular pathway and cell state responsible for dissociation-induced apoptosis in human pluripotent stem cells. *Cell Stem Cell,* 7**,** 225-39.

OHKAWARA, J. I., IKEBUCHI, K., FUJIHARA, M., SATO, N., HIRAYAMA, F., YAMAGUCHI, M., MORI, K. J. & SEKIGUCHI, S. 1998. Culture system for extensive production of CD19+IgM+ cells by human cord blood CD34+ progenitors. *Leukemia,* 12**,** 764-71.

OHNO, S., MORI, N. & MATSUNAGA, T. 1985. Antigen-binding specificities of antibodies are primarily determined by seven residues of VH. *Proc Natl Acad Sci U S A,* 82**,** 2945-9.

OKITA, K., MATSUMURA, Y., SATO, Y., OKADA, A., MORIZANE, A., OKAMOTO, S., HONG, H., NAKAGAWA, M., TANABE, K., TEZUKA, K., SHIBATA, T., KUNISADA, T., TAKAHASHI, M., TAKAHASHI, J., SAJI, H. & YAMANAKA, S. 2011. A more efficient method to generate integration-free human iPS cells. *Nat Methods,* 8**,** 409-12.

OKUDA, T., VAN DEURSEN, J., HIEBERT, S. W., GROSVELD, G. & DOWNING, J. R. 1996. AML1, the target of multiple chromosomal translocations in human leukemia, is essential for normal fetal liver hematopoiesis. *Cell,* 84**,** 321-30.

OLTZ, E. M., YANCOPOULOS, G. D., MORROW, M. A., ROLINK, A., LEE, G., WONG, F., KAPLAN, K., GILLIS, S., MELCHERS, F. & ALT, F. W. 1992. A novel regulatory myosin light chain gene distinguishes pre-B cell subsets and is IL-7 inducible. *EMBO J,* 11**,** 2759-67.

OSAWA, M., HANADA, K., HAMADA, H. & NAKAUCHI, H. 1996. Long-term lymphohematopoietic reconstitution by a single CD34-low/negative hematopoietic stem cell. *Science,* 273**,** 242-5.

OTTERSBACH, K. & DZIERZAK, E. 2005. The murine placenta contains hematopoietic stem cells within the vascular labyrinth region. *Dev Cell,* 8**,** 377-87.

PALACIOS, R., GOLUNSKI, E. & SAMARIDIS, J. 1995. In vitro generation of hematopoietic stem cells from an embryonic stem cell line. *Proc Natl Acad Sci U S A,* 92**,** 7530-4.

PALIS, J., CHAN, R. J., KONISKI, A., PATEL, R., STARR, M. & YODER, M. C. 2001. Spatial and temporal emergence of high proliferative potential hematopoietic precursors during murine embryogenesis. *Proc Natl Acad Sci U S A,* 98**,** 4528-4533.

PALIS, J., ROBERTSON, S., KENNEDY, M., WALL, C. & KELLER, G. 1999. Development of erythroid and myeloid progenitors in the yolk sac and embryo proper of the mouse. *Development,* 126**,** 5073-84.

PALIS, J. & YODER, M. C. 2001. Yolk-sac hematopoiesis: the first blood cells of mouse and man. *Exp Hematol,* 29**,** 927-36.

PARDANAUD, L., ALTMANN, C., KITOS, P., DIETERLEN-LIEVRE, F. & BUCK, C. A. 1987. Vasculogenesis in the early quail blastodisc as studied with a monoclonal antibody recognizing endothelial cells. *Development,* 100**,** 339-49.

PARDANAUD, L., LUTON, D., PRIGENT, M., BOURCHEIX, L. M., CATALA, M. & DIETERLEN-LIEVRE, F. 1996. Two distinct endothelial lineages in ontogeny, one of them related to hemopoiesis. *Development,* 122**,** 1363-71.

PARK, L. S., MARTIN, U., GARKA, K., GLINIAK, B., DI SANTO, J. P., MULLER, W., LARGAESPADA, D. A., COPELAND, N. G., JENKINS, N. A., FARR, A. G., ZIEGLER, S. F., MORRISSEY, P. J., PAXTON, R. & SIMS, J. E. 2000. Cloning of the murine thymic

stromal lymphopoietin (TSLP) receptor: Formation of a functional heteromeric complex requires interleukin 7 receptor. *J Exp Med,* 192**,** 659-70.

PARRISH, Y. K., BAEZ, I., MILFORD, T. A., BENITEZ, A., GALLOWAY, N., ROGERIO, J. W., SAHAKIAN, E., KAGODA, M., HUANG, G., HAO, Q. L., SEVILLA, Y., BARSKY, L. W., ZIELINSKA, E., PRICE, M. A., WALL, N. R., DOVAT, S. & PAYNE, K. J. 2009. IL-7 Dependence in human B lymphopoiesis increases during progression of ontogeny from cord blood to bone marrow. *J Immunol,* 182**,** 4255-66.

PASCUAL, V., VERKRUYSE, L., CASEY, M. L. & CAPRA, J. D. 1993. Analysis of Ig H chain gene segment utilization in human fetal liver. Revisiting the "proximal utilization hypothesis". *J Immunol,* 151**,** 4164-72.

PEARSON, S., SROCZYNSKA, P., LACAUD, G. & KOUSKOFF, V. 2008. The stepwise specification of embryonic stem cells to hematopoietic fate is driven by sequential exposure to Bmp4, activin A, bFGF and VEGF. *Development,* 135**,** 1525-35.

PEAULT, B., COLTEY, M. & LE DOUARIN, N. M. 1988. Ontogenic emergence of a quail leukocyte/endothelium cell surface antigen. *Cell Differ,* 23**,** 165-74.

PEREZ-ANDRES, M., GROSSERICHTER-WAGENER, C., TEODOSIO, C., VAN DONGEN, J. J., ORFAO, A. & VAN ZELM, M. C. 2011. The nature of circulating CD27+CD43+ B cells. *J Exp Med,* 208**,** 2565-6; author reply 2566-9.

PERLMUTTER, R. M., KEARNEY, J. F., CHANG, S. P. & HOOD, L. E. 1985. Developmentally controlled expression of immunoglobulin VH genes. *Science,* 227**,** 1597-601.

PESCHON, J. J., MORRISSEY, P. J., GRABSTEIN, K. H., RAMSDELL, F. J., MARASKOVSKY, E., GLINIAK, B. C., PARK, L. S., ZIEGLER, S. F., WILLIAMS, D. E., WARE, C. B., MEYER, J. D. & DAVISON, B. L. 1994. Early lymphocyte expansion is severely impaired in interleukin 7 receptor-deficient mice. *J Exp Med,* 180**,** 1955-60.

PICK, M., AZZOLA, L., MOSSMAN, A., STANLEY, E. G. & ELEFANTY, A. G. 2007. Differentiation of human embryonic stem cells in serum-free medium reveals distinct roles for bone morphogenetic protein 4, vascular endothelial growth factor, stem cell factor, and fibroblast growth factor 2 in hematopoiesis. *Stem Cells,* 25**,** 2206-14.

PLANELLES, L., CARVALHO-PINTO, C. E., HARDENBERG, G., SMANIOTTO, S., SAVINO, W., GOMEZ-CARO, R., ALVAREZ-MON, M., DE JONG, J., ELDERING, E., MARTINEZ, A. C., MEDEMA, J. P. & HAHNE, M. 2004. APRIL promotes B-1 cell-associated neoplasm. *Cancer Cell,* 6**,** 399-408.

PONCE, M. L. 2009. Tube formation: an in vitro matrigel angiogenesis assay. *Methods Mol Biol,* 467**,** 183-8.

POUGET, C., GAUTIER, R., TEILLET, M. A. & JAFFREDO, T. 2006. Somite-derived cells replace ventral aortic hemangioblasts and provide aortic smooth muscle cells of the trunk. *Development,* 133**,** 1013-22.

PRADO-LOPEZ, S., CONESA, A., ARMINAN, A., MARTINEZ-LOSA, M., ESCOBEDO-LUCEA, C., GANDIA, C., TARAZONA, S., MELGUIZO, D., BLESA, D., MONTANER, D., SANZ-GONZALEZ, S., SEPULVEDA, P., GOTZ, S., O'CONNOR, J. E., MORENO, R., DOPAZO, J., BURKS, D. J. & STOJKOVIC, M. 2010. Hypoxia promotes efficient differentiation of human embryonic stem cells to functional endothelium. *Stem Cells,* 28**,** 407-18.

PRICE, K. M., LITTLER, W. A. & CUMMINS, P. 1980. Human atrial and ventricular myosin light-chains subunits in the adult and during development. *Biochem J,* 191**,** 571-80.

PRIEYL, J. A. & LEBIEN, T. W. 1996. Interleukin 7 independent development of human B cells. *Proc Natl Acad Sci U S A,* 93**,** 10348-53.

PUEL, A., ZIEGLER, S. F., BUCKLEY, R. H. & LEONARD, W. J. 1998. Defective IL7R expression in T(-)B(+)NK(+) severe combined immunodeficiency. *Nat Genet,* 20**,** 394-7.

PURPURA, K. A., MORIN, J. & ZANDSTRA, P. W. 2008. Analysis of the temporal and concentration-dependent effects of BMP-4, VEGF, and TPO on development of embryonic stem cell-derived mesoderm and blood progenitors in a defined, serum-free media. *Exp Hematol,* 36**,** 1186-98.

RAFII, S., KLOSS, C. C., BUTLER, J. M., GINSBERG, M., GARS, E., LIS, R., ZHAN, Q., JOSIPOVIC, P., DING, B. S., XIANG, J., ELEMENTO, O., ZANINOVIC, N., ROSENWAKS, Z., SADELAIN, M., RAFII, J. A. & JAMES, D. 2012. Human ESC-derived hemogenic endothelial cells undergo distinct waves of endothelial to hematopoietic transition. *Blood*.

RAFII, S., KLOSS, C. C., BUTLER, J. M., GINSBERG, M., GARS, E., LIS, R., ZHAN, Q., JOSIPOVIC, P., DING, B. S., XIANG, J., ELEMENTO, O., ZANINOVIC, N., ROSENWAKS, Z., SADELAIN, M., RAFII, J. A. & JAMES, D. 2013. Human ESC-derived hemogenic endothelial cells undergo distinct waves of endothelial to hematopoietic transition. *Blood,* 121**,** 770-80.

RAMPON, C. & HUBER, P. 2003. Multilineage hematopoietic progenitor activity generated autonomously in the mouse yolk sac: analysis using angiogenesis-defective embryos. *Int J Dev Biol,* 47**,** 273-80.

RAWLINGS, D. J., QUAN, S. G., KATO, R. M. & WITTE, O. N. 1995a. Long-term culture system for selective growth of human B-cell progenitors. *Proc Natl Acad Sci U S A,* 92**,** 1570-4.

RAWLINGS, D. J., QUAN, S. G., KATO, R. M. & WITTE, O. N. 1995b. Long-Term Culture System for Selective Growth of Human B-Cell Progenitors. *Proc Natl Acad Sci U S A,* 92**,** 1570-1574.

RAY, A. & DITTEL, B. N. 2010. Isolation of mouse peritoneal cavity cells. *J Vis Exp*.

RAY, R. J., STODDART, A., PENNYCOOK, J. L., HUNER, H. O., FURLONGER, C., WU, G. E. & PAIGE, C. J. 1998. Stromal cell-independent maturation of IL-7-responsive pro-B cells. *J Immunol,* 160**,** 5886-97.

RAYA, A., RODRIGUEZ-PIZA, I., GUENECHEA, G., VASSENA, R., NAVARRO, S., BARRERO, M. J., CONSIGLIO, A., CASTELLA, M., RIO, P., SLEEP, E., GONZALEZ, F., TISCORNIA, G., GARRETA, E., AASEN, T., VEIGA, A., VERMA, I. M., SURRALLES, J., BUEREN, J. & IZPISUA BELMONTE, J. C. 2009. Disease-corrected haematopoietic progenitors from Fanconi anaemia induced pluripotent stem cells. *Nature,* 460**,** 53-9.

REIJMERS, R. M., GROEN, R. W., KUIL, A., WEIJER, K., KIMBERLEY, F. C., MEDEMA, J. P., VAN KUPPEVELT, T. H., LI, J. P., SPAARGAREN, M. & PALS, S. T. 2011. Disruption of heparan sulfate proteoglycan conformation perturbs B-cell maturation and APRIL-mediated plasma cell survival. *Blood,* 117**,** 6162-71.

RENNO, T., HAHNE, M., TSCHOPP, J. & MACDONALD, H. R. 1996. Peripheral T cells undergoing superantigen-induced apoptosis in vivo express B220 and upregulate Fas and Fas ligand. *J Exp Med,* 183**,** 431-7.

REUBINOFF, B. E., PERA, M. F., FONG, C. Y., TROUNSON, A. & BONGSO, A. 2000. Embryonic stem cell lines from human blastocysts: somatic differentiation in vitro. *Nat Biotechnol,* 18**,** 399-404.

REYA, T., DUNCAN, A. W., AILLES, L., DOMEN, J., SCHERER, D. C., WILLERT, K., HINTZ, L., NUSSE, R. & WEISSMAN, I. L. 2003. A role for Wnt signalling in self-renewal of haematopoietic stem cells. *Nature,* 423**,** 409-14.

REYNAUD, C. A. & WEILL, J. C. 2012. Gene profiling of CD11b(+) and CD11b(-) B1 cell subsets reveals potential cell sorting artifacts. *J Exp Med,* 209**,** 433-4; author reply 434-6.

RICHARD, C., DREVON, C., CANTO, P. Y., VILLAIN, G., BOLLEROT, K., LEMPEREUR, A., TEILLET, M. A., VINCENT, C., ROSSELLO CASTILLO, C., TORRES, M., PIWARZYK, E., SPECK, N. A., SOUYRI, M. & JAFFREDO, T. 2013. Endothelio-mesenchymal interaction controls runx1 expression and modulates the notch pathway to initiate aortic hematopoiesis. *Dev Cell,* 24**,** 600-11.

RICHIE EHRLICH, L. I., SERWOLD, T. & WEISSMAN, I. L. 2011. In vitro assays misrepresent in vivo lineage potentials of murine lymphoid progenitors. *Blood,* 117**,** 2618-24.

ROBB, L., LYONS, I., LI, R., HARTLEY, L., KONTGEN, F., HARVEY, R. P., METCALF, D. & BEGLEY, C. G. 1995. Absence of yolk sac hematopoiesis from mice with a targeted disruption of the scl gene. *Proc Natl Acad Sci U S A,* 92**,** 7075-9.

ROBERTSON, S. M., KENNEDY, M., SHANNON, J. M. & KELLER, G. 2000. A transitional stage in the commitment of mesoderm to hematopoiesis requiring the transcription factor SCL/tal-1. *Development,* 127**,** 2447-59.

ROBIN, C., OTTERSBACH, K., BOISSET, J. C., OZIEMLAK, A. & DZIERZAK, E. 2011. CD41 is developmentally regulated and differentially expressed on mouse hematopoietic stem cells. *Blood,* 117**,** 5088-91.

ROITT, I. M., GREAVES, M. F., TORRIGIANI, G., BROSTOFF, J. & PLAYFAIR, J. H. 1969. The cellular basis of immunological responses. A synthesis of some current views. *Lancet,* 2**,** 367-71.

ROLINK, A., KUDO, A., KARASUYAMA, H., KIKUCHI, Y. & MELCHERS, F. 1991. Long-term proliferating early pre B cell lines and clones with the potential to develop to surface Ig-positive, mitogen reactive B cells in vitro and in vivo. *EMBO J,* 10**,** 327-36.

ROLINK, A. G., WINKLER, T., MELCHERS, F. & ANDERSSON, J. 2000. Precursor B cell receptor-dependent B cell proliferation and differentiation does not require the bone marrow or fetal liver environment. *J Exp Med,* 191**,** 23-32.

ROUBELAKIS, M. G., TSAKNAKIS, G., PAPPA, K. I., ANAGNOU, N. P. & WATT, S. M. 2013. Spindle shaped human mesenchymal stem/stromal cells from amniotic fluid promote neovascularization. *PLoS One,* 8**,** e54747.

RUIZ-HERGUIDO, C., GUIU, J., D'ALTRI, T., INGLES-ESTEVE, J., DZIERZAK, E., ESPINOSA, L. & BIGAS, A. 2012. Hematopoietic stem cell development requires transient Wnt/beta-catenin activity. *J Exp Med,* 209**,** 1457-68.

RYBTSOV, S., SOBIESIAK, M., TAOUDI, S., SOUILHOL, C., SENSERRICH, J., LIAKHOVITSKAIA, A., IVANOVS, A., FRAMPTON, J., ZHAO, S. & MEDVINSKY, A. 2011. Hierarchical organization and early hematopoietic specification of the developing HSC lineage in the AGM region. *J Exp Med,* 208**,** 1305-15.

SABIN, F. R. 1920. Studies on the origin of blood vessels and of red corpuscles as seen in the living blastoderm of the chick during the second day of incubation. *Contributions to Embryology,* 9**,** 213-262.

SAKURAI, H., ERA, T., JAKT, L. M., OKADA, M., NAKAI, S. & NISHIKAWA, S. 2006. In vitro modeling of paraxial and lateral mesoderm differentiation reveals early reversibility. *Stem Cells,* 24**,** 575-86.

SAKURAI, H., SAKAGUCHI, Y., SHOJI, E., NISHINO, T., MAKI, I., SAKAI, H., HANAOKA, K., KAKIZUKA, A. & SEHARA-FUJISAWA, A. 2012. In vitro modeling of paraxial mesodermal progenitors derived from induced pluripotent stem cells. *PLoS One,* 7**,** e47078.

SALVAGIOTTO, G., BURTON, S., DAIGH, C. A., RAJESH, D., SLUKVIN, II & SEAY, N. J. 2011. A defined, feeder-free, serum-free system to generate in vitro hematopoietic progenitors and differentiated blood cells from hESCs and hiPSCs. *PLoS One,* 6**,** e17829.

SAMOKHVALOV, I. M., SAMOKHVALOVA, N. I. & NISHIKAWA, S. 2007. Cell tracing shows the contribution of the yolk sac to adult haematopoiesis. *Nature,* 446**,** 1056-61.

SANZ, E., MUNOZ, A. N., MONSERRAT, J., VAN-DEN-RYM, A., ESCOLL, P., RANZ, I., ALVAREZ-MON, M. & DE-LA-HERA, A. 2010. Ordering human CD34+CD10-CD19+ pre/pro-B-cell and CD19- common lymphoid progenitor stages in two pro-B-cell development pathways. *Proc Natl Acad Sci U S A,* 107**,** 5925-30.

SCHATTEMAN, G. C., MORRISON-GRAHAM, K., VAN KOPPEN, A., WESTON, J. A. & BOWEN-POPE, D. F. 1992. Regulation and role of PDGF receptor alpha-subunit expression during embryogenesis. *Development,* 115**,** 123-31.

SCHEID, J. F., MOUQUET, H., FELDHAHN, N., SEAMAN, M. S., VELINZON, K., PIETZSCH, J., OTT, R. G., ANTHONY, R. M., ZEBROSKI, H., HURLEY, A., PHOGAT, A., CHAKRABARTI, B., LI, Y., CONNORS, M., PEREYRA, F., WALKER, B. D., WARDEMANN, H., HO, D., WYATT, R. T., MASCOLA, J. R., RAVETCH, J. V. & NUSSENZWEIG, M. C. 2009. Broad diversity of neutralizing antibodies isolated from memory B cells in HIV-infected individuals. *Nature,* 458**,** 636-40.

SCHMIDT, M. R., APPEL, M. C., GIASSI, L. J., GREINER, D. L., SHULTZ, L. D. & WOODLAND, R. T. 2008. Human BLyS facilitates engraftment of human PBL derived B cells in immunodeficient mice. *PLoS One,* 3**,** e3192.

SCHROEDER, H. W., JR., HILLSON, J. L. & PERLMUTTER, R. M. 1987. Early restriction of the human antibody repertoire. *Science,* 238**,** 791-3.

SCHULZ, C., GOMEZ PERDIGUERO, E., CHORRO, L., SZABO-ROGERS, H., CAGNARD, N., KIERDORF, K., PRINZ, M., WU, B., JACOBSEN, S. E., POLLARD, J. W., FRAMPTON, J., LIU, K. J. & GEISSMANN, F. 2012. A lineage of myeloid cells independent of Myb and hematopoietic stem cells. *Science,* 336**,** 86-90.

SCOTT, E. W., SIMON, M. C., ANASTASI, J. & SINGH, H. 1994. Requirement of transcription factor PU.1 in the development of multiple hematopoietic lineages. *Science,* 265**,** 1573-7.

SEIDL, K. J., WILSHIRE, J. A., MACKENZIE, J. D., KANTOR, A. B. & HERZENBERG, L. A. 1999. Predominant VH genes expressed in innate antibodies are associated with distinctive antigen-binding sites. *Proc Natl Acad Sci U S A,* 96**,** 2262-7.

SEKIYA, S. & SUZUKI, A. 2011. Direct conversion of mouse fibroblasts to hepatocyte-like cells by defined factors. *Nature,* 475**,** 390-3.

SERWOLD, T., HOCHEDLINGER, K., SWINDLE, J., HEDGPETH, J., JAENISCH, R. & WEISSMAN, I. L. 2010. T-cell receptor-driven lymphomagenesis in mice derived from a reprogrammed T cell. *Proc Natl Acad Sci U S A,* 107**,** 18939-43.

SHALABY, F., ROSSANT, J., YAMAGUCHI, T. P., GERTSENSTEIN, M., WU, X. F., BREITMAN, M. L. & SCHUH, A. C. 1995. Failure of blood-island formation and vasculogenesis in Flk-1-deficient mice. *Nature,* 376**,** 62-6.

SHEPARD, J. L. & ZON, L. I. 2000. Developmental derivation of embryonic and adult macrophages. *Curr Opin Hematol,* 7**,** 3-8.

SHU, J., WU, C., WU, Y., LI, Z., SHAO, S., ZHAO, W., TANG, X., YANG, H., SHEN, L., ZUO, X., YANG, W., SHI, Y., CHI, X., ZHANG, H., GAO, G., SHU, Y., YUAN, K., HE, W., TANG, C., ZHAO, Y. & DENG, H. 2013. Induction of pluripotency in mouse somatic cells with lineage specifiers. *Cell,* 153**,** 963-75.

SHULTZ, L. D., BREHM, M. A., GARCIA-MARTINEZ, J. V. & GREINER, D. L. 2012. Humanized mice for immune system investigation: progress, promise and challenges. *Nat Rev Immunol,* 12**,** 786-98.

SHULTZ, L. D., LYONS, B. L., BURZENSKI, L. M., GOTT, B., CHEN, X., CHALEFF, S., KOTB, M., GILLIES, S. D., KING, M., MANGADA, J., GREINER, D. L. & HANDGRETINGER, R. 2005. Human lymphoid and myeloid cell development in NOD/LtSz-scid IL2R gamma null mice engrafted with mobilized human hemopoietic stem cells. *J Immunol,* 174**,** 6477-89.

SIEBURG, H. B., CHO, R. H., DYKSTRA, B., UCHIDA, N., EAVES, C. J. & MULLER-SIEBURG, C. E. 2006. The hematopoietic stem compartment consists of a limited number of discrete stem cell subsets. *Blood,* 107**,** 2311-6.

SITNICKA, E., BRAKEBUSCH, C., MARTENSSON, I. L., SVENSSON, M., AGACE, W. W., SIGVARDSSON, M., BUZA-VIDAS, N., BRYDER, D., CILIO, C. M., AHLENIUS, H., MARASKOVSKY, E., PESCHON, J. J. & JACOBSEN, S. E. 2003. Complementary signaling through flt3 and interleukin-7 receptor alpha is indispensable for fetal and adult B cell genesis. *J Exp Med,* 198**,** 1495-506.

SITNICKA, E., BRYDER, D., THEILGAARD-MONCH, K., BUZA-VIDAS, N., ADOLFSSON, J. & JACOBSEN, S. E. 2002. Key role of flt3 ligand in regulation of the common lymphoid progenitor but not in maintenance of the hematopoietic stem cell pool. *Immunity,* 17**,** 463-72.

SOLAR, G., DESAUVAGE, F., EATON, D. & COHEN, B. 1997. Role of c-Mpl in early hematopoiesis. *Blood,* 90**,** 2544-2544.

SOLDNER, F., HOCKEMEYER, D., BEARD, C., GAO, Q., BELL, G. W., COOK, E. G., HARGUS, G., BLAK, A., COOPER, O., MITALIPOVA, M., ISACSON, O. & JAENISCH, R. 2009. Parkinson's disease patient-derived induced pluripotent stem cells free of viral reprogramming factors. *Cell,* 136**,** 964-77.

SOZA-RIED, C., HESS, I., NETUSCHIL, N., SCHORPP, M. & BOEHM, T. 2010. Essential role of c-myb in definitive hematopoiesis is evolutionarily conserved. *Proc Natl Acad Sci U S A,* 107**,** 17304-8.

SPANGRUDE, G. J., HEIMFELD, S. & WEISSMAN, I. L. 1988. Purification and characterization of mouse hematopoietic stem cells. *Science,* 241**,** 58-62.

STADTFELD, M., APOSTOLOU, E., AKUTSU, H., FUKUDA, A., FOLLETT, P., NATESAN, S., KONO, T., SHIODA, T. & HOCHEDLINGER, K. 2010. Aberrant silencing of imprinted genes on chromosome 12qF1 in mouse induced pluripotent stem cells. *Nature,* 465**,** 175-81.

STADTFELD, M., APOSTOLOU, E., FERRARI, F., CHOI, J., WALSH, R. M., CHEN, T., OOI, S. S., KIM, S. Y., BESTOR, T. H., SHIODA, T., PARK, P. J. & HOCHEDLINGER, K. 2012. Ascorbic acid prevents loss of Dlk1-Dio3 imprinting and facilitates generation of

all-iPS cell mice from terminally differentiated B cells. *Nat Genet,* 44**,** 398-405, S1-2.

SUBRAMANIAN, A., GUO, B., MARSDEN, M. D., GALIC, Z., KITCHEN, S., KACENA, A., BROWN, H. J., CHENG, G. & ZACK, J. A. 2009. Macrophage differentiation from embryoid bodies derived from human embryonic stem cells. *J Stem Cells,* 4**,** 29-45.

SUGIYAMA, D., OGAWA, M., HIROSE, I., JAFFREDO, T., ARAI, K. & TSUJI, K. 2003. Erythropoiesis from acetyl LDL incorporating endothelial cells at the preliver stage. *Blood,* 101**,** 4733-8.

SUGIYAMA, D., OGAWA, M., NAKAO, K., OSUMI, N., NISHIKAWA, S., NISHIKAWA, S., ARAI, K., NAKAHATA, T. & TSUJI, K. 2007. B cell potential can be obtained from pre-circulatory yolk sac, but with low frequency. *Dev Biol,* 301**,** 53-61.

SUMNER, R., CRAWFORD, A., MUCENSKI, M. & FRAMPTON, J. 2000. Initiation of adult myelopoiesis can occur in the absence of c-Myb whereas subsequent development is strictly dependent on the transcription factor. *Oncogene,* 19**,** 3335-42.

SUN, N., PANETTA, N. J., GUPTA, D. M., WILSON, K. D., LEE, A., JIA, F., HU, S., CHERRY, A. M., ROBBINS, R. C., LONGAKER, M. T. & WU, J. C. 2009. Feeder-free derivation of induced pluripotent stem cells from adult human adipose stem cells. *Proc Natl Acad Sci U S A,* 106**,** 15720-5.

SZILVASSY, S. J., HUMPHRIES, R. K., LANSDORP, P. M., EAVES, A. C. & EAVES, C. J. 1990. Quantitative assay for totipotent reconstituting hematopoietic stem cells by a competitive repopulation strategy. *Proc Natl Acad Sci U S A,* 87**,** 8736-40.

TADA, S., ERA, T., FURUSAWA, C., SAKURAI, H., NISHIKAWA, S., KINOSHITA, M., NAKAO, K. & CHIBA, T. 2005. Characterization of mesendoderm: a diverging point of the definitive endoderm and mesoderm in embryonic stem cell differentiation culture. *Development,* 132**,** 4363-74.

TAKAHASHI, K., TANABE, K., OHNUKI, M., NARITA, M., ICHISAKA, T., TOMODA, K. & YAMANAKA, S. 2007. Induction of pluripotent stem cells from adult human fibroblasts by defined factors. *Cell,* 131**,** 861-72.

TAKAHASHI, K. & YAMANAKA, S. 2006. Induction of pluripotent stem cells from mouse embryonic and adult fibroblast cultures by defined factors. *Cell,* 126**,** 663-76.

TAOUDI, S., GONNEAU, C., MOORE, K., SHERIDAN, J. M., BLACKBURN, C. C., TAYLOR, E. & MEDVINSKY, A. 2008. Extensive hematopoietic stem cell generation in the AGM region via maturation of VE-cadherin+CD45+ pre-definitive HSCs. *Cell Stem Cell,* 3**,** 99-108.

TAURA, D., SONE, M., HOMMA, K., OYAMADA, N., TAKAHASHI, K., TAMURA, N., YAMANAKA, S. & NAKAO, K. 2009. Induction and isolation of vascular cells from human induced pluripotent stem cells--brief report. *Arterioscler Thromb Vasc Biol,* 29**,** 1100-3.

TAVIAN, M., COULOMBEL, L., LUTON, D., CLEMENTE, H. S., DIETERLEN-LIEVRE, F. & PEAULT, B. 1996. Aorta-associated CD34+ hematopoietic cells in the early human embryo. *Blood,* 87**,** 67-72.

TAVIAN, M., HALLAIS, M. F. & PEAULT, B. 1999. Emergence of intraembryonic hematopoietic precursors in the pre-liver human embryo. *Development,* 126**,** 793-803.

TAVIAN, M., ROBIN, C., COULOMBEL, L. & PEAULT, B. 2001. The human embryo, but not its yolk sac, generates lympho-myeloid stem cells: mapping multipotent hematopoietic cell fate in intraembryonic mesoderm. *Immunity,* 15**,** 487-95.

TAYLOR, E., TAOUDI, S. & MEDVINSKY, A. 2010. Hematopoietic stem cell activity in the aorta-gonad-mesonephros region enhances after mid-day 11 of mouse development. *Int J Dev Biol,* 54**,** 1055-60.

TCHIEU, J., KUOY, E., CHIN, M. H., TRINH, H., PATTERSON, M., SHERMAN, S. P., AIMIUWU, O., LINDGREN, A., HAKIMIAN, S., ZACK, J. A., CLARK, A. T., PYLE, A. D., LOWRY, W. E. & PLATH, K. 2010. Female human iPSCs retain an inactive X chromosome. *Cell Stem Cell,* 7**,** 329-42.

TESAR, P. J., CHENOWETH, J. G., BROOK, F. A., DAVIES, T. J., EVANS, E. P., MACK, D. L., GARDNER, R. L. & MCKAY, R. D. 2007. New cell lines from mouse epiblast share defining features with human embryonic stem cells. *Nature,* 448**,** 196-9.

THOMSON, J. A., ITSKOVITZ-ELDOR, J., SHAPIRO, S. S., WAKNITZ, M. A., SWIERGIEL, J. J., MARSHALL, V. S. & JONES, J. M. 1998. Embryonic stem cell lines derived from human blastocysts. *Science,* 282**,** 1145-7.

THROSBY, M., VAN DEN BRINK, E., JONGENEELEN, M., POON, L. L., ALARD, P., CORNELISSEN, L., BAKKER, A., COX, F., VAN DEVENTER, E., GUAN, Y., CINATL, J., TER MEULEN, J., LASTERS, I., CARSETTI, R., PEIRIS, M., DE KRUIF, J. & GOUDSMIT, J. 2008. Heterosubtypic neutralizing monoclonal antibodies cross-protective against H5N1 and H1N1 recovered from human IgM+ memory B cells. *PLoS One,* 3**,** e3942.

TIAN, X., HEXUM, M. K., PENCHEV, V. R., TAYLOR, R. J., SHULTZ, L. D. & KAUFMAN, D. S. 2009. Bioluminescent imaging demonstrates that transplanted human embryonic stem cell-derived CD34(+) cells preferentially develop into endothelial cells. *Stem Cells,* 27**,** 2675-85.

TIAN, X., WOLL, P. S., MORRIS, J. K., LINEHAN, J. L. & KAUFMAN, D. S. 2006. Hematopoietic engraftment of human embryonic stem cell-derived cells is regulated by recipient innate immunity. *Stem Cells,* 24**,** 1370-80.

TIMMERMANS, F., VELGHE, I., VANWALLEGHEM, L., DE SMEDT, M., VAN COPPERNOLLE, S., TAGHON, T., MOORE, H. D., LECLERCQ, G., LANGERAK, A. W., KERRE, T., PLUM, J. & VANDEKERCKHOVE, B. 2009. Generation of T cells from human embryonic stem cell-derived hematopoietic zones. *J Immunol,* 182**,** 6879-88.

TOMODA, K., TAKAHASHI, K., LEUNG, K., OKADA, A., NARITA, M., YAMADA, N. A., EILERTSON, K. E., TSANG, P., BABA, S., WHITE, M. P., SAMI, S., SRIVASTAVA, D., CONKLIN, B. R., PANNING, B. & YAMANAKA, S. 2012. Derivation conditions impact X-inactivation status in female human induced pluripotent stem cells. *Cell Stem Cell,* 11**,** 91-9.

TONEGAWA, S. 1983. Somatic generation of antibody diversity. *Nature,* 302**,** 575-81.

TRUMPP, A., ESSERS, M. & WILSON, A. 2010. Awakening dormant haematopoietic stem cells. *Nat Rev Immunol,* 10**,** 201-9.

TSAI, F. Y., KELLER, G., KUO, F. C., WEISS, M., CHEN, J., ROSENBLATT, M., ALT, F. W. & ORKIN, S. H. 1994a. An early haematopoietic defect in mice lacking the transcription factor GATA-2. *Nature,* 371**,** 221-6.

TSAI, F. Y. & ORKIN, S. H. 1997. Transcription factor GATA-2 is required for proliferation/survival of early hematopoietic cells and mast cell formation, but not for erythroid and myeloid terminal differentiation. *Blood,* 89**,** 3636-43.

TSAI, L. H., WHITE, L., RAINES, E., ROSS, R., SMITH, R. G., CUSHLEY, W. & OZANNE, B. 1994b. Expression of platelet-derived growth factor and its receptors by two pre-B acute lymphocytic leukemia cell lines. *Blood,* 83**,** 51-5.

UCKUN, F. M., SUN, L., QAZI, S., MA, H. & OZER, Z. 2011. Recombinant human CD19-ligand protein as a potent anti-leukaemic agent. *Br J Haematol,* 153**,** 15-23.

VALLIER, L., TOUBOUL, T., CHNG, Z., BRIMPARI, M., HANNAN, N., MILLAN, E., SMITHERS, L. E., TROTTER, M., RUGG-GUNN, P., WEBER, A. & PEDERSEN, R. A. 2009. Early cell fate decisions of human embryonic stem cells and mouse epiblast stem cells are controlled by the same signalling pathways. *PLoS One,* 4**,** e6082.

VAN WYNSBERGHE, P. M., KAI, Z. S., MASSIRER, K. B., BURTON, V. H., YEO, G. W. & PASQUINELLI, A. E. 2011. LIN-28 co-transcriptionally binds primary let-7 to regulate miRNA maturation in Caenorhabditis elegans. *Nat Struct Mol Biol,* 18**,** 302-8.

VIERBUCHEN, T., OSTERMEIER, A., PANG, Z. P., KOKUBU, Y., SUDHOF, T. C. & WERNIG, M. 2010. Direct conversion of fibroblasts to functional neurons by defined factors. *Nature,* 463**,** 1035-U50.

VODYANIK, M. A., BORK, J. A., THOMSON, J. A. & SLUKVIN, II 2005. Human embryonic stem cell-derived CD34+ cells: efficient production in the coculture with OP9 stromal cells and analysis of lymphohematopoietic potential. *Blood,* 105**,** 617-26.

VODYANIK, M. A. & SLUKVIN, II 2007. Hematoendothelial differentiation of human embryonic stem cells. *Curr Protoc Cell Biol,* Chapter 23**,** Unit 23 6.

VODYANIK, M. A., THOMSON, J. A. & SLUKVIN, II 2006. Leukosialin (CD43) defines hematopoietic progenitors in human embryonic stem cell differentiation cultures. *Blood,* 108**,** 2095-105.

VON FREEDEN-JEFFRY, U., VIEIRA, P., LUCIAN, L. A., MCNEIL, T., BURDACH, S. E. & MURRAY, R. 1995. Lymphopenia in interleukin (IL)-7 gene-deleted mice identifies IL-7 as a nonredundant cytokine. *J Exp Med,* 181**,** 1519-26.

VOSSHENRICH, C. A., CUMANO, A., MULLER, W., DI SANTO, J. P. & VIEIRA, P. 2003. Thymic stromal-derived lymphopoietin distinguishes fetal from adult B cell development. *Nat Immunol,* 4**,** 773-9.

WADA, H., KOJO, S., KUSAMA, C., OKAMOTO, N., SATO, Y., ISHIZUKA, B. & SEINO, K. 2011. Successful differentiation to T cells, but unsuccessful B-cell generation, from B-cell-derived induced pluripotent stem cells. *Int Immunol,* 23**,** 65-74.

WADDINGTON, C. H. 1957. The Strategy of the Genes. *Geo Allen & Unwin*.

WAGAR, E. J., CROMWELL, M. A., SHULTZ, L. D., WODA, B. A., SULLIVAN, J. L., HESSELTON, R. M. & GREINER, D. L. 2000. Regulation of human cell engraftment and development of EBV-related lymphoproliferative disorders in Hu-PBL-scid mice. *J Immunol,* 165**,** 518-27.

WAGNER, J. E., KERNAN, N. A., STEINBUCH, M., BROXMEYER, H. E. & GLUCKMAN, E. 1995. Allogeneic sibling umbilical-cord-blood transplantation in children with malignant and non-malignant disease. *Lancet,* 346**,** 214-9.

WAKAO, H., YOSHIKIYO, K., KOSHIMIZU, U., FURUKAWA, T., ENOMOTO, K., MATSUNAGA, T., TANAKA, T., YASUTOMI, Y., YAMADA, T., MINAKAMI, H., TANAKA, J., ODA, A., SASAKI, T., WAKAO, R., LANTZ, O., UDAGAWA, T., SEKIYA, Y., HIGUCHI, K., HARADA, N., NISHIMURA, K., OHTAKA, M., NAKANISHI, M. & FUJITA, H. 2013. Expansion of functional human mucosal-associated invariant T cells via reprogramming to pluripotency and redifferentiation. *Cell Stem Cell,* 12**,** 546-58.

WALLS, J. R., COULTAS, L., ROSSANT, J. & HENKELMAN, R. M. 2008. Three-dimensional analysis of vascular development in the mouse embryo. *PLoS One,* 3**,** e2853.

WANDEL, E., SAALBACH, A., SITTIG, D., GEBHARDT, C. & AUST, G. 2012. Thy-1 (CD90) is an interacting partner for CD97 on activated endothelial cells. *J Immunol,* 188**,** 1442-50.

WANG, C., TANG, X., SUN, X., MIAO, Z., LV, Y., YANG, Y., ZHANG, H., ZHANG, P., LIU, Y., DU, L., GAO, Y., YIN, M., DING, M. & DENG, H. 2012. TGFbeta inhibition enhances the generation of hematopoietic progenitors from human ES cell-derived hemogenic endothelial cells using a stepwise strategy. *Cell Res,* 22**,** 194-207.

WANG, L., MENENDEZ, P., CERDAN, C. & BHATIA, M. 2005a. Hematopoietic development from human embryonic stem cell lines. *Exp Hematol,* 33**,** 987-96.

WANG, L., MENENDEZ, P., SHOJAEI, F., LI, L., MAZURIER, F., DICK, J. E., CERDAN, C., LEVAC, K. & BHATIA, M. 2005b. Generation of hematopoietic repopulating cells from human embryonic stem cells independent of ectopic HOXB4 expression. *J Exp Med,* 201**,** 1603-14.

WANG, Q., STACY, T., BINDER, M., MARIN-PADILLA, M., SHARPE, A. H. & SPECK, N. A. 1996. Disruption of the Cbfa2 gene causes necrosis and hemorrhaging in the central nervous system and blocks definitive hematopoiesis. *Proc Natl Acad Sci U S A,* 93**,** 3444-9.

WARREN, L., MANOS, P. D., AHFELDT, T., LOH, Y. H., LI, H., LAU, F., EBINA, W., MANDAL, P. K., SMITH, Z. D., MEISSNER, A., DALEY, G. Q., BRACK, A. S., COLLINS, J. J., COWAN, C., SCHLAEGER, T. M. & ROSSI, D. J. 2010. Highly efficient reprogramming to pluripotency and directed differentiation of human cells with synthetic modified mRNA. *Cell Stem Cell,* 7**,** 618-30.

WATANABE, K., UENO, M., KAMIYA, D., NISHIYAMA, A., MATSUMURA, M., WATAYA, T., TAKAHASHI, J. B., NISHIKAWA, S., MUGURUMA, K. & SASAI, Y. 2007. A ROCK inhibitor permits survival of dissociated human embryonic stem cells. *Nat Biotechnol,* 25**,** 681-6.

WATERSTON, R. H., LINDBLAD-TOH, K., BIRNEY, E., ROGERS, J., ABRIL, J. F., AGARWAL, P., AGARWALA, R., AINSCOUGH, R., ALEXANDERSSON, M., AN, P., ANTONARAKIS, S. E., ATTWOOD, J., BAERTSCH, R., BAILEY, J., BARLOW, K., BECK, S., BERRY, E., BIRREN, B., BLOOM, T., BORK, P., BOTCHERBY, M., BRAY, N., BRENT, M. R., BROWN, D. G., BROWN, S. D., BULT, C., BURTON, J., BUTLER, J., CAMPBELL, R. D., CARNINCI, P., CAWLEY, S., CHIAROMONTE, F., CHINWALLA, A. T., CHURCH, D. M., CLAMP, M., CLEE, C., COLLINS, F. S., COOK, L. L., COPLEY, R. R., COULSON, A., COURONNE, O., CUFF, J., CURWEN, V., CUTTS, T., DALY, M., DAVID, R., DAVIES, J., DELEHAUNTY, K. D., DERI, J., DERMITZAKIS, E. T., DEWEY, C., DICKENS, N. J., DIEKHANS, M., DODGE, S., DUBCHAK, I., DUNN, D. M., EDDY, S. R., ELNITSKI, L., EMES, R. D., ESWARA, P., EYRAS, E., FELSENFELD, A., FEWELL, G. A., FLICEK, P., FOLEY, K., FRANKEL, W. N., FULTON, L. A., FULTON, R. S., FUREY, T. S., GAGE, D., GIBBS, R. A., GLUSMAN, G., GNERRE, S., GOLDMAN, N., GOODSTADT, L., GRAFHAM, D., GRAVES, T. A., GREEN, E. D., GREGORY, S., GUIGO, R., GUYER, M., HARDISON, R. C., HAUSSLER, D., HAYASHIZAKI, Y., HILLIER, L. W., HINRICHS, A., HLAVINA, W., HOLZER, T., HSU, F., HUA, A., HUBBARD, T., HUNT, A., JACKSON, I., JAFFE, D. B., JOHNSON, L. S., JONES, M., JONES, T. A., JOY, A., KAMAL, M., KARLSSON, E. K., et al. 2002. Initial sequencing and comparative analysis of the mouse genome. *Nature,* 420**,** 520-62.

WATT, S. M., ATHANASSOPOULOS, A., HARRIS, A. L. & TSAKNAKIS, G. 2010. Human endothelial stem/progenitor cells, angiogenic factors and vascular repair. *J R Soc Interface,* 7 Suppl 6**,** S731-51.

WEINSTEIN, J. A., JIANG, N., WHITE, R. A., 3RD, FISHER, D. S. & QUAKE, S. R. 2009. High-throughput sequencing of the zebrafish antibody repertoire. *Science,* 324**,** 807-10.

WEISSMAN, I. L., ANDERSON, D. J. & GAGE, F. 2001. Stem and progenitor cells: origins, phenotypes, lineage commitments, and transdifferentiations. *Annu Rev Cell Dev Biol,* 17**,** 387-403.

WESEMANN, D. R., PORTUGUESE, A. J., MAGEE, J. M., GALLAGHER, M. P., ZHOU, X., PANCHAKSHARI, R. A. & ALT, F. W. 2012. Reprogramming IgH isotype-switched B cells to functional-grade induced pluripotent stem cells. *Proc Natl Acad Sci U S A,* 109**,** 13745-50.

WETZEL, A., CHAVAKIS, T., PREISSNER, K. T., STICHERLING, M., HAUSTEIN, U. F., ANDEREGG, U. & SAALBACH, A. 2004. Human Thy-1 (CD90) on activated endothelial cells is a counterreceptor for the leukocyte integrin Mac-1 (CD11b/CD18). *J Immunol,* 172**,** 3850-9.

WHITLOCK, C. A., ROBERTSON, D. & WITTE, O. N. 1984. Murine B cell lymphopoiesis in long term culture. *J Immunol Methods,* 67**,** 353-69.

WHITLOCK, C. A. & WITTE, O. N. 1982. Long-term culture of B lymphocytes and their precursors from murine bone marrow. *Proc Natl Acad Sci U S A,* 79**,** 3608-12.

WILSON, A., MACDONALD, H. R. & RADTKE, F. 2001. Notch 1-deficient common lymphoid precursors adopt a B cell fate in the thymus. *J Exp Med,* 194**,** 1003-12.

WINTER, J., JUNG, S., KELLER, S., GREGORY, R. I. & DIEDERICHS, S. 2009. Many roads to maturity: microRNA biogenesis pathways and their regulation. *Nat Cell Biol,* 11**,** 228-34.

WOLF, M. L., BUCKLEY, J. A., GOLDFARB, A., LAW, C. L. & LEBIEN, T. W. 1991. Development of a bone marrow culture for maintenance and growth of normal human B cell precursors. *J Immunol,* 147**,** 3324-30.

WU, A. M., TILL, J. E., SIMINOVITCH, L. & MCCULLOCH, E. A. 1967. A cytological study of the capacity for differentiation of normal hemopoietic colony-forming cells. *J Cell Physiol,* 69**,** 177-84.

YAHATA, T., MUGURUMA, Y., YUMINO, S., SHENG, Y., UNO, T., MATSUZAWA, H., ITO, M., KATO, S., HOTTA, T. & ANDO, K. 2008. Quiescent human hematopoietic stem cells in the bone marrow niches organize the hierarchical structure of hematopoiesis. *Stem Cells,* 26**,** 3228-36.

YAMASHITA, J., ITOH, H., HIRASHIMA, M., OGAWA, M., NISHIKAWA, S., YURUGI, T., NAITO, M. & NAKAO, K. 2000. Flk1-positive cells derived from embryonic stem cells serve as vascular progenitors. *Nature,* 408**,** 92-6.

YANG, L., SOONPAA, M. H., ADLER, E. D., ROEPKE, T. K., KATTMAN, S. J., KENNEDY, M., HENCKAERTS, E., BONHAM, K., ABBOTT, G. W., LINDEN, R. M., FIELD, L. J. & KELLER, G. M. 2008. Human cardiovascular progenitor cells develop from a KDR+ embryonic-stem-cell-derived population. *Nature,* 453**,** 524-8.

YE, M., ERMAKOVA, O. & GRAF, T. 2005. PU.1 is not strictly required for B cell development and its absence induces a B-2 to B-1 cell switch. *J Exp Med,* 202**,** 1411-22.

YIN, A. H., MIRAGLIA, S., ZANJANI, E. D., ALMEIDA-PORADA, G., OGAWA, M., LEARY, A. G., OLWEUS, J., KEARNEY, J. & BUCK, D. W. 1997. AC133, a novel marker for human hematopoietic stem and progenitor cells. *Blood,* 90**,** 5002-12.

YODER, M. C. & HIATT, K. 1997. Engraftment of embryonic hematopoietic cells in conditioned newborn recipients. *Blood,* 89**,** 2176-83.

YODER, M. C., HIATT, K., DUTT, P., MUKHERJEE, P., BODINE, D. M. & ORLIC, D. 1997a. Characterization of definitive lymphohematopoietic stem cells in the day 9 murine yolk sac. *Immunity,* 7**,** 335-44.

YODER, M. C., HIATT, K. & MUKHERJEE, P. 1997b. In vivo repopulating hematopoietic stem cells are present in the murine yolk sac at day 9.0 postcoitus. *Proc Natl Acad Sci U S A,* 94**,** 6776-80.

YOKOTA, T., HUANG, J., TAVIAN, M., NAGAI, Y., HIROSE, J., ZUNIGA-PFLUCKER, J. C., PEAULT, B. & KINCADE, P. W. 2006. Tracing the first waves of lymphopoiesis in mice. *Development,* 133**,** 2041-51.

YOKOTA, T., MEKA, C. S., KOURO, T., MEDINA, K. L., IGARASHI, H., TAKAHASHI, M., ORITANI, K., FUNAHASHI, T., TOMIYAMA, Y., MATSUZAWA, Y. & KINCADE, P. W. 2003. Adiponectin, a fat cell product, influences the earliest lymphocyte precursors in bone marrow cultures by activation of the cyclooxygenase-prostaglandin pathway in stromal cells. *J Immunol,* 171**,** 5091-9.

YONA, S., KIM, K. W., WOLF, Y., MILDNER, A., VAROL, D., BREKER, M., STRAUSS-AYALI, D., VIUKOV, S., GUILLIAMS, M., MISHARIN, A., HUME, D. A., PERLMAN, H., MALISSEN, B., ZELZER, E. & JUNG, S. 2013. Fate mapping reveals origins and dynamics of monocytes and tissue macrophages under homeostasis. *Immunity,* 38**,** 79-91.

YOSHIMOTO, M., MONTECINO-RODRIGUEZ, E., FERKOWICZ, M. J., PORAYETTE, P., SHELLEY, W. C., CONWAY, S. J., DORSHKIND, K. & YODER, M. C. 2011. Embryonic day 9 yolk sac and intra-embryonic hemogenic endothelium independently generate a B-1 and marginal zone progenitor lacking B-2 potential. *Proc Natl Acad Sci U S A,* 108**,** 1468-73.

YOSHIMOTO, M., PORAYETTE, P., GLOSSON, N. L., CONWAY, S. J., CARLESSO, N., CARDOSO, A. A., KAPLAN, M. H. & YODER, M. C. 2012. Autonomous murine T-cell progenitor production in the extra-embryonic yolk sac before HSC emergence. *Blood,* 119**,** 5706-14.

YOUNG, P. E., BAUMHUETER, S. & LASKY, L. A. 1995. The sialomucin CD34 is expressed on hematopoietic cells and blood vessels during murine development. *Blood,* 85**,** 96-105.

YU, J., CHAU, K. F., VODYANIK, M. A., JIANG, J. & JIANG, Y. 2011. Efficient feeder-free episomal reprogramming with small molecules. *PLoS One,* 6**,** e17557.

YU, J., HU, K., SMUGA-OTTO, K., TIAN, S., STEWART, R., SLUKVIN, II & THOMSON, J. A. 2009. Human induced pluripotent stem cells free of vector and transgene sequences. *Science,* 324**,** 797-801.

YU, J., VODYANIK, M. A., SMUGA-OTTO, K., ANTOSIEWICZ-BOURGET, J., FRANE, J. L., TIAN, S., NIE, J., JONSDOTTIR, G. A., RUOTTI, V., STEWART, R., SLUKVIN, II & THOMSON, J. A. 2007. Induced pluripotent stem cell lines derived from human somatic cells. *Science,* 318**,** 1917-20.

YUAN, J., NGUYEN, C. K., LIU, X., KANELLOPOULOU, C. & MULJO, S. A. 2012. Lin28b reprograms adult bone marrow hematopoietic progenitors to mediate fetal-like lymphopoiesis. *Science,* 335**,** 1195-200.

ZAMBIDIS, E. T., PARK, T. S., YU, W., TAM, A., LEVINE, M., YUAN, X., PRYZHKOVA, M. & PEAULT, B. 2008. Expression of angiotensin-converting enzyme (CD143) identifies and regulates primitive hemangioblasts derived from human pluripotent stem cells. *Blood,* 112**,** 3601-14.

ZHANG, Y., FISHER, N., NEWEY, S. E., SMYTHE, J., TATTON, L., TSAKNAKIS, G., FORDE, S. P., CARPENTER, L., ATHANASSOPOULOS, T., HALE, S. J., FERGUSON, D. J., TYLER, M. P. & WATT, S. M. 2009. The impact of proliferative potential of umbilical cord-derived endothelial progenitor cells and hypoxia on vascular tubule formation in vitro. *Stem Cells Dev,* 18**,** 359-75.

ZHAO, T., ZHANG, Z. N., RONG, Z. & XU, Y. 2011. Immunogenicity of induced pluripotent stem cells. *Nature,* 474**,** 212-5.

ZHOU, H., WU, S., JOO, J. Y., ZHU, S., HAN, D. W., LIN, T., TRAUGER, S., BIEN, G., YAO, S., ZHU, Y., SIUZDAK, G., SCHOLER, H. R., DUAN, L. & DING, S. 2009. Generation of induced pluripotent stem cells using recombinant proteins. *Cell Stem Cell,* 4**,** 381-4.

ZHOU, T., BENDA, C., DUNZINGER, S., HUANG, Y., HO, J. C., YANG, J., WANG, Y., ZHANG, Y., ZHUANG, Q., LI, Y., BAO, X., TSE, H. F., GRILLARI, J., GRILLARI-VOGLAUER, R., PEI, D. & ESTEBAN, M. A. 2012. Generation of human induced pluripotent stem cells from urine samples. *Nat Protoc,* 7**,** 2080-9.

ZHU, Z. & HUANGFU, D. 2013. Human pluripotent stem cells: an emerging model in developmental biology. *Development,* 140**,** 705-17.

ZIMMERLIN, L., DONNENBERG, V. S., PFEIFER, M. E., MEYER, E. M., PEAULT, B., RUBIN, J. P. & DONNENBERG, A. D. 2010. Stromal vascular progenitors in adult human adipose tissue. *Cytometry A,* 77**,** 22-30.